eman ta zabal zazu

Universidad del País Vasco

Euskal Herriko Unibertsitatea

Properties and applications of antioxidant bilayer films based on fish skin gelatin containing epigallocatechin gallate

Krisana Nilsuwan

Supervisors: Koro de la Caba & Soottawat Benjakul

Department of Chemical and Environmental Engineering

Properties and applications of antioxidant bilayer films based on fish skin gelatin containing epigallocatechin gallate

Krisana Nilsuwan

A Thesis Submitted in Fulfillment of the Requirements for the Degree of Doctor of Philosophy in Food Science and Technology

Prince of Songkla University

2020

Título de la tesis: Properties and applications of antioxidant bilayer films based on fish skin gelatin containing epigallocatechin gallate

Autor: Mr. Krisana Nilsuwan

Programa de doctorado: Ingeniería de Materiales Renovables

Año académico: 2019/2020

RESUMEN

Se han preparado y caracterizado films bicapa por laminación de films de gelatina de pescado (GF) y su correspondiente film emulsificado (EF) con diferentes ratios de espesores (7:3, 5:5 and 3:7). La formación de las dos capas se pudo observar por microscopia electrónica de barrido (SEM). Los films bicapa presentaron valores de resistencia a tracción (TS) similares ($P > 0,05$) a los films EF, pero mostraron menor ($P < 0,05$) elongación a rotura (EAB). Asimismo, todos los films bicapa presentaron menor ($P < 0,05$) permeabilidad al vapor de agua (WVP) y mayor ($P < 0,05$) permeabilidad al oxígeno (OP) que los films GF. La mayor ($P < 0,05$) diferencia de color (ΔE^*) se observó para los films bicapa con mayor espesor en el film EF. Además, el valor de transmisión de luz fue menor, mientras que el valor de transparencia fue mayor ($P < 0,05$) para los films bicapa que para los monocapa de GF. El análisis por calorimetría diferencial de barrido (DSC) reveló que los films bicapa presentan mayor temperature de transción vítrea (T_g) que los monocapa GF, aunque menor que los monocapa EF. Todos los films bicapa son termosellables, aunque los films monocapa de GF presentaron mayor ($P < 0,05$) resistencia y eficiencia de sellado.

De cara a mejorar la permeabilidad al vapor de agua de los films de gelatina de pescado (GF), se llevó a cabo la laminación con films de ácido poliláctico (PLAF), preparándose films bicapa GF/PLAF con diferentes ratios de

espesor (9:1, 8:2, 7:3, 6:4 and 5:5) mediante el método de solution casting. Los films bicapa exhibieron menor ($P < 0,05$) TS, pero mayor ($P < 0,05$) EAB que los monocapa de PLAF. Además, todos los films bicapa presentaron menor WVP y transparencia en comparación con los monocapa GF. Asimismo, los films bicapa presentaron menor barrera a la transmisión de luz UV, especialmente para los films con un mayor espesor de PLAF. Sin embargo, todos los films bicapa presentaron mejores propiedades barrera al oxígeno que los films monocapa, independientemente de los espesores de las capas. Las imágenes de SEM mostraron que la superficie del film era lisa, lo que no impidió que los films bicapa fuesen termosellables, observándose la menor ($P < 0,05$) eficiencia de sellado para los films bicapa GF/PLAF la ratio de espesor 5:5. Por otra parte, el análisis térmico por DSC reveló que los films GF/PLAF (6:4) presentan dos picos endotérmicos diferenciados, correspondientes a la fusión de la gelatina y del PLA.

En relación con las propiedades antioxidantes de los films, se incorporó epigalocatequina galato (EGCG) en distintas concentraciones (0 – 5,71 % en peso, en base al contenido de proteína) en las formulaciones de gelatina de pescado, investigándose las propiedades de los films de gelatina de pescado resultantes. Todos los films mostraron una superficie lisa, observándose la mayor ($P < 0,05$) eficiencia de sellado para los films con el 5,71 % en peso de EGCG. La capacidad antioxidante de los mismos se determinó mediante distintos análisis, incluyendo el test de absorbancia del catión radical 2,2'-azinobis (3-etilbenzotiazolina-6-sulfonato) (ABTS), la capacidad de atrapar radicales libres con el 2,2-difenil-1-picrilhidrazilo (DPPH), y la capacidad de reducción férrica (FRAP), así como la absorbancia de radicales de oxígeno (ORAC). Los films que

contienen 4,29 y 5,71 % en peso de EGCG presentan mayor ($P < 0,05$) TS y WVP, pero menor ($P < 0,05$) EAB y transmisión de luz en comparación con los films control (sin EGCG). Todos los films con EGCG mostraron valores mayores ($P < 0,05$) de a^*, b^* y ΔE^* que los films sin EGCG. La incorporación del 5,71 % en peso de EGCG aumentó la T_g de los films de gelatina, debido a la interacción entre la proteína y la EGCG, como se pudo observar por FTIR. Asimismo, la mayor liberación de EGCG desde los films de gelatina se observó para los films con el 5,71 % en peso de EGCG.

Analizando las propiedades de los films monocapa, bicapa y aquellos con EGCG como antioxidante, se puede concluir que los films bicapa presentan mayor TS y propiedades barrera al vapor de agua y a la luz, pero también son más opacos que los films monocapa. Sin embargo, no se observaron diferencias significativas ($P > 0,05$) en las propiedades barrera al oxígeno entre los films bicapa y monocapa. Estos films se han empleado para fabricar bolsas, en las que se ha envasado aceite de pollo (CSO). El aceite envasado en las bolsas preparadas con los films que contienen EGCG mostraron menores valores de peróxido (PV), sustancias reactivas con ácido tiobarbitúrico (TBARS), y compuestos volátiles, después de 30 días de almacenamiento, en comparación con el aceite envasado en bolsas comerciales de polietileno lineal de baja densidad (LLDPE). Asimismo, al final del almacenamiento, se observó una mayor retención del ácido linoleico (C18:2 *n*-6) y del ácido linolénico (C18:3 *n*-9) en el aceite envasado en las bolsas preparadas con los films de gelatina con EGCG.

Una vez analizadas las propiedades de los films monocapa y bicapa preparados por el método de solution casting, se analizó la viabilidad del

procesado en seco por termo-compresión como estrategia alternativa y más apropiada para el escalado industrial, ya que permite la reducción de los tiempos de producción. Los films de gelatina con EGCG preparados por esta técnica son homogéneos, como se comprueba a través de las imágenes de SEM, que muestran una buena compatibilidad entre los componentes de la mezcla, y presentan menor brillo. El análisis por FTIR, rayos X (XRD) y termogravimetría (TGA) mostró que se producen interacciones entre la gelatina y la EGCG utilizada como antioxidante natural, disminuyendo la solubilidad de los films. Los films con un contenido de EGCG de 5,71 % y 17,14 % mostraron un buen comportamiento mecánico, con buenos valores tanto de TS como de EAB. Además, los films mostraron actividad antioxidante y la curva migración de EGCG mostró una liberación controlada del bioactivo.

Finalmente, la estrategia de producción de films por termo-compresión también se empleó para la fabricación de films bicapa, de cara a eliminar el uso de disolventes orgánicos en la preparación de los films de PLA, en línea con los principios de la química verde. Los films resultantes son transparentes, fácilmente manejables y presentan valores bajos de WVP por la adición de la capa de PLA. Además, la incorporación de EGCG promueve las interacciones con la gelatina, como se observa por FTIR, dando lugar a films bicapa homogéneos, como se observa por SEM. Los films bicapa con 12 % de EGCG muestran buenas propiedades mecánicas, barrera al agua y a la luz, y alta capacidad antioxidante. Estos films bicapa obtenidos por compression se utilizaron para preparer bolsas, en las que se envasaron filetes de pescado (SCS). Después de 7 días de almacenamiento a 4 °C, los filetes de pescado envasados en las bolsas de gelatina con 12 % de EGCG mostraron valores

menores de bacterias psicrofílicas, pérdida de peso, PV y TBARS que los envasados en las bolsas sin EGCG o en las bolsas de LLDPE.

Thesis Title: Properties and applications of antioxidant bilayer films based on fish skin gelatin containing epigallocatechin gallate

Author: Mr. Krisana Nilsuwan

Major Program: Food Science and Technology

Academic Year: 2019/2020

ABSTRACT

Bilayer films prepared by the lamination of fish gelatin film (GF) and its corresponding emulsified film (EF) with different layer thickness ratios (7:3, 5:5 and 3:7) were characterized. Bilayer films had the similar tensile strength (TS) to EF ($P > 0.05$) but showed lower elongation at break (EAB) ($P < 0.05$). All bilayer films showed the lower water vapor permeability (WVP) but higher oxygen permeability (OP) than GF. The highest total color different (ΔE^*) value was observed in bilayer film laminated with higher thickness ratio of EF ($P < 0.05$). Lower light transmission and higher transparency value were obtained for bilayer films, compared to GF ($P < 0.05$). Based on cross-sectional scanning electron microscopic (SEM), all bilayer films consisted of two layers. Differential scanning calorimetric (DSC) analysis revealed that the bilayer films had the higher glass transition temperature (T_g) than GF but lower than EF. All bilayer films were heat sealable, however their seal strength and seal efficiency were lower than those of GF ($P < 0.05$).

In order to improve water vapor permeability of GF by laminating with poly(lactic) acid film (PLAF), GF/PLAF bilayer films with different layer thickness ratios (9:1, 8:2, 7:3, 6:4 and 5:5) were prepared by casting and characterized. Bilayer films exhibited lower TS but higher EAB than PLAF ($P < 0.05$). All bilayer films showed lower WVP and transparency, compared to GF. Bilayer films had

less barrier property toward UV light transmission, especially with increasing PLAF layer thickness ratio. All bilayer films exhibited better oxygen barrier property than PLAF and GF layer thickness had no impact on oxygen permeability of resulting bilayer films. SEM micrographs of all films showed smooth surface and the two layers of cross-section were observed for all bilayer films. Bilayer films were heat sealable. The lowest seal strength and seal efficiency were attained for film with GF/PLAF layer thickness ratio of 5:5 ($P < 0.05$). DSC analysis revealed that the GF/PLAF (6:4) bilayer film exhibited two distinct endothermic peaks, corresponding to the melting transition of gelatin and PLA.

Regarding the enhancement of antioxidant activity, epigallocatechin gallate (EGCG) was incorporated to GF at various concentrations (0-5.71 wt %, based on protein content) and the properties of fish gelatin-based films was also investigated. EGCG had broad antioxidant activities including the 2,2-azino-bis (3-ethylbenzothiazoline-6-sulfonic acid) (ABTS) and 2,2-diphenyl-1-picrylhydrazyl (DPPH) radical scavenging activities, ferric reducing antioxidant power (FRAP), hydrogen peroxide scavenging activity and oxygen radical absorbance capacity (ORAC). Films containing 4.29 and 5.71 wt % EGCG exhibited higher TS and WVP but lower EAB and light transmission, compared with the control film (without EGCG) ($P < 0.05$). All films incorporated with EGCG showed higher a^*-, b^*- and ΔE^* than that without EGCG ($P < 0.05$). All films had smooth surface. The incorporation of 5.71 wt % EGCG increased glass transition temperature (T_g) of gelatin film. FTIR analysis revealed the interaction between protein and EGCG. Higher seal strength and seal efficiency were observed for film incorporated with 5.71 wt % EGCG in comparison with control film (without

EGCG) ($P < 0.05$). When the migration of EGCG from gelatin film was tested, the highest release of EGCG was found for film containing 5.71 wt % EGCG after 18 days of storage.

The properties of monolayer and bilayer fish gelatin films and the corresponding films containing EGCG were examined. Bilayer films showed higher TS, water vapor and light barrier properties but also higher opaqueness and yellowness than monolayer films. No differences in EAB and oxygen barrier property between monolayer and bilayer films were observed. Those films were used to produce pouches, in which chicken skin oil (CSO) was packaged. CSO packaged in the pouches prepared with the films containing EGCG showed lower peroxide value (PV), thiobarbituric acid reactive substances (TBARS) and volatile compounds after 30 days of storage in comparison with that packaged in linear low-density polyethylene (LLDPE) pouch. Additionally, at the end of the storage, linoleic acid (C18:2 *n*-6) and linolenic acid (C18:3 *n*-9) were more retained in CSO packaged in the pouches made from the films containing EGCG.

An alternative approach towards more producible active films based on fish gelatin and EGCG fabricated by thermo-compression molding was investigated in this study. This strategy permitted the reduction of production times. EGCG, used as a natural antioxidant, promoted the interaction with gelatin, as shown by Fourier transform infrared spectroscopy, total soluble matter, X-ray diffraction and thermogravimetric analyses. This interaction led to the formation of homogeneous structures, as observed by SEM, indicating a good compatibility among all the components of the mixture. Films with EGCG at 5.71 wt % and 17.14 wt % showed good mechanical properties, both TS and EAB. In addition,

EGCG provided films with lower gloss and mass loss as well as slow release profile with DPPH radical scavenging activity.

In order to reduce the production times and avoided the uses of inorganic solvents towards production of active bilayer films based on PLA and fish gelatin incorporated with EGCG. An alternative approach fabricated by thermo-compression molding was investigated. Thermo-compression molded bilayer films showed good handling, transparency and low WVP. The incorporation of EGCG promoted interactions with gelatin, as shown by Fourier transform infrared spectroscopy. These interactions contributed to homogeneous structures, as observed by SEM. Bilayer films with 12 wt % EGCG showed good mechanical properties, high water and UV-visible light barrier properties as well as a high DPPH radical scavenging activity. These bilayer films were used to produce bags, in which striped catfish slices (SCS) were packaged. After 7 days of storage at 4 °C, SCS packaged in bags prepared with 12 wt % EGCG had lower psychrophilic bacteria count, weight loss, peroxide value, and thiobarbituric acid reactive substances (TBARS) value along with higher docosahexaenoic acid (C22:6 *n*-3) content than those packaged in bags prepared without EGCG or in LLDPE bags. No difference in overall likeness score was found among all the samples packaged in different bags after 7 days of storage.

ชื่อวิทยานิพนธ์ คุณสมบัติและการประยุกต์ใช้ฟิล์มสองชั้นที่มีฤทธิ์ต้านออกซิเดชันจากฟิล์มเจลาตินที่เติมสารอีพิกัลโลคาเทชินกัลเลต

ผู้เขียน นายกฤษณะ นิลสุวรรณ

สาขาวิชา วิทยาศาสตร์และเทคโนโลยีอาหาร

ปีการศึกษา 2562

บทคัดย่อ

จากการวิเคราะห์ฟิล์มสองชั้นที่เตรียมจากการประกบระหว่างฟิล์มเจลาตินหนังปลา (GF) และฟิล์มอิมัลชัน (EF) ด้วยอัตราส่วนชั้นความหนาที่ต่างกัน (7 ต่อ 3, 5 ต่อ 5 และ 3 ต่อ 7) พบว่าฟิล์มสองชั้นมีค่าการทนแรงดึง (TS) ไม่แตกต่างจาก EF แต่มีค่าการยืดสูงสุดเมื่อขาด (EAB) ต่ำกว่า ฟิล์มสองชั้นทั้งหมดมีค่าการซึมผ่านไอน้ำ (WVP) ต่ำกว่าแต่มีค่าการซึมผ่านออกซิเจน (OP) สูงกว่า GF ค่า ΔE^* สูงที่สุดพบในฟิล์มสองชั้นที่มีชั้น EF หนากว่า ฟิล์มสองชั้นมีค่าการส่องผ่านของแสงต่ำกว่าและค่าความโปร่งแสงสูงกว่า GF จากกล้องจุลทรรศน์แบบส่องกราดแสดงให้เห็นว่าฟิล์มมีสองชั้น การวิเคราะห์ค่าพลังงานความร้อนและอุณหภูมิของสารตัวอย่างเปรียบเทียบกับสารมาตรฐาน (DSC) บ่งชี้ว่าฟิล์มสองชั้นมีอุณหภูมิการเปลี่ยนสถานะจากแก้วเป็นยาง (T_g) สูงกว่า GF แต่ต่ำกว่า EF ฟิล์มสองชั้นทั้งหมดสามารถซีลได้แต่ความแข็งแรงของรอยซีลและประสิทธิภาพของการซีลต่ำกว่า GF

เพื่อที่จะปรับปรุงสมบัติการป้องกันไอน้ำของ GF โดยการประกบด้วยฟิล์มพอลิแลคติกแอซิส (PLAF) จากการเตรียมฟิล์มสองชั้น GF/PLAF ที่อัตราส่วนความหนาที่แตกต่างกัน (9 ต่อ 1 8 ต่อ 2 7 ต่อ 3 6 ต่อ 4 และ 5 ต่อ 5) ด้วยวิธีเทฟิล์ม พบว่าฟิล์มสองชั้นมีค่า TS ต่ำกว่าแต่มีค่า EAB สูงกว่า PLAF ฟิล์มสองชั้นทั้งหมดมีค่า WVP และค่าความโปร่งแสงต่ำกว่า GF ฟิล์มสองชั้นมีสมบัติการป้องกันการส่องผ่านของแสงยูวีต่ำลงโดยเฉพาะเมื่อชั้นของ PLAF หนาขึ้น ฟิล์มสองชั้นมีสมบัติการป้องกันออกซิเจนที่ดีกว่า PLAF และการเปลี่ยนแปลงความหนาของชั้น GF ไม่มีผลต่อการเปลี่ยนการซึมผ่านของออกซิเจนของฟิล์มสองชั้น รูปภาพจากกล้องจุลทรรศน์แบบส่องกราดแสดงให้เห็นว่าผิวฟิล์มเรียบและภาคตัดขวางแสดงให้เห็นทั้งลักษณะสองชั้นของฟิล์มสองชั้น ฟิล์มสองชั้นสามารถซีลได้ ฟิล์มสองชั้นที่ใช้อัตราส่วน 5 ต่อ 5 มีค่าความแข็งแรงรอยของซีลและประสิทธิภาพของการซีลต่ำที่สุด การวิเคราะห์ DSC บ่งชี้ว่าฟิล์มสองชั้นมีอุณหภูมิการหลอมเหลว 2 จุด ซึ่งเกี่ยวข้องกับการหลอมเหลวของเจลาตินและพอลิแลคติกแอซิส

สำหรับการเพิ่มฤทธิ์การต้านออกซิเดชันของฟิล์มเจลาติน สารอีพิกัลโลคาเทชินกัลเลต (EGCG) ที่ความเข้มข้นแตกต่างกัน (ร้อยละ 0 ถึง 5.71 ฐานโปรตีน) ถูกเติมลงในฟิล์มเจ

ลาติน จากการศึกษากิจกรรมการออกฤทธิ์การต้านออกซิเดชันของสาร EGCG พบว่าสาร EGCG แสดงกิจกรรมการกำจัดอนุมูล ABTS และ DPPH การกำจัดอนุมูลโลหะของเหล็ก การกำจัดอนุมูลไฮโดรเจนเพอร์ออกไซด์และการดูดซับอนุมูลออกซิเจน ฟิล์มที่เติมสาร EGCG ที่ความเข้มข้นร้อยละ 4.29 และ 5.71 มีค่า TS และ WVP สูงกว่า แต่มีค่า EAB และค่าการส่องผ่านของแสงต่ำกว่าฟิล์มที่ไม่เติมสาร EGCG ฟิล์มทั้งหมดที่เติมสาร EGCG มีค่า a^* ค่า b^* และค่า ΔE^* สูงกว่าฟิล์มที่ไม่ได้เติมสาร EGCG ผิวหน้าของฟิล์มเจลาตินทั้งหมดมีลักษณะเรียบ การเติมสาร EGCG ทำให้ค่า T_g ของฟิล์มเจลาตินมีค่าเพิ่มขึ้น การวิเคราะห์ฟลูเรียร์ทรานส์ฟอร์มอินฟราเรดสเปคโทรไมโครสโคปี (FTIR) บ่งชี้การเกิดอันตรกิริยาระหว่างโปรตีนและสาร EGCG ค่าความแข็งแรงรอยของซีลและประสิทธิภาพของการซีลของฟิล์มที่เติมสาร EGCG ร้อยละ 5.71 มีค่าสูงกว่าฟิล์มที่ไม่เติมสาร EGCG สำหรับการวิเคราะห์การปลดปล่อยของสาร EGCG พบว่าฟิล์มที่เติมสาร EGCG ร้อยละ 5.71 มีค่าการปลดปล่อยสาร EGCG สูงที่สุดภายหลังการเก็บรักษานาน 18 วัน

จากการศึกษาคุณสมบัติของฟิล์มชั้นเดียวและฟิล์มสองชั้นจากเจลาตินปลาทั้งที่เติมและไม่เติมสาร EGCG พบว่าฟิล์มสองชั้นมีค่า TS ค่าการป้องกันการซึมผ่านไอน้ำ ค่าการป้องกันการส่องผ่านของแสง ความขุ่นและความเหลืองสูงกว่าฟิล์มชั้นเดียว ค่า EAB และสมบัติการป้องกันออกซิเจนของฟิล์มชั้นเดียวและฟิล์มสองชั้นไม่แตกต่างกัน เมื่อนำฟิล์มทั้งหมดมาขึ้นรูปเป็นซองเพื่อใช้บรรจุน้ำมันจากหนังไก่ (CSO) พบว่า CSO ที่บรรจุในซองจากฟิล์มที่เติมสาร EGCG มีค่าเพอร์ออกไซด์ (PV) ค่า thiobarbituric acid reactive substances (TBARS) และปริมาณสารระเหยได้ต่ำกว่าซองจากฟิล์มพอลิเอทิลีนความหนาแน่นต่ำสายตรง (LLDPE) นอกจากนี้พบว่าปริมาณของกรดลิโนเลอิก (C18:2 *n*-6) และกรดลิโนเลนิค (C18:3 *n*-9) คงเหลืออยู่มากใน CSO ที่บรรจุในซองจากฟิล์มที่เติมสาร EGCG

จากการศึกษาวิธีการทางเลือกในการผลิตฟิล์มแอคทีฟจากเจลาตินหนังปลาและสาร EGCG ให้มากขึ้นด้วยวิธีการกดขึ้นรูปด้วยความร้อน พบว่าวิธีดังกล่าวสามารถลดระยะเวลาในการผลิต สาร EGCG ซึ่งเป็นสารต้านออกซิเดชันจากธรรมชาติส่งเสริมการเกิดอันตรกิริยาของเจลาตินโดยแสดงจากผลการวิเคราะห์ FTIR ค่าการละลาย ค่าการสะท้อนของแสงรังสีเอกซ์และการวิเคราะห์ความโน้มถ่วงความร้อน (TGA) อันตรกิริยาดังกล่าวส่งผลให้เกิดโครงสร้างที่เป็นเนื้อเดียวกัน ซึ่งสังเกตได้ด้วย SEM ที่แสดงให้เห็นความเข้ากันได้ดีขององค์ประกอบทั้งหมด ฟิล์มที่เติมสาร EGCG ความเข้มข้นร้อยละ 5.71 และ 17.14 มีค่าสมบัติเชิงกลที่ดี ทั้งค่า TS และค่า EAB นอกจากนี้ สาร EGCG ทำให้ฟิล์มมีค่าความวาวและค่าการสูญเสียน้ำหนักน้อยกว่า รวมถึงทำให้เกิดรูปแบบการปลดปล่อยค่ากิจกรรมการกำจัดอนุมูล DPPH แบบช้า

นอกจากนี้ เพื่อลดระยะเวลาการผลิตและหลีกเลี่ยงการใช้ตัวทำละลายในการผลิตฟิล์มสองชั้นแอคทีฟจากพอลิแลคติกและเจลาตินจากปลาที่เติมสาร EGCG จากการศึกษาวิธีการกดขึ้นรูปด้วยความร้อน พบว่าฟิล์มสองชั้นมีลักษณะที่ดี มีความโปร่งแสงและมีค่า WVP ต่ำ การเติมสาร EGCG ทำให้เกิดอันตรกิริยากับเจลาติน สังเกตได้จากผลการวิเคราะห์ FTIR ซึ่งอันตรกิริยาที่เกิดขึ้นนี้ส่งผลให้โครงสร้างมีความเป็นเนื้อเดียวกัน สังเกตได้จากผลการวิเคราะห์ SEM ฟิล์มที่เติมสาร EGCG ความเข้มข้นร้อยละ 12 มีค่าสมบัติเชิงกลที่ดี มีค่าการป้องกันการซึมผ่านไอน้ำและการส่องผ่านของแสงสูง รวมถึงมีกิจกรรมการกำจัดอนุมูล DPPH สูง เมื่อฟิล์มสองชั้นนี้ถูกขึ้นรูปเป็นถุงสำหรับบรรจุเนื้อปลาสวาย (SCS) พบว่าภายหลังการเก็บรักษาที่อุณหภูมิ 4 องศาเซลเซียส เป็นเวลา 7 วัน SCS ที่บรรจุในถุงจากฟิล์มสองชั้นที่เติมสาร EGCG มีปริมาณแบคทีเรียที่เจริญได้ดีที่อุณหภูมิต่ำ ค่าการสูญเสียน้ำหนัก ค่า PV ค่า TBARS ต่ำกว่า ตลอดจนมีปริมาณกรดโดโคซะเฮกซะอีโนอิก (C22:6 *n*-3) สูงกว่า SCS ที่บรรจุในถุงจากฟิล์มสองชั้นที่ไม่เติมสาร EGCG หรือถุงจากฟิล์ม LLDPE นอกจากนี้คะแนนความชอบโดยรวมของทุกตัวอย่างภายหลังจากการเก็บรักษาเป็นเวลา 7 วัน ไม่แตกต่างกัน

ACKNOWLEDGEMENT

I would like to express my deepest appreciation and sincere gratitude to my advisor, Prof. Dr. Soottawat Benjakul of the Department of Food Technology, Faculty of Agro-Industry, Prince of Songkla University, for his kindness, guidance and assistance during my study since the first day of being his student. Not only the academic knowledge dedicate to me, but also invaluable suggestion and lessons for my personal life have been kindly provided. His determination and perseverance to train me to be a good researcher with responsibility, vigilance and honesty are always acknowledged.

I sincerely thank to my co-advisor, Asst. Prof. Dr. Thummanoon Prodpran of the Department of Material Product Technology, Faculty of Agro-Industry, Prince of Songkla University, for his kindness and helpful guidance in consultation, particularly during my research on characterization part.

I would like to express my profound gratitude to my co-advisor, Prof. Dr. Koro de la Caba of the department of Chemical and Environmental Engineering, University of the Basque Country (UPV/EHU), Spain for her warm welcome, kindness, generous contribution and unconditional help, particularly during my one academic year internship under Ph.D. Cotutelle Program (2018-2019) in San-Sebastian, Spain.

I am grateful to my examining committee, Asst. Prof. Dr. Kongkarn Kijroongrojana of the Department of Food Technology, Faculty of Agro-Industry, Prince of Songkla University, Asst. Prof. Dr. Supachai Pisuchpen of the Department of Material Product Technology, Faculty of Agro-Industry, Prince of Songkla University, and Assoc. Prof. Dr. Rungsinee Sothornvit for the valuable time devoted to my thesis and their kindness, comments and helpful suggestion.

I would like to express my deepest appreciation to my beloved family for the great encouragement and support. Finally, my deep gratitude is also dedicated to my dear friends and colleagues of Seafood Chemistry and Biochemistry lab (2205) and BIOMAT research group (UPV/EHU) particularly Dr. Pedro Guerrero who shared the hard time with me during my study and gave me their help.

This study could not be succeeded without the financial support from Thailand Research Fund under the Royal Golden Jubilee PhD Program (PHD/0158/2558) and the Grant-in-Aid for dissertation from Graduate School, Prince of Songkla University, Thailand. The Ministry of Science, Innovation and Universities (RTI2018-097100-B-C22), the Basque Government (Department of Quality and Food Industry), and the Provincial Council of Gipuzkoa (Department of Economic Development, the Rural Environment and Territorial Balance) are also acknowledged for the financial support.

Krisana Nilsuwan

CONTENTS

CONTENTS (Continued)

CONTENTS (Continued)

CONTENTS (Continued)

CONTENTS (Continued)

CONTENTS (Continued)

LIST OF TABLES

LIST OF TABLES (Continued)

LIST OF TABLES (Continued)

LIST OF FIGURES

LIST OF FIGURES (Continued)

LIST OF FIGURES (Continued)

CHAPTER 1

INTRODUCTION AND REVIEW OF LITERATURE

1.1 Introduction

Packaging materials are widely used to protect the product from surroundings, retard deterioration, extend the shelf-life, maintain the quality of foods, and distribute foods and products conveniently. Petroleum-based materials are commonly used and have a wide range of advantages. However, these materials are not biodegraded easily and generate a global pollution (Zhang and Mittal, 2010). Biopolymer films have gained interest in their use as edible food packaging. Edible films can be defined as thin continuous layer of biopolymer materials which can be applied as a coating on food, used as a wrap or made into pouch to hold the food or to protect it against external factors (Kester and Fennema, 1986; Krochta, 1997). Proteins are heteropolymers containing a variety of amino acids, which can undergo a wide range of interactions and chemical reactions (Stevens, 1990). Proteins have been extensively used for the development of biodegradable films due to their abundance and good film-forming ability. Among the proteins, gelatin possesses an excellent film-forming property, and is one of the first materials applied to edible coatings and films (McHugh and Krochta, 1994b). Gelatin yields transparent, colorless and highly extensible films (Núñez-Flores *et al.*, 2012). Nevertheless, it has high water absorptivity due to hydrophilicity of gelatin molecules and the presence of hydrophilic plasticizers such as glycerol, etc. (Gennadios *et al.*, 1994; Krochta, 1997; McHugh and Krochta, 1994b). This can limit the applications of gelatin films in food products with high moisture content (Núñez-Flores *et al.*, 2012). Several strategies such as chemical and enzymatic crosslinking (Bigi *et al.*, 2001; de Carvalho and Grosso, 2004), the incorporation of hydrophobic substances such as lipid, fatty acid and wax (Limpisophon *et al.*, 2010; Prodpran *et al.*, 2007; Soazo *et al.*, 2011), etc. have been implemented to improve the moisture resistance of gelatin-based films. Additionally, lamination can be another means to improve the performance of polymeric films by combining the properties of different films into one sheet (Rakotonirainy and Padua, 2001). Regarding the laminated film, the outer layers impart moisture resistance and mechanical stability, while the inner one acts as a gas barrier (Fang *et al.*, 2005). Moreover, thickness layer ratios mostly have the impact on

properties of bilayer films. Among promising outer layer films, emulsified gelatin film (EF) and poly(lactic) acid film (PLAF) have gained increasing attention as renewable and readily biodegradable materials (Cabedo *et al.*, 2006; Jongjareonrak *et al.*, 2006c; Tongnuanchan *et al.*, 2012). Lamination of EF and PLAF, which possess high water vapor barrier, onto the gelatin film (GF), which has the excellent oxygen barrier property, could render the bilayer film having both aforementioned barrier properties.

Regarding the manufacture processes, there are two main methods used to prepare protein films and bilayer films: wet and dry processes (Guerrero *et al.*, 2010; Martucci and Ruseckaite, 2010; Prodpran *et al.*, 2017). The wet process is based on the dispersion or solubilization of proteins in a solvent medium, while the dry process includes hot-pressing or compression molding as well as melt and extrusion techniques to prepare films (Ciannamea *et al.*, 2016; Guerrero *et al.*, 2010). Compression and extrusion techniques are faster and more efficient and, thus, more appropriate for industrial scale production, but research on both formulations and processing conditions are still needed to improve the properties of the final products (Chuaynukul *et al.*, 2018; Guerrero *et al.*, 2010). In this regard, compression molding could use with the aim of avoiding the use of inorganic solvents and reducing the production times of gelatin and bilayer films production.

Phenolic compounds or plant extracts have been incorporated into protein-based film to improve mechanical properties due to their protein cross-linking activity (Maryam Adilah *et al.*, 2018; Nuthong *et al.*, 2009b). Those phenolic compounds could also act as antioxidant, making the film more active (Gómez-Estaca *et al.*, 2009a; Maryam Adilah *et al.*, 2018). The antioxidant power was generally proportional to the amount of the added extract (Gómez-Estaca *et al.*, 2009a). Epigallocatechin gallate (EGCG) is one of major flavanols obtained from tea extract, containing 10-60% of dry weight (Zaveri, 2006). EGCG has been reported to exhibit antioxidant activity and play a role in preventing the lipid oxidation in foods (Lu *et al.*, 2010).

As a consequence, the smart active films with varying properties can be produced, especially for shelf-life extension of foods. Packaging from gelatin-based and bilayer films incorporated with antioxidant, particularly natural antioxidant e.g. EGCG is able to retard deterioration caused by chemical reaction, especially lipid oxidation, which prevent the water migration into foods, especially dry food with crispy

texture. Therefore, foods can be stored for an extended time. Gelatin from fish processing byproduct also can be better used, thereby increasing the market value and bring about the new environmental friendly and edible packaging.

1.2 Review of literature

1.2.1 Biodegradable and edible film

Biodegradable or compostable packaging is preferable to recyclable packaging because the latter still requires external energy to be provided to bring about the recycling process. Nevertheless, biodegradable or compostable packaging is difficult to be recycled (Guilbert *et al.*, 1997). Also, owing to the environment protection from packaging based on petroleum, which are not decomposed, biodegradable film has been an alternative packaging to those synthetic packaging material (Kester and Fennema, 1986). With regard to biodegradability, all components should be biodegradable and environmentally safe (Witt *et al.*, 1996).

Edible packaging is another type of material, which can provide the convenience to consumer. Edible packaging material must meet requirements related with their transport properties (mainly water vapor, carbon dioxide and oxygen permeabilities), mechanical properties (especially their resistance to stretching and rupture), optical properties (mainly related with their opacity and color) and flavor (in most cases, flavorless coatings are needed) (Cerqueira *et al.*, 2011). Edible films can be used to extend the shelf-life of food products by reducing moisture and solute migration, gas exchange, respiration and oxidative reaction rates (Han and Gennadios, 2005). The most beneficial characteristics of edible films are their edibility and inherent biodegradability (Guilbert *et al.*, 1996; Krochta and De Mulder-Johnston, 1997). To maintain their edibility, all film components (i.e., biopolymers, plasticizers, and other additives) should be food-grade ingredients, and all process facilities and equipment should be acceptable for food processing (Guilbert *et al.*, 1996).

1.2.2 Protein-based film

Proteins are heteropolymers containing different 20 amino acids. They are macromolecules with specific amino acid sequences and there are limitless number of sequential arrangements with a wide range of interactions and chemical reactions (Pommet *et al.*, 2003; Stevens, 1990). All structures of proteins can be easily modified

by heat, pressure, irradiation, mechanical treatment, acids, alkalines, metal ions, salts, chemical hydrolysis, enzymatic treatment and chemical cross-linking (Han and Gennadios, 2005; Krochta and De Mulder-Johnston, 1997). The most distinctive characteristics of proteins, compared to other film-forming materials, are conformational denaturation, electrostatic charges, and amphiphilic nature. Many factors can affect the conformation, charge density and hydrophilic-hydrophobic balance of proteins, thereby influencing the physical and mechanical properties of prepared films and coatings (Gontard *et al.*, 1996; Park *et al.*, 1996). In addition, properties of protein-based films depend on various factors such as the source of protein, pH of protein solution, heating temperature, plasticizers, film thickness, preparation conditions, formation process and additives incorporated into the film-forming solutions (Benjakul *et al.*, 2008; Paulo *et al.*, 2005).

Protein-based films show the impressive gas barrier properties and mechanical properties, compared to those prepared from polysaccharides and fat-based films (Cao *et al.*, 2007). However, the poor water vapor resistance limits their application. Improvement of protein film properties could be attained by modifying the properties of protein by chemical and enzymatic methods (Kester and Fennema, 1986; Krochta, 1997). Additionally, several approaches such as enzymatic modifications (de Carvalho and Grosso, 2004; Staroszczyk *et al.*, 2012), incorporation of appropriate plasticizers (Vanin *et al.*, 2005) and hydrophobic materials (Limpan *et al.*, 2010; Prodpran *et al.*, 2007), etc. have been implemented.

There are two categories of film formation processes: dry and wet (Guilbert *et al.*, 1997) (Figure 1). For the dry process, film production does not use liquid solvents, such as water or alcohol. Heat is applied to the film-forming materials to increase the temperature to above the melting point of the film-forming materials, to cause them to flow. Molten casting, extrusion, and heat pressing are good examples of dry processes (Han and Gennadios, 2005). Therefore, the thermoplastic properties of the film-forming materials should be identified in order to design film-manufacturing processes. It is necessary to determine the effects of plasticizers and any other additives on the thermoplasticity of film-forming materials (Guilbert *et al.*, 1997; Krochta, 2002).

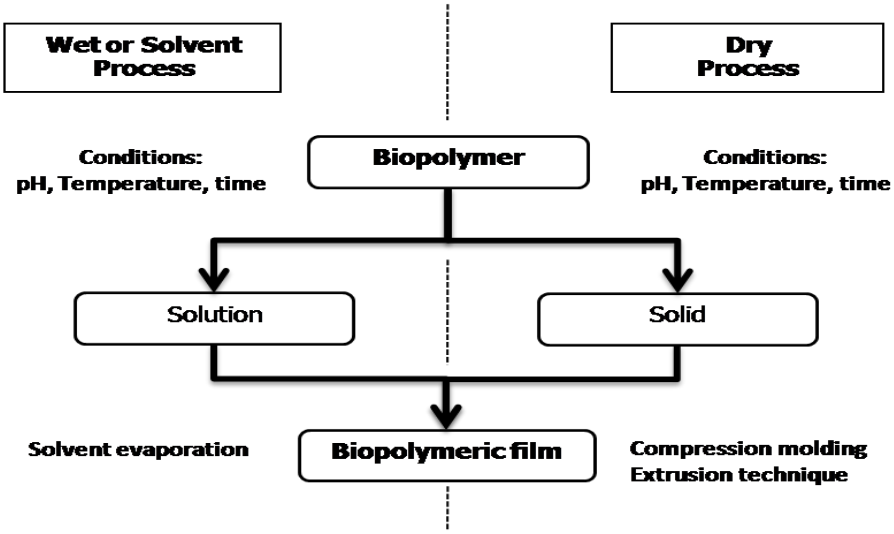

Figure 1. Processing methods: wet (or solvent) and dry process.
Source: Adapted from Guerrero *et al.* (2010)

For the wet process, the solvents are used for the dispersion of film-forming materials, followed by drying to remove the solvent and form a film structure. The selection of solvents is one of the most important factors. For edible film preparation, all the film-forming solutions should be edible and biodegradable. Only water, ethanol, and their mixtures are appropriate as solvents (Krochta, 2002). All the ingredients of film-forming materials should be dissolved or homogeneously dispersed in the solvents to produce film-forming solutions (Han and Floros, 1997; Han and Gennadios, 2005). The film-forming solution should be applied to flat surfaces using a sprayer, spreader or dipping roller, and dried to eliminate the solvent, forming a film structure. Several protein-based films from different sources, e.g. fish gelatin (Tongnuanchan *et al.*, 2012), fish muscle protein (Oujifard *et al.*, 2013; Prodpran *et al.*, 2012), porcine plasma protein (Nuthong *et al.*, 2009a), etc. were prepared by casting methods, in which film-forming solutions were firstly prepared prior to casting.

Film is essentially a dried and extensively interacted polymer network. Film-forming materials should form a spatially rearranged gel structure with all incorporated film-forming agents, such as biopolymers, plasticizers, other additives, and solvents in the case of wet casting (Felton, 2013; Rhim and Ng, 2007). Biopolymers as film-forming materials are generally dissolved or dispersed to produce film-forming solutions. Further drying of the hydrogels eliminates the excess solvents from the gel structure. Whey protein emulsion films are produced from whey-protein gels by

dehydration after heat-set or cold-set gel formation (Soazo *et al.*, 2011). There could be a critical stage of a transition from a wet gel to a dry film, which relates to a phase transition from a polymer-in-water (or other solvents) system to a water-in-polymer system (Han and Gennadios, 2005).

Protein-based film can be formed in three steps (Figure 2) (Marquié and Guilbert, 2002):

(1) Break intermolecular bonds (non-covalent and covalent bonds) that stabilize polymers in their native forms by using chemical or physical rupturing agents (by solubilization or thermal treatment). Polymer chains become mobile.

(2) Arrange and orient mobile polymer chains in the desired shape.

(3) Allow the formation of new intermolecular bonds and interactions to stabilize the three-dimensional network. The shape obtained in step 2 is maintained by eliminating the agents used in step 1 (e.g., solvent removal or cooling).

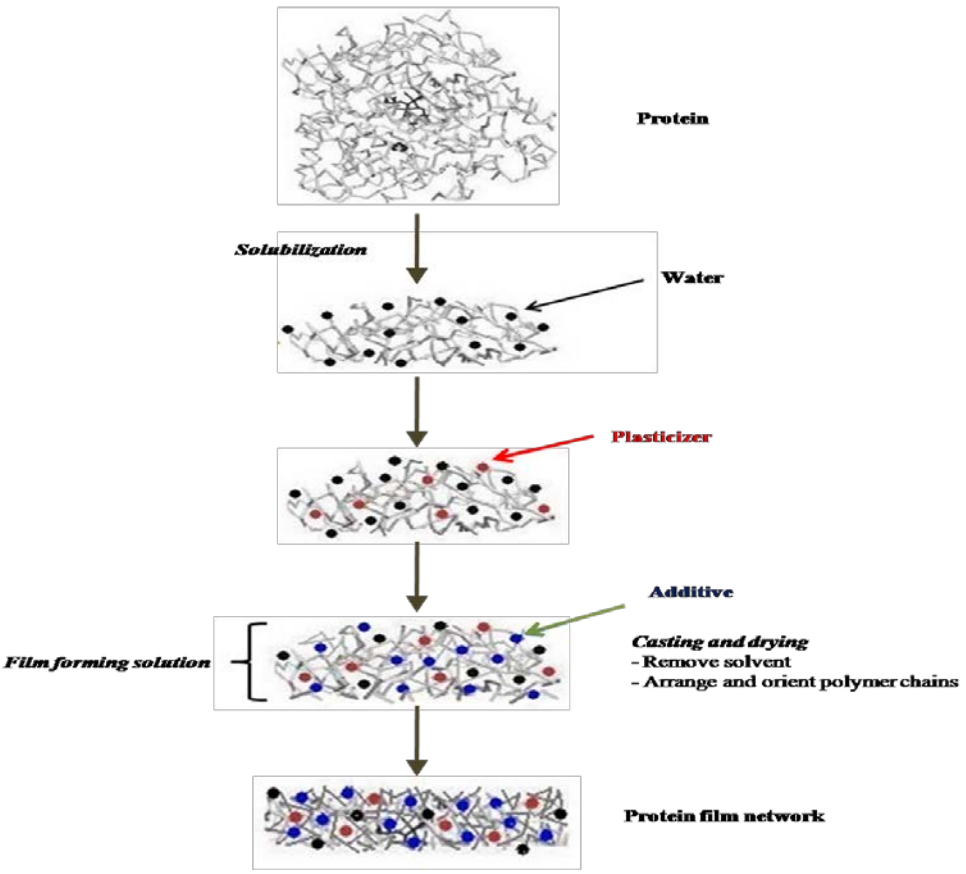

Figure 2. Mechanism of protein film formation.

Source: Adapted from Marquié and Guilbert (2002)

Potential chemical and physical approaches have been implemented for the modification of film-forming mechanisms by altering film-forming raw materials, varying film-forming processing conditions, and applying treatments on formed films (Figure 3). Potential chemical methods of modifying the film-forming mechanisms of protein-based films include pH changes, salt addition, heat denaturation, solvent changes, chemical modification of the side chains of peptides, cross-linking, and hydrolysis of peptides (Kowalczyk and Baraniak, 2011; Were *et al.*, 1999; Yildirim and Hettiarachchy, 1997), irradiation of peptides (Lacroix and Ouattara, 2000), and the addition of foreign proteins (Denavi *et al.*, 2009; Mecitoğlu *et al.*, 2006).

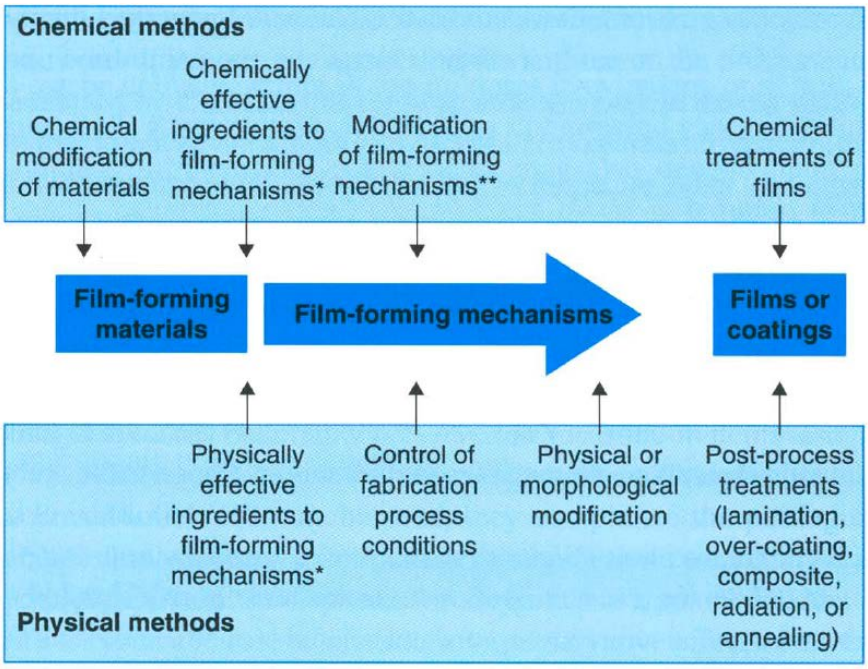

Figure 3. Chemical and physical modifying methods for preparation of film and coatings. * indicates the addition of chemically or physically active ingredients, which may enhance or interfere with the film-forming mechanisms. ** includes any chemical cross-linking, chemical substitution of side chains to create hydrophobic interactions or electrostatic interactions, and other extra mechanisms caused by chemical modifications.

Source: Han and Gennadios (2005)

Physicochemical properties of proteins determine the behavior of proteins during preparation, processing, storage and consumption. These properties are not only

important to facilitate processing, but also to determine the quality of the final product (Ralston and Osswald, 2008). Physical and chemical modifications of edible films and coatings include lamination, formation of composites, addition of particles or emulsions, perforation, over-coating, annealing heat curing (Gennadios *et al.*, 1996; Miller *et al.*, 1997), orientation, radiation (Gennadios *et al.*, 1998; Micard *et al.*, 2000), and ultrasound treatment (Banerjee *et al.*, 1996). Lamination of soy protein isolate with corn zein led to increase tensile strength and water vapor and oxygen barrier properties of the resulting bilayer film (Cho *et al.*, 2010). The incorporation of sea weed extract (6%, w/w, based on protein) enhanced the elongation at break and water vapor barrier property of bigeye snapper skin gelatin film (Rattaya *et al.*, 2009). Additionally, Bhat and Karim (2014) have been documented that fish gelatin film cross-linked with 1-2% (w/w) ribose film exhibited the increasing in TS and water vapor barrier property.

Macroscopic phase separation of incompatible ingredients from the film-forming solution is not generally desirable unless the phase separation is intentionally designed for the formation of a bilayer film structure (Han and Gennadios, 2005). To produce a homogeneous film structure avoiding macroscopic phase separation, various emulsifiers can be added to the film-forming solution (Andreuccetti *et al.*, 2009; Krochta, 2002; Tongnuanchan *et al.*, 2014). The solvent compatibility of ingredients is very important to develop homogeneous edible film and coating systems carrying active agents. All ingredients, including active agents as well as biopolymers and plasticizers, should be homogeneously dissolved in the solvent to produce film-forming solutions. Most film-forming solutions possess much higher surface tension than the surface energy of dried films, since they contain excessive amounts of water or ethanol (Han and Gennadios, 2005). During the solvent drying process, the film-forming solution is concentrated and its surface energy is decreased due to the loss of solvent (Guerrero *et al.*, 2010; Marquié and Guilbert, 2002).

1.2.3 Gelatin-based film

Gelatin is a water soluble protein obtained by thermal denaturation or partial hydrolysis of collagen, which is the main fibrous protein in bones, cartilages and skins. In general, the source, age of animal, and type of collagen are all intrinsic factors influencing the properties of gelatins (Johnston-Banks, 1990). Gelatin possesses an excellent film-forming property, and is one of the first materials applied to edible

coatings and films (Gennadios *et al.*, 1994). Edible films have been prepared from gelatin of different fish skins including bigeye snapper and brown stripe red snapper (Jongjareonrak *et al.*, 2006a) baltic cod (Kołodziejska and Piotrowska, 2007), tilapia (Tongnuanchan *et al.*, 2012), tuna (Gómez-Estaca *et al.*, 2009c), blue shark (Limpisophon *et al.*, 2009), unicorn leatherjacket (Ahmad *et al.*, 2012b).

Gelatin from varying fish species are different in terms of amino acid composition, chain length, etc., depending on extraction processes used. With different molecular properties, resulting films have different properties (Table 1). Gelatin from different chain length and amino acid composition, have been documented to yield film with different property (Jongjareonrak *et al.*, 2006a; Nagarajan *et al.*, 2012). Hoque *et al.* (2011) reported that shorter gelatin molecules generated by enzyme hydrolysis (Alcalase) yielded the film with the lower junction zone or shorter strands via weak bonds during film formation. This led to the lower mechanical properties and thermal stability of the resulting films. Hydrolysis process increased hydrophilic groups, which can interact with water molecules, leading to the increased WVP of the film. Furthermore, edible films prepared by enzyme hydrolysis (pepsin) had the disruption of the smooth, compact and homogenous structure of films (Jridi *et al.*, 2013). Apart from the chain length of gelatin molecules, plasticizer concentration was another crucial factor governing the properties of gelatin-based films from cuttlefish skin (Hoque *et al.*, 2011). Nagarajan *et al.* (2013) studied the properties of gelatin films from splendid squid (*Loligo formosana*) skin bleached with hydrogen peroxide (H_2O_2) at various concentrations (0–8% w/v). TS and WVP of films decreased, but elongation at break (EAB) increased as the concentration of H_2O_2 increased. The shorter chain peptides found in gelatin caused by fragmentation induced by H_2O_2 at high levels might be associated with lower intermolecular interaction in the film matrix. Cleavage of the glutamyl side chain and proline residue of the protein in the presence of high concentration of H_2O_2 via excessive amounts of the $HO^{\bullet}$ radical was reported (Stadtman, 2001).

Protein content, type and concentration of plasticizers were reported to affect the properties of gelatin based films (Vanin *et al.*, 2005). TS of gelatin film from shark (*Prionace glauca*) skin was affected by the protein concentration (1, 2 and 3%) of FFS (Limpisophon *et al.*, 2009). TS of film made from 2% protein FFS was the highest.

EAB and WVP of film increased with increasing protein concentration. Addition of glycerol improved flexibility and enhanced UV barrier property at 280 nm. Transparency and WVP increased with increasing glycerol. TS of gelatin film from the skin of brownstripe red snapper (*Lutjanus vitta*) and bigeye snapper (*Priacanthus macracanthus*) decreased with increasing glycerol concentration from 25 to 75% (Jongjareonrak *et al.*, 2006a). The proteins network becomes less dense, and more permeable with the plasticizer incorporation. The increase in free volume of the system also raises the solvent mobility, thereby increasing the water diffusion in the matrix of the film (Cuq *et al.*, 1997). Moreover, at the same plasticizer concentration, fish skin gelatin from the two different species plasticized with glycerol (Gly) showed the highest EAB, whereas ethylene glycol (EG) plasticized film showed the highest TS (Jongjareonrak *et al.*, 2006b). Cao *et al.* (2009) also studied the effects of different plasticizers including oligosaccharide-sucrose, some organic acids and polyethylene glycol (PEG) with different molecular weight (300, 400, 600, 800, 1500, 4000, 10000, 20000 Da). It was found that PEG of lower molecular weights exhibited the better plasticizing effects for gelatin film and such films had the better visual properties than others.

Heat treatment at appropriate temperature (70 °C) brought about the stretching or unfolding of gelatin molecule, in which higher inter-chain interaction could be formed via hydrogen bond or hydrophobic interaction. As a consequence, the improved mechanical property was obtained. Heat treatment of film-forming solution was also documented to have the impact on the properties of film from cuttlefish skin gelatin (Hoque *et al.*, 2010).

Drying condition, e.g. temperature and time also show the impact on properties of films. Gelatin films dried at different temperatures had varying physical properties (Chiou *et al.*, 2009). Gelatin chains in a solution dried below gelation temperature can form triple helical structures before complete evaporation of water. The dried film, usually termed cold-cast gelatin film, can then retain these helical structures, depending on moisture content (Chiou *et al.*, 2009). In contrast, gelatin chains in a solution dried above gelation temperature remain as random coils during the drying process (Bradbury and Martin, 1952). The dried film, usually termed hot-cast gelatin film, then retain this amorphous structure (Chiou *et al.*, 2009). Fish gelatin solutions, especially those

derived from cold-water species, have much lower gelation temperatures than mammalian gelatin solutions. This is mainly due to the fact that fish gelatin has the lower concentrations of proline and hydroxyproline (Bradbury and Martin, 1952; Kozlov and Burdygina, 1983). Fish gelatin films made from Alaska pollock (*Theragra chalcogramma*) and Alaska pink salmon (*Oncorhynchus gorbuscha*) were dried at 4 °C, 23 °C, 40 °C, and 60 °C. Cold-cast gelatin films (dried below gelation temperature at 4 °C) had higher tensile strength, percent elongation values and water sorption isotherms than hot-cast (dried above gelation temperature at the higher temperatures) gelatin films. Water vapor permeability of cold-cast gelatin films was 2-3 fold higher than that of hot-cast counterpart (Chiou *et al.*, 2009).

Casting methods are time consuming and are not appropriate for commercial production. A large scale production method such as extrusion is imperative for industrial production (Wang and Padua, 2003). Most extrusion processes are for polymer films and are often followed by compression molding to reduce the thickness of the extruded sheets (Fishman *et al.*, 2004; Liu *et al.*, 2008; Selling *et al.*, 2009). Extrusion can be implemented as a continuous unit operation with control of temperature, size, shape, and moisture (Gómez-Guillén *et al.*, 2009). Krishna *et al.* (2012) reported that WVP of extruded gelatin films was higher than that of solution-cast films, while the glass transition temperatures (T_g) of the extruded films were generally lower than those of solution-cast films.

Table 1. Properties of gelatin-based films from different fish species and sources.

Fish Species	Sources	Protein Conc.	Plasticizer Conc.	Additive Conc.	Thickness (mm)	Mechanical properties		WVP ($\times 10^{-10}$g m^{-1} s^{-1} Pa^{-1})	References
						TS (MPa)	EAB (%)		
Alaska pollock (*Theragra chalcogramma*)	Skin	5% (w/v) of FFS	-	Glutaraldehyde, 0.25 – 0.75% (w/w) of gelatin	-	45.9-50.1	3.23-3.44	0.73-0.86[a]	Chiou *et al.* (2008)
Alaska pink salmon (*Oncorhynchus gorbuscha*)	Skin	5% (w/v) of FFS	-	Glutaraldehyde, 0.25 – 0.75% (w/w) of gelatin	-	49.7-60.0	3.36-3.8	0.85-1.08[a]	Chiou *et al.* (2008)
Atlantic halibut (*Hippoglossus hippoglossus*)	Skin	2% (w/v) of FFS	Sorbitol, 30% (w/w) of protein	-	0.080 ± 0.006	3.8 ± 0.8	294.5 ± 47.8	12.0 ± 2.2 [d]	Carvalho *et al.* (2008)
Blue shark (*Prionace glauca*)	Skin	1-3% (w/v) of FFS	Glycerol, 50% (w/w) of protein	-	0.011-0.043	12.58 – 27.29	61.13 – 74.17	0.4 – 1.12	Limpisophon *et al.* (2009)
Bigeye snapper (*Priacanthus tayenus*)	Skin	2% (w/v) of FFS	Glycerol, 50% (w/w) of protein	Sea weed extract, 6% (w/w) of protein	0.029-0.030	10.04 – 11.43	12.11 – 25.98	0.89 – 1.28	Rattaya et al. (2009)

Table 1. Properties of gelatin-based films from different fish species and sources (cont.)

Fish Species	Sources	Protein Conc.	Plasticizer Conc.	Additive Conc.	Thickness (mm)	Mechanical properties		WVP ($\times 10^{-10}$ g m^{-1} s^{-1} Pa^{-1})	References
						TS (MPa)	EAB (%)		
Cod (*Godus morhua*)	Skin	4% (w/v) of FFS	Glycerol and sorbitol, 0.75 and 0.75 g/g gelatin	Soy protein isolate, 0 - 100% (w/w) of gelatin	0.047-0.086	2.83 - 8.25 N (Puncture force)	10 - 100 (Puncture deformation)	1.75 - 3.86 [b]	Denavi *et al.* (2009)
Grouper (*Epinephelus chlorostigma*)	Bone	3% (w/v) of FFS	Sorbitol, 30% (w/w) of protein	-	0.076	9.25	37.48	975 [c]	Jeya Shakila *et al.* (2012)
Red snapper (*Lutjanus campechanus*)	Bone	3% (w/v) of FFS	Sorbitol, 30% (w/w) of protein	-	0.065	8.53	59.50	1040 [c]	Jeya Shakila *et al.* (2012)
Sole (*Solea spp.*)	Skin	4% (w/v) of FFS	Glycerol and sorbitol, 0.15 and 0.15 g/g gelatin	-	-	11.4	18.1	1.77 [d]	Gómez-Estaca *et al.* (2009b)
Tuna (*Thunnus tynnus*)	Skin	2% (w/v) of FFS	Glycerol, 0.25 g/g protein	Murta leaves extract, 3.75 g/g gelatin	0.098 – 0.10	2.75 – 5.91 N (Puncture force)	3.56 – 13.77 (Puncture deformation)	1.83 - 2.87 [b]	Gómez-Guillén *et al.* (2007)

Table 1. Properties of gelatin-based films from different fish species and sources (cont.)

Fish Species	Sources	Protein Conc.	Plasticizer Conc.	Additive Conc.	Thickness (mm)	Mechanical properties		WVP ($\times 10^{-10}$g m^{-1} s^{-1} Pa^{-1})	References
						TS (MPa)	EAB (%)		
Unicorn leatherjacket	Skin	3% (w/v) of FFS	Glycerol, 0-25% (w/w) of protein	Bergamot oil, 5-25% (w/w) of protein	0.042-0.048	23.75-36.34	3.06-8.76	1.21-1.94	Ahmad *et al.* (2012a)
Warm-water tilapia	Skin	4, 6, and 8% (w/v) of FFS	Glycerol, 40% (w/w) of protein	-	0.039, 0.051 and 0.063	3.42, 3.47 and 5.85	53.05, 56.07 and 100.91	55.20, 78.10 and 110.55 [e]	Nur Hanani *et al.* (2012)
Horse Mackerel (*Trachurus japonicus*)	Scale	2% (w/v) of FFS	Glycerol, 20% (w/w) of protein	-	0.022-0.024	13.14-36.48	19.74-46.09	0.98-1.14	Le *et al.* (2015)
Puffer fish	Skin	5% (w/v) of FFS	Sorbitol, 40% (w/w) of protein	*Moringa oleifera* Lam. leaf extract, 0.03, 0.05, 0.07 and 0.1 g/5 g gelatin	-	50.60 - 84.49	18.90 – 65.93	13.8 - 17.0 [d]	Lee *et al.* (2016a)

Table 1. Properties of gelatin-based films from different fish species and sources (cont.)

Fish Species	Sources	Protein Conc.	Plasticizer Conc.	Additive Conc.	Thickness (mm)	Mechanical properties		WVP ($\times 10^{-10}$ g m^{-1} s^{-1} Pa^{-1})	References
						TS MPa)	EAB (%)		
Skate	Skin	5% (w/v) of FFS	Sorbitol, 1.50% (w/w) of protein	Thyme essential oil (0.5 – 1.5%, w/w) of protein	0.051 – 0.075	17.68 – 33.84	153.96 – 274.69	1.84 – 2.17 [g]	Lee *et al.* (2016b)
Olive flounder (*Paralichthys olivaceus*)	Skin	5% (w/v) of FFS	Fructose, 1.5% (w/w) of FFS	-	0.10	31.14	46.69	2.17 [g]	Lee and Song (2017)
Whitemouth croaker	Bone	2% (w/v) of FFS	-	-	0.08	2.4 - 23.2	2.2 – 3.5	3.17 – 4.80 [e]	Bandeira *et al.* (2017)
Whitemouth croaker	Skin	2% (w/v) of FFS	-	-	0.08	2.4 - 23.2	2.2 – 3.5	3.17 – 4.80 [e]	Bandeira *et al.* (2017)
Common carp	Skin	2% (w/v) of FFS	Glycerol, 0.40% (w/w) of protein	-	0.054	17.73	10.52	2.70 [f]	Santos *et al.* (2018)
Nile tilapia	Skin	2% (w/v) of FFS	Glycerol, 0.40% (w/w) of protein	-	0.052	19.52	9.45	2.12 [f]	Santos *et al.* (2018)

[*] FFS= film-forming solution; [a] WVP unit (g mm/m^2 h kPa); [b] WVP unit (10^{-8} g mm h^{-1} cm^{-2} Pa^{-1}); [c] WVP unit (g/m^2/day at 90% RH at 25 °C); [d] WVP unit (10^{-8} g mm/h cm^2 Pa); [e] WVP unit (g mm/ kPa d m^2); [f] WVP unit (10^{-11} g mm h^{-1} cm^{-2} Pa^{-1}); [g] WVP unit (10^{-9} g m/ m^2 s Pa).

1.2.4 Emulsion and emulsion-based film

1.2.4.1 Emulsion system

Emulsion is defined as a system, which consists of two immiscible liquids (usually oil and water). One of the liquids is dispersed as small spherical droplets (dispersed phase) in the other (continuous phase). The process of converting two immiscible liquids into an emulsion is known as *homogenization* (Walstra, 1993). The creation of an emulsion directly from two separate liquids is defined as *primary* homogenization, whereas the reduction in size of the droplets in an already existing emulsion is defined as *secondary* homogenization (McClements, 2005) (**Figure 4**). The separate oil and water phases are firstly converted to a coarse emulsion that contains fairly large droplets using one type of homogenizer (e.g., a high-speed blender), and then the size of the droplets is reduced using another type of homogenizer (e.g., a high-pressure valve homogenizer). Emulsion can be categorized into three main systems including coarse or macroemulsion, microemulsion and nanoemulsion (Burguera and Burguera, 2012). Coarse emulsion has cloudy appearance. The droplet size is typically between 0.5 and 50 μm. The appearance of microemulsions is optically transparent. For a mini- or nanoemulsion, the appearance may be translucent (0.05-0.2 μm) or turbid (up to 0.5 μm), depending upon the droplet size and the refractive index difference between the droplets and the continuous phase (Burguera and Burguera, 2012).

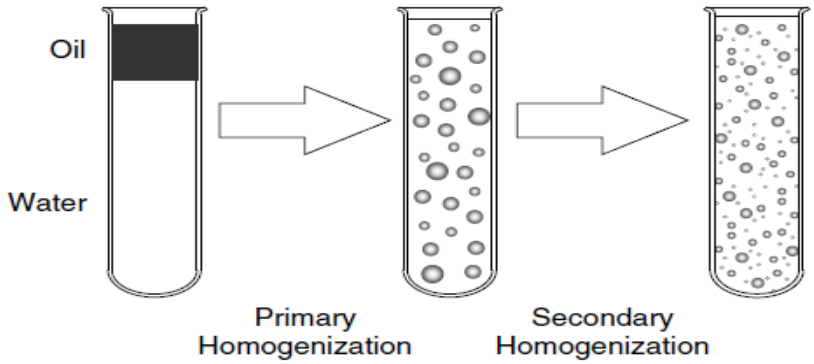

Figure 4. Primary and secondary homogenization.
Source: McClements (2005).

Lipid particle size is determined as the droplet size distribution measured by laser light scattering (McClements, 2005; McHugh and Krochta, 1994a). Volume-surface mean diameter (d_{32}) is widely used to express the volume-surface mean

diameter, which is related to the average surface area of droplets exposed to the continuous phase per unit volume of emulsion. Weighted mean diameter (d_{43}) is another method of expressing the volume-length diameter of a polydisperse emulsion, which is the sum of the volume ratio of droplets in each size-class multiplied by the mid-point diameter of the size-class. d_{43} is more sensitive to the presence of large particles in an emulsion than d_{32}, hence it is often more sensitive to monitor the phenomenon such as flocculation (McClements, 2005).

1.2.4.2 Emulsion-based film

The protein-based films have excellent barrier properties toward oxygen, carbon dioxide and volatile compounds (Limpan *et al.*, 2010). However, protein-based films have poor water vapor barrier property due to their hydrophilicity in nature, thereby limiting the use as potential packaging (Gennadios *et al.*, 1997; Gómez-Guillén *et al.*, 2009). To tackle this problem, the hydrophobic substances such as oil, fatty acid and wax have been incorporated into protein-based film to improve water vapor barrier property and to take advantage of the special functional characteristics of compounds added (Limpisophon *et al.*, 2010; Soazo *et al.*, 2011; Tongnuanchan *et al.*, 2012). To obtain protein-lipid composite films, a lipid can be incorporated into a protein matrix dispersing a lipid in the protein aqueous solution to obtain an emulsified film. The emulsified films exhibiting good water vapor barrier capacity were governed by several parameters such as preparation techniques used (Fabra *et al.*, 2011; Perez-Gago and Krochta, 2001), etc. Emulsified films require only a single step and exhibit good mechanical properties. They also have low water vapor barrier property. In general, water vapor can migrate through the continuous hydrophilic matrix but the dispersed lipid phase increases the tortuosity factor for mass transfer in the matrix (Fabra *et al.*, 2011; Kamper and Fennema, 1984; Quezada Gallo *et al.*, 2000). A decrease of lipid particle sizes was well correlated with the reduction of water vapor permeability (Perez-Gago and Krochta, 2001). Small particles and high emulsion stability during the film drying give rise to a homogeneous distribution of the lipid particles in the film, which in turn contributes to a more efficient control of water transfer (Debeaufort *et al.*, 1993). To reduce lipid droplet size of film-forming emulsion, mechanical devices such as rotor-stator homogenizers, high-pressure homogenizers, microfluidizers, etc. are used.

Those aforementioned equipment generates the intense disruptive forces that breakup the lipid and water phases and finally lead to the formation of tiny lipid droplets before film casting (Qian and McClements, 2011). In general, rotor-stator homogenizer is used to reduce the lipid droplet size in film-forming emulsion. Speed and time of homogenization have the influence on the reduction of lipid droplet size in film-forming emulsion. Fabra *et al.* (2011) reported that the homogenization of sodium caseinate incorporated with oleic acid at 9,500 rpm for 3 min reduced d_{32} and d_{43} values of oleic acid to 22.8 and 37 μm, respectively. However, the rotor-stator homogenizer provides a lower energy input, thus producing the largest particles, which tended to develop pinholes or cracks and exhibited non-uniform surface. Nevertheless, the resulting films formed the bilayer structure and exhibited excellent water barrier ability, but poor mechanical resistance (Park *et al.*, 1996; Quezada Gallo *et al.*, 2000). High-energy approach is capable of generating intense disruptive forces that breakup the oil and water phases. Microfluidization technique utilizes the shearing forces of high-pressure homogenization as well as the severe stress of head-on collision to create a finer particle size emulsion (Keane *et al.*, 2000; Strawbridge *et al.*, 1995). Diagram of microfluidization process is illustrated in **Figure 5**.

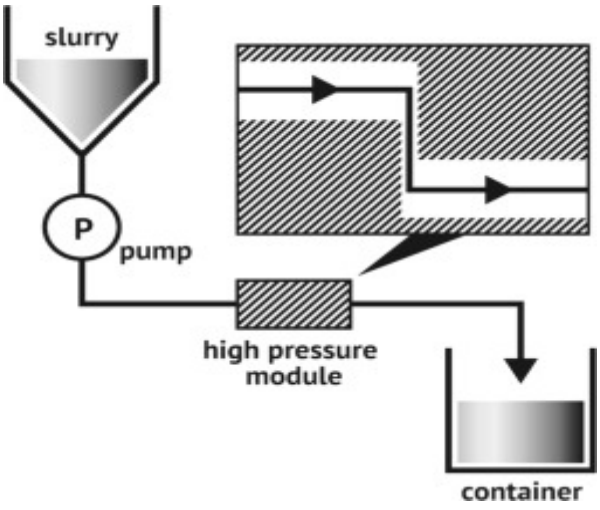

Figure 5. Schematic diagram of microfluidization process.
Source: Kim *et al.* (2015).

Particle size distribution produced by microfluidizers tends to be narrower and smaller than those produced by other homogenization devices (Jafari *et al.*, 2007; Perrier-Cornet *et al.*, 2005; Wooster *et al.*, 2008). The microfluidized lemongrass oil-

loaded nanoemulsions exhibited a dramatic reduction of their average droplet size, down to 5.5±0.3 nm, in comparison with the values of the coarse emulsion (prepared with rotor-stator homogenizer), with the average size of 1120 ± 230 nm (Salvia-Trujillo *et al.*, 2015). Fabra *et al.* (2011) prepared sodium caseinate-based films containing oleic acid by using a rotor-stator and a microfluidizer. When microfluidizer was used at 103.39 MPa for 3 cycle, d_{32} and d_{43} values of film-forming emulsion were 0.236 and 0.402 μm, respectively, which were smaller than those homogenized with a rotor-stator (d_{32} = 22.8 μm; d_{43} = 37 μm). Thus, filmogenic dispersions with narrower particle size distributions promoted better mechanical and water barrier properties of the emulsified films. Ma *et al.* (2012) reported that properties of films prepared from different homogenization techniques (rotor-stator homogenizer at 10,000 for 4 min or microfluidizer at 138 MPa for 3 cycles) were different. TS and EAB of gelatin film (5%, w/w) containing 12.5% olive oil increased from 17.1 MPa (rotor-stator homogenizer) to 23.2 MPa (microfluidizer) and from 39.5% to 106.7%, respectively, while WVP was decreased from $5.6 \times 10^{-10} gs^{-1}m^{-1}Pa^{-1}$ to $3.7 \times 10^{-10} gs^{-1}m^{-1}Pa^{-1}$. It was noted that the microfluidized gelatin–olive oil films exhibited the excellent barrier ability to UV light. The transparency values and surface irregularity of the films were decreased when lipid droplets in the film-forming dispersion (FFD) decreased (Ma *et al.*, 2012).

1.2.5 Poly(lactic) acid (PLA) based film

Lactic acid (2-hydroxy propionic acid), the single monomer of PLA, is produced via fermentation or chemical synthesis (Jamshidian *et al.*, 2010). Fermentation has been used for industrial lactic acid production rather than synthesis due to higher capacity and lower manufacturing costs (Datta and Henry, 2006). PLA has a wide range of molecular weight and only high molecular weight one (Figure 6) is used in the packaging industry. There are three possible ways for the polymerization of lactic acid; (a) direct condensation polymerization; (b) direct polycondensation in an azeotropic solution and (c) polymerization through lactide formation (Jamshidian *et al.*, 2010). Among those processes, polymerization through lactide formation is industrially accomplished for PLA production. Lactide is a cyclic dimer formed by removing water under mild conditions without solvent (Jamshidian *et al.*, 2010).

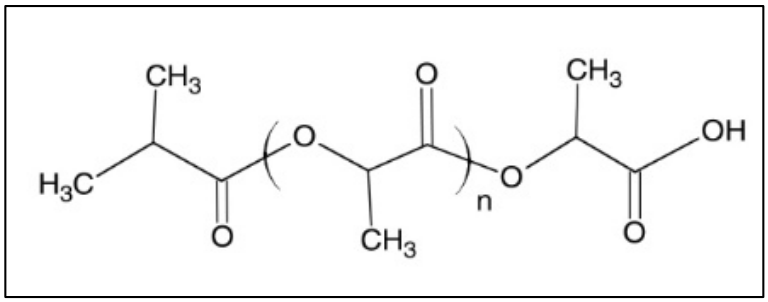

Figure 6. Structural illustration of high molecular weight PLA.
Source: Modified from Jamshidian *et al.* (2010).

PLA, classified as GRAS (Generally Recognized as Safe), is allowed for using as food contact (Conn *et al.*, 1995). As a food packaging, PLA films has been produced by various techniques: injection molding, thermoforming and film casting (Lim *et al.*, 2008). PLA film has good optical, physical, mechanical, and barrier properties, compared to some existing petroleum-based polymers (Auras *et al.*, 2003). To improve properties of PLA film, the different methods have been applied such as using modifier, blending and adding the selected additives (Jamshidian *et al.*, 2010). Sung *et al.* (2017) reported that bio-nanocomposite films based on PLA matrix reinforced with cellulose nanocrystals (CNCs) at different concentrations (1%, 3%, and 5% w/w) had the increases in tensile strength (3% and 10%) and Young's modulus (15% and 22%) along with the decreasing water vapor permeability (20% and 31%) when CNCs at 1% and 3% were incorporated. All composite films based on PLA and CNCs had good oxygen barrier properties (87.1-120.9 cc·μm/m^2·day·kPa) (Sung *et al.*, 2017). To solve inherent problem of brittleness, the monomeric and oligomeric plasticizers were added into PLA film. Ljungberg and Wesslén (2005) found that the incorporation of tributyl citrate and diethyl bishydroxymethyl malonate at level of 17.6% (w/w) drastically decreased the *T*g of PLA from 52 °C to 25-29 °C, which attributed to the increased of flexibility of resulting film. Xiong *et al.* (2010) reported that the blending of PLA with soluble egg shell membrane can improve mechanical property of the films. The PLA/SEP (9:1, w/w) film had good mechanical (22.4-32.9 MPa) property, and was much better than SEP film (Xiong *et al.*, 2010).

PLA films can be added with bioactive compounds and became active. Green tea extract (GTE) with DPPH radical capacity (EC50 = 0.12 ± 0.00 mg/mL) and the

highest TPC (416 ± 9.95 mg gallic acid equivalents (GAE)/g extract), at concentration of 1% and 2% (w/w) was immobilized into PLA film (Martins *et al.*, 2018). The incorporation of GTE in the PLA films protected the smoked salmon from lipid oxidation as indicated by lower increases in peroxide value, *p*-anisidine value, thiobarbituric acid reactive substances (TBARS) and hexanal content during the storage of 60 days at 5 °C (Martins *et al.*, 2018).

1.2.6 Bilayer film

Bilayer film combine materials with different properties in order to improve film functional properties (Kurek *et al.*, 2014). It consists of a second distinguishable layer film laminated over a preformed hydrocolloids film (Slavutsky and Bertuzzi, 2016). The bilayer films exhibiting good properties are governed by several parameters such as preparation techniques used, types of material and layer thickness ratios (Cho *et al.*, 2010; Valencia-Sullca *et al.*, 2018). The preparation method used depends on the characteristics of film components and the desired structure and properties of the resulting film. Casting is a general method to produce bilayer film, in which two steps of casting are employed. The first solution was poured and dried to form the first layer film. Consequently, the second film-forming solution was overlaid onto the formed film to obtain the resulting bilayer film (Slavutsky and Bertuzzi, 2016).

Recently, various materials have been utilized to form bilayer films as shown in Table 2. Generally, the different bilayer films such as olive flounder skin gelatin/PLA (Lee and Song, 2017), SPI/corn zein (Cho *et al.*, 2010), chitosan/whey protein (Kurek *et al.*, 2014), fish gelatin/agar (Vejdan *et al.*, 2016) and polyvinyl alcohol/chitosan (Zhuang *et al.*, 2018), have been formed by casting method. Nevertheless, it also can be produced via themocompression method such as chitosan incorporated without and with oregano essential oil laminated with starch (Valencia-Sullca *et al.*, 2018). The mechanical and barrier properties are mainly improved in the resulting bilayer films. Increased in tensile strength (TS) (from 31.14 to 37.56 MPa) and decreased in water vapor permeability (WVP) (from 2.17 to 0.92 × 10^{-9} g·m/m^2·s·Pa) were observed for bilayer film prepared from olive flounder skin gelatin film (5% w/v) laminated with PLA (7% w/v) (Lee and Song, 2017). Cho *et al.* (2010) documented that TS of bilayer film prepared from 5% (w/v) soy protein isolate (SPI) laminated with 6.67% (w/v) corn

zein (CZ) was 5.9 MPa, which was higher than TS obtained from monolayer SPI film (2.5 MPa). WVP of SPI film was lowered from 0.94 to 0.61 $\times 10^{-12}$·kg·m/m^2·s·Pa when CZ was laminated (Cho *et al.*, 2010). Arabestani *et al.* (2016) also documented that the bilayer film prepared from 5% (w/v) bitter vetch seed protein concentrated (BVPC) containing 50% (w/w) glycerol laminated with 6.67% (w/v) corn zein containing 1.67% PEG-400 had higher TS (18.03 MPa) than the monolayer BVPC film (5.04 MPa). Corn zein has a high hydrophobic amino acid content and produces films with lower water vapor permeability and higher tensile strength in comparison with other protein-based films (Cho *et al.*, 2010; Ghanbarzadeh and Oromiehi, 2009). Furthermore, bilayer film also can prepared by thermocompression. Valencia-Sullca *et al.* (2018) reported that cassava starch (CS)/chitosan bilayer film obtained by compressing CS film and chitosan film at 100 °C for 2 min by means of the hot-plates hydraulic press exhibited the lower WVP (7.3 g·mm/m^2·h·kPa) and higher TS (20 MPa) than starch monolayer film (WVP: 9.38 g·mm/m^2·h·kPa; TS: 17.3 MPa). However, the thermal treatment applied to obtain bilayer reduced their antimicrobial properties (total aerobial and coliform microorganisms) as compared to chitosan. This was probably due to the activity losses occurred during film processing (Valencia-Sullca *et al.*, 2018). Additionally, the thickness ratios of both layers had a marked effect on the mechanical and barrier properties (Kurek *et al.*, 2014). Bilayer film based on chitosan (CS) and whey protein (WP) at different CS:WP thickness ratios (20:60, 40:40 and 60:20 µm) showed different TS and WVP. When a thicker chitosan layer (40 and 60 µm) was used, higher TS (17.50 and 15.30 MPa) were obtained for bilayer film, while the lower TS (5.80 MPa) was noted when a CS:WP at ratio of 20:60 was used, compared to CS film (8.90 MPa). All CS/WP bilayer film exhibited lower WVP values (0.79-1.74 $\times 10^{-10}$·g/m·s·Pa) than CS film (2.37 $\times 10^{-10}$·g/m·s·Pa) (Kurek *et al.*, 2014). This was noted that the increasing chitosan content yielded the stronger chitosan/whey protein bilayer films (Kurek *et al.*, 2014). Therefore, the mechanical and barrier properties of bilayer film are influenced by various factors including preparation technique, types of materials used and layer thickness ratios.

Table 2 Bilayer film from various material sources.

Bilayer film		TS (MPa)	EAB (%)	WVP	OP	References
Alginate	Chitosan	0.96 ± 0.22	16.62 ± 4.18	6.31 ± 0.7 [a]	-	Reyes-Avalos *et al.* (2016)
Chitosan	Cassava starch	20 ± 2	2.28 ± 0.14	7.3 ± 0.6 [b]	0.097 ± 0.003 [1]	Valencia-Sullca *et al.* (2018)
Chitosan	Whey protein	5.80 - 17.50	1.44 - 35.70	0.79 - 1.74 [c]	-	Kurek *et al.* (2014)
Bitter vetch seed protein	corn zein	18.03 ± 0.95	3.54 ± 0.59	0.55 ± 0.03 [d]	-	Arabestani *et al.* (2016)
Corn zein	Soy protein isolate	5.9 ± 0.4	7.3 ± 2.0	0.61 ± 0.05 [e]	0.81 ± 0.05 [2]	Cho *et al.* (2010)
Gelatin	Agar	10.80 ± 0.46	48.17 ± 1.75	3.26 ± 10 [f]	-	Vejdan *et al.* (2016)
Poly(lactic) acid	Gliadin	11.46 - 21.21	114.72 - 151.6	1.91 - 4.23 [g]	0.86 - 8.33 [3]	Zhu *et al.* (2017)
Polyvinyl alcohol	Chitosan	14.16 ± 1.62	111.47 ± 1.10	188.07 ± 14.56 [h]	-	Zhuang *et al.* (2018)

TS: Tensile strength; EAB: Elongation at break; WVP: Water vapor permeability; OP: Oxygen permeability. [a] WVP unit (× 10^{-12} g m^{-1} h^{-1} Pa^{-1}); [b] WVP unit (g mm kPa^{-1} h^{-1} m^{-2}); [c] WVP unit (×$10^{-10}$$gm^{-1}$ s^{-1} Pa^{-1}); [d] WVP unit (gmm/mhKPa); [e] WVP unit (×10^{-12} kg m/m^2 s Pa); [f] WVP unit (×10 g/m^2 s Pa); [g] WVP unit (×10^6 g m m^{-2} 24h Pa); [h] WVP unit (g mm m^{-2} d^{-1} kPa^{-1}). [1] OP unit (× 10^{-13} cm^3 $m^{-1}s^{-1}$ Pa^{-1}); [2] OP unit (×10^{-18} m^3 m/m^2 s Pa); [3] OP unit (×10^{15} cm^3 cm cm^{-2} s Pa).

1.2.7 Antioxidantive compounds and antioxidant films

1.2.7.1 Antioxidative compounds

Antioxidants are a group of chemicals effective in extending the shelf-life of a wide variety of food products via their inhibition of lipid oxidation. The use of antioxidants was extended to a wide variety of food products including high-fat foods, cereal and even products containing very low levels of lipids. The addition of antioxidants is one effective way to retard lipid oxidation. The most widely used antioxidants include free radical scavengers (also known as chain-breaking antioxidants) that inactivate free radicals formed in the initiation and propagation steps of lipid oxidation, and metal chelators (Shahidi and Zhong, 2010). Lipid peroxidation is a free-radical chain reaction that causes a total change in the sensory properties and nutritive value of food products (Rajapakse *et al.*, 2005). Decomposition of hydroperoxides by heating or by transition metal ion catalysis can produce both peroxyl and alkoxyl radicals. The formation of peroxyl radical is the major chain-propagation step in lipid peroxidation (Headlam and Davies, 2003). In bulk lipids, hydrophilic antioxidants locate preferentially at the oil-air interface and better protect the lipid from oxidation. In O/W emulsions, lipophilic antioxidants concentrate at the oil-water interface and inhibit lipid oxidation more effectively than hydrophilic antioxidants that partition into the water phase (Atarés *et al.*, 2012).

1.2.7.2 Classification of food antioxidants

Antioxidants counteract the oxidation in two different ways, by protecting target lipids from oxidation initiators or by stalling the propagation phase. Antioxidants can be broadly classified by the mechanism of action as primary antioxidants (chain breaking antioxidants) and secondary antioxidants (preventive antioxidants) (Sun *et al.*, 2011).

1.2.7.2.1 Primary antioxidants

Primary antioxidants or chain-breaking antioxidants are free radical acceptors that delay or inhibit the initiation step or interrupt the propagation step of autoxidation through reaction with lipid and peroxy radicals and convert them to more stable, non-radical products (Gil, 2011). Primary antioxidants are most effective if they are added during the induction and initiation stages of oxidation when the propagation steps have

not occurred. The most commonly used primary antioxidants in foods are synthetic compounds such as phenolic antioxidants including butylated hydroxyanisole (BHA), butylated hydroxytoluene (BHT), propyl gallate (PG), and tertiary butylhydroquinone (TBHQ) (Sun *et al.*, 2011). However, a few natural primary antioxidants such as tocopherols, flavonoids, as well as carotenoids are used in foods and products (Sun *et al.*, 2011). The activity of phenolic antioxidants is often lost at high concentrations and they may become prooxidative (Sun *et al.*, 2011). Different plant phenolics showed varying antioxidant activity, depending on their structure (Woong *et al.*, 2018). Maqsood and Benjakul (2010) documented that tannic acid showed higher antioxidant activity than catechin, caffeic acid and ferulic acid; when assayed using DPPH, ABTS radical scavenging activities and ferric reducing antioxidant power (FRAP). Catechin showed the highest metal chelating activity, whereas caffeic acid had the highest lipoxygenase (LOX) inhibitory activity (Maqsood and Benjakul, 2010). Yu *et al.* (2017) noted that among different phenolic compounds purified from *Stevia rebaudiana* stem (SRS) waste extract, chlorogenic acid and cryptochlorogenic acid each showed significantly higher DPPH radical scavenging activity than sodium L-ascorbate (SA). However, protocatechuic acid, chlorogenic acid, cryptochlorogenic acid and caffeic acid showed higher ORAC than SA (Yu *et al.*, 2017). Carotenoids belong to the most common auxiliary antioxidants. They are thought to be singlet oxygen quenchers and also react with chain-carrying peroxy radicals or alkyl-radical intermediates (Matsushita *et al.*, 2000).

1.2.7.2.2 Secondary antioxidants

Secondary antioxidants or preventive antioxidants act through numerous possible mechanisms other than converting free radicals to more stable products to slow the rate of oxidation. They can hinder reactive oxygen species (ROS) formation or scavenge species responsible for oxidation initiation (O^{-2}, $^1O_2$, etc.) (Sun *et al.*, 2011). There are many different preventive antioxidation pathways including chelation of transition metals, singlet oxygen deactivation, enzymatic ROS detoxification, UV filtration, inhibition of proxidant enzymes, antioxidant enzyme cofactors, etc (Laguerre et al., 2007). Moreover, they can replenish hydrogen to primary antioxidants, decompose hydroperoxides to nonradical species and act as oxygen scavengers, and

also act as reducing agent (Akoh, 2017). Because these secondary antioxidants can enhance the antioxidant activity of primary antioxidants, they are also called synergists. The commonly used secondary antioxidants are citric acid, ascorbic acid, ascorbyl palmitate, lecithin, and tartaric acid (Eitenmiller and Lee, 2004).

1.2.7.3 Types of antioxidants

1.2.7.3.1 Synthetic antioxidants

Synthetic antioxidants commonly used in foods include sodium erythorbate, sodium ascorbate, BHA, BHT, TBHQ, PG, nitrite (NO_2) and nitrate (NO_3) (Valencia *et al.*, 2007). However, the use of these synthetic antioxidants is negatively perceived by consumer due to potential toxicity and their connotation as chemicals in food (Georgantelis *et al.*, 2007). Synthetic antioxidants have varying activity, depending on the ability to scavenge radicals, etc. Sun and Ho (2005) tested various compounds using the DPPH radical scavenging assay and found that BHT and TBHQ (0.1-1.0 mg/ml) had similar free radical scavenging activities. However, TBHQ had a higher free radical scavenging capacity than BHT (Devi and Arumughan, 2007). The number of hydroxyl groups on an aromatic ring is the major factor contributing to the efficacy of phenolic antioxidants (Chen *et al.*, 1996). This may explain the higher activity of TBHQ (a diphenolic antioxidant) compared to that of BHT, a monophenolic antioxidant (Devi and Arumughan, 2007).

1.2.7.3.2 Natural antioxidants

The demand for using natural antioxidants has been increased due to the potential hazardous effects of synthetic counterparts. Natural antioxidants have fascinated an immense deal of interest because of their health effects and positive image against degenerative diseases and certain cancers (Iqbal and Bhanger, 2007). In addition, a list of artificial compounds on food product labels seems incompatible with functional or organic claims. Based on this, food companies are trying to replace artificial additives with natural compounds, thus conferring a healthier image to their products (Botsoglou *et al.*, 2002). However, very few antioxidants from natural sources have reached the market due to problems associated with regulatory issues, among others (Embuscado and Shahidi, 2015). The antioxidant potency of the natural antioxidant or phenolic compounds, is dictated by their structural characteristics as well

as the medium, in which they are used. Polar antioxidants are generally more effective in bulk oil while nonpolar antioxidants are superior in their action in oil-in-water emulsions, as explained by polar paradox theory (Embuscado and Shahidi, 2015). The antioxidant activity of phenolic acids and their esters depends on the number of hydroxyl groups in the molecule, and this would be strengthened by steric hindrance (Naczk and Shahidi, 2004). Hydroxylated cinnamic acids with extended conjugation are more effective than their corresponding benzoic acid counterparts. Furthermore, the special arrangement of hydroxyl groups or hydroxyl and keto groups, such as 3-hydroxy-4-keto group and/or 5-hydroxy-4-keto group (when the A-ring is hydroxylated at the 5th position) in flavonols, allows chelation of prooxidant metal ions. An o-quinol group at the B-ring also demonstrates metal chelating activity (Pratt and Hudson, 1990). Hence, the antioxidant efficacies can be rendered by one or more mechanisms. Reducing power of phenolics is another mechanism.

1.2.7.3.3 Epigallocatechin gallate (EGCG)

Epigallocatechin gallate (EGCG) is one of major flavanols obtained from tea extract, which contains 10-60% of EGCG (dry weight) (Zaveri, 2006). It has trihydroxyl group in the B ring at carbons 3′, 4′, and 5′, and a gallate moiety esterified at carbon 3 of the C ring (Graham, 1992) (Figure 7).

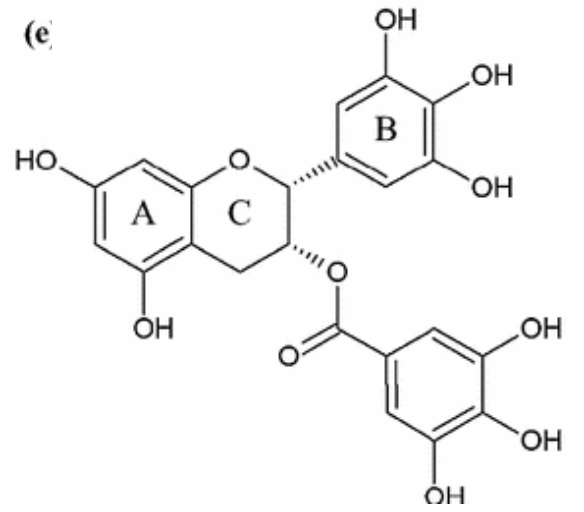

Figure 7. Chemical structures of epigallocatechin gallate.

Source: Modified from Sae-leaw *et al.* (2017).

EGCG has been reported to exhibit antioxidant activity and play a role in preventing the lipid oxidation in foods (Lu *et al.*, 2010). Refined, bleached and

deodorized seal blubber oil and menhaden oil treated with tea catechins (epicatechin (EC), (-)epigallocatechin (EGC), (-)epicatechin gallate (ECG) and (-)epigallocatechin gallate) at 200 ppm showed excellent oxidative stability (peroxide value, conjugated diene, and TBARS) as compared with samples that contained commonly used antioxidants such as α-tocopherol, BHA, BHT, and TBHQ (Wanasundara and Shahidi, 1996). The potential of catechins in prevention of oxidation of marine oils was in the decreasing order: ECG > EGCG > EGC > EC (Wanasundara and Shahidi, 1996). Moreover, EGCG showed a synergistic effect on oxidative stability with other components in emulsions. Almajano *et al.* (2007) reported that EGCG (0.5 mM) and ovalbumin (0.2%) showed the longest times for refined sunflower oil-in-water emulsions stored at 50 °C to reach PV = 40 meq/kg. The emulsion containing EGCG and ovalbumin also had the lowest concentration of hexanal at 37 days (Almajano *et al.*, 2007). Furthermore, EGCG is the most effective cancer chemopreventive. Du *et al.* (2012) documented that EGCG showed the most potent antiproliferative effects on the HCT-116 and SW-480 human colorectal cancer cells when evaluated using an MTS assay, compared to other polyphenols (caffeic acid, gallic acid, catechin, epicatechin, gallocatechin, catechin gallate, gallocatechin gallate, epicatechin gallate and epigallocatechin). The significant induced cell cycle arrest in the G1 phase and apoptosis were observed for cell after being treated with EGCG (Du *et al.*, 2012). Addionally, green tea catechins and EGCG were shown to ameliorate diabetes and to improve metabolic phenotype in rodent models of diabetes (Franko *et al.*, 2018). Yan *et al.* (2012) reported that green tea catechins (GTCs) significantly decreased glucose levels and ROS content as well as increased glucose tolerance in obese KK-ay mice and high-fat diet-induced obese rats. EGCG attenuated dexamethasone and TNF-α promoted ROS generation and increased glucose uptake ability (Yan *et al.*, 2012). Therefore, EGCG has a wide range of bioactivity.

1.2.7.4 Influence of antioxidants on lipid oxidation in bulk lipid and food emulsion

1.2.7.4.1 Use of antioxidant in bulk lipid

The effectiveness of antioxidants depends on several factors such as the polarity of the antioxidants, lipid substrate, pH, temperature, concentration of antioxidants, and

the physical properties of the food (Huang *et al.*, 1997). Nonpolar antioxidants are gradually localized in the lipid phase of o/w emulsions. Polar antioxidants to have a higher affinity toward the air-oil interface or reverse micelles, and thus they are able to concentrate on oil-air interfaces where oxidative reaction takes place (Sun *et al.*, 2011). An antioxidant added to food must be effective at low concentrations (Sun *et al.*, 2011). A combination of antioxidants is used to obtain a synergistic effect. In a food product, a synergy is obtained by combining the added and inherent antioxidants. However, the behavior of antioxidants in food and their antioxidative ability can vary markedly, depending on the lipid-containing systems (Sikorski and Kolakowska, 2010). Food products are predominantly multiphase systems. One of the most effective ways of inhibiting lipid oxidation in bulk lipid is to incorporate antioxidants (Decker *et al.*, 2005). Hydrophilic antioxidants (Trolox or ascorbic acid) possess better antioxidant activity than their hydrophobic analogues (tocopherol and ascorbyl palmitate) in some bulk lipid systems (Huang *et al.*, 1996). The greater tendency for hydrophilic antioxidants to accumulate at the air–water interface where oxidation may be expected to begin is one of the mechanisms proposed to account for their better antioxidant activity in bulk lipid (Huang *et al.*, 1996). However, other mechanisms have also been proposed to account for the ability of hydrophilic antioxidants to act as better antioxidants than their hydrophobic analogs in bulk lipid (Vaisali *et al.*, 2017). Air is more hydrophobic than lipid and thus there is no driving force to concentrate hydrophilic antioxidants at the oil-air interface (Chaiyasit *et al.*, 2007). In bulk menhaden lipid, BHT was a more effective antioxidant than 4-hydroxymethyl-2,6-ditertiarybutylphenol, while α-tocopherol was more effective than δ-tocopherol (Chaiyasit *et al.*, 2005). The fractionated polyphenols from both dried and frozen apple peel showed higher inhibition of lipid oxidation, compared to α-tocopherol, BHT and crude apple peel extracts (Sekhon-Loodu *et al.*, 2013).

1.2.7.4.2 Use of antioxidant in food emulsion

In oil-in-water (O/W) emulsion, chelating agents can inhibit lipid oxidation by decreasing metal reactivity or by physically partitioning the metal away from the lipid. Cho *et al.* (2006) found that chelating agents in the aqueous phase of an O/W emulsion could facilitate the transfer of iron out of the lipid droplets. EDTA has been shown to

remove iron from the surface emulsions droplets. Overall, EDTA was found to be more effective in preventing lipid oxidation in O/W emulsions than sodium tripolyphosphate and citric acid (Hu *et al.*, 2004). Hu *et al.* (2004) indicated that the oxidative stability of whey protein isolate stabilized o/w emulsion could be increased by EDTA without having any impact on physical stability. Phenolic compound also can improve stability of O/W by act as a radical scavenging to donate a hydrogen atom to free radicals, thereby terminating chain reaction (Gülçin, 2006). Menhaden oil-in-water emulsions stabilized by *p*-hydroxyphenylacetic acid (HPA) (5 mM) had lower lipid hydroperoxides and thiobarbituric acid reactive substances, compared to that without HPA (Yuji *et al.*, 2007). In addition, the synergistic effect was observed for caffeic acid and bovine serum albumin (BSA) in retarding oxidation of sunflower oil/water emulsions. This O/W emulsion sample took 8.19 days to reach a total oxidation (TOTOX) of 3.7, while the O/W emulsion containing caffeic acid (5 mmol/kg emulsion) and BSA (0.2%) reached the same value at 42 days during storage at 50 °C (Conde *et al.*, 2011). Nevertheless, the surface activity of antioxidants could be increased by modification of phenolic compound with hydrocarbon chains (Yuji *et al.*, 2007). Emulsions containing rosmarinate with 4 and 8 alkyl esters showed lower lipid hydroperoxides and headspace volatiles than those without rosmarinate and those with 0, 12, 18, and 20 alkyl esters (Lee *et al.*, 2012). This was noted that modified phenolic with proper hydrocarbon chain length is mainly located on the interface, thus providing a high antioxidant activity toward lipid radicals (Lee *et al.*, 2012).

1.2.7.5 Antioxidant films

Consumer concerns of food quality and safety lead to the development of active packaging, which is innovative packaging possessing some functions, particularly for shelf-life extension of food products (Kaewprachu *et al.*, 2015). Active compounds can be incorporated into packaging materials to provide antioxidant and/or antimicrobial agents (Kaewprachu *et al.*, 2015). Among all biomaterials, gelatin is a proteinacious material and has several advantages, which can be incorporated with several active compounds with various activities. Among active substances, phenolic compounds or plant extracts have been incorporated into fish gelatin-based film to improve the properties (Etxabide *et al.*, 2017b) (Table 4). Ferulic acid and caffeic acid at different

concentrations (1-5%, w/v) were added into cold fish gelatin film. Caffeic acid (5%) could lower solubility, oxygen permeability and water vapor permeability of the film (Araghi *et al.*, 2015). Limpisophon and Schleining (2017) reported that the addition of gallic acid (0.05-0.15%, w/w of FFS) increased the tensile strength, elongation at break and UV barrier property of cold water fish skin gelatin film. Apart from acting as protein cross-linkers, those phenolic compounds could serve as antioxidant, making the film more active (Gómez-Estaca *et al.*, 2009a; Maryam Adilah *et al.*, 2018). Antioxidant power is generally governed by types and concentrations of antioxidant used. Gómez-Estaca *et al.* (2009a) reported that ferric-reducing antioxidant power and ABTS radical-scavenging capacity of tuna skin gelatin film containing oregano extract (1.25%, w/v) were higher than those of films containing rosemary extract (2.5 and 20%, w/v). The antioxidant capacity of fish gelatin film was generally governed by types and concentrations of antioxidants used. Silver crap skin gelatin films added with high amount of green tea extract (0.7%, w/v) showed the increased total phenolic content (39.05 mg gallic acid/g film) and DPPH radical scavenging activity (31.4%) (Wu *et al.*, 2013). Li *et al.* (2014) also reported that DPPH radical scavenging activity of silver carp skin gelatin films was increased when the concentration of natural extracts (green tea extract, proanthocyanidins, grape seed polyphenols, ginger extract and gingko leaf extract) was increased from 0.001 to 0.1% (w/v). Moreover, the DPPH scavenging capacity of films was decreased to a certain degree when the concentration of natural extracts was increased up to 0.5% (w/v) (Li *et al.*, 2014). High quantity of extracts in films can form aggregation. As a result, compatibility of gelatin and natural extracts became less (Shen *et al.*, 2011). Furthermore, EGCG also has been reported to exhibit antioxidant activity and play a role in preventing the lipid oxidation in foods (Lu *et al.*, 2010; Wang *et al.*, 2019). Due to its antioxidative activity with safety concern, it can be employed as natural antioxidant in packaging, particularly gelatin-based films. Films could serve as carrier for control release of active components. Etxabide *et al.* (2017a) reported that the release of curcumin derivatives from gelatin films. It was possible to deliver the curcumin over an extended period of time due to the controlled release from gelatin films. The antioxidant activity of Atlantic Bluefin tuna (*Thunnus thynnus*) gelatin films was significantly enhanced when brown algae *(Cystoseira barbata)*

Table 3 Fish gelatin film incorporated with various natural antioxidants.

Antioxidants	Concentration	References
Gallic acid	0.05, 0.10 and 0.15%(w/v)	Limpisophon and Schleining (2017)
Moringa oleifera Lam. leaf extract	0.6, 1.0, 1.4 and 2% (based on gelatin)	Lee *et al.* (2016a)
Ferulic acid and caffeic acid	0, 1, 3, and 5%(w/v)	Araghi *et al.* (2015)
Coconut husk ethanolic extract	0.05 and 0.4% (w/w, based on protein)	Nagarajan *et al.* (2015)
Green tea extract, proanthocyanidins, grape seed polyphenols, ginger extract and gingko leaf extract	0.001, 0.1 and 0.5% (w/v)	Li *et al.* (2014)
Green tea extract	0.3 and 0.7% (w/v)	Wu *et al.* (2013)
Brown algae *(Cystoseira barbata)* extract	5% (based on gelatin)	Haddar *et al.* (2012)
Oregano and rosemary extracts	0.3-1.25 and 2.5-20% (w/v) respectively	Gómez-Estaca *et al.* (2009a)
Seaweed (*Turbinaria ornata*) extract	6% (w/w, based on protein)	Rattaya *et al.* (2009)
Murta leaves extract	3.75 g/g gelatin	Gómez-Guillén *et al.* (2007)

seaweed extract was added. This was directly governed by phenolic and flavonoids compounds present in this extract (Haddar *et al.*, 2012). The level of 5% (based on gelatin) rendered the film with highest antioxidant activity.

1.2.7.6 Application of antioxidant film as food packaging

Lipid oxidation is one of the most important mechanisms in food deterioration. It leads to a reduction in shelf-life due to the changes in taste and/or odor as well as the texture. Furthermore, functionality of muscle foods and nutritional quality are also reduced (Pereira de Abreu *et al.*, 2010). The radicals, mainly hydroxyl and superoxide originated from oxygen, are the main initiators of lipid oxidation (Nerín *et al.*, 2008). To avoid the formation of radicals or eliminating prooxidants, different active substances with different mechanisms have been incorporated into packaging, in which active packaging possessing free radical scavengers, metal chelators, ultraviolet (UV) absorbers, oxygen scavengers, and singlet oxygen quenchers can be prepared and used for prolonging the shelf-life of foods (Tian *et al.*, 2013; Yildirim *et al.*, 2017). Such packaging is intended to prevent or slow down the oxidation reactions that affect the quality of food (Vejdan *et al.*, 2016). Antioxidants can also be immobilized on the polymeric surface, exerting their activity by direct contact with the food product without mass transfer. Since the agent does not migrate, its activity is limited to the contact surface only (Gómez-Estaca *et al.*, 2014). In solid or semi-solid foods, the activity is limited to the area of contact between the packaging system and the food, and therefore these systems have found applications in vacuum packaging and/or the manufacture of slide separators (Gómez-Estaca *et al.*, 2014). In this context, the antioxidant film for food applications has been developed. Generally, synthetic antioxidants, such as butylated hydroxytoluene (BHT) and butylated hydroxyanisole (BHA) have been used in food packaging to prevent lipid oxidation. Torres-Arreola *et al.* (2007) reported a delay in lipid oxidation and protein denaturation in fresh sierra fish fillets through the incorporation of BHT into LDPE packaging. Compared to LDPE films, samples packed in BHT-LDPE films demonstrated lower lipid oxidation, expressed as thiobarbituric acid-reactive substances (TBARS) values (4.20 ± 0.52 mg), compared to 11.95 ±1.06 mg malonaldehyde (MDA)/kg), peroxide index values (7.20 ± 1.38 meq/kg, compared with 15.15 ±1.48 meq/kg), and free fatty acid contents (7.98

± 0.43, compared with 11.83 ± 1.26 of oleic acid) (Torres-Arreola *et al.*, 2007). Jongjareonrak *et al.* (2008) documented that bigeye snapper skin gelatin film and brownstripe red snapper skin gelatin film incorporated without and with BHT or α-tocopherol (200 ppm) showed a preventive effect on lard oxidation as evidenced by the retardation of thiobarbituric acid reactive substances (TBARS) and peroxide formation. Moreover, being natural products, both pure phenolic compounds and plant polyphenolic extracts, have been increasingly preferred over synthetic antioxidants for the reasons of being nontoxic and posing no health concerns (Maqsood *et al.*, 2014). The incorporation of phenolic compound could therefore provide antioxidant activity for resulting films (Maqsood *et al.*, 2014). Colín-Chávez *et al.* (2012) compared the efficiency of different pouches made from four different films (a monolayer low-density polyethylene (LDPE) film added with 2.90% of marigold (*Tagetes erecta*) extract; a two-layer high-density polyethylene/LDPE film added with 3.59% of the extract in the LDPE layer and the corresponding two control films without addition of the extract) on soybean oil stability. PV increased from 1.78±0.29 mEq/kg to 49.97±4.87 mEq/kg (LDPE without extract film), 41.28±1.64 mEq/kg (LDPE with 2.9% extract film), 46.97±1.49 mEq/kg (HDPE/LDPE film without extract) and 39.96±0.94 mEq/kg (HDPE/LDPE film with 3.59% extract) after 16 days of storage at 30 °C (Colín-Chávez *et al.*, 2012). The sealable LDPE films containing 1.9% and 3% of α-tocopherol maintained the oxidation stability (hexanal content) of corn oil for 16 weeks at 30 °C, compared to 12 weeks for the oil in a control bag (without antioxidant) (Graciano-Verdugo *et al.*, 2010). Manzanarez-López *et al.* (2011) reported that PLA films containing 2.58% α-tocopherol (PT2.5 film) were also able to delay the induction of the oxidation, compared to PLA film without α-tocopherol (PT0 film). The maximum peroxide values (PV) of soybean oil contact with PT0 film for 15 days at 20, 30 and 40 °C were 19.5, 27.5 and 33.9 meq/kg, respectively. Nevertheless, the maximal PV as 9.9, <10 and 13.5 meq/kg was observed for soybean oil contact with PT2.5 film at same storage time. Thus, the incorporation of antioxidants into films could be a means to being about active packaging, especially for food storage. As a consequence, active components could be released during the storage, thus extending the shelf-life of packaging foods.

References

Ahmad, M., Benjakul, S., Prodpran, T. and Agustini, T. W. 2012a. Physico-mechanical and antimicrobial properties of gelatin film from the skin of unicorn leatherjacket incorporated with essential oils. Food Hydrocolloid. 28: 189-199.

Ahmad, M., Benjakul, S., Sumpavapol, P. and Nirmal, N. P. 2012b. Quality changes of sea bass slices wrapped with gelatin film incorporated with lemongrass essential oil. Int. J. Food Microbiol. 155: 171-178.

Akoh, C. C. 2017. Food lipids: chemistry, nutrition, and biotechnology. CRC press.

Almajano, M. P., Delgado, M. E. and Gordon, M. H. 2007. Albumin causes a synergistic increase in the antioxidant activity of green tea catechins in oil-in-water emulsions. Food Chem. 102: 1375-1382.

Andreuccetti, C., Carvalho, R. A. and Grosso, C. R. F. 2009. Effect of hydrophobic plasticizers on functional properties of gelatin-based films. Food Res. Int. 42: 1113-1121.

Arabestani, A., Kadivar, M., Amoresano, A., Illiano, A., Di Pierro, P. and Porta, R. 2016. Bitter vetch (*Vicia ervilia*) seed protein concentrate as possible source for production of bilayered films and biodegradable containers. Food Hydrocolloid. 60: 232-242.

Araghi, M., Moslehi, Z., Mohammadi Nafchi, A., Mostahsan, A., Salamat, N. and Daraei Garmakhany, A. 2015. Cold water fish gelatin modification by a natural phenolic cross-linker (ferulic acid and caffeic acid). Food Sci. Nutr. 3: 370-375.

Atarés, L., Marshall, L. J., Akhtar, M. and Murray, B. S. 2012. Structure and oxidative stability of oil in water emulsions as affected by rutin and homogenization procedure. Food Chem. 134: 1418-1424.

Auras, R. A., Harte, B., Selke, S. and Hernandez, R. 2003. Mechanical, physical, and barrier properties of poly(lactide) films. J. Plast. Film Sheet. 19: 123-135.

Bandeira, S. F., Silva, R. S. G., Moura, J. M. and Pinto, L. A. A. 2017. Characterization and film-forming properties of gelatins from whitemouth croaker (*Micropogonias furnieri*) skin and bones. J. Aquat. Food Prod. Technol. 26: 447-456.

Banerjee, R., Chen, H. and Wu, J. 1996. Milk protein-based edible film mechanical strength changes due to ultrasound process. J. Food Sci. 61: 824-828.

Benjakul, S., Artharn, A. and Prodpran, T. 2008. Properties of protein-based film from round scad (*Decapterus maruadsi*) muscle as influenced by fish quality. LWT-Food Sci. Technol. 41: 753-763.

Bhat, R. and Karim, A. A. 2014. Towards producing novel fish gelatin films by combination treatments of ultraviolet radiation and sugars (ribose and lactose) as cross-linking agents. J. Food Sci. Technol. 51: 1326-1333.

Bigi, A., Cojazzi, G., Panzavolta, S., Rubini, K. and Roveri, N. 2001. Mechanical and thermal properties of gelatin films at different degrees of glutaraldehyde cross-linking. Biomaterials. 22: 763-768.

Botsoglou, N. A., Christaki, E., Fletouris, D. J., Florou-Paneri, P. and Spais, A. B. 2002. The effect of dietary oregano essential oil on lipid oxidation in raw and cooked chicken during refrigerated storage. Meat Sci. 62: 259-265.

Bradbury, E. and Martin, C. 1952. The effect of the temperature of preparation on the mechanical properties and structure of gelatin films. Proc. R. Soc. London, Series A. 214: 183-192.

Burguera, J. L. and Burguera, M. 2012. Analytical applications of emulsions and microemulsions. Talanta. 96: 11-20.

Cabedo, L., Luis Feijoo, J., Pilar Villanueva, M., Lagarón, J. M. and Giménez, E. 2006. Optimization of biodegradable nanocomposites based on a PLA/PCL blends for food packaging applications. Macromol. Symp. 233: 191-197.

Cao, N., Fu, Y. and He, J. 2007. Mechanical properties of gelatin films cross-linked, respectively, by ferulic acid and tannin acid. Food Hydrocolloid. 21: 575-584.

Cao, N., Yang, X. and Fu, Y. 2009. Effects of various plasticizers on mechanical and water vapor barrier properties of gelatin films. Food Hydrocolloid. 23: 729-735.

Carvalho, R. A., Sobral, P. J. A., Thomazine, M., Habitante, A. M. Q. B., Giménez, B., Gómez-Guillén, M. C. and Montero, P. 2008. Development of edible films based on differently processed Atlantic halibut (*Hippoglossus hippoglossus*) skin gelatin. Food Hydrocolloid. 22: 1117-1123.

Cerqueira, M. A., Bourbon, A. I., Pinheiro, A. C., Martins, J. T., Souza, B. W. S., Teixeira, J. A. and Vicente, A. A. 2011. Galactomannans use in the development of edible films/coatings for food applications. Trends Food Sci. Technol. 22: 662-671.

Chaiyasit, W., Elias, R. J., McClements, D. J. and Decker, E. A. 2007. Role of physical structures in bulk oils on lipid oxidation. Crit. Rev. Food Sci. Nutr. 47: 299-317.

Chaiyasit, W., McClements, D. J. and Decker, E. A. 2005. The relationship between the physicochemical properties of antioxidants and their ability to inhibit lipid oxidation in bulk oil and oil-in-water emulsions. J. Agric. Food Chem. 53: 4982-4988.

Chen, Z. Y., Chan, P. T., Ho, K. Y., Fung, K. P. and Wang, J. 1996. Antioxidant activity of natural flavonoids is governed by number and location of their aromatic hydroxyl groups. Chem. Phys. Lipids. 79: 157-163.

Chiou, B.-S., Avena-Bustillos, R. J., Bechtel, P. J., Imam, S. H., Glenn, G. M. and Orts, W. J. 2009. Effects of drying temperature on barrier and mechanical properties of cold-water fish gelatin films. J. Food Eng. 95: 327-331.

Chiou, B.-S., Avena-Bustillos, R. J., Bechtel, P. J., Jafri, H., Narayan, R., Imam, S. H., Glenn, G. M. and Orts, W. J. 2008. Cold water fish gelatin films: Effects of cross-linking on thermal, mechanical, barrier, and biodegradation properties. Eur. Polym. J. 44: 3748-3753.

Cho, S. Y., Lee, S. Y. and Rhee, C. 2010. Edible oxygen barrier bilayer film pouches from corn zein and soy protein isolate for olive oil packaging. LWT-Food Sci. Technol. 43: 1234-1239.

Cho, Y. J., Alamed, J., McClements, D. J. and Decker, E. A. 2006. Ability of chelators to alter the physical location and prooxidant activity of iron in oil-in-water emulsions. J. Food Sci. 68: 1952-1957.

Chuaynukul, K., Nagarajan, M., Prodpran, T., Benjakul, S., Songtipya, P. and Songtipya, L. 2018. Comparative characterization of bovine and fish gelatin films fabricated by compression molding and solution casting methods. J. Polym. Mater. 26: 1239-1252.

Ciannamea, E. M., Stefani, P. M. and Ruseckaite, R. A. 2016. Properties and antioxidant activity of soy protein concentrate films incorporated with red grape extract processed by casting and compression molding. LWT-Food Sci. Technol. 74: 353-362.

Colín-Chávez, C., Soto-Valdez, H., Peralta, E., Lizardi-Mendoza, J. and Balandrán-Quintana, R. R. 2012. Fabrication and properties of antioxidant polyethylene-based films containing marigold (*Tagetes erecta*) extract and application on soybean oil stability. Packag. Technol. Sci. 26: 267-280.

Conde, E., Gordon, M. H., Moure, A. and Dominguez, H. 2011. Effects of caffeic acid and bovine serum albumin in reducing the rate of development of rancidity in oil-in-water and water-in-oil emulsions. Food Chem. 129: 1652-1659.

Conn, R. E., Kolstad, J. J., Borzelleca, J. F., Dixler, D. S., Filer Jr, L. J., LaDu Jr, B. N. and Pariza, M. W. 1995. Safety assessment of polylactide (PLA) for use as a food-contact polymer. Food Chem. Toxicol. 33: 273-283.

Cuq, B., Gontard, N. and Guilbert, S. 1997. Thermal properties of fish myofibrillar protein-based films as affected by moisture content. Polymer. 38: 2399-2405.

Datta, R. and Henry, M. 2006. Lactic acid: recent advances in products, processes and technologies — a review. J. Chem. Technol. Biot. 81: 1119-1129.

de Carvalho, R. A. and Grosso, C. R. F. 2004. Characterization of gelatin based films modified with transglutaminase, glyoxal and formaldehyde. Food Hydrocolloid. 18: 717-726.

Debeaufort, F., Martin-Polo, M. and Voilley, A. 1993. Polarity homogeneity and structure affect water vapor permeability of model edible films. J. Food Sci. 58: 426-429.

Decker, E. A., Warner, K., Richards, M. P. and Shahidi, F. 2005. Measuring antioxidant effectiveness in food. J. Agric. Food Chem. 53: 4303-4310.

Denavi, G. A., Pérez-Mateos, M., Añón, M. C., Montero, P., Mauri, A. N. and Gómez-Guillén, M. C. 2009. Structural and functional properties of soy protein isolate and cod gelatin blend films. Food Hydrocolloid. 23: 2094-2101.

Devi, R. R. and Arumughan, C. 2007. Antiradical efficacy of phytochemical extracts from defatted rice bran. Food Chem. Toxicol. 45: 2014-2021.

Du, G.-J., Zhang, Z., Wen, X.-D., Yu, C., Calway, T., Yuan, C.-S. and Wang, C.-Z. 2012. Epigallocatechin gallate (EGCG) is the most effective cancer chemopreventive polyphenol in green tea. Nutr. 4: 1679-1691.

Eitenmiller, R. R. and Lee, J. 2004. Vitamin E: food chemistry, composition, and analysis. CRC Press.

Embuscado, M. and Shahidi, F. 2015. Handbook of antioxidants for food preservation. A volume in Woodhead Publishing Series in Food Science. UK: Technology and Nutrition. 251-283.

Etxabide, A., Coma, V., Guerrero, P., Gardrat, C. and de la Caba, K. 2017a. Effect of cross-linking in surface properties and antioxidant activity of gelatin films incorporated with a curcumin derivative. Food Hydrocolloid. 66: 168-175.

Etxabide, A., Uranga, J., Guerrero, P. and de la Caba, K. 2017b. Development of active gelatin films by means of valorisation of food processing waste: A review. Food Hydrocolloid. 68: 192-198.

Fabra, M. J., Pérez-Masiá, R., Talens, P. and Chiralt, A. 2011. Influence of the homogenization conditions and lipid self-association on properties of sodium caseinate based films containing oleic and stearic acids. Food Hydrocolloid. 25: 1112-1121.

Fang, J. M., Fowler, P. A., Escrig, C., Gonzalez, R., Costa, J. A. and Chamudis, L. 2005. Development of biodegradable laminate films derived from naturally occurring carbohydrate polymers. Carbohydr Polym. 60: 39-42.

Felton, L. A. 2013. Mechanisms of polymeric film formation. Int. J. Pharm. 457: 423-427.

Fishman, M. L., Coffin, D. R., Onwulata, C. I. and Konstance, R. P. 2004. Extrusion of pectin and glycerol with various combinations of orange albedo and starch. Carbohydr Polym. 57: 401-413.

Franko, A., Rodriguez Camargo, D. C., Böddrich, A., Garg, D., Rodriguez Camargo, A., Rathkolb, B., Janik, D., Aichler, M., Feuchtinger, A., Neff, F., Fuchs, H., Wanker, E. E., Reif, B., Häring, H.-U., Peter, A. and Hrabě de Angelis, M. 2018. Epigallocatechin gallate (EGCG) reduces the intensity of pancreatic amyloid

fibrils in human islet amyloid polypeptide (hIAPP) transgenic mice. Sci. Rep. 8: 1116.

Gennadios, A., Handa, A., Froning, G. W., Weller, C. L. and Hanna, M. A. 1998. Physical properties of egg white-dialdehyde starch films. J. Agric. Food Chem. 46: 1297-1302.

Gennadios, A., Hanna, M. A. and Kurth, L. B. 1997. Application of edible coatings on meats, poultry and seafoods: a review. LWT-Food Sci. Technol. 30: 337-350.

Gennadios, A., McHugh, T. H., Weller, C. L. and Krochta, J. M. 1994. Edible coatings and films based on proteins. *In* Edible coatings and films to improve food quality. (Krochta, J. M. *et al.*, eds.). p. 210–278. Technomic Pub. Co., Inc. Lancaster, NC.

Gennadios, A., Weller, C. L., Hanna, M. A. and Froning, G. W. 1996. Mechanical and barrier properties of egg albumen films. J. Food Sci. 61: 585-589.

Georgantelis, D., Blekas, G., Katikou, P., Ambrosiadis, I. and Fletouris, D. J. 2007. Effect of rosemary extract, chitosan and α-tocopherol on lipid oxidation and colour stability during frozen storage of beef burgers. Meat Sci. 75: 256-264.

Ghanbarzadeh, B. and Oromiehi, A. R. 2009. Thermal and mechanical behavior of laminated protein films. J. Food Eng. 90: 517-524.

Gil, D. M. d. A. 2011. Biosensor evaluation of the antioxidant activity of wines and teas. Interference studies and comparison with other. Ph.D. Dissertation. Lisbon University, Protugal.

Gómez-Estaca, J., Bravo, L., Gómez-Guillén, M. C., Alemán, A. and Montero, P. 2009a. Antioxidant properties of tuna-skin and bovine-hide gelatin films induced by the addition of oregano and rosemary extracts. Food Chem. 112: 18-25.

Gómez-Estaca, J., Giménez, B., Montero, P. and Gómez-Guillén, M. C. 2009b. Incorporation of antioxidant borage extract into edible films based on sole skin gelatin or a commercial fish gelatin. J. Food Eng. 92: 78-85.

Gómez-Estaca, J., López-de-Dicastillo, C., Hernández-Muñoz, P., Catalá, R. and Gavara, R. 2014. Advances in antioxidant active food packaging. Trends. Food Sci. Technol. 35: 42-51.

Gómez-Estaca, J., Montero, P., Fernández-Martín, F. and Gómez-Guillén, M. C. 2009c. Physico-chemical and film-forming properties of bovine-hide and tuna-skin gelatin: A comparative study. J. Food Eng. 90: 480-486.

Gómez-Guillén, M. C., Ihl, M., Bifani, V., Silva, A. and Montero, P. 2007. Edible films made from tuna-fish gelatin with antioxidant extracts of two different murta ecotypes leaves (*Ugni molinae Turcz*). Food Hydrocolloid. 21: 1133-1143.

Gómez-Guillén, M. C., Pérez-Mateos, M., Gómez-Estaca, J., López-Caballero, E., Giménez, B. and Montero, P. 2009. Fish gelatin: A renewable material for developing active biodegradable films. Trends Food Sci. Technol. 20: 3-16.

Gontard, N., Thibault, R., Cuq, B. and Guilbert, S. 1996. Influence of relative humidity and film composition on oxygen and carbon dioxide permeabilities of edible films. J. Agric. Food Chem. 44: 1064-1069.

Graciano-Verdugo, A. Z., Soto-Valdez, H., Peralta, E., Cruz-Zárate, P., Islas-Rubio, A. R., Sánchez-Valdes, S., Sánchez-Escalante, A., González-Méndez, N. and González-Ríos, H. 2010. Migration of α-tocopherol from LDPE films to corn oil and its effect on the oxidative stability. Food Res. Int. 43: 1073-1078.

Graham, H. N. 1992. Green tea composition, consumption, and polyphenol chemistry. Preventive medicine. 21: 334-350.

Guerrero, P., Retegi, A., Gabilondo, N. and de la Caba, K. 2010. Mechanical and thermal properties of soy protein films processed by casting and compression. J. Food Eng. 100: 145-151.

Guilbert, S., Cuq, B. and Gontard, N. 1997. Recent innovations in edible and/or biodegradable packaging materials. Food Addit. Contam. 14: 741-751.

Guilbert, S., Gontard, N. and Gorris, L. G. M. 1996. Prolongation of the shelf-life of perishable food products using biodegradable films and coatings. LWT-Food Sci. Technol. 29: 10-17.

Gülçin, İ. 2006. Antioxidant activity of caffeic acid (3,4-dihydroxycinnamic acid). Toxicol. 217: 213-220.

Haddar, A., Sellimi, S., Ghannouchi, R., Alvarez, O. M., Nasri, M. and Bougatef, A. 2012. Functional, antioxidant and film-forming properties of tuna-skin gelatin with a brown algae extract. Int. J. Biol. Macromol. 51: 477-483.

Han, J. H. and Floros, J. D. 1997. Casting antimicrobial packaging films and measuring their physical properties and antimicrobial activity. J. Plast. Film Sheet. 13: 287-298.

Han, J. H. and Gennadios, A. 2005. Edible films and coatings: A review. *In* Innovations in Food Packaging. (Han, J. H., ed.). p. 239-262. Academic Press. London.

Headlam, H. A. and Davies, M. J. 2003. Cell-mediated reduction of protein and peptide hydroperoxides to reactive free radicals. Free Rad. Biol. Med. 34: 44-55.

Hoque, M. S., Benjakul, S. and Prodpran, T. 2010. Effect of heat treatment of film-forming solution on the properties of film from cuttlefish (*Sepia pharaonis*) skin gelatin. J. Food Eng. 96: 66-73.

Hoque, M. S., Benjakul, S. and Prodpran, T. 2011. Effects of partial hydrolysis and plasticizer content on the properties of film from cuttlefish (*Sepia pharaonis*) skin gelatin. Food Hydrocolloid. 25: 82-90.

Hu, M., Julian McClements, D. and Decker, E. A. 2004. Impact of chelators on the oxidative stability of whey protein isolate-stabilized oil-in-water emulsions containing ω-3 fatty acids. Food Chem. 88: 57-62.

Huang, S.-W., Frankel, E. N., Aeschbach, R. and German, J. B. 1997. Partition of selected antioxidants in corn oil− water model systems. J. Agric. Food Chem. 45: 1991-1994.

Huang, S.-W., Hopia, A., Schwarz, K., Frankel, E. N. and German, J. B. 1996. Antioxidant activity of α-tocopherol and trolox in different lipid substrates: bulk oils vs oil-in-water emulsions. J. Agric. Food Chem. 44: 444-452.

Iqbal, S. and Bhanger, M. I. 2007. Stabilization of sunflower oil by garlic extract during accelerated storage. Food Chem. 100: 246-254.

Jafari, S., He, Y. and Bhandari, B. 2007. Optimization of nano-emulsions production by microfluidization. Eur. Food Res. Technol. 225: 733-741.

Jamshidian, M., Tehrany, E. A., Imran, M., Jacquot, M. and Desobry, S. 2010. Poly-lactic acid: Production, applications, nanocomposites, and release studies. Compr. Rev. Food Sci. Food Saf. 9: 552-571.

Jeya Shakila, R., Jeevithan, E., Varatharajakumar, A., Jeyasekaran, G. and Sukumar, D. 2012. Comparison of the properties of multi-composite fish gelatin films with that of mammalian gelatin films. Food Chem. 135: 2260-2267.

Johnston-Banks, F. A. 1990. Gelatine. *In* Food Gels. (Harris, P., ed.). p. 233-289. Elsevier Applied Food Science Series, Springer. Dordrecht, the Netherlands.

Jongjareonrak, A., Benjakul, S., Visessanguan, W., Prodpran, T. and Tanaka, M. 2006a. Characterization of edible films from skin gelatin of brownstripe red snapper and bigeye snapper. Food Hydrocolloid. 20: 492-501.

Jongjareonrak, A., Benjakul, S., Visessanguan, W. and Tanaka, M. 2006b. Effects of plasticizers on the properties of edible films from skin gelatin of bigeye snapper and brownstripe red snapper. Eur. Food Res. Technol. 222: 229-235.

Jongjareonrak, A., Benjakul, S., Visessanguan, W. and Tanaka, M. 2006c. Fatty acids and their sucrose esters affect the properties of fish skin gelatin-based film. Eur. Food Res. Technol. 222: 650-657.

Jongjareonrak, A., Benjakul, S., Visessanguan, W. and Tanaka, M. 2008. Antioxidative activity and properties of fish skin gelatin films incorporated with BHT and α-tocopherol. Food Hydrocolloid. 22: 449-458.

Jridi, M., Souissi, N., Mbarek, A., Chadeyron, G., Kammoun, M. and Nasri, M. 2013. Comparative study of physico-mechanical and antioxidant properties of edible gelatin films from the skin of cuttlefish. Int. J. Biol. Macromol. 61: 17-25.

Kaewprachu, P., Osako, K., Benjakul, S. and Rawdkuen, S. 2015. Quality attributes of minced pork wrapped with catechin–lysozyme incorporated gelatin film. Food Pack. Shelf Life. 3: 88-96.

Kamper, S. L. and Fennema, O. 1984. Water vapor permeability of edible bilayer films. J. Food Sci. 49: 1478-1481.

Keane, M. A., Boyer, M. C., Biggs, S. R., Galvin, K. P. and Hosken, R. W. 2000. Particle size analysis of microfluidised dairy emulsions. Aust. J. Dairy Technol. 55: 94.

Kester, J. J. and Fennema, O. R. 1986. Edible films and coatings: A review. Food Technology. 40: 47-59.

Kim, J.-M., Kim, H.-N., Park, Y.-J., Ko, J.-W., Lee, J.-W. and Kim, H.-D. 2015. Fabrication of transparent $MgAl_2O_4$ spinel through homogenous green compaction by microfluidization and slip casting. Ceram. Int. 41: 13354-13360.

Kołodziejska, I. and Piotrowska, B. 2007. The water vapour permeability, mechanical properties and solubility of fish gelatin–chitosan films modified with transglutaminase or 1-ethyl-3-(3-dimethylaminopropyl) carbodiimide (EDC) and plasticized with glycerol. Food Chem. 103: 295-300.

Kowalczyk, D. and Baraniak, B. 2011. Effects of plasticizers, pH and heating of film-forming solution on the properties of pea protein isolate films. J. Food Eng. 105: 295-305.

Kozlov, P. V. and Burdygina, G. I. 1983. The structure and properties of solid gelatin and the principles of their modification. Polymer. 24: 651-666.

Krishna, M., Nindo, C. I. and Min, S. C. 2012. Development of fish gelatin edible films using extrusion and compression molding. J. Food Eng. 108: 337-344.

Krochta, J. M. 1997. Edible protein films and coatings. *In* Food protein and their applications. (Damodaran, S. and Paraf, A., eds.). p. 529-550. Marcel Dekker Inc. New York.

Krochta, J. M. 2002. Proteins as raw materials for films and coatings: definitions, current status, and opportunities. *In* Protein-based films and coatings. (Gennadios, A., ed.). p. 1-41. CRC Press. Boca Raton, FL.

Krochta, J. M. and De Mulder-Johnston, C. 1997. Edible and biodegradable polymer films: Challenges and opportunities. Food Technology. 51: 61-72.

Kurek, M., Galus, S. and Debeaufort, F. 2014. Surface, mechanical and barrier properties of bio-based composite films based on chitosan and whey protein. Food Pack. Shelf Life. 1: 56-67.

Lacroix, M. and Ouattara, B. 2000. Combined industrial processes with irradiation to assure innocuity and preservation of food products — a review. Food Res. Int. 33: 719-724.

Laguerre, M., Lecomte, J. and Villeneuve, P. 2007. Evaluation of the ability of antioxidants to counteract lipid oxidation: Existing methods, new trends and challenges. Prog. Lipid Res. 46: 244-282.

Le, T., Maki, H., Takahashi, K., Okazaki, E. and Osako, K. 2015. Properties of gelatin film from horse mackerel (*Trachurus japonicus*) scale. J. Food Sci. 80: E734-E741.

Lee, J. H., Panya, A., Laguerre, M., Bayrasy, C., Lecomte, J., Villeneuve, P. and Decker, E. A. 2012. Comparison of antioxidant capacities of rosmarinate alkyl esters in riboflavin photosensitized oil-in-water emulsions. J. Am. Oil Chem. Soc. 90: 225-232.

Lee, K.-Y. and Song, K. B. 2017. Preparation and characterization of an olive flounder (*Paralichthys olivaceus*) skin gelatin and polylactic acid bilayer film. J. Food Sci. 82: 706-710.

Lee, K.-Y., Yang, H.-J. and Song, K. B. 2016a. Application of a puffer fish skin gelatin film containing *Moringa oleifera* Lam. leaf extract to the packaging of Gouda cheese. J. Food Sci. Technol. 53: 3876-3883.

Lee, K. Y., Lee, J. H., Yang, H. J. and Song Kyung, B. 2016b. Production and characterisation of skate skin gelatin films incorporated with thyme essential oil and their application in chicken tenderloin packaging. Int. J. Food Sci. Technol. 51: 1465-1472.

Li, J.-H., Miao, J., Wu, J.-L., Chen, S.-F. and Zhang, Q.-Q. 2014. Preparation and characterization of active gelatin-based films incorporated with natural antioxidants. Food Hydrocolloid. 37: 166-173.

Lim, L. T., Auras, R. and Rubino, M. 2008. Processing technologies for poly(lactic acid). Prog. Polym. Sci. 33: 820-852.

Limpan, N., Prodpran, T., Benjakul, S. and Prasarpran, S. 2010. Properties of biodegradable blend films based on fish myofibrillar protein and polyvinyl alcohol as influenced by blend composition and pH level. J. Food Eng. 100: 85-92.

Limpisophon, K. and Schleining, G. 2017. Use of gallic acid to enhance the antioxidant and mechanical properties of active fish gelatin film. J. Food Sci. 82: 80-89.

Limpisophon, K., Tanaka, M. and Osako, K. 2010. Characterisation of gelatin–fatty acid emulsion films based on blue shark (*Prionace glauca*) skin gelatin. Food Chem. 122: 1095-1101.

Limpisophon, K., Tanaka, M., Weng, W., Abe, S. and Osako, K. 2009. Characterization of gelatin films prepared from under-utilized blue shark (*Prionace glauca*) skin. Food Hydrocolloid. 23: 1993-2000.

Liu, L., Jin, T., Liu, C.-K., Hicks, K., Mohanty, A. K., Bhardwaj, R. and Misra, M. 2008. A preliminary study on antimicrobial edible films from pectin and other food hydrocolloids by extrusion method. J. Nat. Fibers. 5: 366-382.

Ljungberg, N. and Wesslén, B. 2005. Preparation and properties of plasticized poly(lactic acid) films. Biomacromolecules. 6: 1789-1796.

Lu, T.-M., Lee, C.-C., Mau, J.-L. and Lin, S.-D. 2010. Quality and antioxidant property of green tea sponge cake. Food Chem. 119: 1090-1095.

Ma, W., Tang, C.-H., Yin, S.-W., Yang, X.-Q., Qi, J.-R. and Xia, N. 2012. Effect of homogenization conditions on properties of gelatin–olive oil composite films. J. Food Eng. 113: 136-142.

Manzanarez-López, F., Soto-Valdez, H., Auras, R. and Peralta, E. 2011. Release of α-tocopherol from poly(lactic acid) films, and its effect on the oxidative stability of soybean oil. J. Food Eng. 104: 508-517.

Maqsood, S. and Benjakul, S. 2010. Comparative studies of four different phenolic compounds on in vitro antioxidative activity and the preventive effect on lipid oxidation of fish oil emulsion and fish mince. Food Chem. 119: 123-132.

Maqsood, S., Benjakul, S., Abushelaibi, A. and Alam, A. 2014. Phenolic compounds and plant phenolic extracts as natural antioxidants in prevention of lipid oxidation in seafood: A detailed review. Compr. Rev. Food Sci. Food Saf. 13: 1125-1140.

Marquié, C. and Guilbert, S. 2002. Formation and properties of cottonseed protein films and coatings. CRC Press, New York, NY, USA.

Martins, C., Vilarinho, F., Sanches Silva, A., Andrade, M., Machado, A. V., Castilho, M. C., Sá, A., Cunha, A., Vaz, M. F. and Ramos, F. 2018. Active polylactic acid film incorporated with green tea extract: Development, characterization and effectiveness. Ind. Crops Prod. 123: 100-110.

Martucci, J. F. and Ruseckaite, R. A. 2010. Three-layer sheets based on gelatin and poly(lactic acid), part 1: Preparation and properties. J. Appl. Polym. Sci. 118: 3102-3110.

Maryam Adilah, Z. A., Jamilah, B. and Nur Hanani, Z. A. 2018. Functional and antioxidant properties of protein-based films incorporated with mango kernel extract for active packaging. Food Hydrocolloid. 74: 207-218.

Matsushita, Y., Suzuki, R., Nara, E., Yokoyama, A. and Miyashita, K. 2000. Antioxidant activity of polar carotenoids including astaxanthin-β-glucoside from marine bacterium on PC liposomes. Fish. Sci. 66: 980-985.

McClements, D. J. 2005. Food emulsions: principles, practices, and techniques. CRC press. Boca Raton, Florida.

McHugh, T. H. and Krochta, J. M. 1994a. Dispersed phase particle size effects on water vapor permeability of whey protein-beeswax edible emulsion films. J. Food Process. Preserv. 18: 173-188.

McHugh, T. H. and Krochta, J. M. 1994b. Permeability properties of edible films. *In* Edible coatings and films to improve food quality. (Krochta, J. M. *et al.*, eds.). p. 139-187. Technomic Pub. Co., Inc. Lancaster, NC.

Mecitoğlu, Ç., Yemenicioğlu, A., Arslanoğlu, A., Elmacı, Z. S., Korel, F. and Çetin, A. E. 2006. Incorporation of partially purified hen egg white lysozyme into zein films for antimicrobial food packaging. Food Res. Int. 39: 12-21.

Micard, V., Belamri, R., Morel, M. H. and Guilbert, S. 2000. Properties of chemically and physically treated wheat gluten films. J. Agric. Food Chem. 48: 2948-2953.

Miller, K. S., Chiang, M. T. and Krochta, J. M. 1997. Heat curing of whey protein films. J. Food Sci. 62: 1189-1193.

Naczk, M. and Shahidi, F. 2004. Extraction and analysis of phenolics in food. J. Chromatogr. A. 1054: 95-111.

Nagarajan, M., Benjakul, S., Prodpran, T. and Songtipya, P. 2012. Properties of film from splendid squid (*Loligo formosana*) skin gelatin with various extraction temperatures. Int. J. Biol. Macromol. 51: 489-496.

Nagarajan, M., Benjakul, S., Prodpran, T. and Songtipya, P. 2015. Effects of bio-nanocomposite films from tilapia and squid skin gelatins incorporated with

ethanolic extract from coconut husk on storage stability of mackerel meat powder. Food Pack. Shelf Life. 6: 42-52.

Nagarajan, M., Benjakul, S., Prodpran, T., Songtipya, P. and Nuthong, P. 2013. Film forming ability of gelatins from splendid squid (*Loligo formosana*) skin bleached with hydrogen peroxide. Food Chem. 138: 1101-1108.

Nerín, C., Tovar, L. and Salafranca, J. 2008. Behaviour of a new antioxidant active film versus oxidizable model compounds. J. Food Eng. 84: 313-320.

Núñez-Flores, R., Giménez, B., Fernández-Martín, F., López-Caballero, M. E., Montero, M. P. and Gómez-Guillén, M. C. 2012. Role of lignosulphonate in properties of fish gelatin films. Food Hydrocolloid. 27: 60-71.

Nur Hanani, Z. A., Roos, Y. H. and Kerry, J. P. 2012. Use of beef, pork and fish gelatin sources in the manufacture of films and assessment of their composition and mechanical properties. Food Hydrocolloid. 29: 144-151.

Nuthong, P., Benjakul, S. and Prodpran, T. 2009a. Characterization of porcine plasma protein-based films as affected by pretreatment and cross-linking agents. Int. J. Biol. Macromol. 44: 143-148.

Nuthong, P., Benjakul, S. and Prodpran, T. 2009b. Effect of phenolic compounds on the properties of porcine plasma protein-based film. Food Hydrocolloid. 23: 736-741.

Oujifard, A., Benjakul, S., Prodpran, T. and Seyfabadi, J. 2013. Properties of red tilapia (*Oreochromis niloticus*) protein based film as affected by cryoprotectants. Food Hydrocolloid. 32: 245-251.

Park, J. W., Testin, R. F., Vergano, P. J., Park, H. J. and Weller, C. L. 1996. Fatty acid distribution and its effect on oxygen permeability in laminated edible films. J. Food Sci. 61: 401-406.

Paulo, J. d. A., dos Santos, J. S. and García, F. T. 2005. Effect of protein and plasticizer concentrations in film forming solutions on physical properties of edible films based on muscle proteins of a Thai tilapia. J. Food Eng. 70: 93-100.

Pereira de Abreu, D. A., Losada, P. P., Maroto, J. and Cruz, J. M. 2010. Evaluation of the effectiveness of a new active packaging film containing natural antioxidants

(from barley husks) that retard lipid damage in frozen Atlantic salmon (*Salmo salar* L.). Food Res. Int. 43: 1277-1282.

Perez-Gago, M. B. and Krochta, J. M. 2001. Lipid particle size effect on water vapor permeability and mechanical properties of whey protein/beeswax emulsion films. J. Agric. Food Chem. 49: 996-1002.

Perrier-Cornet, J. M., Marie, P. and Gervais, P. 2005. Comparison of emulsification efficiency of protein-stabilized oil-in-water emulsions using jet, high pressure and colloid mill homogenization. J. Food Eng. 66: 211-217.

Pommet, M., Redl, A., Morel, M.-H., Domenek, S. and Guilbert, S. 2003. Thermoplastic processing of protein-based bioplastics: chemical engineering aspects of mixing, extrusion and hot molding. Macromol. Symp. 197: 207-218.

Pratt, D. E. and Hudson, B. J. F. 1990. Natural antioxidants not exploited commercially. *In* Food antioxidants. p. 171-191. Springer.

Prodpran, T., Benjakul, S. and Artharn, A. 2007. Properties and microstructure of protein-based film from round scad (*Decapterus maruadsi*) muscle as affected by palm oil and chitosan incorporation. Int. J. Biol. Macromol. 41: 605-614.

Prodpran, T., Benjakul, S. and Phatcharat, S. 2012. Effect of phenolic compounds on protein cross-linking and properties of film from fish myofibrillar protein. Int. J. Biol. Macromol. 51: 774-782.

Prodpran, T., Chuaynukul, K., Nagarajan, M., Benjakul, S. and Prasarpran, S. 2017. Impacts of plasticizer and pre-heating conditions on properties of bovine and fish gelatin films fabricated by thermo-compression molding technique. Italian Journal of Food Science. 29: 487-504.

Qian, C. and McClements, D. J. 2011. Formation of nanoemulsions stabilized by model food-grade emulsifiers using high-pressure homogenization: Factors affecting particle size. Food Hydrocolloid. 25: 1000-1008.

Quezada Gallo, J.-A., Debeaufort, F., Callegarin, F. and Voilley, A. 2000. Lipid hydrophobicity, physical state and distribution effects on the properties of emulsion-based edible films. J. Membr. Sci. Technol. 180: 37-46.

Rajapakse, N., Mendis, E., Byun, H.-G. and Kim, S.-K. 2005. Purification and *in vitro* antioxidative effects of giant squid muscle peptides on free radical-mediated oxidative systems. J. Nutr. Biochem. 16: 562-569.

Rakotonirainy, A. M. and Padua, G. W. 2001. Effects of lamination and coating with drying oils on tensile and barrier properties of zein films. J. Agric. Food Chem. 49: 2860-2863.

Ralston, B. E. and Osswald, T. A. 2008. Viscosity of soy protein plastics determined by screw-driven capillary rheometry. J. Polym. Mater. 16: 169-176.

Rattaya, S., Benjakul, S. and Prodpran, T. 2009. Properties of fish skin gelatin film incorporated with seaweed extract. J. Food Eng. 95: 151-157.

Reyes-Avalos, M. C., Femenia, A., Minjares-Fuentes, R., Contreras-Esquivel, J. C., Aguilar-González, C. N., Esparza-Rivera, J. R. and Meza-Velázquez, J. A. 2016. Improvement of the quality and the shelf life of figs (*Ficus carica*) using an alginate–chitosan edible film. Food Bioprocess Tech. 9: 2114-2124.

Rhim, J.-W. and Ng, P. K. W. 2007. Natural biopolymer-based nanocomposite films for packaging applications. Crit. Rev. Food Sci. Nutr. 47: 411-433.

Sae-leaw, T., Benjakul, S. and Simpson, B. K. 2017. Effect of catechin and its derivatives on inhibition of polyphenoloxidase and melanosis of Pacific white shrimp. J. Food Sci. Technol. 54: 1098-1107.

Salvia-Trujillo, L., Rojas-Graü, A., Soliva-Fortuny, R. and Martín-Belloso, O. 2015. Physicochemical characterization and antimicrobial activity of food-grade emulsions and nanoemulsions incorporating essential oils. Food Hydrocolloid. 43: 547-556.

Santos, J. P., Esquerdo, V. M., Moura, C. M. and Pinto, L. A. A. 2018. Crosslinking agents effect on gelatins from carp and tilapia skins and in their biopolymeric films. Colloid. Surface. A. 539: 184-191.

Sekhon-Loodu, S., Warnakulasuriya, S. N., Rupasinghe, H. P. V. and Shahidi, F. 2013. Antioxidant ability of fractionated apple peel phenolics to inhibit fish oil oxidation. Food Chem. 140: 189-196.

Selling, G. W., Woods, K. K., Biswas, A. and Willett, J. L. 2009. Reactive extrusion of zein with glyoxal. J. Appl. Polym. Sci. 113: 1828-1835.

Shahidi, F. and Zhong, Y. 2010. Lipid oxidation and improving the oxidative stability. Chem. Soc. Rev. 39: 4067-4079.

Shen, J., Wang, J. J., Liu, X. X. and Fan, J. Y. 2011. The structure and antioxidant activity of procyanidins/cellulose acetate biodegradable packaging film. J. Zhejiang Univ. Sci. B. 28: 865-870.

Sikorski, Z. E. and Kolakowska, A. 2010. Chemical and functional properties of food lipids. CRC press.

Slavutsky, A. M. and Bertuzzi, M. A. 2016. Standard and new processing techniques used in the preparation of films and coatings at the lab level and scale-up. *In* Edible Films and Coatings. p. 21-42. CRC Press.

Soazo, M., Rubiolo, A. C. and Verdini, R. A. 2011. Effect of drying temperature and beeswax content on physical properties of whey protein emulsion films. Food Hydrocolloid. 25: 1251-1255.

Stadtman, E. R. 2001. Protein oxidation in aging and age-related diseases. Ann. NY. Acad. Sci. 928: 22-38.

Staroszczyk, H., Pielichowska, J., Sztuka, K., Stangret, J. and Kołodziejska, I. 2012. Molecular and structural characteristics of cod gelatin films modified with EDC and TGase. Food Chem. 130: 335-343.

Stevens, M. P. 1990. Polymer chemistry. Oxford university press. New York.

Strawbridge, K. B., Ray, E., Hallett, F. R., Tosh, S. M. and Dalgleish, D. G. 1995. Measurement of particle size distributions in milk homogenized by a microfluidizer: Estimation of populations of particles with radii less than 100 nm. J. Colloid Interf. Sci. 171: 392-398.

Sun, T. and Ho, C.-T. 2005. Antioxidant activities of buckwheat extracts. Food Chem. 90: 743-749.

Sun, Y.-E., Wang, W.-D., Chen, H.-W. and Li, C. 2011. Autoxidation of unsaturated lipids in food emulsion. Crit. Rev. Food Sci. Nutr. 51: 453-466.

Sung, S. H., Chang, Y. and Han, J. 2017. Development of polylactic acid nanocomposite films reinforced with cellulose nanocrystals derived from coffee silverskin. Carbohydr Polym. 169: 495-503.

Tian, F., Decker, E. A. and Goddard, J. M. 2013. Controlling lipid oxidation of food by active packaging technologies. Food Funct. 4: 669-680.

Tongnuanchan, P., Benjakul, S. and Prodpran, T. 2012. Properties and antioxidant activity of fish skin gelatin film incorporated with citrus essential oils. Food Chem. 134: 1571-1579.

Tongnuanchan, P., Benjakul, S. and Prodpran, T. 2014. Structural, morphological and thermal behaviour characterisations of fish gelatin film incorporated with basil and citronella essential oils as affected by surfactants. Food Hydrocolloid. 41: 33-43.

Torres-Arreola, W., Soto-Valdez, H., Peralta, E., Cárdenas-López, J. L. and Ezquerra-Brauer, J. M. 2007. Effect of a low-density polyethylene film containing butylated hydroxytoluene on lipid oxidation and protein quality of sierra fish (*Scomberomorus sierra*) muscle during frozen storage. J. Agric. Food Chem. 55: 6140-6146.

Vaisali, C., Belur, P. D. and Iyyaswami, R. 2017. Effectiveness of rutin and its lipophilic ester in improving oxidative stability of sardine oil containing trace water. Int. J. Food Sci. Technol. 53: 541-548.

Valencia-Sullca, C., Vargas, M., Atarés, L. and Chiralt, A. 2018. Thermoplastic cassava starch-chitosan bilayer films containing essential oils. Food Hydrocolloid. 75: 107-115.

Valencia, I., Ansorena, D. and Astiasarán, I. 2007. Development of dry fermented sausages rich in docosahexaenoic acid with oil from the microalgae Schizochytrium sp.: Influence on nutritional properties, sensorial quality and oxidation stability. Food Chem. 104: 1087-1096.

Vanin, F. M., Sobral, P. J. A., Menegalli, F. C., Carvalho, R. A. and Habitante, A. M. Q. B. 2005. Effects of plasticizers and their concentrations on thermal and functional properties of gelatin-based films. Food Hydrocolloid. 19: 899-907.

Vejdan, A., Ojagh, S. M., Adeli, A. and Abdollahi, M. 2016. Effect of TiO_2 nanoparticles on the physico-mechanical and ultraviolet light barrier properties of fish gelatin/agar bilayer film. LWT-Food Sci. Technol. 71: 88-95.

Walstra, P. 1993. Principles of emulsion formation. Chemical Engineering Science. 48: 333-349.

Wanasundara, U. N. and Shahidi, F. 1996. Stabilization of seal blubber and menhaden oils with green tea catechins. J. Am. Oil Chem. Soc. 73: 1183-1190.

Wang, Q., Cao, J., Yu, H., Zhang, J., Yuan, Y., Shen, X. and Li, C. 2019. The effects of EGCG on the mechanical, bioactivities, cross-linking and release properties of gelatin film. Food Chem. 271: 204-210.

Wang, Y. and Padua, G. W. 2003. Tensile properties of extruded zein sheets and extrusion blown films. Macromol. Mater. Eng. 288: 886-893.

Were, L., Hettiarachchy, N. S. and Coleman, M. 1999. Properties of cysteine-added soy protein-wheat gluten films. J. Food Sci. 64: 514-518.

Witt, U., Müller, R. J. and Deckwer, W. D. 1996. Evaluation of the biodegradability of copolyesters containing aromatic compounds by investigations of model oligomers. J. Environ. Polym. Degrad. 4: 9-20.

Woong, K., Beomgi, L., Jaeyoung, P., Ho-Joong, K. and Hyeonsook, C. 2018. Comparative antioxidant activity and structural feature of protocatechuic acid and phenolic acid derivatives by DPPH and intracellular ROS. Letters in Drug Design & Discovery. 15: 612-620.

Wooster, T. J., Golding, M. and Sanguansri, P. 2008. Impact of oil type on nanoemulsion formation and Ostwald ripening stability. Langmuir. 24: 12758-12765.

Wu, J., Chen, S., Ge, S., Miao, J., Li, J. and Zhang, Q. 2013. Preparation, properties and antioxidant activity of an active film from silver carp (*Hypophthalmichthys molitrix*) skin gelatin incorporated with green tea extract. Food Hydrocolloid. 32: 42-51.

Xiong, X., Li, Q., Lu, J. W., Guo, Z. X. and Yu, J. 2010. Poly(lactic acid)/soluble eggshell membrane protein blend films: Preparation and characterization. J. Appl. Polym. Sci. 117: 1955-1959.

Yan, J., Zhao, Y., Suo, S., Liu, Y. and Zhao, B. 2012. Green tea catechins ameliorate adipose insulin resistance by improving oxidative stress. Free Rad. Biol. Med. 52: 1648-1657.

Yildirim, M. and Hettiarachchy, N. S. 1997. Biopolymers produced by cross-linking soybean 11S globulin with whey proteins using transglutaminase. J. Food Sci. 62: 270-275.

Yildirim, S., Röcker, B., Pettersen, M. K., Nilsen-Nygaard, J., Ayhan, Z., Rutkaite, R., Radusin, T., Suminska, P., Marcos, B. and Coma, V. 2017. Active packaging applications for food. Compr. Rev. Food Sci. Food Saf. 17: 165-199.

Yu, H., Yang, G., Sato, M., Yamaguchi, T., Nakano, T. and Xi, Y. 2017. Antioxidant activities of aqueous extract from *Stevia rebaudiana* stem waste to inhibit fish oil oxidation and identification of its phenolic compounds. Food Chem. 232: 379-386.

Yuji, H., Weiss, J., Villeneuve, P., López Giraldo, L. J., Figueroa-Espinoza, M.-C. and Decker, E. A. 2007. Ability of surface-active antioxidants to inhibit lipid oxidation in oil-in-water emulsion. J. Agric. Food Chem. 55: 11052-11056.

Zaveri, N. T. 2006. Green tea and its polyphenolic catechins: Medicinal uses in cancer and noncancer applications. Life Sci. 78: 2073-2080.

Zhang, H. and Mittal, G. 2010. Biodegradable protein-based films from plant resources: A review. Environ Prog. Sustain. Energy. 29: 203-220.

Zhu, J. Y., Tang, C. H., Yin, S. W. and Yang, X. Q. 2017. Development and characterisation of polylactic acid–gliadin bilayer/trilayer films as carriers of thymol. International Journal of Food Science and Technology. 53: 608-618.

Zhuang, C., Jiang, Y., Zhong, Y., Zhao, Y., Deng, Y., Yue, J., Wang, D., Jiao, S., Gao, H., Chen, H. and Mu, H. 2018. Development and characterization of nano-bilayer films composed of polyvinyl alcohol, chitosan and alginate. Food Control. 86: 191-199.

CHAPTER 2

PROPERTIES, MICROSTRUCTURE AND HEAT SEAL ABILITY OF BILAYER FILMS BASED ON FISH GELATIN AND EMULSIFIED GELATIN FILMS

2.1 Abstract

Bilayer films prepared by the lamination of fish gelatin film (GF) and its corresponding emulsified film (EF) with different thickness ratios (7:3, 5:5 and 3:7) were characterized. Bilayer films had the similar tensile strength (TS) to EF ($P > 0.05$) but showed lower elongation at break (EAB) ($P < 0.05$). All bilayer films showed the lower water vapor permeability (WVP) but higher oxygen permeability (OP) than GF. Bilayer films had varying ΔE^* (total color different), where the highest value was observed in that laminated with higher thickness ratio of EF ($P < 0.05$). Lower light transmission and higher transparency value were obtained for bilayer films, compared to GF ($P < 0.05$). Based on scanning electron microscopic (SEM) cross-section micrographs, all bilayer films consisted of two layers. Differential scanning calorimetric (DSC) analysis revealed that the bilayer films had the higher glass transition temperature (T_g) than GF but lower than EF. All bilayer films were heat sealable, however their seal strength and seal efficiency were lower than those of GF ($P < 0.05$). Therefore, the thickness ratios of GF and EF had a marked effect on the mechanical and barrier properties as well as heat sealing ability of resulting bilayer films.

2.2 Introduction

Biodegradable films from bio-based materials have been intensively developed since the commercial plastic packaging produced from petrochemical products are associated with environmental pollution and serious ecological problems (Arvanitoyannis, 2002). Proteins from various sources have been used as packaging materials due to good film formation as well as excellent barrier properties against gas and volatile compounds, oils and UV light (Cho *et al.*, 2010; Krochta, 2002). Gelatin is

one of proteinaceous materials, known to have an excellent film forming ability. Currently, marine gelatin, particularly from fish skin, has gained attention as biodegradable material without religious constraint (Aewsiri *et al.*, 2009; Jongjareonrak *et al.*, 2006a; Yi *et al.*, 2006). Gelatin film (GF) generally has good mechanical property with an excellent oxygen barrier property (Jongjareonrak *et al.*, 2006a; Nilsuwan *et al.*, 2016c). Nevertheless, it has high water absorptivity due to hydrophilicity of gelatin molecules and the presence of hydrophilic plasticizers such as glycerol (Gennadios *et al.*, 1994; Krochta, 1997; McHugh and Krochta, 1994). The hydrophobic substances such as fats and oils have been added to improve water vapor barrier properties of the gelatin films (Tongnuanchan *et al.*, 2012; Wang *et al.*, 2017). Palm oil must be emulsified in gelatin solution using soy lecithin as the surfactant, in which the emulsified film was obtained after casting (Nilsuwan *et al.*, 2016b). Emulsified gelatin based films generally had the higher water vapor barrier property than non-emulsified counterpart (Jongjareonrak *et al.*, 2006b; Tongnuanchan *et al.*, 2012). However, the direct incorporation of hydrophobic substances resulted in the decreased oxygen gas barrier property of obtained emulsified gelatin film (EF) (Nilsuwan *et al.*, 2016c). Film lamination is a one of potential means for the improvement of film properties, in which bilayer film can be formed. As a consequence, the advantages of each film can be exploited. Soy protein isolate/corn zein bilayer film with the increased water barrier property was developed (Cho *et al.*, 2010). Properties of gelatin films were improved via laminating with desired films such as chitosan film (Nowzari *et al.*, 2013). However, little information regarding bilayer film based on GF and EF exists. Lamination of EF, which possesses high water vapor barrier, onto the GF, which has the excellent oxygen barrier property could render the bilayer film having both aforementioned barrier properties.

2.3 Objective

To characterize the physical and thermal properties as well as heat seal ability of bilayer films (GF/EF) as influenced by thickness ratio of both layers.

2.4 Materials and methods

2.4.1 Materials

Fish gelatin produced from tilapia skin (~240 bloom) was procured from Lapi Gelatine S.p.A (Empoli, Italy). Palm oil was obtained from Oleen Co., Ltd. (Samutsakorn, Thailand). Glycerol was purchased from Merck (Darmstadt, Germany). Soy lecithin (L-α-phosphatidylcholine, HLB~4.0) was obtained from Sigma-Aldrich (St. Louis, MO, USA). All chemicals were of analytical grade.

2.4.2 Preparation of film forming solution and emulsion

Film forming solution and emulsion from fish gelatin were prepared according to the method of Nilsuwan *et al.* (2016c). Gelatin powder was mixed with distilled water to obtain protein content of 3.5% (wet basis) and the mixture was heated at 70 °C for 30 min. Glycerol at a concentration of 30% (w/w, based on protein content) was added into solution. The resulting solution was termed as ‘film forming solution’. To prepare film forming emulsion, glycerol was added to gelatin solution at the level of 10% (w/w, based on protein content). Palm oil previously mixed with soy lecithin, used as a surfactant, at a level of 50% (based on palm oil) was transferred into prepared gelatin solution to obtain a final concentration of 75% (w/w, based on protein content). The mixture was homogenized at 22,000 rpm for 3 min using a rotor-stator homogenizer (IKA Labortechnik homogeniser, Selangor, Malaysia). The coarse emulsion was passed through a Microfluidizer (Microfluidics, Model HC-5000, Newton, MA, USA) at 20.68 MPa for 2 passes. Fine emulsion was referred to ‘film forming emulsion’. Both film forming solution and emulsion were used for film preparation.

2.4.3 Preparation of bilayer films

Firstly, the thickness of films prepared from film forming solution or emulsion, named as ‘gelatin film, GF’ and ‘emulsified gelatin film, EF’, respectively, was estimated from the plot between amount of prepared film forming solution or emulsion (mL) and thickness of the resulting films (mm). All the films were expected

to have the final thickness of approximately 0.10 mm. GF and EF were also prepared and used as the control films. The bilayer films including GF laminated with EF with different layer thickness ratios (7:3, 5:5 and 3:7) were constructed. Briefly, gelatin film forming solution was firstly cast onto a plastic petri dish with a diameter of 89 mm (Hycon Plastics Inc., Manchester, NH, USA) and air-blown for 12 h at 25 °C and 60 ± 5% relative humidity (RH). Thereafter, gelatin film forming emulsion with a known volume was overlaid on GF previously formed to obtain the designated final thickness ratios. After the second casting, the samples were air-blown for 12 h prior to drying at 25 °C and 50 ± 5% RH for 48 h in an environmental chamber. All the films were peeled off and subjected to analyses.

2.4.4 Film analyses

2.4.4.1 Film thickness

The thickness of film was measured using a micrometer (Mitutoyo, Model ID-C112PM, Serial No. 00320, Mitutoyo Corp., Kawasaki-shi, Japan). Five random locations around each film of ten film samples were used for determination of average thickness.

2.4.4.2 Mechanical properties

Prior to testing, films were conditioned for 48 h at 25 °C and 50 ± 5% RH. Tensile strength (TS) and elongation at break (EAB) were determined as described by Iwata *et al.* (2000) using the Universal Testing Machine (Lloyd Instrument, Hampshire, UK) equipped with tensile load cell of 100 N. Ten samples (2×5 cm^2) with an initial grip length of 3 cm were used for testing. Cross-head speed was set at 30 mm/min. Tensile strength (MPa) was calculated by dividing the maximum load (N) necessary to pull the sample film apart by the cross-sectional area (m^2). Average thickness of the film strip was used to estimate the cross-sectional area of the sample. Percentage elongation at break was calculated by dividing film elongation at the moment of rupture by the initial grip length of samples. The value was then multiplied by 100.

2.4.4.3 Water vapor permeability (WVP)

WVP was measured using a modified ASTM method (ASTM, 1989) as modified by Shiku *et al.* (2004). Bilayer films with the GF layer facing down were sealed on an aluminium permeation cup containing dried silica gel (0% RH) with silicone vacuum grease and a rubber gasket to hold the films in place. The cups were placed in a desiccator containing the distilled water at 30 °C. The cups were weighed at 1-h interval over a 10-h period. WVP of the film was calculated as follows:

$$\text{WVP (g.m/m}^2\text{.s.Pa)} = \frac{wl}{At(P_2 - P_1)}$$

where w is the weight gain of the cup (g); l is the film thickness (m); A is the exposed area of film (m^2); t is the time of gain (s); P_1 and P_2 are the vapor pressure in the aluminium cup and desiccator, respectively; P_2-P_1 is the vapor pressure difference across the film (4242.31 Pa at 30 °C).

2.4.4.4 Oxygen permeability (OP)

OP of films was measured according to the ASTM D3985-05 method. An Oxygen Permeation Analyzer (Illinois model 8000, Illinois Instruments Inc., Johnsburg, IL, USA) was used to measure oxygen transmission rate (OTR) through the film. Each film was placed on a stainless steel mask. The mask was then placed in a test cell and exposed to an oxygen atmosphere flow on the EF side and a nitrogen atmosphere flow on the GF side. OTR was measured at 25 °C and 50% RH (Nilsuwan *et al.*, 2016c). The film was allowed to equilibrate for 10 h before measurements. OP was calculated using following equation:

$$\text{OP (mol.m/m}^2\text{.s.Pa)} = \frac{\text{OTR} \cdot l}{\Delta P}$$

where OTR is the oxygen transmission rate (mol/m^2 s); l is the film thickness (m); ΔP is the partial pressure of oxygen (Pa).

2.4.4.5 Color

Film samples were subjected to color measurement using a CIE colorimeter (Hunter associates laboratory, Inc., Reston, VA, USA). D_{65} (day light) and a measure cell with opening of 3 cm was used. The color of the films was expressed as L^*-value (lightness), a^*-value (redness/greenness) and b^*-value (yellowness/blueness). Total difference of color (ΔE^*) was calculated as follows (Gennadios *et al.*, 1996):

$$\Delta E^* = \sqrt{(\Delta L^*)^2 + (\Delta a^*)^2 + (\Delta b^*)^2}$$

where ΔL^*, Δa^* and Δb^* are the differences between the color parameter of the samples and those of the white standard (L^* = 92.82, a^* = -1.24, b^* = 0.46).

2.4.4.6 Light transmittance and transparency

The light transmittance of films was measured at the ultraviolet and visible range (200-800 nm) using a UV-vis spectrophotometer (UV-1800, Shimadzu, Kyoto, Japan) according to the method of Shiku *et al.* (2004). The transparency value of film was calculated using the following equation (Han and Floros, 1997):

$$\text{Transparency value} = \frac{-\log T_{600}}{x}$$

where T_{600} is the fractional transmittance at 600 nm and x is the film thickness (mm). The greater transparency value represents the lower transparency of film.

2.4.4.7 Film microstructure

Morphology of the upper surface (EF surface) and cross-section of film samples was visualized using a scanning electron microscope (SEM) (Quanta 400, FEI, Eindhoven, the Netherlands). For cross-section, samples were fractured under liquid nitrogen prior to visualization. Then, the samples were mounted on bronze stub and sputtered with gold (Sputter coater SPI-Module, West Chester, PA, USA) in order to make the sample conductive. The photographs were taken at an acceleration voltage of 15 kV.

2.4.4.8 Film microstructure

Morphology of the upper surface (EF surface) and cross-section of film samples was visualized using a scanning electron microscope (SEM) (Quanta 400, FEI, Eindhoven, the Netherlands). For cross-section, samples were fractured under liquid nitrogen prior to visualization. Then, the samples were mounted on bronze stub and sputtered with gold (Sputter coater SPI-Module, West Chester, PA, USA) in order to make the sample conductive. The photographs were taken at an acceleration voltage of 15 kV.

2.4.4.9 Water contact angle

Contact angle was determined using a contact angle meter (model OCA15EC, dataphysics instruments, Stuttgart, BW, Germany) as described by Guerrero *et al.* (2011). A film sample was put on a movable sample stage and levelled horizontally; then a drop of approximately 3 μL of distilled water was placed on the upper surface of the films using a microsyringe. The contact angle (CA) was immediately measured at room temperature (25 °C). Contact angle values were recorded. Average CA values were calculated from values obtained at five different positions on the same sample.

2.4.4.10 Differential scanning calorimetry

Thermal properties of films were determined using a differential scanning calorimeter (DSC) (Perkin Elmer, Model DSC-7, Norwalk, CT, USA) as described by Nilsuwan *et al.* (2016a). Temperature calibration was performed using the indium thermogram. Film samples (2-5 mg) were accurately weighed into aluminium pans, hermetically sealed, and scanned over the temperature range of -20 to 150 °C, with a heating rate of 5 °C/min. Liquid nitrogen was used as a cooling medium and the system was equilibrated at -20 °C for 5 min prior to the scan. An empty aluminium pan was used as the reference. The maximum transition temperature was estimated from the endothermic peak of the DSC thermogram and transition enthalpy was determined from

the area under the endothermic peak. A second scan was also performed in the same manner, followed by quench-cooling of the sample after completing the first scan.

2.4.4.11 Seal ability

Seal strength and seal efficiency were determined as described by Tongnuanchan *et al.* (2016). Film samples were cut into strips (25 × 20 mm^2). Two strips of bilayer films were faced together, in which the GF sides of both films were heat-sealed using an impulse sealer with a magnet Model ME-300HIM (S.N.MARK Ltd., Park, Nonthaburi, Thailand) at 150 ± 0.5 °C for 1.25 s, followed by cooling for 1.50 s. The width of seal area was 2 mm.

Before testing, all sealed film samples were conditioned at 25 ± 2 °C and 50 ± 5% relative humidity (RH) for 48 h. The heat-seal strength was estimated using the peel test. The peel strength and seal efficiency of the heat-sealed films were determined according to the Standard ASTM F-88 (ASTM., 2001) with slight modifications using Universal Testing Machine (Lloyd Instruments, Hampshire, UK) at 25 ± 2 °C and 50 ± 5% RH. Each leg of the sealed film was clamped to a 100 N static load cell of the machine, in which each end of the sealed film was held perpendicularly to the direction of the pull. The distance between the clamps was 50 mm. The samples were subjected to tensile loaded at 100 N until seal failure was obtained. Both seal strength and seal efficiency were calculated as follows:

$$\text{Seal strength (N/m)} = \frac{\text{Peak force}}{\text{Film width}}$$

$$\text{Seal efficiency (\%)} = \frac{\text{Peak force}}{\text{Tensile force}} \times 100$$

2.4.5 Statistical analysis

All experiments were run in triplicate with different three lots of films. Data were subjected to analysis of variance (ANOVA) and mean comparisons were carried out by the Duncan's multiple range test. Analysis was performed using the SPSS package (SPSS for windows, SPSS Inc., Chicago, IL, USA).

2.5 Results and discussion

2.5.1 Appearance and thickness of bilayer films

Photographs of bilayer films with different thickness ratios of GF/EF (7:3, 5:5 and 3:7) are illustrated in Figure 8. Generally, individual GF and EF had the obviously different appearance. GF was colorless and transparent, while EF was yellowish and opaque. Coloring components in palm oil and soy lecithin more likely contributed to the yellowish color of EF (Tongnuanchan *et al.*, 2016). When the bilayer films were formed by lamination of GF and EF, the resulting film became more opaque, especially when the higher thickness ratio of EF was used.

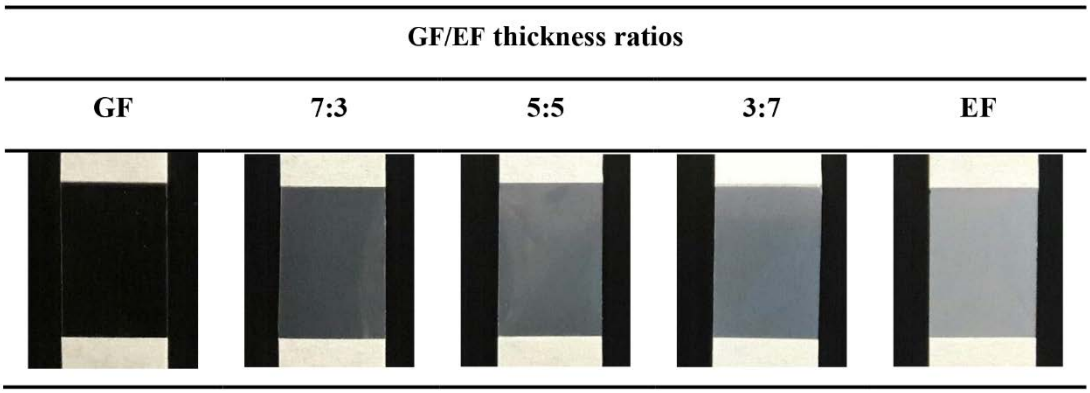

Figure 8. Photographs of bilayer films with different GF/EF thickness ratios. GF: fish gelatin film; EF: emulsion film

The overall thickness of bilayer film with different thickness GF/EF ratios is shown in Table 4. All films tested had thickness in the range of 0.083-0.098 mm. Both GF and EF showed the similar thickness ($P > 0.05$) but their thickness was higher than that of bilayer films ($P < 0.05$). The bilayer film with GF/EF thickness ratio of 7:3 was thicker than those having the ratios of 5:5 and 3:7 ($P < 0.05$). The lowering in thickness of bilayer films, compared to GF and EF was plausibly associated with the mergence of both films during lamination. Gelatin in GF might be partially solubilized and penetrated into EF when being laminated. Therefore, lamination of GF and EF affected the appearance and thickness of resulting bilayer films.

Table 4. Thickness, mechanical properties, water vapor permeability and oxygen transmission rate of bilayer films with different GF/EF thickness ratios.

GF/EF	Thickness (mm)	TS (MPa)	EAB (%)	WVP ($*10^{-12}$ g m/m^2 s Pa)	OP ($*10^{-18}$ mol m/m^2 s Pa)
GF	0.097±0.003 a	26.93±3.05 b	33.87±4.57 a	14.15±0.30 a	4.67±0.08 e
7:3	0.088±0.002 b	30.32±2.08 ab	15.71±3.59 b	11.42±0.28 b	8.43±0.12 d
5:5	0.083±0.004 c	32.45±1.21 a	14.23±1.74 b	10.34±0.21 c	8.67±0.12 c
3:7	0.084±0.005 c	31.95±1.11 a	16.44±1.84 b	9.78±0.02 d	9.85±0.31 b
EF	0.098±0.004 a	32.47±2.08 a	34.25±0.85 a	7.61±0.06 e	21.08±0.82 a

GF: fish gelatin film; EF: emulsion film TS: Tensile strength; EAB: Elongation at break; WVP: Water vapor permeability; OP: Oxygen permeability. Different lowercase letters in the same column indicate significant differences ($P < 0.05$).

2.5.2 Mechanical properties

Mechanical properties of bilayer films having different GF/EF thickness ratios expressed as tensile strength (TS) and elongation at break (EAB) are given in Table 4. EF generally showed higher TS than GF ($P < 0.05$). This result was in accordance with Nilsuwan *et al.* (2016c) who reported that emulsion gelatin film containing palm oil showed the increased TS. Lecithin used as the surfactant in emulsion gelatin film was mainly located at oil/water interface, in which polar heads of phosphate groups were exposed to the aqueous phase. As a result, the ionic interaction between lecithin and positively charged domain of gelatin chain occurred. This might help strengthen the film network. However, Sahraee *et al.* (2017) reported that the incorporation of corn oil lowered TS of gelatin-based nanocomposite films containing nano chitin. Generally, the mechanical properties of EF are governed by several factors including oil, surfactant type as well as emulsification technique (Nilsuwan *et al.*, 2016a; Tongnuanchan *et al.*, 2014). All bilayer films had no difference in TS, compared with EF, regardless of GF/EF thickness ratios used ($P > 0.05$). Bilayer films with GF/EF thickness ratio of 5:5 and 3:7 had the higher TS than GF ($P < 0.05$). Both GF and EF had the similar EAB ($P > 0.05$), which was higher than those of bilayer films ($P < 0.05$). All bilayer films exhibited the similar EAB ($P > 0.05$). The lower EAB value of bilayer films might be attributed to the limitation of both films at interface, thereby reducing stretch ability of resulting films. Merging of interfaces between GF and EF might increase the strength and rigidity of bilayer films as indicated by the lower EAB but higher TS as compared to GF. Cho *et al.* (2010) also reported that corn zein/soy protein isolate bilayer film showed the lower EAB, in comparison with soy protein isolate film. Thus, mechanical properties of bilayer films were different from those of GF and EF as governed by laminating process.

2.5.3 Barrier properties

Water vapor permeability (WVP) and oxygen permeability (OP) of bilayer films in comparison with those of GF and EF are shown in Table 4. WVP of EF was lower than that of GF by approximately two times ($P < 0.05$). For the bilayer films, in which EF layer was exposed to saturated water vapor, WVP were 11.42, 10.34 and

9.78×10^{-12} g m/m^2 s Pa when the GF/EF thickness ratios of 7:3, 5:5 and 3:7 were used, respectively. It was noted that WVP was decreased as the thickness of EF of bilayer film increased ($P < 0.05$). Oil droplets in EF more likely functioned as the barrier toward water vapor. All bilayer films showed the lower WVP than GF ($P < 0.05$). WVP of bilayer film is generally determined by the thickness and WVP of each film layer (McHugh *et al.*, 1993; Yong Cho *et al.*, 2002). This result indicated that the lamination of EF onto GF could enhance water vapor barrier property of the resulting bilayer films, compared to individual GF. Hydrophobic substances such as palm oil in emulsion film could increase the hydrophobicity of films, thereby retarding water vapor migration through the film (Nilsuwan *et al.*, 2016b).

Oxygen permeability (OP) of films is also very important since it has been used as the index of efficiency in preventing lipid oxidation of packaged oily foods (Cho *et al.*, 2010). Among all film samples, EF had the highest OP (21.08×10^{-18} mol m/m^2 s Pa) ($P < 0.05$) (Table 4), indicating the lowest ability in preventing oxygen migration through the films. Oil droplets distributed in EF might disrupt the continuity or uniformity of gelatin matrix. As a result, interconnectivity or compactness of protein film matrix was lowered, thus allowing the oxygen to pass through more easily. After lamination with GF, all bilayer films showed the lower OP than EF alone ($P < 0.05$). Continuous decrease in OP was obtained for bilayer film as the thickness ratio of GF was increased ($P < 0.05$). This result indicated that the lowered oxygen transmission was associated with the excellent oxygen barrier of GF as reported by Nilsuwan *et al.* (2016c). Thus, the lamination of GF and EF could augment the barrier property toward oxygen permeability and improve water vapor barrier property of bilayer films effectively.

2.5.4 Color, light transmission and transparency value

The color of bilayer films with different GF/EF thickness ratios is presented in Table 5. In general, EF had the highest b^* and ΔE^* but lowest L^* and a^* than others ($P < 0.05$). The opposite results were noticeable for GF. For bilayer films, the higher thickness ratio of EF increased b^* and ΔE^* of the films. More yellowness

and higher Δ*E** were mainly due to the color of palm oil and lecithin used in film forming emulsion.

Table 5. Color of bilayer films with different GF/EF thickness ratios.

GF/EF	*L**	*a**	*b**	Δ*E**
GF	89.76±0.14 a	-1.42±0.02 a	1.65±0.04 a	3.29±0.13 a
7:3	89.63±0.13 b	-1.84±0.06 b	4.42±0.43 b	5.13±0.35 b
5:5	89.58±0.12 b	-1.91±0.08 c	5.00±0.62 c	5.63±0.56 c
3:7	89.36±0.16 c	-2.18±0.05 d	7.40±0.67 d	7.82±0.63 d
EF	89.03±0.11 d	-2.41±0.02 e	11.34±0.5 e	11.48±0.48 e

GF: fish gelatin film; EF: emulsion film

Different lowercase letters in the same column indicate significant differences ($P < 0.05$).

Light transmission at selected wavelengths from 200 to 800 nm in UV and visible ranges and transparency value of bilayer films in comparison with GF and EF are shown in Table 6. All films had a good barrier property in the UV-ranges (200–280 nm). Light transmission at 280 nm of EF was lowest, whereas the value increased in bilayer films, particularly those with increasing GF thickness ratio. It was noted that GF showed the highest transmission at 280 nm. High UV light barrier capacity was reported for gelatin films from cuttlefish skin (Hoque *et al.*, 2011a). EF and bilayer films showed the better barrier properties toward visible light transmission than GF. It was suggested that the increase in opaqueness of films containing oil lowered the visible light transmission through the film. Oil droplets distributed throughout the film might prevent the light to transmit through the films. With increasing GF thickness ratio, visible light transmission of bilayer films increased. Similar trend was observed for opaqueness. Bilayer films became more opaque as indicated by the higher transparency value as the EF thickness ratio was increased. The increasing thickness ratio of GF decreased the transparency value of the resulting films ($P < 0.05$), indicating that films became more transparent. Therefore, the lamination of EF and GF affected the color and light transmission of bilayer films.

Table 6. Light transmittance and transparency value of bilayer films with different GF/EF thickness ratios.

GF/EF	Light transmittance (%) at different wave number (nm)								Transparency value
	200	280	350	400	500	600	700	800	
GF	0.00	25.50	84.79	88.95	90.75	91.32	91.50	91.64	0.41±0.01 e
7:3	0.00	7.56	40.64	51.38	62.19	67.30	71.87	74.13	1.72±0.09 d
5:5	0.00	4.44	30.20	42.28	56.06	64.01	69.13	72.97	2.14±0.06 c
3:7	0.00	2.53	21.86	34.14	49.98	59.76	66.27	70.89	2.82±0.24 b
EF	0.00	0.25	7.15	15.63	31.01	42.92	51.88	58.69	3.77±0.19 a

GF: fish gelatin film; EF: emulsion film

Different lowercase letters in the same column indicate significant differences ($P < 0.05$).

2.5.5 Scanning electron microscopy

SEM micrographs of the upper surface and freeze-fractured cross section of bilayer films with different GF/EF thickness ratios, GF and EF are illustrated in Figure 9. The similar surface of all film samples was observed. However, slightly rougher surface was found for EF. For cross section, GF showed high smoothness, while EF exhibited more roughness. As expected, the cross section of bilayer films showed two layers including upper (EF) and lower (GF) layers with various thickness. In the present study, GF was firstly cast and EF was subsequently cast on the firstly formed GF. The result indicated that GF had the highest protein–protein interaction with high compactness and smooth surface. When oil was incorporated, disruption of protein-protein interaction in the emulsion film matrix arising from droplets of palm oil occurred as evidenced by the increased roughness of the film cross-section (Tongnuanchan *et al.*, 2013). Oil droplets with hydrophobic nature might serve as barrier for water vapor adsorption and migration as indicated by low WVP of EF (Table 4). Based on microscopic image, the lamination of GF and EF lowered the thickness of resulting bilayer films. This might be related with the mergence of GF and EF, especially at the connected area.

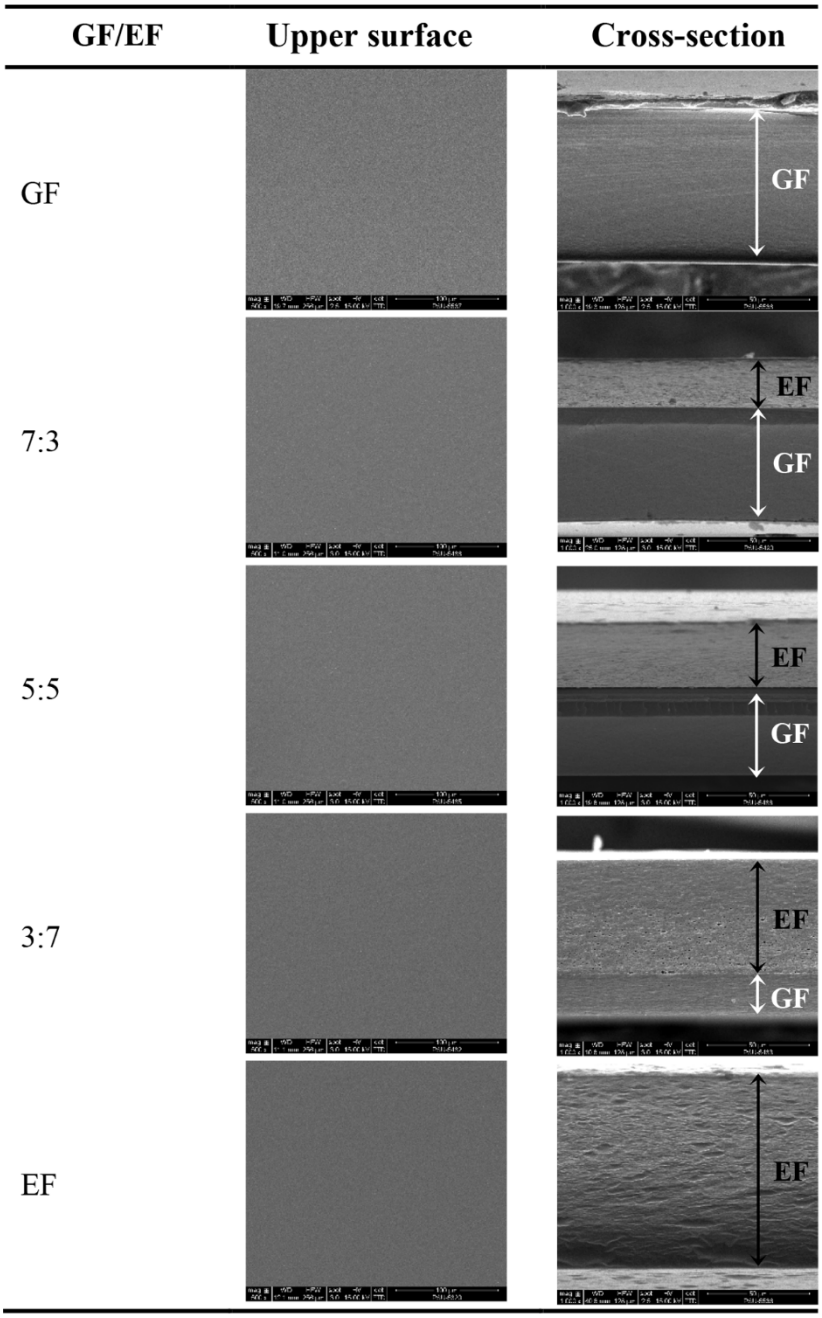

Figure 9. SEM micrographs of upper surface (500×) and cross-section (1000×) of bilayer films with different GF/EF thickness ratios. GF: fish gelatin film; EF: emulsion film

2.5.6 Water contact angle

Upper surface of bilayer films with different GF/EF thickness ratios had contact angles in the range of 64.75°-72.43° (Table 7). The contact angles of GF and

EF were 104.27° and 66.86°, respectively. EF was incorporated with palm oil, which is hydrophobic in nature. Therefore, it could be considered more hydrophobic and showed lower affinity for water contact. However, it was found that EF had higher affinity for water than GF in the present study. This might be due to the rougher surface and the presence of soy lecithin, which was located surrounding oil droplets. Lecithin contains one polar head of phosphate group and two non-polar tails of hydrocarbon chain (McClements, 2005). The hydrophilicity from polar head exposed to aqueous phase might contribute to the increased hydrophilicity of EF. Surface morphology could also affect the contact angle (Yuan and Lee, 2013). GF generally exhibited the smoother surface, while the EF had slightly rough surface (Figure 9). Rougher surface might favor the migration of water through the groove of the film surface.

Table 7. Water contact angle and images of water droplet over upper layer of bilayer films with different GF/EF thickness ratios.

GF/EF	Water contact angle (°)	Water contact image
GF	104.27±2.09 a	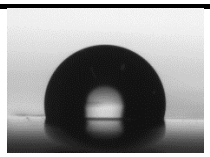
7:3	72.43±2.87 b	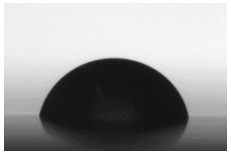
5:5	65.33±4.04 c	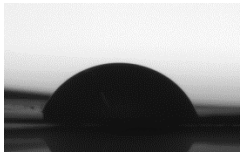
3:7	64.75±2.22 c	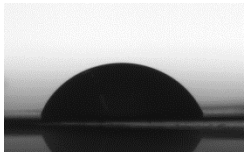
EF	66.86±3.85 c	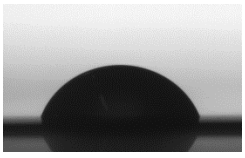

GF: fish gelatin film; EF: emulsion film. Different lowercase letters in the same column indicate significant differences ($P < 0.05$).

2.5.7 Differential scanning calorimetry

DSC thermograms of the 1st and 2nd -heating scans of GF, EF and different bilayer films are shown in Figure 10. From thermogram of the 1st heating scan (from -20 to 150 °C), all film samples exhibited a step-like transitions, indicating the glass transition temperature (T_g) and an endothermic melting transition (T_{max}). T_g of GF was observed at temperature of 53.87 °C, which was likely associated with T_g of plasticized gelatin-rich phase. All bilayer films had higher T_g, compared to GF but lower than T_g of EF. This result was in agreement with lower tensile strength (TS) of GF in comparison with EF (Table 1). For endothermic/melting transition, thermograms of EF and bilayer films exhibited endothermic transition peak ($T_{max,1}$) at temperature range of -3.15 to -3.98 °C. As expected, $T_{max,1}$ was not observed in GF. This endothermic transition was most likely attributed to the melting transition of palm oil droplets dispersed in the film matrix. Moreover, GF showed the endothermic peak with $T_{max,2}$ of 125.85 °C, whereas $T_{max,2}$ of EF was not detected. $T_{max,2}$ of bilayer films were 136.60, 147.02 and 148.60 °C when the GF/EF thickness ratios of 7:3, 5:5 and 3:7 were used, respectively. The difference in $T_{max,2}$ of bilayer films might be determined by different moisture contents in film matrix. The melting transition is generally associated with the disruption of ordered or aggregated molecular structure (Jongjareonrak *et al.*, 2006a; Tang *et al.*, 2009). The observed endothermic peak at $T_{max,2}$ was possibly arisen from the helix-coil transition of gelatin coupled with desorption/evaporation of molecularly bound water (Rahman *et al.*, 2008). The result suggested that the gelatin molecules could undergo partial renaturation, thereby transforming themselves into a more ordered structure during casting and drying (Hoque *et al.*, 2011b; Rahman *et al.*, 2008). Furthermore, GF exhibited the highest ΔH (12.77 J/g), compared with bilayer films. ΔH were 10.96, 9.43 and 0.275 J/g for bilayer films with GF/EF thickness ratios of 7:3, 5:5 and 3:7, respectively. This result indicated that the lesser portion of ordered structure was formed in the bilayer films upon EF lamination as indicated by the lower enthalpy for disruption of the inter-chain interaction in the matrix of films. Enthalpy or area under endothermic melting peak generally corresponded with the amount of ordered phase structure (Vanin *et al.*, 2005).

For the 2nd scan, it was found that the endothermic peak, which was related to gelatin-rich phase transition ($T_{max,2}$), was not observed for all film samples. It was suggested that gelatin was not able to rearrange themselves into ordered structure upon quench cooling during DSC scan (Tongnuanchan *et al.*, 2015). Additionally, gelatin molecules might be completely disrupted along with the loss of adsorbed water after the first-heating scan. Nevertheless, the endothermic melting peak ($T_{max,1}$) was still observed for EF and bilayer films, but it was not found for the GF. This endothermic transition was correlated with the melting transition of palm oil as previously described. Therefore, the GF/EF thickness ratio had the influence on thermal transition characteristics of bilayer films.

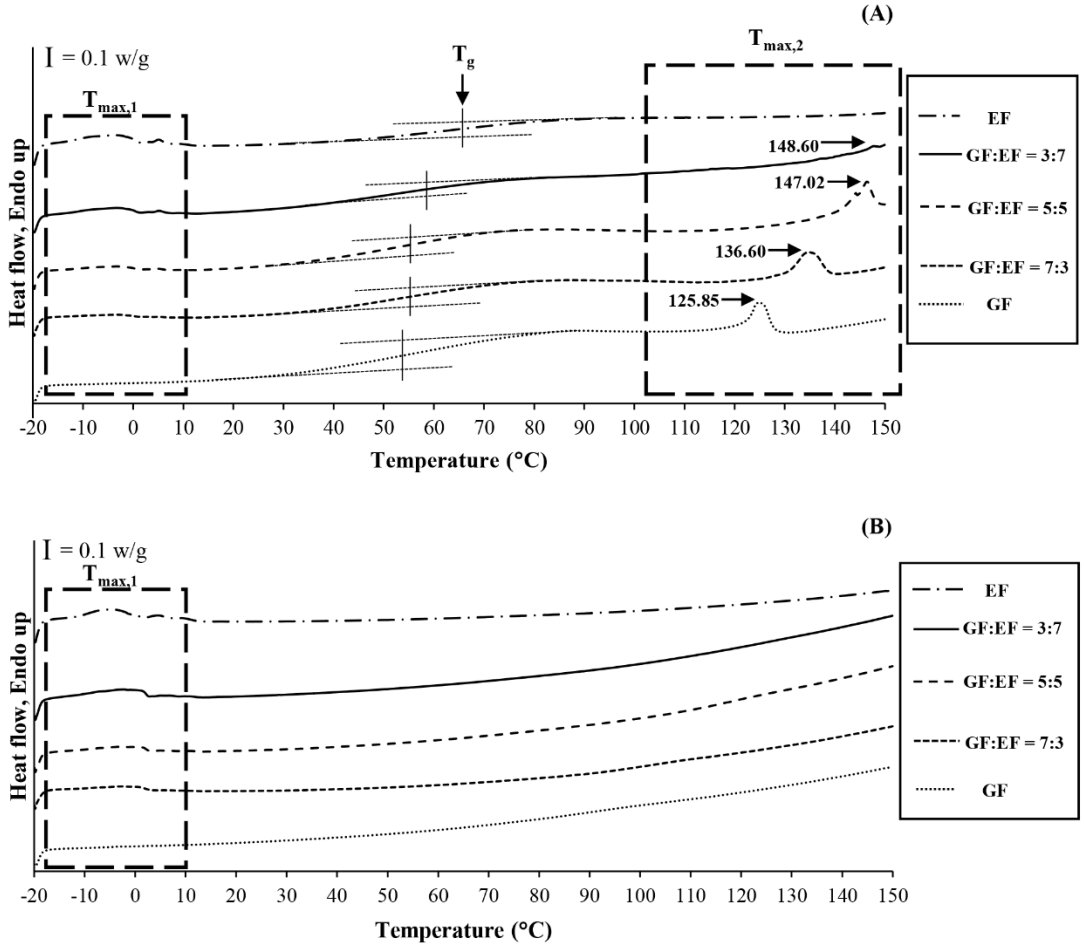

Figure 10. DSC thermograms of 1st-heating scan (A) and 2nd-heating scan (B) of bilayer films with different GF/EF thickness ratios. GF: fish gelatin film; EF: emulsion film

2.5.8 Seal ability

Seal strength and seal efficiency of GF, EF and bilayer films with different GF/EF thickness ratios are shown in Table 8. During heat sealing process, the surface of 2 films underwent melting via applied heat. This could promote the interfacial interactions across the contact surfaces, thus yielding the sufficient seal strength to the sealed film (Tongnuanchan *et al.*, 2016). All film samples were heat sealable except EF. GF showed the highest seal strength and seal efficiency, compared with all bilayer films ($P < 0.05$). Among all bilayer films, that with the GF/EF thickness ratio of 7:3 exhibited the highest seal strength and seal efficiency ($P < 0.05$). GF side (bottom part of film) of one film was attached to the same side of another film prior to sealing. During the lamination, GF of both films was molten by heat and the interfacial interaction between two films could be enhanced, favoring the sealing ability of bilayer films. Nevertheless, EF was unsealable, plausibly due to the high oil content in film matrix, which could interrupt the interfacial protein-protein interaction during sealing process. Thus, the seal strength and seal efficiency of bilayer films were directly affected by the GF/EF thickness ratios.

Table 8. Seal strength and seal efficiency for peel test of bilayer films with different GF/EF thickness ratios.

GF/EF	Sealed films*	Seal strength (N/m)	Seal efficiency (%)
GF	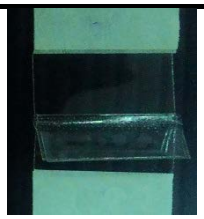	998.33±15.28 a	74.14±1.13 a
7:3	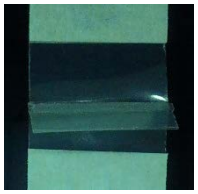	400.50±17.33 b	25.57±1.11 b
5:5	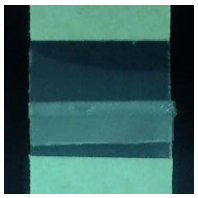	314.33±48.20 c	17.57±2.69 c
3:7	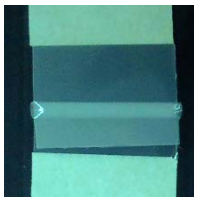	205.17±70.94 d	12.00±4.15 d
EF		ND	ND

GF: fish gelatin film; EF: emulsion film

Different lowercase letters in the same column indicate significant differences ($P < 0.05$). ND: Not determined (Unable to seal)

*Sealing of bilayer films was conducted via facing GF layers of two strips.

2.6 Conclusions

Properties of bilayer film prepared from GF and EF were influenced by the GF/EF thickness ratio. Increasing thickness ratio of GF increased the oxygen barrier property, while increasing ratio of EF decreased water permeability of bilayer film. Thermal stability of GF was increased when laminated with EF and it was governed by GF/EF thickness ratio. All bilayer films were heat sealable. The seal strength and seal efficiency of bilayer films proportionally increased as the thickness of GF layer increased. Therefore, the bilayer films prepared using the appropriate GF/EF thickness ratio had the combined nature between gelatin film and emulsified film. The developed film could be further used as the edible food packaging.

2.7 References

Aewsiri, T., Benjakul, S. and Visessanguan, W. 2009. Functional properties of gelatin from cuttlefish (*Sepia pharaonis*) skin as affected by bleaching using hydrogen peroxide. Food Chem. 115: 243-249.

Arvanitoyannis, I. S. 2002. Formation and properties of collagen and gelatin films and coatings. *In* Protein-based films and coatings. (Gennadios, A., ed.). p. 275–304. CRC Press. Boca Raton.

Cho, S. Y., Lee, S. Y. and Rhee, C. 2010. Edible oxygen barrier bilayer film pouches from corn zein and soy protein isolate for olive oil packaging. LWT-Food Sci. Technol. 43: 1234-1239.

Gennadios, A., McHugh, T. H., Weller, C. L. and Krochta, J. M. 1994. Edible coatings and films based on proteins. *In* Edible coatings and films to improve food quality. (Krochta, J. M. *et al.*, eds.). p. 210–278. Technomic Pub. Co., Inc. Lancaster, NC.

Gennadios, A., Weller, C. L., Hanna, M. A. and Froning, G. W. 1996. Mechanical and barrier properties of egg albumen films. J. Food Sci. 61: 585-589.

Guerrero, P., Stefani, P. M., Ruseckaite, R. A. and de la Caba, K. 2011. Functional properties of films based on soy protein isolate and gelatin processed by compression molding. J. Food Eng. 105: 65-72.

Han, J. H. and Floros, J. D. 1997. Casting antimicrobial packaging films and measuring their physical properties and antimicrobial activity. J. Plast. Film Sheet. 13: 287-298.

Hoque, M. S., Benjakul, S. and Prodpran, T. 2011a. Effects of hydrogen peroxide and Fenton's reagent on the properties of film from cuttlefish (*Sepia pharaonis*) skin gelatin. Food Chem. 128: 878-888.

Hoque, M. S., Benjakul, S., Prodpran, T. and Songtipya, P. 2011b. Properties of blend film based on cuttlefish (*Sepia pharaonis*) skin gelatin and mungbean protein isolate. Int. J. Biol. Macromol. 49: 663-673.

Iwata, K. I., Ishizaki, S. H., Handa, A. K. and Tanaka, M. U. 2000. Preparation and characterization of edible films from fish water-soluble proteins. Fish. Sci. 66: 372-378.

Jongjareonrak, A., Benjakul, S., Visessanguan, W., Prodpran, T. and Tanaka, M. 2006a. Characterization of edible films from skin gelatin of brownstripe red snapper and bigeye snapper. Food Hydrocolloid. 20: 492-501.

Jongjareonrak, A., Benjakul, S., Visessanguan, W. and Tanaka, M. 2006b. Fatty acids and their sucrose esters affect the properties of fish skin gelatin-based film. Eur. Food Res. Technol. 222: 650-657.

Krochta, J. M. 1997. Edible protein films and coatings. *In* Food protein and their applications. (Damodaran, S. and Paraf, A., eds.). p. 529-550. Marcel Dekker Inc. New York.

Krochta, J. M. 2002. Proteins as raw materials for films and coatings: definitions, current status, and opportunities. *In* Protein-based films and coatings. (Gennadios, A., ed.). p. 1-41. CRC Press. Boca Raton, FL.

McClements, D. J. 2005. Emulsion ingredients. *In* Food emulsions: principles, practices, and techniques. (McClements, D. J., ed.). p. 95-174. CRC Press. Boca Raton, Florida.

McHugh, T. H., Avena-Bustillos, R. and Krochta, J. M. 1993. Hydrophilic edible films: Modified procedure for water vapor permeability and explanation of thickness effects. J. Food Sci. 58: 899-903.

McHugh, T. H. and Krochta, J. M. 1994. Permeability properties of edible films. *In* Edible coatings and films to improve food quality. (Krochta, J. M. *et al.*, eds.). p. 139-187. Technomic Pub. Co., Inc. Lancaster, NC.

Nilsuwan, K., Benjakul, S. and Prodpran, T. 2016a. Effects of soy lecithin levels and microfluidization conditions on properties of fish gelatin-based film incorporated with palm oil. Int. J. Food Eng. 12: 647-660.

Nilsuwan, K., Benjakul, S. and Prodpran, T. 2016b. Emulsion stability and properties of fish gelatin-based films as affected by palm oil and surfactants. J. Sci. Food Agric. 96: 2504-2513.

Nilsuwan, K., Benjakul, S. and Prodpran, T. 2016c. Quality changes of shrimp cracker covered with fish gelatin film without and with palm oil incorporated during storage. Int. Aquat. Res. 8: 227-238.

Nowzari, F., Shábanpour, B. and Ojagh, S. M. 2013. Comparison of chitosan–gelatin composite and bilayer coating and film effect on the quality of refrigerated rainbow trout. Food Chem. 141: 1667-1672.

Rahman, M. S., Al-Saidi, G. S. and Guizani, N. 2008. Thermal characterisation of gelatin extracted from yellowfin tuna skin and commercial mammalian gelatin. Food Chem. 108: 472-481.

Sahraee, S., Milani, J. M., Ghanbarzadeh, B. and Hamishehkar, H. 2017. Effect of corn oil on physical, thermal, and antifungal properties of gelatin-based nanocomposite films containing nano chitin. LWT-Food Sci. Technol. 76: 33-39.

Shiku, Y., Hamaguchi, P. Y., Benjakul, S., Visessanguan, W. and Tanaka, M. 2004. Effect of surimi quality on properties of edible films based on Alaska pollack. Food Chem. 86: 493-499.

Tang, C.-H., Xiao, M.-L., Chen, Z., Yang, X.-Q. and Yin, S.-W. 2009. Properties of cast films of vicilin-rich protein isolates from *Phaseolus legumes*: Influence of heat curing. LWT-Food Sci. Technol. 42: 1659-1666.

Tongnuanchan, P., Benjakul, S. and Prodpran, T. 2012. Properties and antioxidant activity of fish skin gelatin film incorporated with citrus essential oils. Food Chem. 134: 1571-1579.

Tongnuanchan, P., Benjakul, S. and Prodpran, T. 2013. Physico-chemical properties, morphology and antioxidant activity of film from fish skin gelatin incorporated with root essential oils. J. Food Eng. 117: 350-360.

Tongnuanchan, P., Benjakul, S. and Prodpran, T. 2014. Structural, morphological and thermal behaviour characterisations of fish gelatin film incorporated with basil and citronella essential oils as affected by surfactants. Food Hydrocolloid. 41: 33-43.

Tongnuanchan, P., Benjakul, S., Prodpran, T. and Nilsuwan, K. 2015. Emulsion film based on fish skin gelatin and palm oil: Physical, structural and thermal properties. Food Hydrocolloid. 48: 248-259.

Tongnuanchan, P., Benjakul, S., Prodpran, T., Pisuchpen, S. and Osako, K. 2016. Mechanical, thermal and heat sealing properties of fish skin gelatin film containing palm oil and basil essential oil with different surfactants. Food Hydrocolloid. 56: 93-107.

Vanin, F. M., Sobral, P. J. A., Menegalli, F. C., Carvalho, R. A. and Habitante, A. M. Q. B. 2005. Effects of plasticizers and their concentrations on thermal and functional properties of gelatin-based films. Food Hydrocolloid. 19: 899-907.

Wang, W., Liu, Y., Jia, H., Liu, Y., Zhang, H., He, Z. and Ni, Y. 2017. Effects of Cellulose Nanofibers Filling and Palmitic Acid Emulsions Coating on the Physical Properties of Fish Gelatin Films. Food Biophys. 12: 23-32.

Yi, J. B., Kim, Y. T., Bae, H. J., Whiteside, W. S. and Park, H. J. 2006. Influence of transglutaminase-induced cross-linking on properties of fish gelatin films. J. Food Sci. 71: E376-E383.

Yong Cho, S., Park, J.-W. and Rhee, C. 2002. Properties of laminated films from whey powder and sodium caseinate mixtures and zein layers. LWT-Food Sci. Technol. 35: 135-139.

Yuan, Y. and Lee, T. R. 2013. Contact Angle and Wetting Properties. *In* Surface Science Techniques. (Bracco, G. and Holst, B., eds.). p. 3-34. Springer Berlin Heidelberg. Berlin, Heidelberg.

CHAPTER 3

PHYSICAL/THERMAL PROPERTIES AND HEAT SEAL ABILITY OF BILAYER FILMS BASED ON FISH GELATIN AND POLY(LACTIC ACID)

3.1 Abstract

Bilayer films of fish gelatin film (GF) and poly(lactic acid) film (PLAF) with different GF/PLAF layer thickness ratios (9:1, 8:2, 7:3, 6:4 and 5:5) were prepared by casting and characterized. Bilayer films exhibited lower tensile strength (TS) but higher elongation at break (EAB) than PLAF ($P < 0.05$). All bilayer films showed lower water vapor permeability (WVP) and transparency, compared to GF. Bilayer films had the less barrier property toward UV light transmission, especially with increasing PLAF layer thickness ratio. All bilayer films exhibited better oxygen barrier property (oxygen permeability of 5.07-5.88 $\times 10^{-18}$ mol m^{-1} s^{-1} Pa^{-1}) than PLAF and GF layer thickness had no impact on oxygen permeability of resulting bilayer films. Based on scanning electron microscopic (SEM) study, all films showed smooth surface and two layers of cross-section were observed for all bilayer films. Bilayer films were heat sealable. The lowest seal strength and seal efficiency were attained for film with GF/PLAF layer thickness ratio of 5:5 ($P < 0.05$). DSC analysis revealed that the GF/PLAF (6:4) bilayer film exhibited two distinct endothermic peaks, corresponding to the melting transition of gelatin and PLA. Thus, the mechanical and barrier properties as well as heat seal ability of bilayer films were determined by the thickness ratios of GF and PLAF layers.

3.2 Introduction

Polymeric materials for packaging applications have been considered carefully, due to the constraints and regulations related with primary and postconsumer plastic waste management. Environmentally sound materials based on naturally occurring biodegradable polymers, such as carbohydrates, lipids, and proteins have been searched and utilized (Tromp, 1995). Gelatin is one of the important biopolymers widely used in the manufacture of gel desserts in food industries, hard/soft capsules in

pharmaceutical industries and edible films in packaging industries (Choi and Regenstein, 2000). Gelatin is derived from the fibrous insoluble collagen, which is the principal constituent of animal skin, bone, and connective tissue. Gelatin is produced via thermal denaturation or partial hydrolysis of native collagen with molecular weights from 3 to 200 kDa, depending on the raw material used and the extraction conditions (Lacroix and Cooksey, 2005). Gelatin edible films, with high tensile strength and low deformation at break, from bovine and porcine skin were prepared (Sobral *et al.*, 2001). Fish skin gelatin can also be used as film forming material, which showed an excellent oxygen barrier property (Nilsuwan *et al.*, 2016). However, gelatin-based film is still encountering poor barrier property toward water vapor migration, due to the hydrophilic nature of gelatin and the plasticizer required for film production. This restricts their uses as food packing materials (Hoque *et al.*, 2011a). As a consequence, several strategies have been proposed to improve the moisture resistance of gelatin–based films. Chemical and enzymatic crosslinking have been employed to improve properties of gelatin films (Bigi *et al.*, 2001; de Carvalho and Grosso, 2004). Lamination can be another means to improve the performance of polymeric films by combining the properties of different films into one sheet (Rakotonirainy and Padua, 2001). In general, the outer layers impart moisture resistance and mechanical stability, while the inner one acts as a gas barrier (Fang *et al.*, 2005). Among promising biopolymers, poly(lactic acid) (PLA) obtained from sugar feedstock, corn, etc., has gained increasing attention as renewable and readily biodegradable biomaterial (Cabedo *et al.*, 2006). This aliphatic polyester features high strength, high modulus, good process ability and complete biodegradation. PLA being classified as GRAS (Generally Recognized As Safe, GRAS) (Martino *et al.*, 2009) has been used for food packaging applications. Owing to the superior properties of PLA film, it has been used in lamination with other film to overcome drawback (Rhim *et al.*, 2007). Consequently, laminated films with improved properties can be produced. Recently bilayer film based on olive flounder skin gelatin (OSG) and PLA at a ratio of 1:1 (v/v) has been developed (Lee and Song, 2017). OSG/PLA bilayer film provided desirable barrier properties and the mechanical properties of OSG film were improved via lamination with PLA film. Nevertheless, bilayer films with different thickness layer ratios mostly exhibit varying properties. Nilsuwan *et al.* (2017) reported that properties of gelatin (GF)/emulsion

(EF) bilayer film were governed by thickness layer ratios of both films. Nevertheless, no information regarding the impact of gelatin film/PLA thickness ratio on the properties of bilayer films exists.

3.3 Objective

To determine properties of bilayer film based on fish gelatin film (GF) and poly(lactic) film (PLAF) with different layer thickness ratios.

3.4 Materials and methods

3.4.1 Materials

Fish gelatin produced from tilapia skin (~240 bloom) was procured from Lapi Gelatine S.p.A (Empoli, Italy). Poly(lactic acid) (4032D, extrusion grade, Mn = 88,500 g/mol and Mw/Mn = 1.8) with the pellet form was obtained from Nature Work Co. Ltd. (Blair, NE, USA). Chloroform and glycerol were procured from Lab-Scan (Bangkok, Thailand) and Merck (Darmstadt, Germany), respectively. All chemicals were of analytical grade.

3.4.2 Preparation of film forming solutions

Fish gelatin solution was prepared according to the method of Nilsuwan *et al.* (2016). Gelatin powder was mixed with distilled water to obtain the protein concentration of 3.5% (w/v). The mixture was heated at 70 °C for 30 min with continuous stirring to completely solubilize gelatin. Glycerol at a concentration of 30% (w/w, based on protein content) was added into solution. The resulting solution was termed as ‘gelatin film forming solution; GFFS’. To prepare PLA solution, PLA resin was dissolved in chloroform to obtain a final concentration of 5% (w/v). The solution was stirred at room temperature for 3 h using magnetic stirrer (C-MAG HS-7, IKA®-Werke GmbH & Co. KG, Staufen, Germany). The obtained solution was referred to as ‘PLA solution; PLAS’. Both aforementioned solutions were used for film preparation.

3.4.3 Preparation of GF/PLAF bilayer films

GF/PLAF bilayer films with different layer thickness ratios were prepared. The thickness of films prepared from GFFS and PLAS, named as 'fish gelatin film (GF)' and 'PLA film (PLAF)', respectively. The GFFS:PLAS at the amounts of 86.6:13.2, 76.6:27.5, 66.5:41.7, 56.5:56.0 and 46.4:70.3 (mL/mL) were used. The amounts of solutions were estimated from the plot between the volume of GFFS or PLAS (mL) and thickness of the resulting films (mm) to obtain the layer thickness ratios of 9:1, 8:2, 7:3, 6:4 and 5:5, respectively. All the films were expected to have the final thickness of approximately 0.10 mm. GF and PLAF with the thickness of 0.10 mm were also prepared and used as the control films. Briefly, GFFS was firstly cast onto a square stainless plate (20×20 cm^2) and air-blown for 24 h at 25 °C and 60 ± 5% relative humidity (RH). Thereafter, PLAS with a known volume was overlaid on GF previously formed to obtain the designated final thickness ratios. After the second casting, the samples were evaporated at room temperature (25 ± 2 °C) for 48 h prior to drying at 25 ± 2 °C and 50 ± 5% RH for 48 h in an environmental chamber. All the films were peeled off and subjected to analyses.

3.4.4 Determination of films

Bilayer films were subjected to analyses in comparison with GF and PLAF.

3.4.4.1 Film thickness

The thickness of film was measured using a micrometer (Mitutoyo, Model ID-C112PM, Serial No. 00320, Mitutoyo Corp., Kawasaki-shi, Japan). Five random locations around each film of ten film samples were used for determination of average thickness.

3.4.4.2 Mechanical properties

Prior to testing, films were conditioned for 48 h at 25 ± 2 °C and 50 ± 5% RH. Tensile strength (TS) and elongation at break (EAB) were determined as

described by Iwata *et al.* (2000) using the Universal Testing Machine (Lloyd Instrument, Hampshire, UK) equipped with tensile load cell of 100 N. Ten samples (20×50 mm^2) with an initial grip length of 30 mm were used for testing. Cross-head speed was set at 30 mm/min. Tensile strength (MPa) was calculated by dividing the maximum load (N) necessary to pull the sample film apart by the cross-sectional area (m^2). Average thickness of the film strip was used to estimate the cross-sectional area of the sample. Percentage elongation at break was calculated by dividing film elongation at the moment of rupture by the initial grip length of samples, followed by multiplying with 100.

3.4.4.3 Water vapor permeability (WVP)

WVP was measured using a modified ASTM method (ASTM, 1989) as modified by Shiku *et al.* (2004). Bilayer films with the GF layer facing down were sealed on an aluminium permeation cup containing dried silica gel (0% RH) with silicone vacuum grease and a rubber gasket to hold the films in place. The cups were placed in an environmental chamber at 25 ± 2 °C and 50 ± 5% RH. The cups were weighed at 1-h interval over a 10-h period. WVP of the film was calculated as follows:

$$\text{WVP (g m}^{-1}\text{s}^{-1}\text{Pa}^{-1}\text{)} = wl\,A^{-1}\,t^{-1}(P_2\text{-}P_1)^{-1}$$

where w is the weight gain of the cup (g); l is the film thickness (m); A is the exposed area of film (m^2); t is the time of gain (s); P_2-P_1 is the vapor pressure difference across the film (1583.7 Pa at 25 °C).

3.4.4.4 Oxygen permeability (OP)

OP of films was measured according to the ASTM D3985-05 method. An Oxygen Permeation Analyzer (Illinois model 8000, Illinois Instruments Inc., Johnsburg, IL, USA) was used to measure oxygen transmission rate (OTR) through the film. Each film was placed on a stainless steel mask. The mask was then placed in a test cell and exposed to an oxygen atmosphere flow on the PLA film side and a nitrogen atmosphere flow on the GF side. OTR was measured at 25 °C and 50% RH (Nilsuwan

et al., 2016). The film was allowed to equilibrate for 10 h before measurements. OP was calculated using following equation:

$$\text{OP (mol m}^{-1}\text{s}^{-1}\text{Pa}^{-1}) = \text{OTR } l\, \Delta P^{-1}$$

where OTR is the oxygen transmission rate (mol/m^2.s); l is the film thickness (m); ΔP is the partial pressure of oxygen (1.013×10^5 Pa at 25 °C).

3.4.4.5 Color

Film samples were subjected to color measurement using a CIE colorimeter (Hunter associates laboratory, Inc., Reston, VA, USA). D_{65} (day light) and a measure cell with opening of 30 mm was used. The color of the films was expressed as L^* -value (lightness), a^* -value (redness/greenness) and b^* -value (yellowness/blueness). Total difference of color (ΔE^*) was calculated as follows (Gennadios *et al.*, 1996):

$$\Delta E^* = \sqrt{(\Delta L^*)^2 + (\Delta a^*)^2 + (\Delta b^*)^2}$$

where ΔL^*, Δa^* and Δb^* are the differences between the color parameter of the samples and those of the white standard (L^* = 92.82, a^* = -1.24, b^* = 0.46).

3.4.4.6 Light transmittance and transparency

The light transmission of films was measured at the ultraviolet and visible range (200-800 nm) using a UV-vis spectrophotometer (UV-1800, Shimadzu, Kyoto, Japan) according to the method of Shiku *et al.* (2004). The transparency value of film was calculated using the following equation (Han and Floros, 1997):

$$\text{Transparency value} = -\log T_{600}\, x^{-1}$$

where T_{600} is the fractional transmission at 600 nm and x is the film thickness (mm). The greater transparency value represents the lower transparency of film.

3.4.4.7 Film microstructure

Morphology of the upper surface (PLA surface) and cross-section of film samples was visualized using a scanning electron microscope (SEM) (Quanta 400, FEI, Eindhoven, the Netherlands). For cross-section, samples were fractured under liquid nitrogen prior to visualization. Then, the samples were mounted on bronze stub and sputtered with gold (Sputter coater SPI-Module, West Chester, PA, USA) in order to make the sample conductive. The photographs were taken at an acceleration voltage of 20 kV.

3.4.4.8 Seal ability

Seal strength and seal efficiency were determined as detailed by Tongnuanchan *et al.* (2016). Film samples were cut into strips (25×20 mm^2). Two strips of bilayer films were faced together, in which the GF sides of both films were heat-sealed using an impulse sealer with a magnet Model ME-300HIM (S.N.MARK Ltd., Park, Nonthaburi, Thailand) at 150 ± 0.5 °C for 1.25 s, followed by cooling for 1.50 s. The width of seal area was 2 mm.

Before testing, all sealed film samples were conditioned at 25 ± 2 °C and 50 ± 5% relative humidity (RH) for 48 h. The heat-seal strength was estimated using the peel test. The peel strength and seal efficiency of the heat-sealed films were determined according to the Standard ASTM F-88 (ASTM., 2001) with slight modifications using Universal Testing Machine (Lloyd Instruments, Hampshire, UK) at 25 ± 2 °C and 50 ± 5% RH. Each leg of the sealed film was clamped to a 100 N static load cell of the machine, in which each end of the sealed film was held perpendicularly to the direction of the pull. The distance between the clamps (grip length) was 50 mm. The samples were subjected to tensile loaded at 100 N until seal failure was obtained. Both seal strength and seal efficiency were calculated as follows:

$$\text{Seal strength (N/m)} = \text{Peak force/Film width}$$

$$\text{Seal efficiency (\%)} = (\text{Peak force/Tensile force}) \times 100$$

where tensile force is the force (N) obtained from tensile strength testing and peak force (N) is the maximum force obtained from seal testing.

3.4.4.9 Characterization of the selected films

The selected films (GF, PLAF and GF/PLAF (6:4) bilayer films) were further characterized.

3.4.4.9.1 Differential scanning calorimetry

Thermal properties of selected films were determined using a differential scanning calorimeter (DSC) (Perkin Elmer, Model DSC-7, Norwalk, CT, USA) as described by (Nuthong *et al.*, 2009). Temperature calibration was performed using the indium thermogram. Film samples (2-5 mg) were accurately weighed into aluminium pans, hermetically sealed, and scanned over the temperature range of -40 to 180 °C, with a heating rate of 5 °C/min. An empty aluminium pan was used as the reference. The maximum transition temperature was estimated from the endothermic peak of the DSC thermogram and transition enthalpy was determined from the area under the endothermic peak.

3.4.4.9.2 Attenuated total reflectance-Fourier transform infrared (ATR-FTIR) spectroscopy

The selected films were scanned with a Bruker Model Equinox 55 FTIR spectrometer (Bruker Co., Ettlingen, Germany) equipped with a horizontal ATR Trough plate crystal cell (45° ZnSe; 80 mm long, 10 mm wide and 4 mm thick) (PIKE Technology Inc., Madison, WI, USA) at 25 °C (Nuthong *et al.*, 2009). Films were placed onto the crystal cell and the cell was clamped into the mount of FTIR spectrometer. The spectra in the range of 650–4000 cm^{-1} with automatic signal gain were collected in 32 scans at a resolution of 4 cm^{-1} and were ratioed against a background spectrum recorded from the clean empty cell at 25 °C.

3.4.5 Statistical analysis

All experiments were run in triplicate with different three lots of films. Data were subjected to analysis of variance (ANOVA) and mean comparisons were carried out by the Duncan's multiple range test. Analysis was performed using the SPSS package (SPSS for windows, SPSS Inc., Chicago, IL, USA).

3.5 Results and discussion

3.5.1 Properties of bilayer films as affected by GF/PLAF layer thickness ratios

3.5.1.1 Thickness of bilayer films

Average thickness of bilayer films with different GF/PLAF layer thickness ratios is shown in Table 9. All films showed the similar thickness ($P > 0.05$) in the range of 0.100-0.102 mm.

Table 9. Thickness, mechanical properties, water vapor and oxygen permeabilities of bilayer films with different GF/PLAF layer thickness ratios.

GF/PLAF	Thickness (mm)	TS (MPa)	EAB (%)	WVP ($\times 10^{-11}$ g m^{-1} s^{-1} Pa^{-1})	OP ($\times 10^{-18}$ mol m^{-1} s^{-1} Pa^{-1})
GF	0.101 ± 0.002 a	24.23 ± 1.01 c	36.27 ± 2.37 a	7.68 ± 0.08 a	4.94±0.09 b
9:1	0.101 ± 0.001 a	16.47 ± 0.41 e	31.87 ± 0.75 b	4.67 ± 0.14 b	5.07±0.10 b
8:2	0.102 ± 0.001 a	20.69 ± 1.62 d	27.61 ± 2.89 c	3.28 ± 0.18 c	5.23±0.08 b
7:3	0.100 ± 0.001 a	23.85 ± 1.05 c	26.86 ± 3.05 c	2.96 ± 0.19 d	5.32±0.05 b
6:4	0.101 ± 0.001 a	23.35 ± 0.92 c	20.20 ± 2.90 d	2.70 ± 0.11 e	5.59±0.07 b
5:5	0.101 ± 0.001 a	27.23 ± 0.29 b	11.60 ± 0.80 e	2.65 ± 0.04 e	5.88±0.09 b
PLAF	0.102 ± 0.001 a	31.79 ± 2.14 a	8.89 ± 0.75 f	2.15 ± 0.13 f	211.51±7.10 a

Results are given as the mean ± SD (n = 3).

Different lowercase letters in the same column indicate significant differences ($P < 0.05$).

GF: fish gelatin film; PLAF: poly(lactic acid) film; TS: Tensile strength; EAB: Elongation at break; WVP: Water vapor permeability; OP: Oxygen permeability

3.5.1.2 Mechanical properties

Mechanical properties of bilayer films having different GF/PLAF layer thickness ratios expressed as tensile strength (TS) and elongation at break (EAB) are shown in Table 9. The highest TS (31.79 MPa) was found for PLA film ($P < 0.05$), compared to other films. This result was in agreement with Lee and Song (2017) who reported that PLA film had higher TS than olive flounder skin gelatin (OSG) film and OSG/PLA bilayer film. PLA film was brittle with high TS (45.01 MPa) and low elongation at break (8.57%) (Martino *et al.*, 2009). It was noted that GF was plasticized with glycerol and generally had low TS, but high EAB (Jongjareonrak *et al.*, 2006). Overall, TS of bilayer films was increased with increasing PLA layer thickness ratios ($P < 0.05$). The bilayer film with GF/PLAF layer thickness ratios of 6:4 and 5:5 had higher TS, compared to GF ($P < 0.05$). The result indicated that PLA layer directly contributed to the strength of bilayer films. TS of SPS/PLA (sugar palm starch/PLA) bilayer film was increased as PLA layer became thicker (Sanyang *et al.*, 2016). PLA layer served as the load-bearing phase (Sanyang *et al.*, 2016). However, TS of bilayer film was lower than that of GF ($P < 0.05$) when the GF/PLAF layer thickness ratios of 9:1 and 8:2 were used. However, the ratios of 7:3 and 6:4 yielded the bilayer films with similar TS to GF ($P > 0.05$). Insufficient thickness of PLA layer plausibly caused the decreased strength of resulting bilayer films as indicated by lowered TS of films. Moreover, GF had higher EAB than PLAF and all bilayer films ($P < 0.05$). The lowering of EAB was generally occurred in bilayer films when thickness of PLAF layer was increased ($P < 0.05$). The lower EAB of bilayer films was associated with the smaller stretch ability of the PLAF layer, thereby enhancing rigidity of resulting bilayer films. Therefore, the mechanical properties of bilayer films were varied, depending on the GF/PLAF layer thickness ratios used.

3.5.1.3 Barrier properties

Water vapor permeability (WVP) and oxygen permeability (OP) of bilayer films in comparison with those of GF and PLAF are shown in Table 9. WVP of PLAF was lower than that of GF by approximately three times ($P < 0.05$). For the bilayer films, in which PLAF layer was exposed to water vapor, WVP was 4.67, 3.28, 2.96, 2.70 and 2.65 $\times 10^{-11}$ g m^{-1} s^{-1} Pa^{-1} when the GF/PLAF layer thickness ratios of 9:1, 8:2, 7:3, 6:4 and 5:5 were used, respectively. It was noted that WVP was decreased as the thickness of PLAF layer of bilayer film increased ($P < 0.05$). Since PLA had higher hydrophobicity in nature than gelatin, increasing proportion of PLA contributed to the lowered WVP of resulting films. All bilayer films showed lower WVP than GF ($P < 0.05$). WVP of bilayer film is generally determined by the thickness and WVP of each film layer (McHugh *et al.*, 1993; Yong Cho *et al.*, 2002). This result indicated that the lamination of PLAF onto GF could enhance water vapor barrier property of the resulting bilayer films, compared to the individual GF.

PLAF had the highest OP (211.51 $\times 10^{-18}$ mol m^{-1} s^{-1} Pa^{-1}) ($P < 0.05$), compared to GF or GF/PLAF bilayer films (Table 9). The result suggested that PLAF showed the poorest oxygen barrier property. Oxygen permeability (OP) of films is used as the index of efficiency in preventing lipid oxidation of packaged fatty foods (Cho *et al.*, 2010). PLA film, which is hydrophobic in nature, had good water vapor barrier property but showed high oxygen permeability (Lee and Song, 2017; Rhim *et al.*, 2006). After lamination with GF, all GF/PLAF bilayer films showed lower OP than PLAF alone ($P < 0.05$). No differences in OP between GF and all bilayer films was noted ($P > 0.05$). Thus, the presence of GF layer in bilayer films effectively prevented the diffusion of oxygen, regardless of GF layer thickness. GF has been known to possess an excellent oxygen barrier property (Lee and Song, 2017; Nilsuwan *et al.*, 2016). Similarly, the olive flounder skin gelatin/PLA bilayer film had a lower OP than PLA film (Lee and Song, 2017). Thus, the lamination of GF to PLAF could enhance the barrier property toward oxygen migration of resulting bilayer films.

3.5.1.4 Color, light transmission and transparency value

The color of bilayer films with different GF/PLAF layer thickness ratios is shown in Table 10. Among all films tested, GF had the highest *b** and Δ*E* * but lowest *L** and *a** ($P < 0.05$). The opposite results were obtained for PLAF. For bilayer films, the higher layer thickness ratio of PLAF increased *L** but decreased *b** of the films. This results indicated that the yellowish color of GF was reduced, but whiteness was augmented by lamination with PLAF layer (Lee and Song, 2017).

Table 10. Color of bilayer films with different GF/PLAF layer thickness ratios.

GF/PLAF	*L**	*a**	*b**	Δ*E**
GF	89.82 ± 0.03 f	-1.43 ± 0.05 c	1.68 ± 0.03 a	3.90 ± 0.04 a
9:1	89.97 ± 0.15 e	-1.37 ± 0.01 b	1.52 ± 0.04 b	3.67 ± 0.20 b
8:2	90.12 ± 0.05 d	-1.36 ± 0.02 b	1.42 ± 0.11 c	3.47 ± 0.08 c
7:3	90.18 ± 0.01 cd	-1.36 ± 0.02 b	1.30 ± 0.01 d	3.38 ± 0.02 cd
6:4	90.24 ± 0.05 bc	-1.35 ± 0.03 b	1.20 ± 0.04 e	3.27 ± 0.05 de
5:5	90.29 ± 0.03 b	-1.33 ± 0.03 b	1.14 ± 0.03 e	3.22 ± 0.04 e
PLAF	90.53 ± 0.05 a	-1.26 ± 0.03 a	0.78 ± 0.06 f	2.85 ± 0.07 f

Results are given as the mean ± SD ($n = 3$).

Different lowercase letters in the same column indicate significant differences ($P < 0.05$). GF: fish gelatin film; PLAF: poly(lactic acid) film.

Light transmission at selected wavelengths from 200 to 800 nm in UV and visible ranges and transparency value of bilayer films in comparison with GF and PLAF are presented in Table 11. In general, GF had a good barrier property toward UV light (200–280 nm). Light transmission at 280 nm of GF was the lowest (24.52%), whereas the value increased in bilayer films (25.90 to 42.89%), particularly those with increasing PLAF layer thickness ratios. It was suggested that GF effectively prevented the UV light transmission. High UV light barrier capacity was reported for protein film such as a gelatin films from fish skin (Tongnuanchan *et al.*, 2015). Aromatic amino acid content of protein material played an important role in UV barrier properties of protein films (Jongjareonrak *et al.*, 2006). On the other hand, PLAF and bilayer films showed better barrier properties toward visible light transmission (350-800 nm) than GF. It was found that the increase in PLAF layer ratios of films lowered the visible light

transmission through the film. The differences in light transmission of GF and PLAF could be caused by the differences in interaction or alignment of biopolymer chains in film matrix, which determined the light transmission of the films (Jongjareonrak *et al.*, 2008). In general, bilayer films exhibited higher transparency value as the PLAF layer thickness ratio was increased. Among all films tested, GF had the lowest transparency value, indicating that it was the most transparent film. Therefore, the lamination of PLAF with GF affected the color and light transmission of bilayer films and GF/PLAF layer thickness ratio was another key factor influencing color and transparency of films.

Table 11. Light transmission and transparency value of bilayer films with different GF/PLAF layer thickness ratios.

GF/PLAF	Light transmission (%) at different wave number (nm)								Transparency value
	200	280	350	400	500	600	700	800	
GF	0.00	24.52	86.51	89.09	90.86	91.42	91.61	91.76	0.39 ± 0.00 e
9:1	0.00	25.90	85.97	88.75	90.44	91.11	91.48	91.73	0.40 ± 0.02 de
8:2	0.00	30.44	84.97	88.95	90.43	91.01	91.28	91.46	0.40 ± 0.01 de
7:3	0.00	34.16	84.48	87.84	89.93	90.71	91.11	91.27	0.42 ± 0.02 cd
6:4	0.00	37.91	84.91	87.87	89.77	90.45	90.81	91.08	0.43 ± 0.03 c
5:5	0.00	42.89	83.22	86.28	88.67	89.79	90.37	90.84	0.46 ± 0.01 b
PLAF	0.00	69.97	81.10	83.78	86.25	87.66	88.56	89.18	0.56 ± 0.03 a

Results are given as the mean ± SD (n = 3).

Different lowercase letters in the same column indicate significant differences ($P < 0.05$). GF: fish gelatin film; PLAF: poly(lactic acid) film.

3.5.1.5 Scanning electron microscopy

SEM micrographs of the upper surface and freeze-fractured cross section of bilayer films with different GF/PLAF layer thickness ratios, GF and PLAF are illustrated in Figure 11. The smooth and homogenous surface was observed for all film samples. GF and PLAF generally has regular and smooth surface (Sanyang *et al.*, 2016). For the cross-section, the individual GF and PLAF typically showed the dense and compact structure. As expected, the cross section of bilayer films showed two layers including upper (PLAF) and lower (GF) layers with various thickness (Figure 11). GF layer was firstly cast and PLAS was overlaid cast on the firstly formed GF. The

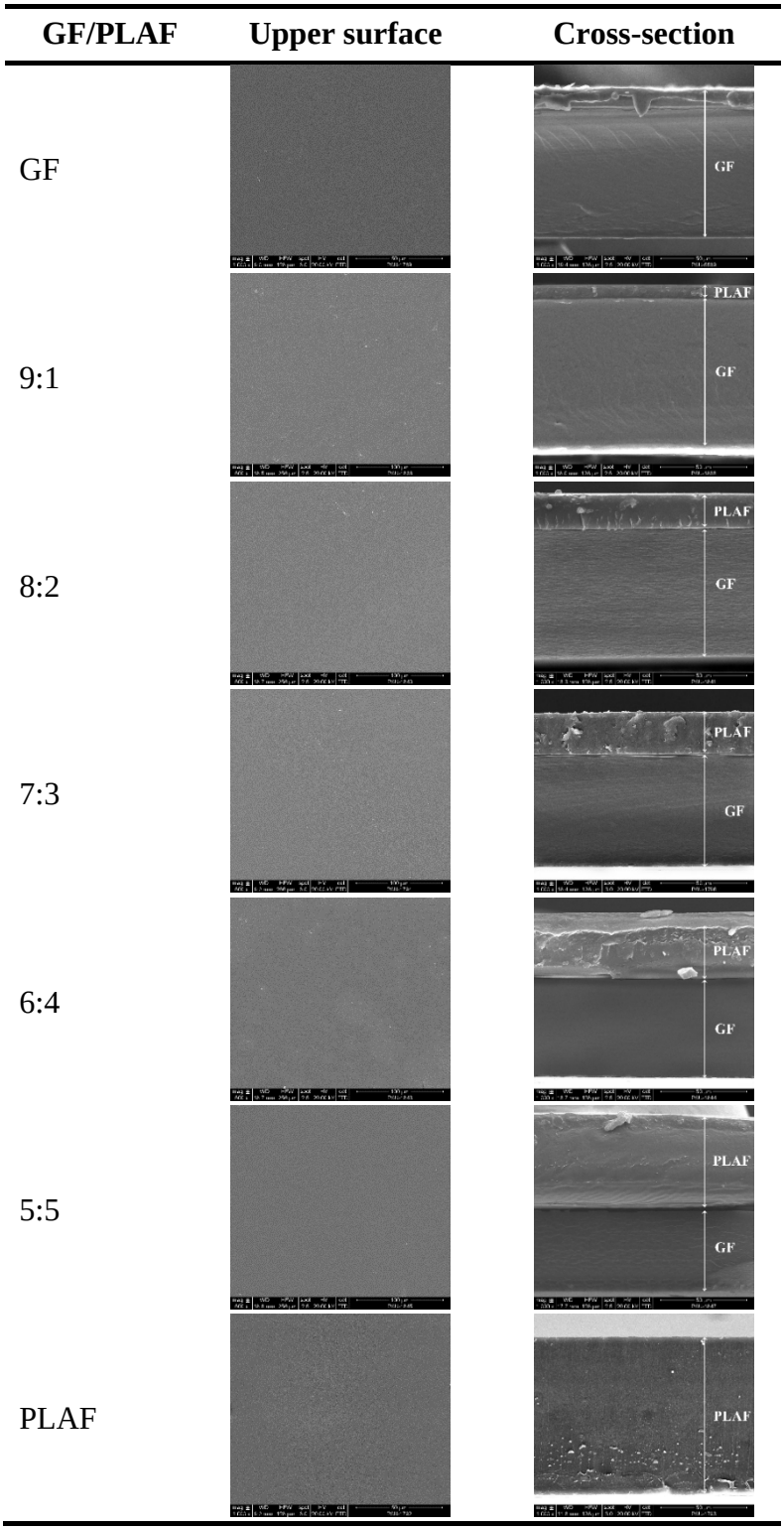

Figure 11. SEM micrographs of upper surface (500×) and cross-section (1000×) of bilayer films with different GF/PLAF layer thickness ratios. GF: fish gelatin film; PLAF: poly(lactic acid) film.

thicker PLAF layer could be easily observed when the PLAF layer thickness ratio was increased. No separation between PLAF and GF layers was noticeable. SEM observations of the cross section of bilayer films revealed that the PLAF layer was tightly bonded to the GF layer, yielding a relatively compact morphology with no obvious interface separation between layers. This result indicated that casting technique used in the present study favored the bridging between layers of both films. Similar result was reported for gelatin-PLA multi-layered film prepared by casting (Nagarajan *et al.*, 2017). Thus, bilayer films having different GF/PLAF layer thickness ratios with good adhesion between layers could be developed.

3.5.1.6 Seal strength and seal efficiency

Seal strength and seal efficiency of GF, PLAF and bilayer films with different GF/PLAF layer thickness ratios are shown in Table 12. During heat sealing process, the surface of the two films underwent melting induced by the introduced heat. This could promote the interfacial interactions across the contact surfaces, thus yielding the sufficient seal strength to the sealed film (Tongnuanchan *et al.*, 2016). All film samples were heat sealable. PLAF showed the higher seal strength and seal efficiency, compared with GF ($P < 0.05$). For bilayer films, the decreases in seal strength and seal efficiency were noticeable when PLAF layer thickness ratios increased ($P < 0.05$). GF side (bottom part of film) of one film was attached to the GF side of another film prior to sealing. During the sealing, GF layers of both films were molten by heat and the molten surfaces of both films were merged and solidified as the single matric after cooling (Nilsuwan *et al.*, 2017). As a result, seal was formed. The seal strength and seal efficiency of bilayer films were therefore affected by the GF/PLAF layer thickness ratios.

Table 12. Seal strength and seal efficiency for peel test of bilayer films with different GF/PLAF layer thickness ratios.

GF/PLAF	Sealed films*	Seal strength (N/m)	Seal efficiency (%)
GF	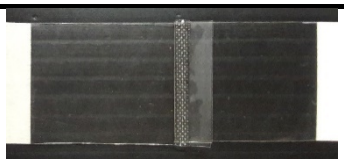	1216.2 ± 89.03 b	49.69 ± 3.64 c
9:1	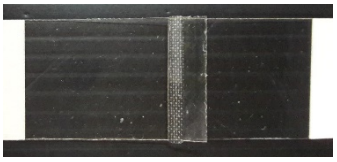	1123.42 ± 19.79 bc	67.55 ± 1.19 a
8:2	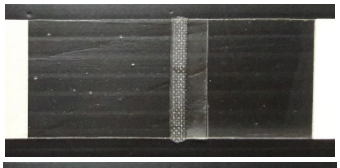	1115.17 ± 11.38 bc	53.05 ± 0.54 c
7:3	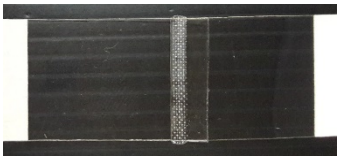	1074.13 ± 91.86 bc	44.84 ± 3.83 d
6:4	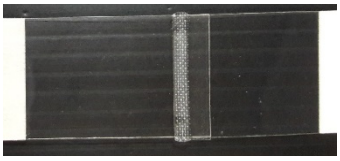	1037.9 ± 11.09 cd	44.21 ± 0.47 d
5:5	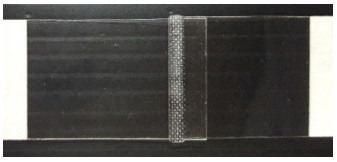	942.12 ± 41.85 d	34.16 ± 1.52 e
PLAF	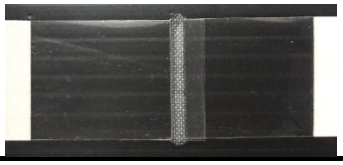	1472.78 ± 53.85 a	61.51 ± 1.39 b

Results are given as the mean ± SD (n = 3).

Different lowercase letters in the same column indicate significant differences ($P < 0.05$). GF: fish gelatin film; PLAF: poly(lactic acid) film.

*Sealing of bilayer films was conducted via facing GF layers of two strips.

3.5.2 Characteristics of the selected GF/PLAF bilayer film

3.5.2.1 Thermal properties

DSC thermograms of the 1st and 2nd-heating scans of GF, PLAF and selected bilayer film (GF/PLAF, 6:4) are shown in Figure 12. From thermogram of the 1st heating scan (from -40 to 180 °C), glass transition temperatures (T_g) of GF and PLAF were 54.08 and 33.25 °C, respectively, representing glass state of plasticized gelatin-rich phase and PLA. The bilayer films had higher T_g (43.09 °C), compared to PLAF but lower than T_g of GF. The T_g of PLAF was lower than the reported values (55-60 °C) (Drumright *et al.*, 2000). This result might be associated with the plasticizing effect of chloroform solvent remaining in the film (Rhim *et al.*, 2006). Additionally, varying molecular weights of PLA were postulated in different studies. Cold crystallization transition temperatures ($T_{c,c}$) were observed for PLAF and bilayer films (GF/PLAF: 6:4) at 88.70 and 89.07 °C, respectively. For melting/order-phase transition, thermograms of all films exhibited endothermic transition peak at temperature (T_{max}) ranging from 145.11 to 156.28 °C. For individual films, $T_{max,1}$ (145.11 °C) was found in GF, whereas PLAF showed the $T_{max,2}$ (156.28 °C). The difference in the thermal transition characteristics is mainly attributed to the component materials of the bilayer film (González and Alvarez Igarzabal, 2013). As expected, GF/PLAF (6:4) bilayer film exhibited two distinct endothermic peaks at 145.54 ($T_{max,1}$) and 154.40 °C ($T_{max,2}$), most likely corresponding to the melting transition of gelatin and PLA, respectively. The melting transition is generally related with the disruption of ordered or aggregated molecular structure (Jongjareonrak *et al.*, 2006; Tang *et al.*, 2009). Gelatin and PLA molecules could undergo partial renaturation and crystallization, respectively, thereby transforming themselves into a more ordered structure during casting and drying (Hoque *et al.*, 2011b; Rahman *et al.*, 2008). Therefore, the GF/PLAF bilayer film had the different thermal transition characteristics, compared with the single film.

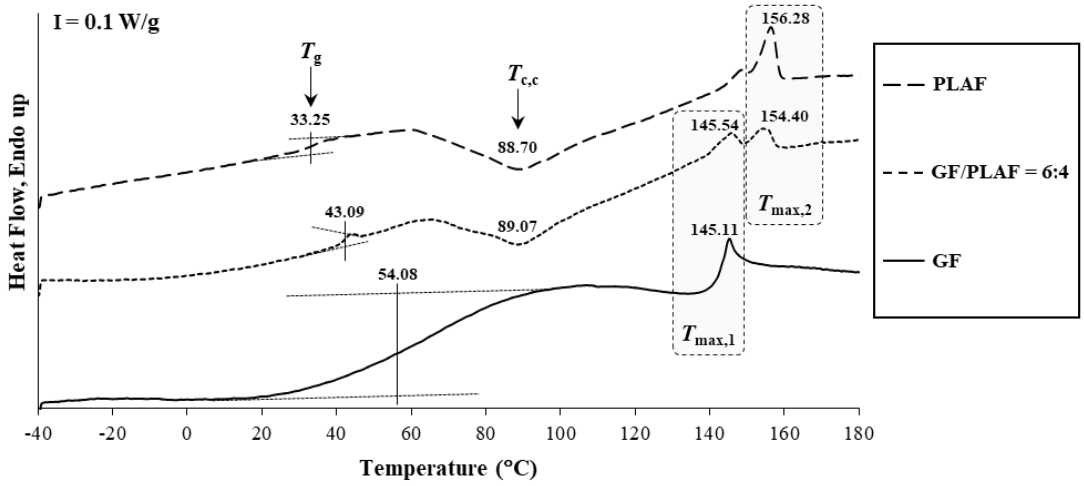

Figure 12. DSC thermograms of GF, PLAF and GF/PLAF (6:4) bilayer films. GF: fish gelatin film; PLAF: poly(lactic acid) film.

3.5.2.2 Attenuated total reflectance-Fourier transform infrared (ATR-FTIR) spectra

FTIR spectra of GF, PLAF and GF/PLAF (6:4) bilayer films are illustrated in Figure 13. GF and GF layer of GF/PLAF bilayer film exhibited major peaks in the amide region. Both GF and GF/PLAF bilayer films had amide-I band at the wavenumber of 1631 cm^{-1}. The amide-I vibration mode is primarily a C=O stretching vibration coupled with the C-N stretch, CCN deformation and in plane N-H bending modes (Aewsiri *et al.*, 2009). The characteristic absorption band of GF and bilayer film in amide-II region was noticeable at the wavenumber of 1546 cm^{-1}, attributing to out-of-plane combination of the N-H in plane bend and the C-N stretching vibration with smaller contributions from the C-O in plane bend and the C-C and N-C stretching vibrations (Aewsiri *et al.*, 2009; Muyonga *et al.*, 2004). GF and bilayer film exhibited the amide-III band at the wavenumber of 1238 cm^{-1}, representing the combination peaks between C-N stretching vibrations and N-H deformation from amide linkages as well as absorptions arising from wagging vibrations from CH_2 groups from the glycine backbone and proline side chains (Aewsiri *et al.*, 2009; Muyonga *et al.*, 2004). The peak situated around 1037 cm^{-1} was related to the interactions arising between plasticizer (OH group of glycerol) and film structure

(Bergo and Sobral, 2007; Tongnuanchan *et al.*, 2016). Amide-A band, arising from the stretching vibrations of the N-H group, appeared at 3288 cm^{-1} for GF and GF layer of bilayer film. Amide-A represents NH-stretching coupled with hydrogen bonding (Doyle *et al.*, 1975). Amide-B was observed at the wavenumber of 3081 cm^{-1} for GF and bilayer films, corresponding to the asymmetric stretching vibration of =C-H as well as $-NH_3^+$. Both GF and GF layer of bilayer film exhibited the peaks with a wavenumber of 2878-2879 cm^{-1} (symmetrical) or 2934-2937 cm^{-1} (asymmetrical), representing C-H stretching vibrations of the $-CH_2$ groups (Kong and Yu, 2007). These characteristic peaks (amide-I, amide-II, amide-III, amide-A and amide-B) of GF and GF layer of bilayer film were not found in the individual PLAF. The IR spectra of PLAF and PLAF layer of bilayer film exhibited peak at 2996-2946 cm^{-1}, corresponding to the C-H stretching of $-CH_3$ characteristic (Ahmed *et al.*, 2016). PLAF and PLAF layer of bilayer film showed the characteristic peaks at 1748 cm^{-1}, representing the -C=O stretching vibration of the ester group of PLA (Li *et al.*, 2012). The asymmetric and symmetric $-CH_3$ deformation vibrational peaks of PLA were observed at the wavenumbers of 1452 and 1360 cm^{-1}, respectively for both PLAF and PLAF layer of bilayer film (Chieng *et al.*, 2013; Nagarajan *et al.*, 2017). In addition, the symmetric C-O-C stretching peak of the PLA ester group was observed at 1181 cm^{-1} for PLAF and PLAF layer of bilayer film. The peaks detected at the wavenumbers of 1128 cm^{-1} for PLAF and PLAF layer of bilayer film were attributed to the stretching vibration of -C-O or -C-OH deformation vibration (Ahmed *et al.*, 2016). Similar characteristic peaks were reported for PLA films (Nagarajan *et al.*, 2017). It was noted that PLAF and PLAF layer of bilayer films showed similar characteristic peaks as analyzed by ATR-FTIR. Since bilayer film contained layers of gelatin and PLA, the characteristic peaks were similar to those of both GF and PLAF. This result suggested that the lamination technique used in the present study did not change the nature of polymer on film surface, while the properties of bilayer film i.e. mechanical and barrier were improved.

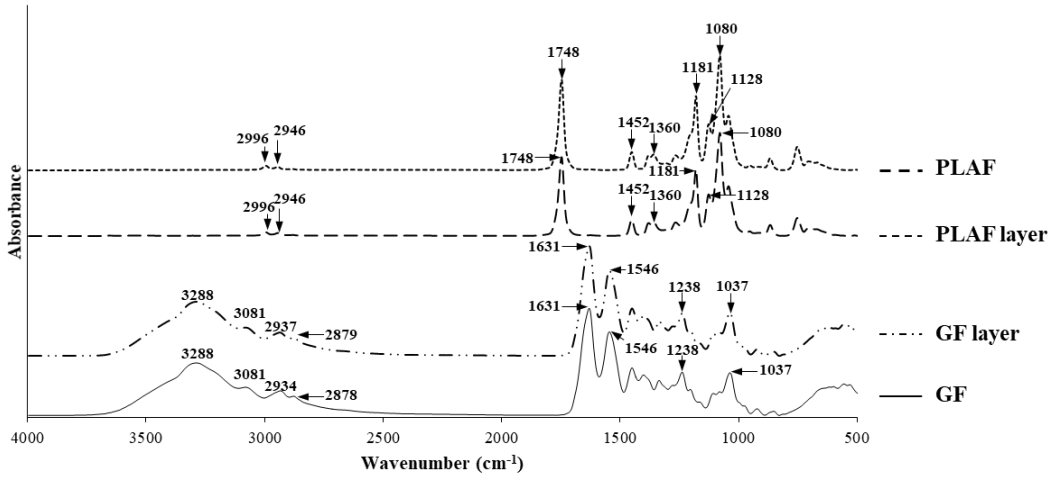

Figure 13. ATR-FTIR of GF, PLAF and GF/PLAF (6:4) bilayer films. GF: fish gelatin film; PLAF: poly(lactic acid) film; PLAF layer: PLAF layer of GF/PLAF (6:4) bilayer film; GF layer: GF layer of GF/PLAF (6:4) bilayer film

3.6 Conclusions

Properties of bilayer film prepared from GF and PLAF were influenced by the GF/PLAF layer thickness ratio. The increasing thickness ratio of PLAF layer increased the water vapor barrier property, while increasing ratio of GF layer increased UV-light barrier properties of bilayer film. All bilayer films showed higher oxygen barrier property than PLAF, but no difference in oxygen permeability was found between all bilayer films and GF. All bilayer films were heat sealable. The seal strength and seal efficiency of bilayer films proportionally increased as the thickness of GF layer increased. Bilayer (GF/PLAF, 6:4) film had improved water vapor barrier property compared to GF. Thus, the developed bilayer films prepared using the appropriate GF/PLAF layer thickness ratio could be further used as the promising biodegradable food packaging.

3.7 References

Aewsiri, T., Benjakul, S. and Visessanguan, W. 2009. Functional properties of gelatin from cuttlefish (*Sepia pharaonis*) skin as affected by bleaching using hydrogen peroxide. Food Chem. 115: 243-249.

Ahmed, J., Hiremath, N. and Jacob, H. 2016. Antimicrobial, rheological, and thermal properties of plasticized polylactide films incorporated with essential oils to inhibit *Staphylococcus aureus* and *Campylobacter jejuni*. J. Food Sci. 81: 419-429.

Bergo, P. and Sobral, P. J. A. 2007. Effects of plasticizer on physical properties of pig skin gelatin films. Food Hydrocolloid. 21: 1285-1289.

Bigi, A., Cojazzi, G., Panzavolta, S., Rubini, K. and Roveri, N. 2001. Mechanical and thermal properties of gelatin films at different degrees of glutaraldehyde cross-linking. Biomaterials. 22: 763-768.

Cabedo, L., Luis Feijoo, J., Pilar Villanueva, M., Lagarón, J. M. and Giménez, E. 2006. Optimization of biodegradable nanocomposites based on a PLA/PCL blends for food packaging applications. Macromol. Symp. 233: 191-197.

Chieng, B. W., Ibrahim, N. A., Yunus, W. M. Z. W. and Hussein, M. Z. 2013. Plasticized poly(lactic acid) with low molecular weight poly(ethylene glycol): Mechanical, thermal, and morphology properties. J. Appl. Polym. Sci. 130: 4576-4580.

Cho, S. Y., Lee, S. Y. and Rhee, C. 2010. Edible oxygen barrier bilayer film pouches from corn zein and soy protein isolate for olive oil packaging. LWT-Food Sci. Technol. 43: 1234-1239.

Choi, S. S. and Regenstein, J. M. 2000. Physicochemical and sensory characteristics of fish gelatin. J. Food Sci. 65: 194-199.

de Carvalho, R. A. and Grosso, C. R. F. 2004. Characterization of gelatin based films modified with transglutaminase, glyoxal and formaldehyde. Food Hydrocolloid. 18: 717-726.

Doyle, B. B., Bendit, E. G. and Blout, E. R. 1975. Infrared spectroscopy of collagen and collagen-like polypeptides. Biopolymers. 14: 937-957.

Drumright, R. E., Gruber, P. R. and Henton, D. E. 2000. Polylactic acid technology. Adv. Mater. 12: 1841-1846.

Fang, J. M., Fowler, P. A., Escrig, C., Gonzalez, R., Costa, J. A. and Chamudis, L. 2005. Development of biodegradable laminate films derived from naturally occurring carbohydrate polymers. Carbohydr Polym. 60: 39-42.

Gennadios, A., Weller, C. L., Hanna, M. A. and Froning, G. W. 1996. Mechanical and barrier properties of egg albumen films. J. Food Sci. 61: 585-589.

González, A. and Alvarez Igarzabal, C. I. 2013. Soy protein – Poly (lactic acid) bilayer films as biodegradable material for active food packaging. Food Hydrocolloid. 33: 289-296.

Han, J. H. and Floros, J. D. 1997. Casting antimicrobial packaging films and measuring their physical properties and antimicrobial activity. J. Plast. Film Sheet. 13: 287-298.

Hoque, M. S., Benjakul, S. and Prodpran, T. 2011a. Effects of partial hydrolysis and plasticizer content on the properties of film from cuttlefish (*Sepia pharaonis*) skin gelatin. Food Hydrocolloid. 25: 82-90.

Hoque, M. S., Benjakul, S., Prodpran, T. and Songtipya, P. 2011b. Properties of blend film based on cuttlefish (*Sepia pharaonis*) skin gelatin and mungbean protein isolate. Int. J. Biol. Macromol. 49: 663-673.

Iwata, K. I., Ishizaki, S. H., Handa, A. K. and Tanaka, M. U. 2000. Preparation and characterization of edible films from fish water-soluble proteins. Fish. Sci. 66: 372-378.

Jongjareonrak, A., Benjakul, S., Visessanguan, W., Prodpran, T. and Tanaka, M. 2006. Characterization of edible films from skin gelatin of brownstripe red snapper and bigeye snapper. Food Hydrocolloid. 20: 492-501.

Jongjareonrak, A., Benjakul, S., Visessanguan, W. and Tanaka, M. 2008. Antioxidative activity and properties of fish skin gelatin films incorporated with BHT and α-tocopherol. Food Hydrocolloid. 22: 449-458.

Kong, J. and Yu, S. 2007. Fourier transform infrared spectroscopic analysis of protein secondary structures. Acta Bioch. Bioph. Sin. 39: 549-559.

Lacroix, M. and Cooksey, K. 2005. Edible films and coatings from animal origin proteins. *In* Innovations in Food Packaging. (Han, J. H., ed.). p. 301-317. Academic Press. London.

Lee, K.-Y. and Song, K. B. 2017. Preparation and characterization of an olive flounder (*Paralichthys olivaceus*) skin gelatin and polylactic acid bilayer film. J. Food Sci. 82: 706-710.

Li, H., Xia, Y., Wu, J., He, Q., Zhou, X., Lu, G., Shang, L., Boey, F., Venkatraman, S. S. and Zhang, H. 2012. Surface modification of smooth poly (L-lactic acid) films for gelatin immobilization. ACS Appl. Mater. Inter. 4: 687-693.

Martino, V. P., Jiménez, A. and Ruseckaite, R. A. 2009. Processing and characterization of poly(lactic acid) films plasticized with commercial adipates. J. Appl. Polym. Sci. 112: 2010-2018.

McHugh, T. H., Avena-Bustillos, R. and Krochta, J. M. 1993. Hydrophilic edible films: Modified procedure for water vapor permeability and explanation of thickness effects. J. Food Sci. 58: 899-903.

Muyonga, J. H., Cole, C. G. B. and Duodu, K. G. 2004. Characterisation of acid soluble collagen from skins of young and adult Nile perch (*Lates niloticus*). Food Chem. 85: 81-89.

Nagarajan, M., Prodpran, T., Benjakul, S. and Songtipya, P. 2017. Properties and characteristics of multi-layered films from tilapia skin gelatin and poly(lactic acid). Food Biophys. 1-12.

Nilsuwan, K., Benjakul, S. and Prodpran, T. 2016. Quality changes of shrimp cracker covered with fish gelatin film without and with palm oil incorporated during storage. Int. Aquat. Res. 8: 227-238.

Nilsuwan, K., Benjakul, S. and Prodpran, T. 2017. Properties, microstructure and heat seal ability of bilayer films based on fish gelatin and emulsified gelatin films. Food Biophys. 1-10.

Nuthong, P., Benjakul, S. and Prodpran, T. 2009. Characterization of porcine plasma protein-based films as affected by pretreatment and cross-linking agents. Int. J. Biol. Macromol. 44: 143-148.

Rahman, M. S., Al-Saidi, G. S. and Guizani, N. 2008. Thermal characterisation of gelatin extracted from yellowfin tuna skin and commercial mammalian gelatin. Food Chem. 108: 472-481.

Rakotonirainy, A. M. and Padua, G. W. 2001. Effects of lamination and coating with drying oils on tensile and barrier properties of zein films. J. Agric. Food Chem. 49: 2860-2863.

Rhim, J.-W., Lee, J. H. and Ng, P. K. W. 2007. Mechanical and barrier properties of biodegradable soy protein isolate-based films coated with polylactic acid. LWT-Food Sci. Technol. 40: 232-238.

Rhim, J.-W., Mohanty, K. A., Singh, S. P. and Ng, P. K. W. 2006. Preparation and properties of biodegradable multilayer films based on soy protein isolate and poly (lactide). Industrial and Engineering Chemistry Research. 45: 3059-3066.

Sanyang, M. L., Sapuan, S. M., Jawaid, M., Ishak, M. R. and Sahari, J. 2016. Development and characterization of sugar palm starch and poly(lactic acid) bilayer films. Carbohydr Polym. 146: 36-45.

Shiku, Y., Hamaguchi, P. Y., Benjakul, S., Visessanguan, W. and Tanaka, M. 2004. Effect of surimi quality on properties of edible films based on Alaska pollack. Food Chem. 86: 493-499.

Sobral, P. J. A., Menegalli, F. C., Hubinger, M. D. and Roques, M. A. 2001. Mechanical, water vapor barrier and thermal properties of gelatin based edible films. Food Hydrocolloid. 15: 423-432.

Tang, C.-H., Xiao, M.-L., Chen, Z., Yang, X.-Q. and Yin, S.-W. 2009. Properties of cast films of vicilin-rich protein isolates from *Phaseolus legumes*: Influence of heat curing. LWT-Food Sci. Technol. 42: 1659-1666.

Tongnuanchan, P., Benjakul, S., Prodpran, T. and Nilsuwan, K. 2015. Emulsion film based on fish skin gelatin and palm oil: Physical, structural and thermal properties. Food Hydrocolloid. 48: 248-259.

Tongnuanchan, P., Benjakul, S., Prodpran, T., Pisuchpen, S. and Osako, K. 2016. Mechanical, thermal and heat sealing properties of fish skin gelatin film containing palm oil and basil essential oil with different surfactants. Food Hydrocolloid. 56: 93-107.

Yong Cho, S., Park, J.-W. and Rhee, C. 2002. Properties of laminated films from whey powder and sodium caseinate mixtures and zein layers. LWT-Food Sci. Technol. 35: 135-139.

CHAPTER 4

PROPERTIES AND ANTIOXIDATIVE ACTIVITY OF FISH GELATIN-BASED FILM INCORPORATED WITH EPIGALLOCATECHIN GALLATE

4.1 Abstract

Antioxidative activity of epigallocatechin gallate (EGCG) was examined. Effect of EGCG at various concentrations (0-5.71 wt %, based on protein content) on the properties of fish gelatin-based films was also investigated. EGCG showed 2,2-Azino-bis (3-ethylbenzothiazoline-6-sulfonic acid) (ABTS) and 2,2-Diphenyl-1-picrylhydrazyl (DPPH) radical scavenging activities, ferric reducing antioxidant power (FRAP), hydrogen peroxide scavenging activity and oxygen radical absorbance capacity (ORAC) of 12.78, 7.68, 11.02, 3.59 and 2.92 mmol Trolox equivalent (TE)/g sample, respectively. Films containing 4.29 and 5.71 wt % EGCG exhibited higher tensile strength (TS) and water vapor permeability (WVP) but lower elongation at break (EAB) and light transmission, compared with the control film ($P < 0.05$). All films incorporated with EGCG showed higher a^*-, b^*- and ΔE^* than the control film ($P < 0.05$). All films had smooth surface. The incorporation of 5.71 wt % EGCG increased glass transition temperature (T_g) of gelatin film. FTIR analysis revealed the interaction between protein and EGCG. Incorporation of EGCG at levels higher than 2.86 wt % yielded more compact films, compared to the control. Higher seal strength and seal efficiency were observed for film incorporated with 5.71 wt % EGCG in comparison with control film ($P < 0.05$). When the migration of EGCG from gelatin film was tested, the highest release of EGCG was found for film containing 5.71 wt % EGCG after 18 days of storage. Therefore, the incorporation of EGCG having antioxidant activity had the impact on properties as well as heat seal ability of gelatin film. The resulting film could be used as antioxidant packaging material.

4.2 Introduction

Consumer concerns of food quality and safety lead to the development of active packaging, which is innovative packaging possessing some functions, particularly for shelf-life extension of food products (Kaewprachu *et al.*, 2015). Active compounds can be incorporated into packaging materials to provide antioxidant and/or antimicrobial agents (Kaewprachu *et al.*, 2015). Among all biomaterials, gelatin is a proteinacious material, which has several advantages. Gelatin has been widely used as a starting material for film formation. Gelatin films have good film forming ability and excellent oxygen barrier properties (Lee and Song, 2017; Nilsuwan *et al.*, 2016). However, gelatin film showed poor water resistance property (Nilsuwan *et al.*, 2016). Phenolic compounds or plant extracts have been incorporated into protein-based film to improve the properties (Maryam Adilah *et al.*, 2018; Nuthong *et al.*, 2009b). Ferulic acid and caffeic acid were added into cold fish gelatin film (Araghi *et al.*, 2015). Gelatin-based film containing oregano or rosemary extracts exhibited higher reducing ability and free radical-scavenging capacity than the control films (Gómez-Estaca *et al.*, 2009). The degree of antioxidant power was generally proportional to the amount of the added extract (Gómez-Estaca *et al.*, 2009). Apart from acting as protein cross-linkers, those phenolic compounds could serve as antioxidant, making the film more active (Gómez-Estaca *et al.*, 2009; Maryam Adilah *et al.*, 2018). Epigallocatechin gallate (EGCG) is one of major flavanols obtained from tea extract, which contained 10-60% of EGCG of dry weight (Zaveri, 2006). EGCG has been reported to exhibit antioxidant activity and play a role in preventing the lipid oxidation in foods (Lu *et al.*, 2010). Due to its antioxidative activity with safety concern, it can be employed as natural antioxidant in packaging, particularly gelatin-based films.

4.3 Objective

To study the effect of EGCG at different concentrations on the physical, thermal properties as well as heat seal ability of fish gelatin-based film. The release of EGCG from film as a function of time was also monitored.

4.4 Materials and methods

4.4.1 Materials

Fish gelatin produced from tilapia skin (~240 bloom) was procured from Lapi Gelatine S.p.A (Empoli, Italy). (-)-epigallocatechin gallate (EGCG) was obtained from Chengdu Biopurify Phytochemicals Ltd., (Sichuan, China). The purity of epigallocatechin gallate was greater than 98% as determined by HPLC. 6-Hydroxy-2,5,7,8-tetramethylchroman-2-carboxylic acid (Trolox) was obtained from Aldrich Chemical Company (Steinheim, Germany). 2,4,6-Tri (2-pyridyl)-S-triazine (TPTZ) was procured from Fluka Chemicals (Buchs, Switzerland). 2,2-diphenyl-1-picryhydrazyl (DPPH), ferrous sulfate ($FeSO_4.7H_2O$), ferric chloride ($FeCl_3.6H_2O$), 2,2-azino-bis-(3-ethylbenzothiazoline-6-sulfonic acid) diammonium salt (ABTS), potassium persulfate, hydrogen peroxide (H_2O_2), 3-(2-pyridyl)-5,6-diphenyl-1,2,4-triazine-4′,4″-disulphonic acid sodium salt (ferrozine) and 2,2′-Azobis (2-amidinopropane) dihydrochloride (AAPH) were purchased from Sigma-Aldrich, Inc. (St. Louis, MO). Glycerol, hydrochloric acid, methanol and ethanol were procured from Merck (Darmstadt, Germany). All chemicals were of analytical grade.

4.4.2 Study on antioxidative activities of epigallocatechin gallate (EGCG)

Antioxidative activities of EGCG were determined by ABTS radical scavenging activity (Binsan *et al.*, 2008), DPPH radical scavenging activity (Brand-Williams *et al.*, 1995), ferric reducing antioxidant power (FRAP) (Benzie and Strain, 1996) and hydrogen peroxide (H_2O_2) scavenging activity (Wettasinghe and Shahidi, 2000). The oxygen radical absorbance capacity (ORAC) was also determined as per method of Kittiphattanabawon *et al.* (2012). The fluorescence decay curves of EGCG (0.05 mg/mL), Trolox (50 mg/mL) and 75 mM phosphate buffer (control) were plotted between relative fluorescence intensity (%) and time (min). All activities were expressed as mmol Trolox equivalent (TE)/g sample.

4.4.3 Effect of EGCG at various concentrations on the properties of fish gelatin-based film

4.4.3.1 Preparation of films

Gelatin films incorporated with EGCG at different concentrations were prepared according to the method of Nuthong *et al.* (2009b) with a slight modification. Fish gelatin powder was dissolved in distilled water to obtain the protein concentration of 3.5% (w/v) and heated at 70 °C for 30 min for complete solubilization. Glycerol at a concentration of 30% (w/w, based on protein content) was used as a plasticizer. Gelatin solution was cooled down to room temperature (28 ± 2 °C). Subsequently, EGCG was added to obtain the final concentrations of 1.43, 2.86, 4.29 and 5.71 wt % (based on protein content). The solution was stirred at room temperature for 1 h and degassed for 5 min using the sonicating bath. The mixture (4 mL) was cast onto a rimmed silicone resin plate (50 × 50 mm^2), air-blown for 12 h at 25 °C, followed by drying in an environmental chamber (Binder GmbH, Tuttlingen, Germany) at 25 ± 0.5 °C and 50 ± 5 % relative humidity (RH) for 48 h. Films were manually peeled off and subjected to analyses.

4.4.3.2 Determination of films

4.4.3.2.1 Film conditioning

Before testing of thickness, mechanical properties, water vapor permeability, color and light transmission, film were conditioned for 48 h at 25 ± 0.5 °C and 50 ± 5% relative humidity (RH). For the rest of characterizations, films were conditioned in a desiccator containing P_2O_5 for 1 week at room temperature (25-30 °C) to obtain the most dehydrated films prior to analyses.

4.4.3.2.2 Film thickness

The thickness of films was measured using a micrometer (Mitutoyo, Model ID-C112PM, Serial No. 00320, Mitutoyo Corp., Kawasaki-shi, Japan). Five

random locations around each film of ten film samples were used for average thickness determination.

4.4.3.2.3 Mechanical properties

Tensile strength (TS) and elongation at break (EAB) were determined as described by Iwata *et al.* (2000) with a slight modification using the Universal Testing Machine (Lloyd Instrument, Hampshire, UK) equipped with tensile load cell of 100 N. Ten film samples (20 × 50 mm^2) with initial grip length of 30 mm were used for testing. Cross-head speed was set at 30 mm/min.

4.4.3.2.4 Water vapor permeability (WVP)

WVP was measured using a modified ASTM method (ASTM, 1989) as modified by Shiku *et al.* (2004). Films were sealed on an aluminium permeation cup containing dried silica gel (0% RH) with silicone vacuum grease and a rubber gasket to hold the films in place. The cups were placed in an environmental chamber at 25 ± 0.5 °C and 50 ± 5% RH. The cups were weighed at 1-h interval over a 10-h period. WVP of the film was calculated as follows:

$$\text{WVP (g m}^{-1}\text{s}^{-1}\text{Pa}^{-1}\text{)} = wl\,A^{-1}\,t^{-1}(P_2\text{-}P_1)^{-1}$$

where w is the weight gain of the cup (g); l is the film thickness (m); A is the exposed area of film (m^2); t is the time of gain (s); P_2-P_1 is the vapor pressure difference across the film (1583.7 Pa at 25 °C).

4.4.3.2.5 Color

Film samples were subjected to color measurement using a CIE colorimeter (Hunter associates laboratory, Inc., Reston, VA, USA). D_{65} (day light) and a measure cell with opening of 30 mm was used. The color of the films was expressed as L^* -value (lightness), a^* -value (redness/greenness) and b^* -value (yellowness/blueness). Total difference of color (ΔE^*) was calculated as follows (Gennadios *et al.*, 1996):

$$\Delta E^* = \sqrt{(\Delta L^*)^2 + (\Delta a^*)^2 + (\Delta b^*)^2}$$

where ΔL^*, Δa^* and Δb^* are the differences between the color parameter of the samples and those of the white standard (L^* = 92.82, a^* = -1.24, b^* = 0.46).

4.4.3.2.6 Light transmittance and transparency

The light transmission of films was measured at the ultraviolet and visible range (200-800 nm) using a UV-vis spectrophotometer (UV-1800, Shimadzu, Kyoto, Japan) according to the method of Shiku *et al.* (2004). The transparency value of film was calculated using the following equation (Han and Floros, 1997):

$$\text{Transparency value} = -logT_{600}\, x^{-1}$$

where T_{600} is the fractional transmission at 600 nm and x is the film thickness (mm). The greater transparency value represents the lower transparency of film.

4.4.3.2.7 Scanning electron microscopic images

Morphology of surface and cross-section of film samples was visualized using a scanning electron microscope (SEM) (Quanta 400, FEI, Eindhoven, the Netherlands). For cross-section, samples were fractured under liquid nitrogen before visualization. Then, the samples were mounted on bronze stub and sputtered with gold (Sputter coater SPI-Module, West Chester, PA, USA) in order to make the sample conductive. The micrographs were taken at an acceleration voltage of 20 kV.

4.4.3.2.8 Heat sealing ability

Seal strength and seal efficiency were determined as detailed by Tongnuanchan *et al.* (2016). Film samples were cut into strips (40 × 20 mm^2). Two strips were faced together and heat-sealed using an impulse sealer with a magnet Model ME-300HIM (S.N.MARK Ltd., Park, Nonthaburi, Thailand) at 150 ± 0.5 °C for 1.25 s, followed by cooling for 1.50 s. The width of seal area was 2 mm. Before testing, all sealed film samples were conditioned at 25 ± 0.5 °C and 50 ± 5% relative humidity (RH) for 48 h. The heat-seal strength was estimated using the peel test. The peel

strength and seal efficiency were determined according to the Standard ASTM F-88 (ASTM, 2001) with slight modifications using Universal Testing Machine (Lloyd Instruments, Hampshire, UK) at 25 ± 0.5 °C and 50 ± 5% RH. The sealed film was clamped to a 100 N static load cell of the machine, in which each end of the sealed film was held perpendicularly to the direction of the pull. The distance between the clamps (grip length) was 50 mm. The samples were subjected to tensile loaded at 100 N until seal failure was obtained. Both seal strength and seal efficiency were calculated as follows:

$$\text{Seal strength (N/m)} = \text{Peak force/Film width}$$

$$\text{Seal efficiency (\%)} = (\text{Peak force/Tensile force}) \times 100$$

where tensile force is the force (N) obtained from tensile strength testing and peak force (N) is the maximum force obtained from seal testing.

4.4.3.2.9 Migration test

Migration test of EGCG from the films was conducted as per the method of Maryam Adilah *et al.* (2018) with some modifications. Film (10 × 30 mm^2) was placed in a screw-cap tube containing 5 mL of 95% (v/v) ethanol (to represent fatty medium). The tube was wrapped with aluminium foil to keep samples in dark. Samples were agitated with orbital shaker (INKUBATOR 1000, Heidolph instruments GmbH & Co.KG, Schwabach, Germany) at a speed of 200 rpm at 25 °C for 24 days. The migration of EGCG into ethanol was monitored by determining total phenolic content (TPC) using Folin Ciocalteu reagent (Slinkard and Singleton, 1977). EGCG solutions (0-250 mg/L) were used as the standards. The release was expressed as mg EGCG equivalent/g film.

EGCG was also identified and quantified by high performance liquid chromatography (HPLC), Waters 2475 (Milford, MA, USA) equipped with a photodiode array detector (Waters 2998, Milford, MA, USA). EGCG was determined by using a Thermo-scientific column (C18, 150 × 4.6 mm, 5 µm). Ethanol added with film showing the higher TPC (5 mL) was flushed with nitrogen gas until the volume of

2 mL was obtained. The concentrated sample was further filtered using a 0.45 µm syringe nylon filter (Agela Technologies, New York). The prepared sample (20 µL) was injected to the HPLC. The elution was performed with the following solvents: 0.1% (v/v) acetic acid (solvent A) and absolute methanol containing 0.1% (v/v) acetic acid (solvent B) with the flow rate of 0.5 mL/min. The gradient used was: 30-45% solvent B (0-20 min). The chromatogram was recorded at 275 nm and EGCG peak was confirmed by comparing the retention time with the EGCG standard.

4.4.3.2.10 Characterization of the selected fish gelatin-based film added with EGCG

Fish gelatin films without and with 5.71 wt % EGCG were selected for further characterization.

4.4.3.2.10 Differential scanning calorimetry

Thermal properties of selected films were determined using a differential scanning calorimeter (DSC) (Perkin Elmer, Model DSC-7, Norwalk, CT, USA) (Nuthong *et al.*, 2009a). Temperature calibration was performed using the indium thermogram. Film samples (2-5 mg) were accurately weighed into aluminium pans, hermetically sealed, and scanned over the temperature range of -40 to 150 °C, with a heating rate of 5 °C/min. An empty aluminium pan was used as the reference. The maximum transition temperature was estimated from the endothermic peak of the DSC thermogram and transition enthalpy was determined from the area under the endothermic peak.

4.4.3.2.11 Attenuated total reflectance-Fourier transform infrared (ATR-FTIR) spectroscopy

The selected films were scanned with a Bruker Model Equinox 55 FTIR spectrometer (Bruker Co., Ettlingen, Germany) equipped with a horizontal ATR Trough plate crystal cell (45° ZnSe; 80 mm long, 10 mm width and 4 mm thickness) (PIKE Technology Inc., Madison, WI, USA) at 25 °C (Nuthong *et al.*, 2009a). Films were placed onto the crystal cell and the cell was clamped into the mount of FTIR

spectrometer. The spectra in the range of 650–4000 cm^{-1} were ratioed against a background spectrum recorded from the clean empty cell at 25 °C.

4.4.4 Statistical analysis

All experiments were run in triplicate with different three lots of films. Data were subjected to analysis of variance (ANOVA) and mean comparisons were carried out by the Duncan's multiple range test. Analysis was performed using the SPSS package (SPSS for windows, SPSS Inc., Chicago, IL, USA).

4.5 Results and discussion

4.5.1 Antioxidative activities of EGCG

Antioxidative activities expressed as ABTS and DPPH radical scavenging activities, FRAP, H_2O_2 scavenging activity and ORAC of EGCG are shown in Table 13. Overall, EGCG showed the antioxidative activities for all assays tested (Table 13). ABTS activity of EGCG was 12.78 mmol TE/g sample. The result indicated the ability of EGCG in scavenging the stable radical cation $ABTS^{\bullet+}$ (2,2′-azinobis(3-ethylbenzothiazoline-6-sulphonic acid)), a blue-green chromophore with maximum absorption at 734 nm. The radical generally has the decrease in its intensity in the presence of antioxidants (Shahidi and Zhong, 2015). EGCG exhibited DPPH radical scavenging activity (7.68 mmol TE/g sample). DPPH is used as a free radical to evaluate antioxidative activity, which is attributed to hydrogen donating ability of test compounds (Shimada *et al.*, 1992). FRAP of EGCG was 11.02 mmol TE/g sample. The FRAP assay is a typical method that measures the reduction of ferric ion (Fe^{3+})-ligand complex to the intensely blue colored ferrous (Fe^{2+}) complex by antioxidants in acidic media (Shahidi and Zhong, 2015). EGCG had the H_2O_2 scavenging activity of 3.59 mmol TE/g sample. Hydrogen peroxide can be implicated indirectly in lipid oxidation. Hydrogen peroxide is the precursor for the generation of hydroxyl radical, which is a strong initiator of lipid oxidation (Choe and Min, 2005). Furthermore, EGCG had ORAC of 2.92 mmol TE/g sample. The ORAC assay measures the radical chain breaking ability of antioxidants by monitoring the inhibition of peroxyl radicals, which are predominant free radicals found in lipid oxidation in foods and biological systems

under physiological conditions (Shahidi and Zhong, 2015). Fluorescence decay curves of fluorescein in the absence and presence of 0.05 mg/mL EGCG are illustrated in Figure 14. The decay was retarded when EGCG was present, in comparison with the control. Additionally, the efficiency of EGCG was higher than Trolox at the concentration of 50 mg/mL as shown by the slower decay in the former. The result indicated that EGCG could prevent the reaction between peroxyl radicals and fluorescein by donating hydrogen atom to the radicals, resulting in the maintenance of fluorescence. Therefore, EGCG was shown to have antioxidant activity with different modes of actions. It could be a potential natural antioxidant to be incorporated into gelatin films.

Table 13. ABTS and DPPH radical scavenging activities, ferric reducing antioxidant power (FRAP), hydrogen peroxide scavenging activity (H_2O_2 scavenging) and oxygen radical absorbance capacity (ORAC) of epigallocatechin gallate (EGCG).

Activities	**mmol TE /g sample**
ABTS scavenging	12.78 ± 0.70
DPPH scavenging	7.68 ± 0.42
FRAP	11.02 ± 0.37
H_2O_2 scavenging	3.59 ± 0.61
ORAC	2.92 ± 0.13

Values are presented as mean ± SD (n = 3).

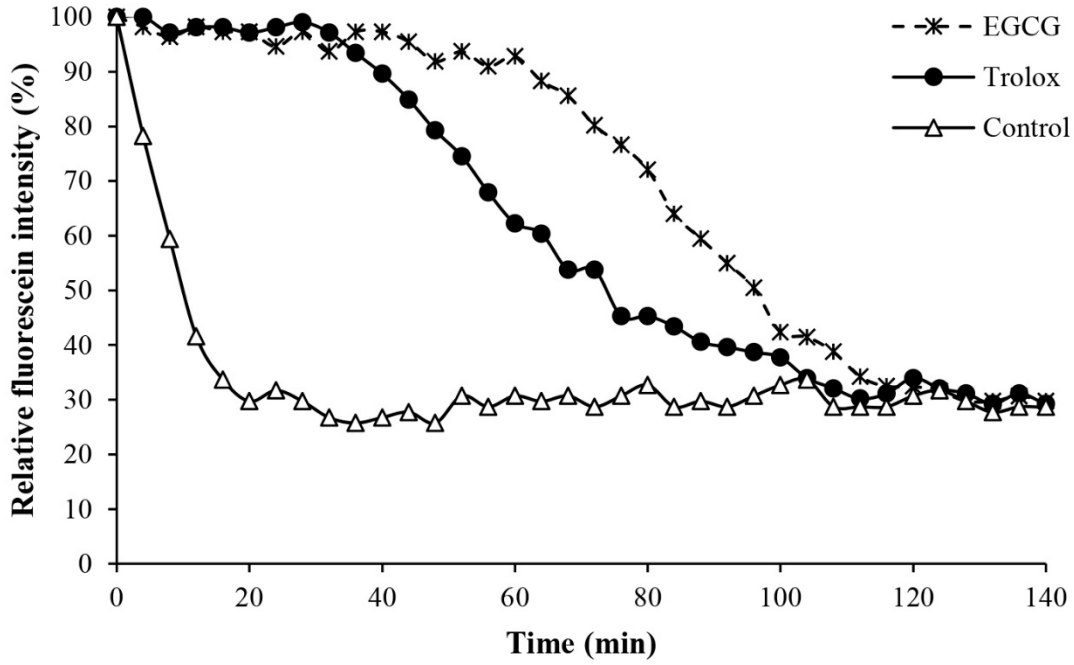

Figure 14. Fluorescence decay curves of fluorescein of epigallocatechin gallate (EGCG) and Trolox at a concentrations of 0.05 and 50 mg/mL, respectively, and the control.

4.5.2 Effect of EGCG at various concentrations on the properties of fish gelatin-based film

4.5.2.1 Film thickness and mechanical properties

Thickness of gelatin film incorporated with EGCG (1.43 – 5.71 wt %) ranged from 0.056 to 0.059 mm, which were slightly higher than the control film ($P < 0.05$) (Table 14). The highest thickness was found for film incorporated with 4.29 and 5.71 wt % EGCG ($P < 0.05$). Tensile strength (TS) and elongation at break (EAB) of fish gelatin films incorporated with EGCG at different concentrations are shown in Table 14. All gelatin films incorporated with EGCG showed higher TS but lower EAB than the control film ($P < 0.05$). TS of the films increased by 118.3, 121.0, 124.0 and 129.2% when EGCG at concentrations of 1.43, 2.86, 4.29 and 5.71 wt % were added, respectively, compared to the control film. It was suggested that EGCG showed the strengthening effect on the resulting film. This was associated with the decrease in film

Table 14. Thickness, mechanical properties, water vapor permeability and color of fish gelatin films incorporated with EGCG at different concentrations.

EGCG concentrations (wt %)	Thickness (mm)	TS (MPa)	EAB (%)	WVP ($\times 10^{-14}$ g m^{-1} s^{-1} Pa^{-1})	*L**	*a**	*b**	Δ*E**
0	0.052 ± 0.001 d	24.08 ± 0.51 c	26.04 ± 0.25 a	7.86 ± 0.27 c	90.32 ± 0.09 a	-1.52 ± 0.11 b	1.68 ± 0.02 b	2.69 ± 0.05 b
1.43	0.056 ± 0.001 c	28.49 ± 0.45 b	11.92 ± 2.21 b	8.17 ± 0.08 bc	89.34 ± 0.42 b	-1.39 ± 0.05 a	1.86 ± 0.05 a	3.91 ± 0.24 a
2.86	0.058 ± 0.000 b	29.13 ± 1.91 b	10.36 ± 1.64 b	8.37 ± 0.17 ab	89.06 ± 0.34 b	-1.36 ± 0.11 a	1.88 ± 0.06 a	3.86 ± 0.19 a
4.29	0.058 ± 0.000 ab	29.86 ± 0.70 ab	9.84 ± 0.73 b	8.69 ± 0.25 a	89.36 ± 0.23 b	-1.36 ± 0.03 a	1.79 ± 0.02 a	3.80 ± 0.07 a
5.71	0.059 ± 0.000 a	31.11 ± 1.60 a	9.55 ± 1.24 b	8.41 ± 0.17 ab	89.36 ± 0.38 b	-1.35 ± 0.02 a	1.83 ± 0.03 a	3.85 ± 0.29 a

Values are given as the mean ± SD (n = 3).

Different lowercase letters in the same column indicate significant differences ($P < 0.05$).

EGCG: Epigallocatechin gallate; TS: Tensile strength; EAB: Elongation at break; WVP: Water vapor permeability.

elasticity/extensibility. Phenolic compound could react with more than one protein site and led to cross-links between proteins (Nuthong *et al.*, 2009b). EGCG has tri-hydroxyl group in the B ring, di-hydroxyl group in the A ring and the tri-hydroxyl group in a gallate moiety (D ring) esterified at carbon 3 of the C ring (Lambert and Elias, 2010; Sae-leaw *et al.*, 2017). These hydroxyl groups could interact with the side chain of gelatin via the formation of H-bonding. Thus, the strength and extensibility of fish gelatin-based films were governed by EGCG concentrations.

4.5.2.2 Water vapor permeability (WVP)

Water vapor permeability of gelatin film incorporated with EGCG at different concentrations (0-5.71 wt %) is shown in Table 14. Generally, high WVP was observed in the films incorporated with EGCG at concentrations higher than 2.86%, compared to the control film ($P < 0.05$). This might be due to the presence of polar groups of EGCG incorporated. This result was in agreement with Nuthong *et al.* (2009b) who reported that the addition of tannic acid, caffeic acid and ferulic acid at 1-3% increased WVP of resulting films. Furthermore, increasing amount of EGCG might induce the formation of protein aggregations. This led to the formation of discontinuous film network with increased free volume of the polymeric matrix. This might contributed to the increased WVP of the resulting films. Therefore, the concentration of phenolic compounds directly affected WVP of the resulting film.

4.5.2.3 Color, light transmission and transparency value

Color of fish gelatin film incorporated with EGCG at various concentrations is shown in Table 14. Decreases in L^*-value and increases in a^*-, b^*- and ΔE^* values were observed in films, when EGCG was incorporated, especially at higher concentrations ($P < 0.05$). Yellowness and redness of resulting films were mostly from the color of EGCG, which was pale yellow in color.

Light transmission at selected wavelengths from 200 to 800 nm in UV and visible ranges and transparency value of gelatin films varied with the levels of EGCG added as shown in Table 15. All gelatin films had an excellent barrier property against UV light at 200 and 280, especially when EGCG was incorporated. Protein-

based films had the excellent UV light barrier capacity, owing to their high amount of aromatic amino acids that absorb UV light (Hamaguchi *et al.*, 2007). All EGCG incorporated films showed the lower transmission of visible light in the range of 350-800 nm, compared to the control film (without EGCG). The higher barrier property toward light transmission was obtained for films incorporated with 4.29 and 5.71 wt % EGCG in comparison with the films containing 1.43 and 2.86 wt % EGCG. This was more likely associated with the increase in opaqueness of films containing phenolic compound (Nuthong *et al.*, 2009b). Transparency values of fish gelatin-based film incorporated with EGCG at concentrations of 4.29 and 5.71 wt % were higher than the control film ($P < 0.05$) as shown in Table 15. This result suggested that the incorporation of EGCG yielded less transparent films. EGCG might act as protein cross-linker and induced the formation of aggregates, which contributed to the turbidity. Simultaneously, the aggregates formed could function as a barrier for light transmission. Therefore, addition of EGCG played an essential role in color, light transmission and transparency of resulting gelatin film.

4.5.2.4 Scanning electron microscopy

Microstructures of fish gelatin films incorporated without and with EGCG at various concentrations are depicted in Figure 15. The smooth and homogenous surface was observed for all film samples. Gelatin-based films generally has regular and smooth surface (Nilsuwan *et al.*, 2017). For the cross-section, the films became denser without any crack when EGCG was incorporated (Figure 15). SEM observations of the cross section of films revealed that the phenolic compound was plausibly bound to the protein matrix, yielding a relatively compact morphology (Nuthong *et al.*, 2009b). This was related with higher transparency value of film containing EGCG (Table 15). Thus, the addition of EGCG provided the compact morphology of resulting gelatin film.

Table 15. Light transmission and transparency value of fish gelatin films incorporated with EGCG at different concentrations.

EGCG concentrations (wt %)	Light transmission (%) at different wavelengths (nm)								Transparency value
	200	280	350	400	500	600	700	800	
0	0.05	39.95	81.16	84.25	86.70	87.83	88.47	88.97	1.09 ± 0.01 b
1.43	0.05	0.55	74.50	80.29	84.42	86.35	87.54	88.37	1.13 ± 0.05 b
2.86	0.05	0.04	73.92	80.72	84.36	85.91	86.83	87.52	1.11 ± 0.01 b
4.29	0.02	0.01	68.83	79.33	82.94	84.71	85.84	86.65	1.23 ± 0.09 a
5.71	0.03	0.02	68.61	79.23	82.51	84.18	85.28	86.13	1.22 ± 0.03 a

Values are given as the mean ± SD (n = 3).

Different lowercase letters in the same column indicate significant differences ($P < 0.05$).

EGCG: Epigallocatechin gallate

EGCG concentrations (wt %)	Surface	Cross-section
0	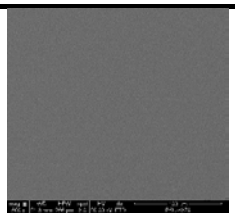	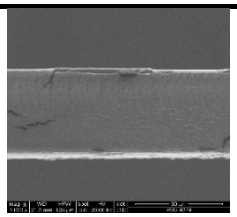
1.43	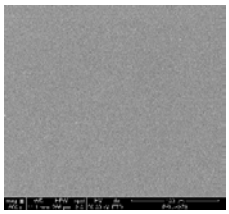	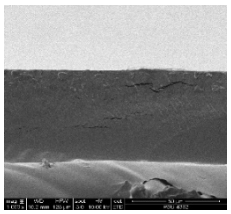
2.86	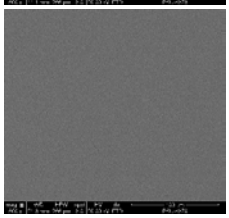	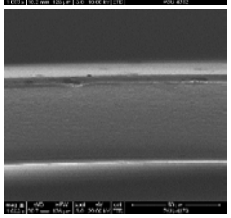
4.29	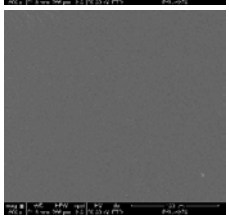	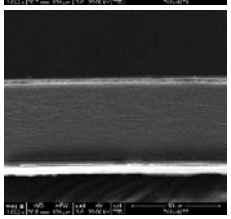
5.71	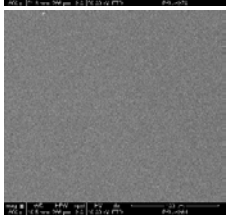	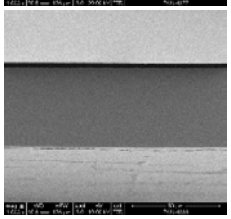

Figure 15. SEM micrograph of fish gelatin films incorporated with EGCG at different concentrations.

4.5.2.5 Heat sealing ability

Seal strength and seal efficiency of fish gelatin-based film incorporated with EGCG at different concentrations are shown in Table 16. All film samples were heat sealable. During heat sealing process, the surface of the two films underwent melting as induced by the introduced heat. This could promote the interfacial interactions across the contact surfaces, thus yielding the sufficient seal strength to the sealed film (Tongnuanchan *et al.*, 2016). Films incorporated with EGCG at levels of 2.86 – 5.71 wt % showed higher seal strength and seal efficiency, compared with

control film ($P < 0.05$). Apart from molecular interdiffusion, polar functional groups of polymers or compounds such as hydroxyl (OH), carboxyl (COOH) or aldehyde (CHO) were directly responsible for chemical interaction taking place at the interface, which contributed to the increase in adhesion strength of film (Lee, 1994). EGCG containing a high amount of hydroxyl group could enhance the interaction with molten gelatin molecules during heat sealing via hydrogen bonding in seal area. This resulted in the increased seal strength and seal efficiency. The seal strength and seal efficiency of fish gelatin films were therefore affected by the addition of EGCG.

4.5.2.6 Migration of EGCG from films

Migration of EGCG from fish gelatin-based film incorporated with EGCG at various concentrations in high fat food simulant (95% ethanol) as monitored by total phenolic content (TPC) during 24 days of storage is illustrated in Figure 16. Overall, low TPC was obtained in 95% ethanol for all films treated. TPC was firstly detected after 6 days and tended to increase up to 18 days of storage. After 18 days, the decrease in TPC was obtained. This might be related with the decomposition of released EGCG present in medium. As a consequence, EGCG lost their ability in reducing Folin-Ciocalteu reagent used for TPC assay. No TPC was detected for control film (without EGCG) throughout 24 days of storage. This result suggested that the slow migration of EGCG from the gelatin films was plausibly associated with the interaction between EGCG and gelatin. This coincided with more compact and denser structure of films added with EGCG (Figure 15). Sukhtezari *et al.* (2017) reported that decreased diffusivity of *Scrophularia striata* Boiss. extract from cellulose matrix was due to the interactions between β-cyclodextrin and cellulose chains. At the same storage time, the highest TPC was found for film incorporated with 5.71 wt % EGCG. With excessive amount of EGCG, free EGCG localized in film matrix could migrate into food simulant with ease. The liberation of EGCG was confirmed by HPLC (Figure 16). Therefore, the concentration of EGCG used in films had the impact on its migration into food simulant or foods, especially high fat foods.

Table 16. Seal strength and seal efficiency of fish gelatin films incorporated with EGCG at different concentrations.

EGCG concentrations (wt %)	Sealed films*	Seal strength (N/m)	Seal efficiency (%)
0	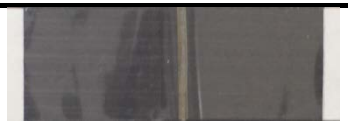	461.23 ± 36.47 b	25.83 ± 2.85 b
1.43		461.64 ± 32.03 b	28.39 ± 1.31 b
2.86		588.6 ± 10.49 a	34.53 ± 0.41 a
4.29		594.02 ± 54.95 a	33.92 ± 1.9 a
5.71		625.64 ± 23.16 a	34.73 ± 0.94 a

Values are given as the mean ± SD (n = 3).

Different lowercase letters in the same column indicate significant differences ($P < 0.05$).

EGCG: Epigallocatechin gallate

*Sealing of films was conducted via facing layers of two strips.

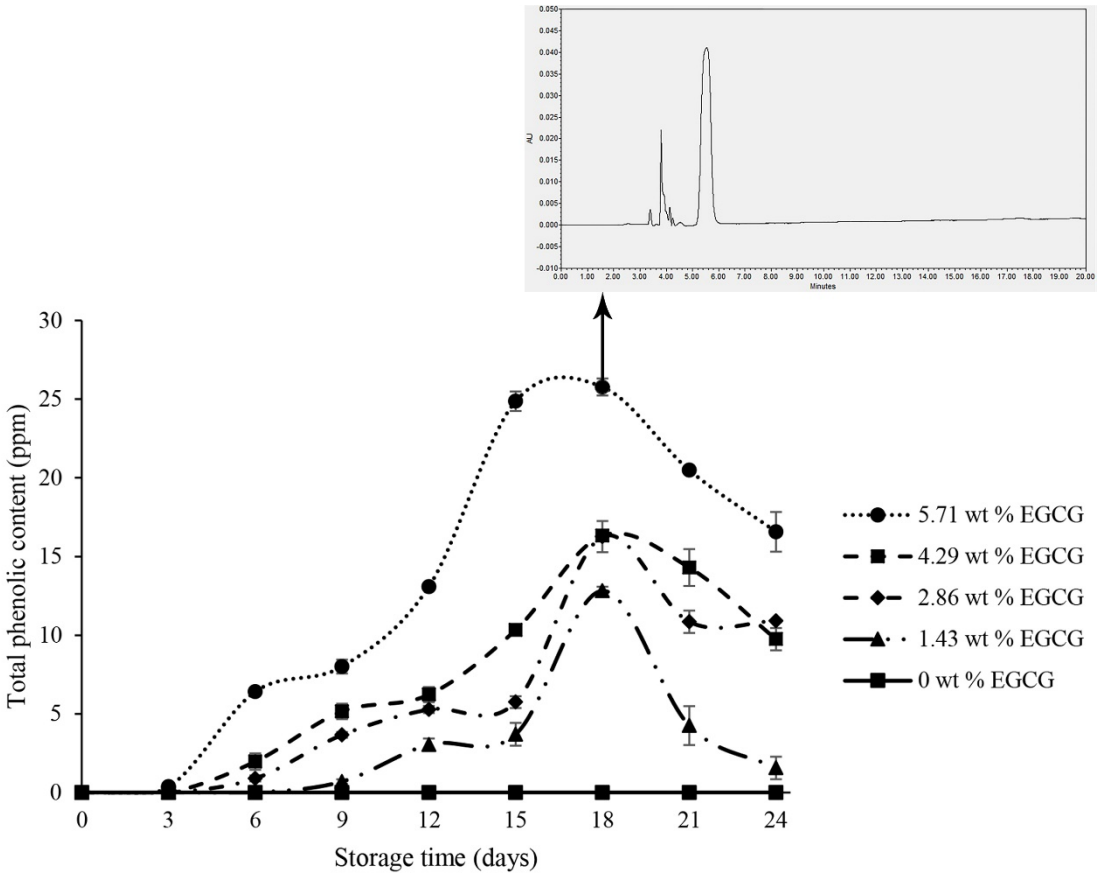

Figure 16. Migration of EGCG from fish gelatin films incorporated with EGCG at concentrations of 0, 1.43, 2.86, 4.29 and 5.71 wt % during 24 days of storage. EGCG content was expressed as total phenolic content. Bars represent the standard deviation (n = 3)

4.5.3 Characterization of selected fish gelatin-based film incorporated with EGCG

4.5.3.1 Differential scanning calorimetry

Thermograms of selected film incorporated without and with 5.71 wt % EGCG are depicted in Figure 17. Glass transition, a step-like transition, temperature (T_g) and an endothermic melting transition (T_{max}) were determined. The glass transition is associated with molecular segmental motion of disordered (amorphous phase) structure, which undergoes from a brittle glassy solid state to a rubbery state, whereas the melting transition of the protein film indicates the temperature causing a disruption of ordered or aggregated structure (Tang *et al.*, 2009). T_g of gelatin film increased from

45.54 °C (control film) to 51.86 °C, when EGCG at the levels of 5.71 wt % was incorporated. It was suggested that the addition of EGCG more likely facilitated protein-protein interaction in film matrix, thereby lowering the mobility of gelatin chain. The enhancement of cohesive structural integrity was found in the film network when phenolic compounds were present (Nuthong *et al.*, 2009a). This result was in agreement with the increased TS and decreased EAB of EGCG incorporated film (Table 14). For endothermic/melting transition, the control film and EGCG incorporated film showed endothermic peak with T_{max} of 129.78 and 129.76 °C, respectively. This endothermic transition obtained after the glass transition was possibly associated with the helix-coil transition of gelatin (Vanin *et al.*, 2005) as well as the disruption of other kinds of ordered or aggregated molecular structure. Gelatin chains could undergo partial renaturation during film formation process (Nilsuwan *et al.*, 2016). Thus, the incorporation of EGCG had the impact on thermal behavior of resulting gelatin film.

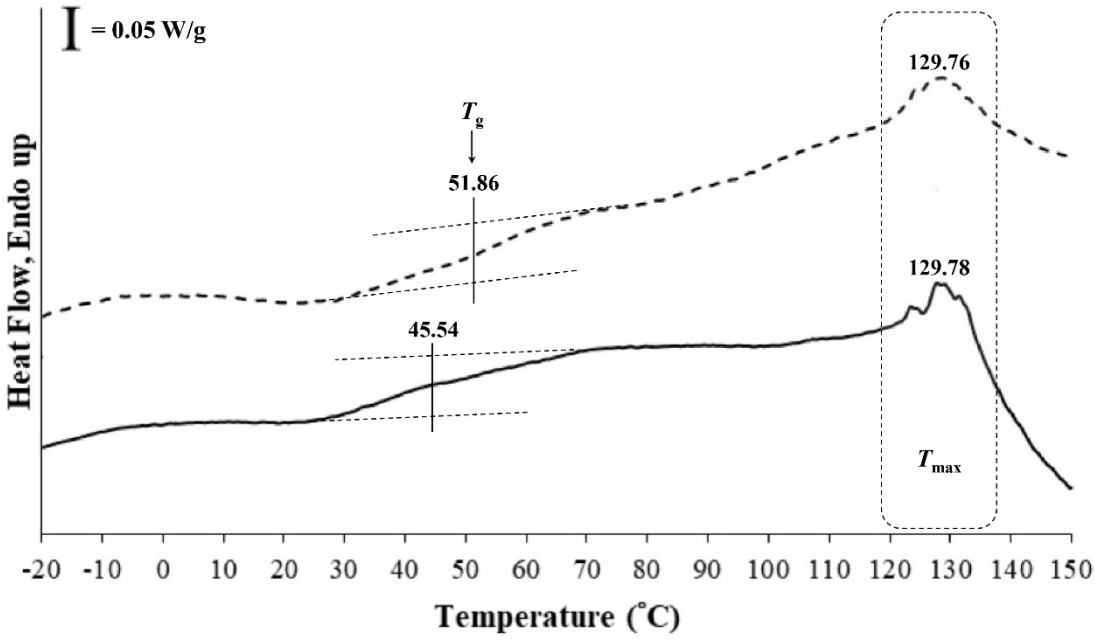

Figure 17. DSC thermogram of fish gelatin films incorporated without and with 5.71 wt % EGCG.

4.5.3.2 Attenuated total reflection-fourier transform infrared spectroscopy (ATR-FTIR)

FT-IR spectra of selected film incorporated without and with 5.71 wt % EGCG are shown in Figure 18. FTIR spectra of control film and film added with EGCG exhibited the similar major characteristic peaks of protein but the amplitudes of peaks varied. The peak situated at the wavenumber of 1036-1038 cm^{-1} in both film samples might be related to the OH group, generally from glycerol added as a plasticizer (Bergo and Sobral, 2007; Nilsuwan *et al.*, 2016). It was noted that the amplitude of peak associated with the OH group of film incorporated with EGCG was higher than that found in control film. It was indicated that EGCG provided the OH group in the resulting film. The EGCG has trihydroxyl group in the B ring at carbons 3′, 4′, and 5′, and a gallate moiety esterified at carbon 3 of the C ring (Lambert and Elias, 2010; Sae-leaw *et al.*, 2017). Both films had similar spectra in the range of 1700–700 cm^{-1}, covering amide-I, II and III bands. FTIR spectra of both films had the major bands at 1630 cm^{-1} (amide-I, illustrating C=O stretching/hydrogen bonding coupled with C-N stretch and CCN deformation), 1538 cm^{-1} (amide-II, representing the bending vibrations of N-H groups and stretching vibrations of C-N groups) and 1237 cm^{-1} (amide-III, illustrating the vibrations in-plane of C-N and N-H groups of bound amide as well as absorptions arising from wagging vibrations from CH_2 groups from the glycine backbone and proline side-chains) (Muyonga *et al.*, 2004). Among these amide bands, the amide-I band (1700-1600 cm^{-1}) has been widely used for infrared analysis to determine the secondary structure of proteins including gelatin (Muyonga *et al.*, 2004). The IR spectra of EGCG incorporated film revealed the notable changes in the wavenumber range of 1500-1000 cm^{-1}, as compared to the control film. The obvious increases in amplitude of peaks at wavenumbers ~1451 and ~1036 cm^{-1} were found in gelatin film incorporated with EGCG. Peaks with wavenumbers at ~1350 and ~1080 cm^{-1}, which were attributed to the bending of the O-H bonds and the stretching of the C-O bonds, respectively, were observed in gelatin modified with TA and OTA (Aewsiri *et al.*, 2010). It reconfirmed that EGCG was present in gelatin film as indicated by the band of OH group in the film. Moreover, the amide-A was found at the wavenumber of 3289 and 3284 cm^{-1} for the control film and film incorporated with EGCG,

respectively. Normally, the vibration at wavenumber ~3300 cm^{-1} of amide-A band represents the NH-stretching coupled with hydrogen bonding (Aewsiri *et al.*, 2010). The shift to lower wavenumber of film containing EGCG indicated the involvement of H-bond between proteins and EGCG. An amide-B band was detected at the wavenumber of 3082 cm^{-1}, representing asymmetric stretching vibration of CH attached to double bond coupled with NH stretching vibration (Muyonga *et al.*, 2004). Peaks at wavenumbers around 2855-2878 cm^{-1} and 2924-2935 cm^{-1} were assigned to the asymmetrical and symmetrical stretching vibrations of the aliphatic C-H in CH_2 and CH_3 groups, respectively (Guillén and Cabo, 2004). Nevertheless, the amplitude of peaks at wavenumber of 1081 cm^{-1} increased when EGCG were incorporated. The peak represents the stretching vibration of the C-O ester group, which is generally found in phenolic compounds (Aewsiri *et al.*, 2010). Therefore, the incorporation of EGCG could affect or modify the functional groups of resulting films.

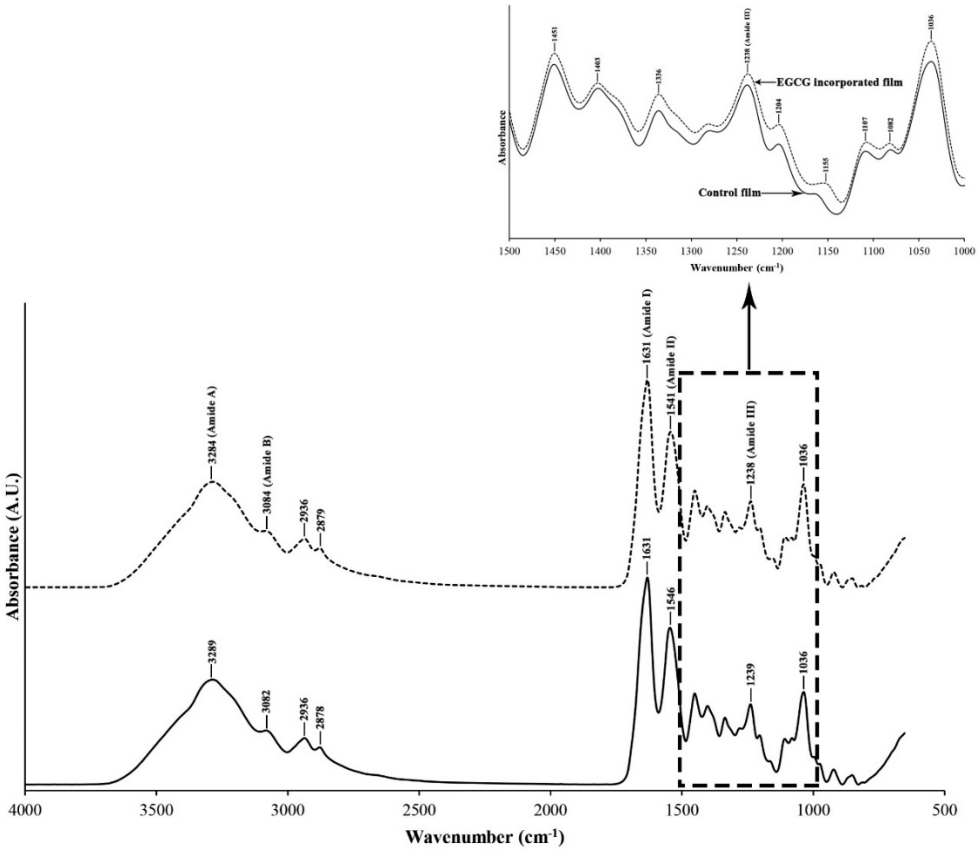

Figure 18. ATR-FTIR spectra of fish gelatin films incorporated without and with 5.71 wt % EGCG.

4.6 Conclusions

EGCG possessed antioxidant activities with varying modes of actions. The properties of fish gelatin-based film was affected by the concentrations of EGCG added. EGCG enhanced the mechanical and UV-light barrier properties of the film. EGCG at 5.71 wt % provided smooth surface and compact cross-section as well as high seal strength and seal efficiency of films. The highest migration of EGCG from film was obtained in film containing 5.71 wt % EGCG. Incorporation of 5.71 wt % EGCG increased glass transition temperature of gelatin film. FTIR analysis revealed that the OH group in film matrix was increased and interaction via H-bond was enhanced when 5.71 wt % EGCG was incorporated. Thus, EGCG could be added into the gelatin film considered as the active packaging material possessing antioxidant activity. Also, it could increase the mechanical properties and heat seal ability of resulting gelatin film.

4.7 References

Aewsiri, T., Benjakul, S., Visessanguan, W., Wierenga, P. A. and Gruppen, H. 2010. Antioxidative activity and emulsifying properties of cuttlefish skin gelatin–tannic acid complex as influenced by types of interaction. Innov. Food Sci. Emerg. Technol. 11: 712-720.

Araghi, M., Moslehi, Z., Mohammadi Nafchi, A., Mostahsan, A., Salamat, N. and Daraei Garmakhany, A. 2015. Cold water fish gelatin modification by a natural phenolic cross-linker (ferulic acid and caffeic acid). Food Sci. Nutr. 3: 370-375.

ASTM. 1989. Annual book of ASTM standards. American Society for Testing and Materials, Philadelphia, PA, USA.

ASTM. 2001. Standard test methods for seal strength of flexible barrier materials - ASTM F88. *In* Annual book of ASTM standards. Vol. 15.09. ASTM. Philadelphia, PA.

Benzie, I. F. F. and Strain, J. J. 1996. The ferric reducing ability of plasma (FRAP) as a measure of “antioxidant power”: the FRAP assay. Anal. Biochem. 239: 70-76.

Bergo, P. and Sobral, P. J. A. 2007. Effects of plasticizer on physical properties of pig skin gelatin films. Food Hydrocolloid. 21: 1285-1289.

Binsan, W., Benjakul, S., Visessanguan, W., Roytrakul, S., Tanaka, M. and Kishimura, H. 2008. Antioxidative activity of mungoong, an extract paste, from the cephalothorax of white shrimp (*Litopenaeus vannamei*). Food Chem. 106: 185-193.

Brand-Williams, W., Cuvelier, M. E. and Berset, C. 1995. Use of a free radical method to evaluate antioxidant activity. LWT-Food Sci. Technol. 28: 25-30.

Choe, E. and Min, D. B. 2005. Chemistry and reactions of reactive oxygen species in foods. J. Food Sci. 70: R142-R159.

Gennadios, A., Weller, C. L., Hanna, M. A. and Froning, G. W. 1996. Mechanical and barrier properties of egg albumen films. J. Food Sci. 61: 585-589.

Gómez-Estaca, J., Bravo, L., Gómez-Guillén, M. C., Alemán, A. and Montero, P. 2009. Antioxidant properties of tuna-skin and bovine-hide gelatin films induced by the addition of oregano and rosemary extracts. Food Chem. 112: 18-25.

Guillén, M. D. and Cabo, N. 2004. Study of the effects of smoke flavourings on the oxidative stability of the lipids of pork adipose tissue by means of Fourier transform infrared spectroscopy. Meat Sci. 66: 647-657.

Hamaguchi, P. Y., Weng, W., Kobayashi, T., Runglertkreingkrai, J. and Tanaka, M. 2007. Effect of fish meat quality on the properties of biodegradable protein films. Food Science and Technology Research. 13: 200-204.

Han, J. H. and Floros, J. D. 1997. Casting antimicrobial packaging films and measuring their physical properties and antimicrobial activity. J. Plast. Film Sheet. 13: 287-298.

Iwata, K. I., Ishizaki, S. H., Handa, A. K. and Tanaka, M. U. 2000. Preparation and characterization of edible films from fish water-soluble proteins. Fish. Sci. 66: 372-378.

Kaewprachu, P., Osako, K., Benjakul, S. and Rawdkuen, S. 2015. Quality attributes of minced pork wrapped with catechin–lysozyme incorporated gelatin film. Food Pack. Shelf Life. 3: 88-96.

Kittiphattanabawon, P., Benjakul, S., Visessanguan, W. and Shahidi, F. 2012. Gelatin hydrolysate from blacktip shark skin prepared using papaya latex enzyme: Antioxidant activity and its potential in model systems. Food Chem. 135: 1118-1126.

Lambert, J. D. and Elias, R. J. 2010. The antioxidant and pro-oxidant activities of green tea polyphenols: A role in cancer prevention. Archives of Biochemistry and Biophysics. 501: 65-72.

Lee, K.-Y. and Song, K. B. 2017. Preparation and characterization of an olive flounder (*Paralichthys olivaceus*) skin gelatin and polylactic acid bilayer film. J. Food Sci. 82: 706-710.

Lee, K. W. 1994. Modification of polyimide surface morphology: relationship between modification depth and adhesion strength. Journal of Adhesion Science and Technology. 8: 1077-1092.

Lu, T.-M., Lee, C.-C., Mau, J.-L. and Lin, S.-D. 2010. Quality and antioxidant property of green tea sponge cake. Food Chem. 119: 1090-1095.

Maryam Adilah, Z. A., Jamilah, B. and Nur Hanani, Z. A. 2018. Functional and antioxidant properties of protein-based films incorporated with mango kernel extract for active packaging. Food Hydrocolloid. 74: 207-218.

Muyonga, J. H., Cole, C. G. B. and Duodu, K. G. 2004. Characterisation of acid soluble collagen from skins of young and adult Nile perch (*Lates niloticus*). Food Chem. 85: 81-89.

Nilsuwan, K., Benjakul, S. and Prodpran, T. 2016. Influence of palm oil and glycerol on properties of fish skin gelatin-based films. J. Food Sci. Technol. 53: 2715-2724.

Nilsuwan, K., Benjakul, S. and Prodpran, T. 2017. Physical/thermal properties and heat seal ability of bilayer films based on fish gelatin and poly(lactic acid). Food Hydrocolloid. In press. https://doi.org/10.1016/j.foodhyd.2017.1010.1001.

Nuthong, P., Benjakul, S. and Prodpran, T. 2009a. Characterization of porcine plasma protein-based films as affected by pretreatment and cross-linking agents. Int. J. Biol. Macromol. 44: 143-148.

Nuthong, P., Benjakul, S. and Prodpran, T. 2009b. Effect of phenolic compounds on the properties of porcine plasma protein-based film. Food Hydrocolloid. 23: 736-741.

Sae-leaw, T., Benjakul, S. and Simpson, B. K. 2017. Effect of catechin and its derivatives on inhibition of polyphenoloxidase and melanosis of Pacific white shrimp. J. Food Sci. Technol. 54: 1098-1107.

Shahidi, F. and Zhong, Y. 2015. Measurement of antioxidant activity. J. Funct. Foods. 18: 757-781.

Shiku, Y., Hamaguchi, P. Y., Benjakul, S., Visessanguan, W. and Tanaka, M. 2004. Effect of surimi quality on properties of edible films based on Alaska pollack. Food Chem. 86: 493-499.

Shimada, K., Fujikawa, K., Yahara, K. and Nakamura, T. 1992. Antioxidative properties of xanthan on the autoxidation of soybean oil in cyclodextrin emulsion. J. Agric. Food Chem. 40: 945-948.

Slinkard, K. and Singleton, V. L. 1977. Total phenol analysis: automation and comparison with manual methods. Am. J. Enol. Vitic. 28: 49-55.

Sukhtezari, S., Almasi, H., Pirsa, S., Zandi, M. and Pirouzifard, M. 2017. Development of bacterial cellulose based slow-release active films by incorporation of *Scrophularia striata* Boiss. extract. Carbohydr Polym. 156: 340-350.

Tang, C.-H., Xiao, M.-L., Chen, Z., Yang, X.-Q. and Yin, S.-W. 2009. Properties of cast films of vicilin-rich protein isolates from *Phaseolus legumes*: Influence of heat curing. LWT-Food Sci. Technol. 42: 1659-1666.

Tongnuanchan, P., Benjakul, S., Prodpran, T., Pisuchpen, S. and Osako, K. 2016. Mechanical, thermal and heat sealing properties of fish skin gelatin film containing palm oil and basil essential oil with different surfactants. Food Hydrocolloid. 56: 93-107.

Vanin, F. M., Sobral, P. J. A., Menegalli, F. C., Carvalho, R. A. and Habitante, A. M. Q. B. 2005. Effects of plasticizers and their concentrations on thermal and functional properties of gelatin-based films. Food Hydrocolloid. 19: 899-907.

Wettasinghe, M. and Shahidi, F. 2000. Scavenging of reactive-oxygen species and DPPH free radicals by extracts of borage and evening primrose meals. Food Chem. 70: 17-26.

Zaveri, N. T. 2006. Green tea and its polyphenolic catechins: Medicinal uses in cancer and noncancer applications. Life Sci. 78: 2073-2080.

CHAPTER 5

FISH GELATIN MONOLAYER AND BILAYER FILMS INCORPORATED WITH EPIGALLOCATECHIN GALLATE: PROPERTIES AND THEIR USE AS POUCHES FOR STORAGE OF CHICKEN SKIN OIL

5.1 Abstract

The properties of monolayer and bilayer fish gelatin films and the corresponding films containing epigallocatechin gallate (EGCG) were examined. Bilayer films showed higher tensile strength, water vapor and light barrier properties but also higher opaqueness and yellowness than monolayer films. No differences in elongation at break and oxygen barrier property between monolayer and bilayer films were observed. Those films were used to produce pouches, in which chicken skin oil (CSO) was packaged. CSO packaged in the pouches prepared with the films containing EGCG showed lower peroxide value (PV), thiobarbituric acid reactive substances (TBARS) and volatile compounds after 30 days of storage in comparison with that packaged in linear low-density polyethylene (LLDPE) pouch. Additionally, at the end of the storage, linoleic acid (C18:2 *n*-6) and linolenic acid (C18:3 *n*-9) were more retained in CSO packaged in the pouches made from the films containing EGCG. Therefore, monolayer or bilayer gelatin films incorporated with EGCG could be used as packaging for oils prone to lipid oxidation.

5.2 Introduction

The interest in biopolymer-based films has been increased due to their advantages over synthetic counterparts, such as their renewable and biodegradable character. Among biopolymers, proteins possess good film-forming ability and have been used as edible food packaging materials (Gennadios *et al.*, 1997; Tongnuanchan *et al.*, 2013). In particular, fish gelatin has been proven as an excellent film-forming material (Gómez-Guillén *et al.*, 2009). Many factors, such as source and concentration of gelatin, have impact on the properties of fish gelatin-based films (Jongjareonrak *et*

al., 2006; Limpisophon and Schleining, 2017; Tongnuanchan *et al.*, 2014). Generally, fish gelatin films exhibit good physical and mechanical properties (Lee and Song, 2017) and have superior oxygen barrier property to synthetic films (Nilsuwan *et al.*, 2017). However, gelatin films have drawback including high water solubility and low water barrier property, owing to their hydrophilicity and the presence of hydrophilic plasticizers such as glycerol (Gennadios *et al.*, 1994; Hoque *et al.*, 2011b; Vanin *et al.*, 2005). The addition of hydrophobic substances, such as fats and oils, into film-forming solutions was implemented to improve the water vapor barrier property of gelatin films (Bertan *et al.*, 2005; Limpisophon *et al.*, 2010). Nevertheless, fish gelatin emulsified with hydrophobic substances had an improvement in water vapor barrier property but showed low oxygen barrier property (Nilsuwan *et al.*, 2016b). In this context, bilayer films from various sources, such as soy protein isolate/corn zein (Cho *et al.*, 2010), chitosan/whey protein (Kurek *et al.*, 2014) and fish gelatin/poly(lactic) acid (Nilsuwan *et al.*, 2018a), have been developed to exploit the advantages of each film (Lee and Song, 2017). Properties of bilayer films were generally governed by layer thickness ratio, being 1:1 ratio the one at which satisfactory water vapor and oxygen barrier properties were found (Nilsuwan *et al.*, 2017).

To enhance the antioxidant activity of gelatin-based films, phenolic compounds or plant extracts have been added (Maryam Adilah *et al.*, 2018; Nuthong *et al.*, 2009). These phenolic compounds could include simple phenols (phenolic acids, coumarins), polyphenols and natural plant extracts (tannins, flavonoids, green tea extract, tea polyphenol) and volatile phenols (essential oils, aromas) (Benbettaïeb *et al.*, 2018). Apart from acting as antioxidants, those phenolic compounds could serve as protein cross-linkers (Gómez-Estaca *et al.*, 2009; Maryam Adilah *et al.*, 2018). Epigallocatechin gallate (EGCG) is one of the major flavanols obtained from tea extract, which contained 10-60% of EGCG of dry weight (Zaveri, 2006). EGCG has been reported to exhibit antioxidant activity and play a role in preventing the lipid oxidation in foods (Lu *et al.*, 2010). Due to its antioxidant activity with safety concern, it can be employed as natural antioxidant in packaging.

Agricultural wastes from animal processing accounted for valuable raw materials for the recovery of valuable compounds (Barker *et al.*, 2004). Chicken skin

is one of the most important by-products of chicken carcass portioning plants, which is normally underutilized. The high content of fat (30-40%, wet basis) was observed in chicken skin (Farmani and Rostammiri, 2015). Chicken skin oil had a lower amount of saturated fatty acids and higher contents of *n*-3 and *n*-6 fatty acids than tallow, lard, and palm oil (Farmani and Rostammiri, 2015; Kallio *et al.*, 2001). However, oil with high unsaturated fatty acid is generally susceptible to lipid oxidation and to development of undesirable odor (Sae-leaw and Benjakul, 2017). The prevention or retardation of those deteriorative reactions of oil during processing and storage is required.

5.3 Objective

To characterize mono and bilayer gelatin-based films incorporated with EGCG and to investigate the quality of chicken skin oil stored in pouches made from those films during the extended storage.

5.4 Materials and methods

5.4.1 Materials

Glycerol, chloroform, trichloroacetic acid and isooctane were obtained from Merck (Darmstadt, Germany). Ammonium thiocyanate, 1,1,3,3-tetramethoxypropane, soy lecithin, oleic acid, cupric acetate and pyridine were purchased from Sigma-Aldrich (St. Louis, MO, USA). All chemicals were of analytical grade. Palm oil was obtained from OLEEN Company Limited (Bangkok, Thailand). Fish gelatin produced from tilapia skin (~240 bloom) was procured from Lapi Gelatine S.p.a (Empoli, Italy). (−)-epigallocatechin gallate (EGCG) was obtained from Chengdu Biopurify Phytochemicals Ltd., (Sichuan, China). Chicken skin was obtained from a local market in Hat Yai (Songkhla, Thailand).

5.4.2 Preparation of films

In order to prepare active film with the highest total phenolic content migration, EGCG at concentration of 5.71 wt % (based on protein content) was incorporated into fish gelatin solution (FFS) (Nilsuwan *et al.*, 2018b). Gelatin powder was mixed with distilled water to obtain a protein concentration of 3.5% (w/v). The

mixture was heated at 70 °C for 30 min with continuous stirring. Glycerol at a concentration of 30% (w/w, based on protein content) was added as plasticizer into solutions. FFS were cooled down to room temperature (28 ± 2 °C) and divided into 2 portions. The first portion was incorporated with EGCG. EGCG was added into FFS to obtain a final concentration of 5.71 wt % (based on protein content). The solution was stirred at room temperature for 1 h and degassed for 5 min using the sonicating bath. Both FFS (without EGCG) and that added with EGCG were used for film preparation.

To prepare film forming emulsions (FFE), 10% glycerol (w/w, based on protein content) was added to gelatin solutions. Palm oil, previously mixed with 50% soy lecithin (w/w based on palm oil) used as a surfactant, which was enough to stabilize the FFE during preparation as well as casting and drying into the film (Nilsuwan *et al.*, 2016b), was transferred into the previously prepared gelatin solution to obtain a final concentration of 75% (w/w, based on protein content). The mixture was homogenized at 22,000 rpm for 3 min using a rotor-stator homogenizer (IKA Labortechnik homogeniser, Selangor, Malaysia). The coarse emulsion was passed through a microfluidizer (Microfluidics, Model HC-5000, Newton, MA, USA) at 20.68 MPa for 2 passes. FFE was further used for film preparation.

In order to obtain monolayer films with an average thickness around 0.100 mm, a known volume of FFS (without or with EGCG) was cast onto a rimmed silicone resin plate (50 × 50 mm^2) and air-blown for 24 h at 25 °C and 60 ± 5% relative humidity (RH). The resulting films were designated as GF (gelatin films without EGCG) or E-GF (gelatin films with EGCG).

In order to obtain bilayer films with a final average thickness around 0.100 mm, a known volume of FFE was cast on monolayer films. After that, the samples were air-blown at room temperature (25 ± 2 °C) for 48 h prior to drying at 25 ± 2 °C and 50 ± 5% RH for 48 h in an environmental chamber. The bilayer films prepared by casting FFE on GF were designated as GF/EF, while the films prepared by casting FFE on E-GF were designated as E- GF/EF. The thickness ratio of two different monolayer films in bilayer film was 1:1.

5.4.3 Properties of monolayer and bilayer gelatin films

5.4.3.1 Film thickness

Film thickness was determined to the nearest 0.001 mm using a micrometer (Mitutoyo, Model ID-C112PM, Serial No. 00320, Mitutoyo Corp., Kawasaki-shi, Japan). Five locations around each film of ten film samples were used for determination of average thickness.

5.4.3.2 Mechanical properties

Prior to testing, films were conditioned for 48 h at 25 ± 2 °C and 50 ± 5% RH. Tensile strength (TS) and elongation at break (EAB) were determined as described by Iwata *et al.* (2000), using the Universal Testing Machine (Lloyd Instrument, Hampshire, UK) equipped with tensile load cell of 100 N. Ten samples (20×50 mm^2) with an initial grip length of 30 mm were used for testing. Cross-head speed was set at 30 mm/min.

5.4.3.3 Water vapor permeability (WVP)

WVP was measured using an ASTM method (ASTM, 1989) modified by Shiku *et al.* (2004). Films were sealed on an aluminium permeation cup containing dried silica gel (0% RH) with silicone vacuum grease and a rubber gasket to hold the films in place. The cups were placed in an environmental chamber at 25 ± 2 °C and 50 ± 5% RH. The cups were weighed at 1-h interval over a 10-h period. WVP of the film was calculated as follows:

$$\text{WVP (g m}^{-1}\text{s}^{-1}\text{Pa}^{-1}\text{)} = \frac{w\,l}{A\,t\,(P_2\text{-}P_1)}$$

where w is the weight gain of the cup (g); l is the film thickness (m); A is the exposed area of film (m^2); t is the time of gain (s); P_2-P_1 is the vapor pressure difference across the film (1583.7 Pa at 25 °C).

5.4.3.4 Oxygen permeability (OP)

OP of films was measured according to the ASTM D3985-05 method. An Oxygen Permeation Analyzer (Illinois model 8000, Illinois Instruments Inc., Johnsburg, IL, USA) was used to measure oxygen transmission rate (OTR) through the film. Each film was placed on a stainless steel mask. OTR was measured at 25 °C and 50% RH (Nilsuwan *et al.*, 2016b). The film was allowed to equilibrate for 10 h before measurements. OP was calculated using the following equation:

$$\text{OP (mol m}^{-1}\text{s}^{-1}\text{Pa}^{-1}) = \frac{\text{OTR } l}{\Delta P}$$

where OTR is the oxygen transmission rate (mol m^{-2} s^{-1}); l is the film thickness (m); ΔP is the partial pressure of oxygen (1.013×10^5 Pa at 25 °C).

5.4.3.5 Color

Film samples were subjected to color measurement using a CIE colorimeter (Hunter associates laboratory, Inc., Reston, VA, USA). D_{65} (day light) and a measure cell with opening of 30 mm was used. The color of the films was expressed as L^* -value (lightness), a^* -value (redness/greenness) and b^* -value (yellowness/blueness). Total difference of color (ΔE^*) was calculated as follows (Gennadios *et al.*, 1996):

$$\Delta E^* = \sqrt{(\Delta L^*)^2 + (\Delta a^*)^2 + (\Delta b^*)^2}$$

where ΔL^*, Δa^* and Δb^* are the differences between the color parameter of the samples and those of the white standard (L^* = 92.82, a^* = -1.24, b^* = 0.46).

5.4.3.6 Light transmittance and transparency

The light transmission of films was measured in the ultraviolet and visible range (200-800 nm) using a UV-vis spectrophotometer (UV-1800, Shimadzu, Kyoto, Japan), according to the method of Shiku *et al.* (2004). The transparency value of films was calculated using the following equation (Han and Floros, 1997):

$$\text{Transparency value} = \frac{-logT_{600}}{x}$$

where T_{600} is the fractional transmission at 600 nm and x is the film thickness (mm).

5.4.4 Quality changes of chicken skin oil (CSO) packaged in gelatin pouches

5.4.4.1 Preparation of CSO

CSO was extracted using the heating method, as described by Sae-leaw and Benjakul (2017), with a slight modification. The extraction was performed in a round bottom flask equipped with a rotary evaporator (N-1000, EYELA, Tokyo Rikakikai Co., Ltd., Tokyo, Japan) under vacuum. Chicken skin was cut into small pieces and ground with a blender. The ground sample (100 g) was heated at 70 °C for 20 min with a continuous swirling. The resulting mixture was centrifuged at 10,000 ×g for 20 min at room temperature to separate residual tissue, and lipid phase was collected.

5.4.4.2 Packaging of CSO in gelatin pouches

All gelatin-based films and LLDPE were used to prepare 3-side seal pouch using an impulse sealer with magnet model ME-300HIM (S.N.MARK Ltd., Park, Nonthaburi, Thailand). Films (50×50 mm^2) were heat-sealed at 150 ± 0.5 °C for 1.25 s, followed by cooling for 1.50 s. The width of seal area was 2 mm.

CSO (2 ml) was transferred manually into the pouches. Subsequently, pouches were heat-sealed. The pouches containing CSO were displayed on the tray and stored at 25-28 °C. The samples were randomly taken for analysis every 5 days up to 30 days.

5.4.4.3 Peroxide value (PV)

PV was determined according to the method of Hu *et al.* (2003) with slight modifications. CSO (0.1 g) was mixed with 5 ml of chloroform/methanol (2:1, v/v). The diluted sample (50 µl) was mixed with 2.35 ml of chloroform/methanol (2:1, v/v), followed by 50 µl of 30% ammonium thiocyanate (w/v) and 50 µl of 20 mM ferrous chloride solution in 3.5% HCl (w/v). After 20 min, the absorbance of the colored

solution was read at 500 nm using a spectrophotometer (UV-1800, Shimadzu, Kyoto, Japan). PV was calculated and expressed as mg cumene hydroperoxide equivalent/100 g oil. A standard curve was prepared using cumene hydroperoxide with the concentration range of 0.5–2 mg/kg.

5.4.4.4 Thiobarbituric acid-reactive substances (TBARS)

TBARS were determined as described by Buege and Aust (1978). The sample (0.5 g) was mixed with 2.5 ml of a solution containing 3.75% thiobarbituric acid (w/v), 15% trichloroacetic acid and 0.25 M HCl. The mixture was heated in boiling water for 10 min to develop a pink color, cooled with running tap water and centrifuged at 3600xg at 25 °C for 20 min using a centrifuge (Beckman Coulter, Avanti J-E Centrifuge, Fullerton, CA, USA). The absorbance of the supernatant was measured at 532 nm using a spectrophotometer. A standard curve was prepared using 1,1,3,3-tetramethoxypropane, a precusor for malonaldehyde, at concentrations ranging from 0 to 2 mg/kg. TBARS were calculated and expressed as mg malonaldehyde/100g oil.

5.4.4.5 Free fatty acid content

The free fatty acid (FFA) content, used as an index of hydrolysis, was determined as described by Takeungwongtrakul *et al.* (2012) with a slight modification. Lipid sample (0.05 g) was dissolved with 2.5 ml of isooctane and added with 1 ml of 5% (w/v) cupric acetate-pyridine reagent. The mixture was shaken vigorously for 90 s using a Vortex-Genie2 mixer (Bohemia, NY, USA) and allowed to stand for 20 s. The upper layer was subjected to absorbance measurements at 715 nm. A standard curve was prepared using oleic acid in isooctane at concentrations ranging from 0 to 50 μmol/2.5 ml. FFA content was expressed as g oleic acid/100 g oil.

5.4.4.6 Volatile compounds

Volatile compounds in CSO were determined at day 0 and 30 of storage, using a solid-phase microextraction gas chromatography mass spectrometry (SPME GC-MS), following the method of Iglesias and Medina (2008), as modified by Intarasirisawat *et al.* (2015).

5.4.4.7 Fatty acid profiles

The fatty acid profile was determined as fatty acid methyl esters (FAMEs), which were prepared according to the method of AOAC (2000). FAMEs were injected to the gas chromatography (7890B GC System, Agilent Technologies, Santa Clara, CA, USA) equipped with a flame ionization detector (FID) at a split ratio of 1:20. A fused silica capillary column (100 m × 0.25 mm × 0.20 µm), coated with bonded polysiloxane, was used. The analytical conditions were: injection port temperature of 250 °C and detector temperature of 270 °C. The oven was programmed from 170 to 225 °C at a rate of 1 °C /min (no initial or final hold). The retention times of FAME standards were used to identify the chromatographic peaks of the samples. Fatty acid content was calculated based on the peak area ratio, and it was expressed as g fatty acid/100 g lipid.

5.4.5 Statistical analysis

All experiments were run in triplicate with different three lots of films. Data were subjected to analysis of variance (ANOVA) and mean comparisons were carried out by the Duncan's multiple range test. Analysis was performed using the SPSS package (SPSS for windows, SPSS Inc., Chicago, IL, USA).

5.5 Results and discussion

5.5.1 Properties of monolayer and bilayer gelatin films

5.5.1.1 Mechanical properties

Mechanical properties of films expressed as tensile strength (TS) and elongation at break (EAB) are shown in Table 17. All gelatin-based films showed higher TS than LLDPE ($P < 0.05$). As can be seen in Table 17, TS values of bilayer films (GF/EF and E-GF/EF) were higher ($P < 0.05$) than those of the corresponding monolayer films (GF and E-GF); therefore, the strength of monolayer films was enhanced by the addition of the second layer. EF which had applied as an overlaid layer generally showed a high TS than GF (Nilsuwan *et al.*, 2017). It was associated with the lecithin used as the surfactant in emulsion gelatin film was mainly located at oil/water

interface, in which polar heads of phosphate groups were exposed to the aqueous phase. As a result, the ionic interaction between lecithin and positively charged domain from amino acid such as lysine, arginine and histidine in gelatin were occurred. This might help strengthen the EF network (Nilsuwan *et al.*, 2016a). Furthermore, gelatin films incorporated with EGCG showed higher TS than those without EGCG ($P < 0.05$). This result suggested that the incorporation of the phenolic compound provided stronger interaction in gelatin films (Hoque *et al.*, 2011a). The hydroxyl groups of EGCG molecules could interact with the side chain of gelatin via the formation of H-bonding, in which EGCG could act as a protein cross-linker (Nilsuwan *et al.*, 2018b). Nevertheless, gelatin films showed lower EAB than commercial LLDPE film, regardless of EGCG incorporation or bilayer formation, as shown in Table 17. However, it is worth noting that the films did not present any handling problem.

5.5.1.2 Barrier properties

Water vapor permeability (WVP) and oxygen permeability (OP) of gelatin-based films in comparison with LLDPE are shown in Table 17. WVP of all gelatin-based films were in the range of 5.35 – 6.64 $\times 10^{-11}$ g m^{-1} s^{-1} Pa^{-1}. In general, bilayer films (GF/EF and E-GF/EF) had lower WVP ($P < 0.05$) than monolayer films (GF and E-GF). Lamination of EF, which had a lower WVP onto GF, which has a higher WVP could render the bilayer film with lower WVP (Nilsuwan *et al.*, 2017). This result indicated that the palm oil droplets distributed in the second layer performed as a barrier against water vapor adsorption and migration through the film as evidenced by the roughness of SEM micrograph of film cross-section arising from droplets of palm oil in the emulsion film matrix (Nilsuwan *et al.*, 2017). Additionally, the contribution of GF or E-GF layer and EF layer on the WVP of resulting bilayer films was not investigate. This was due to the mergence between GF and EF at the interface of resulting bilayer film (Nilsuwan *et al.*, 2017). Nevertheless, the resulting WVP calculating from the whole sample including top/merged domain/bottom was more importantly. Furthermore, the monolayer film without EGCG (GF) exhibited lower WVP ($P < 0.05$) than the monolayer incorporated with EGCG (E-GF), indicating that the addition of EGCG could enhance the hydrophilicity of the gelatin film by interaction with water molecules via H-bonding.

Table 17. Thickness, tensile strength (TS), elongation at break (EAB), water vapor permeability (WVP) and oxygen permeability (OP) of monolayer and bilayer fish gelatin films incorporated without and with epigallocatechin gallate.

Films	**Thickness (mm)**	**TS (MPa)**	**EAB (%)**	**WVP (10^{-11} g m/m^2 s Pa)**	**OP (10^{-18} mol m/m^2 s Pa)**
LLDPE	0.038 ± 0.002 b	25.79 ± 3.25 d	578.07 ± 54.62 a	0.01 ± 0.00 d	1124.36 ± 12.13 a
GF	0.100 ± 0.002 a	29.93 ± 2.15 c	24.11 ± 2.60 b	5.89 ± 0.12 b	4.28 ± 0.03 b
E-GF	0.101 ± 0.005 a	36.43 ± 0.89 b	13.88 ± 1.69 b	6.64 ± 0.25 a	1.86 ± 0.03 b
GF/EF	0.096 ± 0.004 a	33.73 ± 3.21 b	15.47 ± 2.42 b	5.48 ± 0.44 c	7.99 ± 0.01 b
E-GF/EF	0.097 ± 0.006 a	40.70 ± 1.66 a	7.29 ± 0.81 b	5.35 ± 0.30 c	2.78 ± 0.01 b

LLDPE: linear low-density polyethylene film; GF: monolayer gelatin film; E-GF: monolayer gelatin film incorporated with EGCG; GF/EF: bilayer gelatin film; E-GF/EF: bilayer gelatin film incorporated with EGCG. Different lowercase letters in the same column indicate significant differences ($P < 0.05$).

OP of films is used as the index of efficiency in preventing lipid oxidation of packaged fatty foods (Cho *et al.*, 2010). LLDPE, which is hydrophobic in nature, had good water vapor barrier property but showed high oxygen permeability (Lee and Song, 2017; Rhim *et al.*, 2006). However, gelatin films are known to possess an excellent oxygen barrier property (Lee and Song, 2017; Nilsuwan *et al.*, 2016b), and it was noted that no differences in OP between all gelatin-based films were observed (Table 17), regardless of bilayer formation and EGCG incorporation ($P > 0.05$). Additionally, gelatin films with EGCG (E-GF and E-GF/EF) had slightly lower OP than those without EGCG ($P > 0.05$). This result might be related with a compact morphology as indicated by denser cross section of films when EGCG was incorporated (Nilsuwan *et al.*, 2018b).

5.5.1.3 Optical properties

The color of film samples is shown in Table 18. Overall, the color of films, expressed as L^*-, a^*-, b^*- and ΔE^*, varied depending on the number of layers and the addition of EGCG. Generally, gelatin films had lower L^*- and a^*-values and higher b^*- and ΔE^*-values than LLDPE film ($P < 0.05$). Regarding b^*-value, which indicates yellowish color, higher values were found when EGCG was incorporated into the monolayer films ($P < 0.05$). Yellowness and redness of resulting films were mostly from the color of EGCG, which was pale yellow in color (Nilsuwan *et al.*, 2018b). Furthermore, bilayer films showed higher b^* than monolayer films ($P < 0.05$). It was suggested that oil droplets distributed in EF layer contributed to the yellowish of bilayer films. The brownish yellow color of soy lecithin also contributed higher b^*-value of resulting film (Nilsuwan *et al.*, 2016a). ΔE^* values were mostly in line with b^*-values.

Light transmission at the selected wavelengths from 200 to 800 nm in UV and visible ranges, as well as transparency values of all film samples, are presented in Figure 19. In general, all gelatin-based films exhibited a good barrier property toward UV transmission (200–280 nm), compared to LLDPE. UV transmission at 280 nm of GF was 23.76% but markedly decreased when EGCG was incorporated. The value was

Table 18. Color and transparency of monolayer and bilayer fish gelatin films incorporated without and with epigallocatechin gallate.

Films	*L**	*a**	*b**	Δ*E**	Transparency value
LLDPE	91.01 ± 0.02 a	-1.29 ± 0.02 a	0.44 ± 0.02 d	1.83 ± 0.01 e	1.84 ± 0.04 c
GF	90.51 ± 0.04 b	-1.48 ± 0.02 b	1.74 ± 0.03 c	2.70 ± 0.02 d	0.61 ± 0.07 d
E-GF	90.23 ± 0.15 c	-1.29 ± 0.04 a	2.30 ± 0.15 b	3.23 ± 0.06 c	0.86 ± 0.12 d
GF/EF	90.62 ± 0.16 b	-2.14 ± 0.05 d	6.47 ± 0.14 a	6.54 ± 0.16 b	4.40 ± 0.21 b
E-GF/EF	90.22 ± 0.15 c	-1.87 ± 0.05 c	6.64 ± 0.29 a	6.81 ± 0.03 a	5.39 ± 0.30 a

LLDPE: linear low-density polyethylene film; GF: monolayer gelatin film; E-GF: monolayer gelatin film incorporated with EGCG; GF/EF: bilayer gelatin film; E-GF/EF: bilayer gelatin film incorporated with EGCG. Different lowercase letters in the same column indicate significant differences ($P < 0.05$).

lowered in bilayer films, particularly the bilayer film containing EGCG (0 %). This result suggested that the aromatic amino acid residues in gelatin and the aromatic structure of phenolic compounds played an important role in the UV barrier properties of resulting films (Jongjareonrak *et al.*, 2006; Limpisophon and Schleining, 2017). For the light transmission in the visible range (350-800 nm), light transmission was lowered for GF when EGCG was incorporated (E-GF). EGCG might act as protein cross-linker and induced the formation of aggregates, which contributed to the turbidity (Nilsuwan *et al.*, 2018b). Additionally, both bilayer films (GF/EF and E-GF/EF) showed lower light transmission in comparison with monolayer (GF and E-GF) films. This result was associated with the oil droplet distributed in the EF layer, which could impede the light transmission through bilayer films (Tongnuanchan *et al.*, 2015). Furthermore, GF and E-GF had the lowest transparency values ($P < 0.05$) (Table 18), indicating the most transparent films.

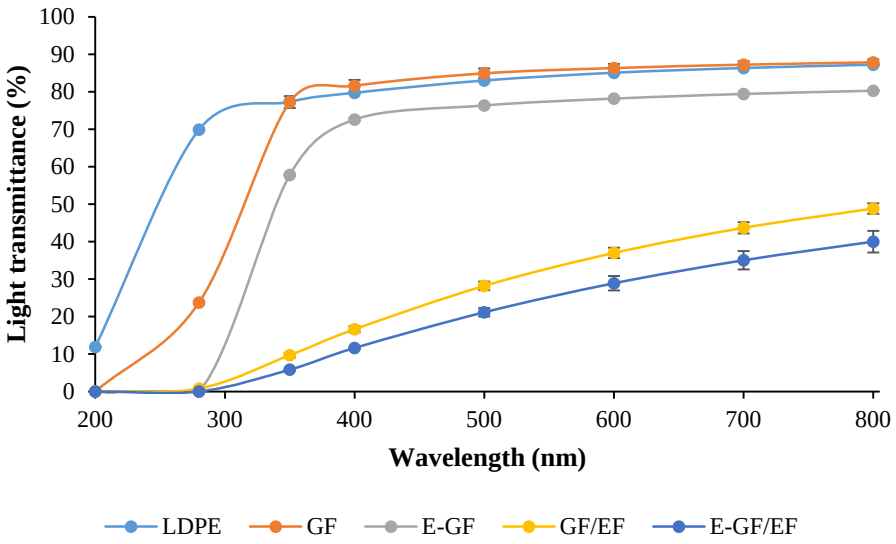

Figure 19. Light transmittance of monolayer and bilayer fish gelatin films incorporated without and with epigallocatechin gallate. LLDPE: linear low-density polyethylene; GF: monolayer gelatin film; E-GF: monolayer gelatin film incorporated with EGCG; GF/EF: bilayer gelatin film; E-GF/EF: bilayer gelatin film incorporated with EGCG.

5.5.2 Oxidative stability of chicken skin oil packaged in gelatin pouches

Photographs of chicken skin oil (CSO) packaged in different pouches made from LLDPE and monolayer (GF and E-GF) and bilayer (GF/EF and E-GF/EF) films are shown in Figure 20. All CSO samples packaged in pouches exhibited yellowish color, mostly attributed to the pigments in CSO. The glossy surface and see-through appearance were found for pouches based on LLDPE, GF and E-GF, while the opaqueness was observed for both pouches made from bilayer films. Therefore, the light barrier property, especially in the visible range, was enhanced for bilayer films, as previously shown by the results presented in Figure 19.

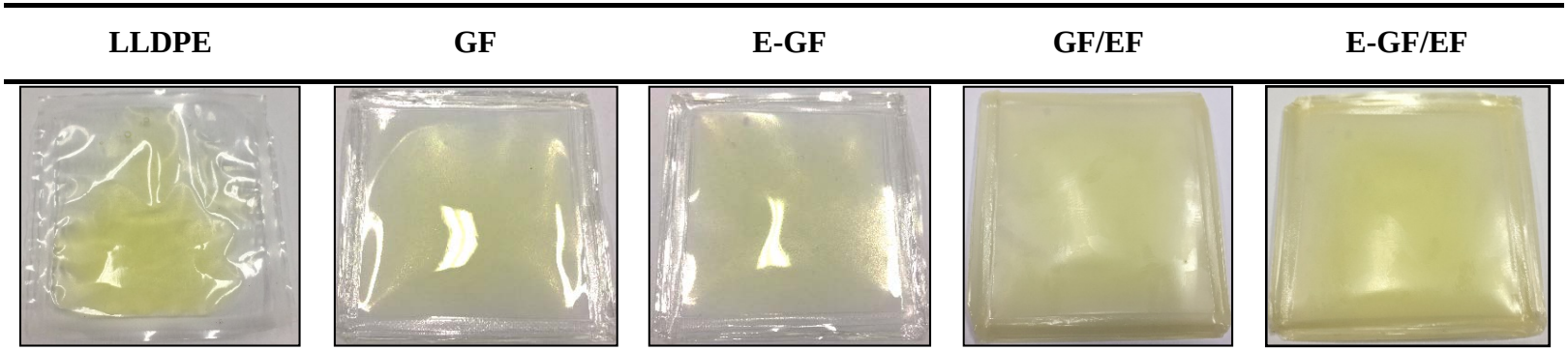

Figure 20. Photographs of chicken skin oil (CSO) packaged in different film pouches. LLDPE: linear low-density polyethylene; GF: monolayer gelatin film; E-GF: monolayer gelatin film incorporated with EGCG; GF/EF: bilayer gelatin film; E-GF/EF: bilayer gelatin film incorporated with EGCG.

5.5.2.1 Peroxide value (PV)

Changes in PV of CSO packaged in different pouches during 30 days of storage are shown in Figure 21A. PV is typically used for measurement of the concentration of hydroperoxides formed at the initial stage of lipid oxidation (Shahidi and Zhong, 2010). PV of CSO packaged in LLDPE pouch sharply increased ($P < 0.05$) up to 20 days of storage. The continuous increases in PV were also observed for the CSO samples packaged in other pouches but the rate of increase was lower ($P < 0.05$) in the samples packaged in E-GF, GF/EF and E-GF/EF pouches. The increase in PV indicated that the samples were in propagation stage of lipid oxidation. Lipid radicals react with oxygen to form peroxyl radicals, which act as the chain carriers of the rapid progressing reaction by attacking a new lipid molecule (Shahidi and Zhong, 2010). PV of all samples decreased after 20 days of storage and slightly increased between 25 – 30 days of storage. The decrease in PV might be due to the decomposition of hydroperoxides to secondary products (Shahidi and Zhong, 2010). It was noted that CSO packaged in gelatin pouches had lower PV than that packaged in the LLDPE pouch. This result was related to the excellent oxygen barrier property of gelatin-based films (Table 17). Cho *et al.* (2010) also documented that the higher oxygen barrier property of protein-based bilayer films (corn zein/soy protein isolate) resulted in a lower oxygen permeation into the pouch headspace than in the nylon/metalocene catalyzed linear low-density polyethylene (NY/mLLDPE) pouch, which led to reduce peroxide value in olive oil packaged in those pouches after 120 days of storage at 50 °C. Additionally, CSO packaged in E-GF and E-GF/EF pouches showed the lower PV values throughout 30 days of storage, compared to GF pouch ($P < 0.05$). This result indicated that the addition of EGCG enhanced the antioxidant activity of gelatin-based films.

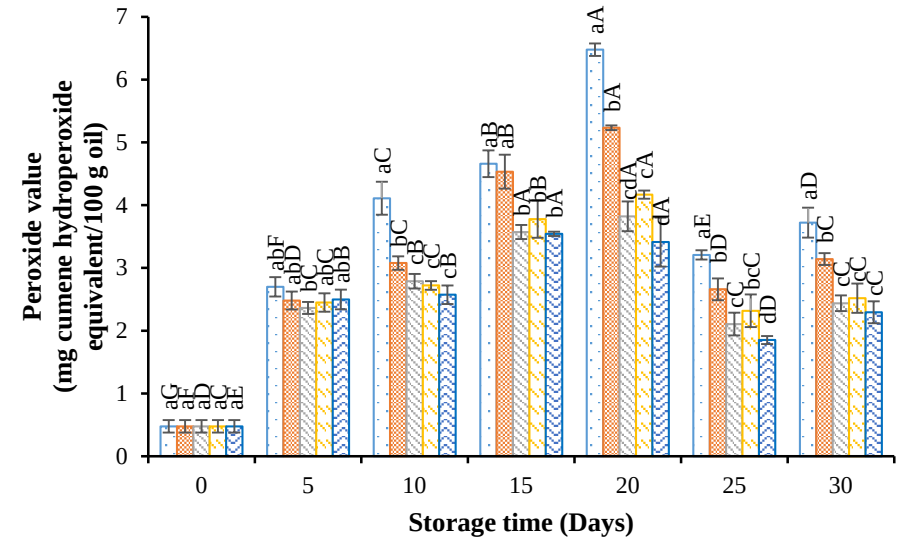
Peroxide value
(mg cumene hydroperoxide equivalent/100 g oil)
Storage time (Days)
0
5
10
15
20
25
30
aG aF aD aC aE
abF abD aC bC abG abB
aC bC cB cC cB
aB aB bA bB bA
aA bA cdA cA dA
aE bD cC bcC dD
aD bC cC cC cC

(A)

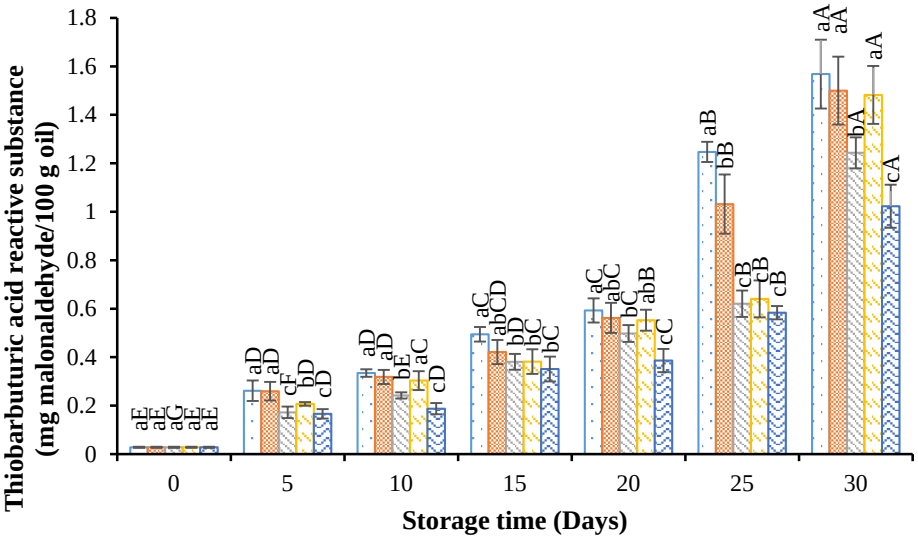
Thiobarbuturic acid reactive substance
(mg malonaldehyde/100 g oil)
Storage time (Days)
0
5
10
15
20
25
30
aE aE aG aE aE
aD aD cF bD cD
aD aD bE aC cD
aC abCD bD bC bC
aC abC bC abB cC
aB bB cB cB cB
aA aA bA aA cA

(B)

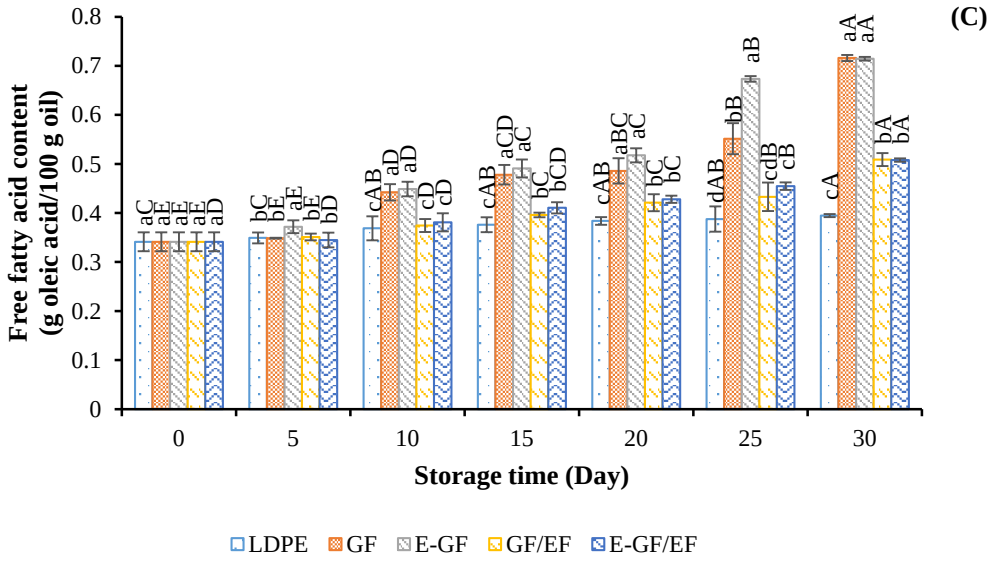

Figure 21. Peroxide value (A), thiobarbituric acid reactive substances (B) and free fatty acid content (C) of chicken skin oil packaged in different film pouches. The relative humidity (RH) and temperature conditions were 73-75% and 25-28 °C, respectively. LLDPE: linear low-density polyethylene; GF: monolayer gelatin film; E-GF: monolayer gelatin film incorporated with EGCG; GF/EF: bilayer gelatin film; E-GF /EF: bilayer gelatin film incorporated with EGCG. Different uppercase letters within the same packaging indicate significant differences ($P < 0.05$). Different lowercase letters within the same storage time indicate significant differences ($P < 0.05$).

5.5.2.2 Thiobarbituric acid reactive substances (TBARS)

TBARS values of CSO packaged in different gelatin pouches during 30 days of storage in comparison with LLDPE pouch are depicted in Figure 21B. Generally, high TBARS values were obtained for CSO packaged in LLDPE throughout 30 days. This result might be related with the lower oxygen barrier property of LLDPE (Table 17). When pouches made from gelatin-based films were used, similar trend of TBARS values was observed for all samples, except for CSO packaged in GF, which had higher TBARS after 20 days, compared with other samples. TBARS values of CSO packaged in GF/EF, E-GF and E-GF/EF gradually increased during the first 25 days and rapidly increased after 25 days of storage. The increases in TBARS values revealed the formation of secondary oxidation products, since TBARS value is an index of

decomposition of hydroperoxides into the secondary oxidation products in the later stages of lipid oxidation (Jacobsen, 2010). Hydroperoxides are decomposed to malonaldehyde, which contributes to off-flavor of oxidized lipids (Sae-leaw and Benjakul, 2017). It is worth noting that TBARS value of CSO packaged in GF/EF pouch was slightly lower than that of CSO packaged in GF pouch, indicating that the EF layer in the bilayer film could enhance the water vapor barrier property along with retaining oxygen barrier property of gelatin film. Also, TBARS values of CSO packaged in E-GF and E-GF/EF pouches generally lowered than those of CSO packaged in GF pouch. The addition of EGCG in gelatin-based film was found to have preventive effects on TBARS formation in the CSO during storage. EGCG possessed a broad antioxidant activity and could lower the formation of free radicals and the decomposition of hydroperoxides into secondary oxidation products (Nilsuwan *et al.*, 2018b). Thus, the packaging used was a prime factor affecting oxygen permeability, thereby influencing oxidative stability of CSO during the storage.

5.5.2.3 Free fatty acid (FFA) content

FFA contents of CSO packaged in different pouches during 30 days of storage are shown in Figure 21C. No differences in FFA contents were observed between all CSO samples during the first 5 days of storage. When pouch made from LLDPE was used, lower FFA content ($P < 0.05$) was obtained for CSO throughout 30 days of storage, compared to those observed in CSO packaged in other pouches, especially after 15 days of storage. This was in agreement with the lowest WVP of LLDPE reported in Table 17. For the CSO packaged in gelatin-based pouches, the continuous increase in FFA contents was obtained for all CSO samples after 10 days of storage but the rate of increase varied, depending on the pouches used. Lower increases ($P < 0.05$) in FFA content were obtained for CSO packaged in pouches made from bilayer-based films (GF/EF and E-GF/EF), compared to those of CSO packaged in monolayer film based pouches (GF and E-GF). Low water vapor barrier property with high moisture adsorption was commonly observed for gelatin films due to their hydrophilic nature; therefore, this result indicated that the additional layer of EF could enhance the water vapor barrier property of gelatin film. Slightly higher FFA contents were found for CSO packaged in the pouches with EGCG (E-GF and E-GF/EF) in

comparison to those observed in CSO packaged in pouches without EGCG incorporation (GF and GF/EF). This was plausibly associated with the high hydrophilicity of EGCG, which made film more hydrophilic. As a consequence, the absorbed water into CSO could induce more hydrolysis. Hydrolysis of glycerol-fatty acid esters is one important change occurring in lipids, thus causing the release of free fatty acids (Sae-leaw and Benjakul, 2017). Generally, lipids can undergo hydrolysis in the presence of moisture and heat (Chantachum *et al.*, 2000). The formation of free fatty acids were likely prone to oxidation. This was coincidental with the increased lipid oxidation as monitored by the increases in PV and TBARS (Figure 21A and 21B). However, the addition of EGCG could lower the oxidation of free fatty acid as indicated by the lowered PV and TBARS of CSO packaged in E-GF pouch, particularly during 10-30 days.

5.5.2.4 Volatile compounds

Selected volatile compounds in CSO packaged in different pouches after 30 days of storage in comparison to freshly prepared oil (day 0) are presented in Table 19. CSO contained polyunsaturated fatty acids (PUFAs), particularly linoleic acid (C18:2) (Kallio *et al.*, 2001). PUFAs are susceptible to oxidation, in which a variety of secondary oxidation products (aldehydes, ketones, and alcohols) can be formed (Thiansilakul *et al.*, 2011). Aldehydes, especially hexanal, were the most prominent volatiles found in CSO. At day 0, the lowest abundance of volatile compounds was found. The major volatile compound found in CSO at day 0 was hexanal, since lipid oxidation might take place in CSO to some degree during extraction. After 30 days of storage, pentanal, hexanal, and 2,4-heptadienal were detected in all CSO samples. Higher abundance of hexanal was found for all CSO samples after storage, in comparison to that present in CSO at 0 day. Hexanal, which contributes to rancid off-odors, is a typical volatile compound formed from linoleic acid during both autoxidation and singlet oxygen promoted oxidation (Thiansilakul *et al.*, 2011). The formation of pentanal may be also explained by the hexanal decomposition (Frankel, 2014). In addition, no nonanal, 2-decenal, 2-propenal and octenal were observed for CSO samples packaged in pouches containing EGCG. Lower abundance of pentanal and hexanal were also found for both aforementioned CSO, compared to others.

Moreover, new alcoholic volatile compounds in all CSO samples, including 1-octen-3-ol, 3-pentanol, 3,5-octadien-2-ol and 2,2-dimethyl propanol, were found after 30 days of storage. Alcohols are known as the secondary products via the decomposition of hydroperoxides (Ross and Smith, 2006). Aliphatic alcohols, particularly unsaturated alcohols, were also alternatively involved in off-flavors due to their lower threshold values than those of the saturated ones (Song *et al.*, 2011). 1-Octen-3-ol was the most predominant volatile occurred in CSO packaged in LLDPE, GF, E-GF and E-GF/EF pouches. 1-Octen-3-ol is a volatile generated from linoleic acid oxidation in the presence of singlet oxygen. 1-Octen-3-ol is originated from n–6 fatty acid autoxidation (Lee and Min, 2010). Additionally, 3-Pentanol, 3,5-octadien-2-ol and 2,2-dimethyl propanol were found for CSO packaged in E-GF/EF, LLDPE and GF/EF pouches, respectively.

Ketones are other secondary lipid oxidation products derived from the decomposition of hydroperoxide (Iglesias and Medina, 2008). 1-Octen-3-one, 2-heptanone, 1-hydroxybutan-2-one and 2-hydroxypentan-3-one were the new volatile compounds observed in CSO after storage. No 2,3-pentanedione or 2,3-octanedione were found in all CSO samples after 30 days of storage, whereas they were found in CSO at day 0.

Among all the pouches used, the lowest abundance of volatile compound was generally found in CSO packaged in E-GF/EF pouch. This result was associated with the lower PV and TBARS values (Figure 3). Therefore, the addition of EGCG into gelatin film forming solutions, together with the addition of a second layer incorporating palm oil, had effectiveness in retarding the formation of secondary lipid oxidation products, responsible for the quality deterioration and unacceptability of CSO.

Table 19. Volatile compounds of chicken skin oil packaged in different pouches at day 0 and 30 of storage at 25-28 °C.

Compounds	Day 0	Day 30				
		LLDPE	GF	E-GF	GF/EF	E-GF/EF
Aldehydes						
Pentanal	ND	2.90	4.94	2.34	4.46	2.65
Hexanal	2.58	28.76	27.38	19.04	25.65	19.16
Heptanal	ND	3.22	ND	1.60	ND	ND
Nonanal	ND	3.92	0.28	ND	0.23	ND
2-Decenal	ND	2.14	ND	ND	ND	ND
2,4-Heptadienal	ND	0.99	2.56	1.58	0.94	0.91
2-Propenal	ND	ND	ND	ND	1.66	ND
Octenal	ND	ND	ND	ND	0.41	ND
Alcohols						
1-Octen-3-ol	ND	1.87	2.50	1.33	ND	1.31
3-Pentanol	ND	ND	ND	ND	ND	0.95
3,5-Octadien-2-ol	ND	0.36	ND	ND	ND	ND
2,2-dimethyl propanol	ND	ND	ND	ND	0.80	ND
Ketone						
2,3-Pentanedione	1.14	ND	ND	ND	ND	ND
1-Octen-3-one	ND	ND	ND	ND	0.33	ND
2,3-Octanedione	0.15	ND	ND	ND	ND	ND
2-Heptanone	ND	0.29	ND	ND	ND	ND
1-Hydroxybutan-2-one	ND	1.56	ND	1.36	2.13	1.26
2-Hydroxypentan-3-one	ND	ND	ND	0.15	ND	0.41

Values are expressed as abundance ($\times 10^6$). ND: not detectable; LLDPE: linear low-density polyethylene film; GF: monolayer gelatin film; E-GF: monolayer gelatin film incorporated with EGCG; GF/EF: bilayer gelatin film; E-GF/EF: bilayer gelatin film incorporated with EGCG.

5.5.2.5 Fatty acid profiles

Fatty acid profiles of CSO packaged in different pouches after 30 days of storage in comparison to freshly prepared CSO (day 0) are shown in Table 20. At day 0, CSO contained 27.19% saturated fatty acid (SFA), 42.73% monounsaturated fatty acid (MUFA) and 29.57% polyunsaturated fatty acid (PUFA). Oleic acid (C18:1 *n*-9) was the most abundant fatty acid (37.15 g/100 g oil), followed by linoleic acid

(C18:2 *n*-6) (26.10 g/100 g oil), and palmitic acid (C16:0) (19.95 g/100 g oil), respectively. This result was in agreement with Kallio *et al.* (2001) who reported that oleic acid, linoleic acid and palmitic acid were the predominant fatty acids in the lipids obtained from chicken skin. After 30 days of storage, MUFA and PUFA contents slightly decreased, along with increasing SFA content ($P < 0.05$) for all CSO samples. The decreases in MUFA and PUFA contents were mostly related with their susceptibility to oxidation during the extended storage (Buamard and Benjakul, 2017). Lower decreases in MUFA and PUFA contents were found for CSO packaged in E-GF and E-GF/EF pouches, compared to those packaged in LLDPE, GF and GF/EF pouches ($P < 0.05$). These results were related with the lower primary and secondary oxidation products present in CSO packaged in E-GF and E-GF/EF pouches after 30 day of storage (Figure 21A-21B). It was indicated that the addition of EGCG into gelatin film forming solutions could lower the oxidation of MUFA and PUFA to some extent, as indicated by the high levels of oleic acid (C18:1 *n*-9) and linoleic acid (C18:2 *n*-6) retained. Furthermore, the *trans* fatty acid was observed for CSO at 0 day, and it was increased after 30 days of storage. A similar trends has also been observed in other works, where C18:1 trans n-9 and C18:2 *trans* n-6 in Altay sheep fat were found at day 0 and increased by 2.3% and 0.4%, respectively, after 50 days of storage (Li *et al.*, 2017). Overall, E-GF/EF pouch could lower the oxidation of CSO more effectively than others due to the antioxidant activity of EGCG (Nilsuwan *et al.*, 2018b).

Table 20. Fatty acid profiles of chicken skin oil packaged in different pouches at day 0 and 30 of storage at 25-28 °C.

Fatty acid (g/100 g oil)	Day 0	Day 30				
		LLDPE	GF	E-GF	GF/EF	E-GF/EF
C14:0	0.81 ± 0.04 b	1.14 ± 0.08 a	1.14 ± 0.00 a	1.11 ± 0.00 a	1.13 ± 0.00 a	1.08 ± 0.00 a
C14:1	0.29 ± 0.02 c	0.46 ± 0.04 a	0.46 ± 0.00 a	0.44 ± 0.00 ab	0.45 ± 0.00 ab	0.43 ± 0.00 b
C15:0	0.24 ± 0.02 c	0.41 ± 0.04 a	0.40 ± 0.00 ab	0.39 ± 0.00 ab	0.40 ± 0.00 ab	0.37 ± 0.00 b
C16:0	19.95 ± 0.01 e	21.41 ± 0.21 b	20.89 ± 0.03 d	21.74 ± 0.01 a	21.1 ± 0.01 c	21.80 ± 0.00 a
C16:1 n-7	4.69 ± 0.00 a	4.61 ± 0.02 c	4.59 ± 0.01 d	4.64 ± 0.01 b	4.58 ± 0.01 d	4.62 ± 0.00 b
C17:0	0.32 ± 0.02 b	0.48 ± 0.04 a	0.47 ± 0.00 a	0.46 ± 0.00 a	0.47 ± 0.00 a	0.44 ± 0.00 a
C17:1	0.23 ± 0.02 c	0.45 ± 0.09 a	0.40 ± 0.00 ab	0.38 ± 0.00 b	0.40 ± 0.00 ab	0.37 ± 0.00 b
C18:0	5.03 ± 0.01 d	5.46 ± 0.08 b	5.33 ± 0.00 c	5.55 ± 0.00 a	5.38 ± 0.00 c	5.58 ± 0.04 a
C18:1 *trans n*-9	0.30 ± 0.02 b	0.47 ± 0.04 a	0.46 ± 0.00 a	0.45 ± 0.00 a	0.46 ± 0.00 a	0.43 ± 0.00 a
C18:1 *n*-9	37.15 ± 0.24 a	34.41 ± 0.02 c	34.36 ± 0.02 c	34.82 ± 0.01 b	34.25 ± 0.02 c	34.89 ± 0.02 b
C18:2 *trans n*-6	0.21 ± 0.02 c	1.33 ± 0.87 b	2.35 ± 0.02 a	0.38 ± 0.00 c	2.32 ± 0.00 a	0.36 ± 0.00 c
C18:2 n-6	26.10 ± 0.16 a	24.32 ± 0.08 c	24.25 ± 0.00 c	24.56 ± 0.00 b	24.22 ± 0.01 c	24.62 ± 0.00 b
C20:0	0.44 ± 0.04 b	0.77 ± 0.08 a	0.77 ± 0.00 a	0.73 ± 0.00 a	0.76 ± 0.00 a	0.70 ± 0.00 a
C18:3 n-6	0.61 ± 0.00 a	0.57 ± 0.04 b	0.57 ± 0.00 b	0.55 ± 0.00 ab	0.56 ± 0.00 ab	0.53 ± 0.00 b
C20:1	0.37 ± 0.13 c	0.52 ± 0.06 ab	0.42 ± 0.00 b	0.60 ± 0.00 a	0.42 ± 0.00 b	0.59 ± 0.00 a
C18:3 n-3 (ALA)	2.17 ± 0.03 a	2.14 ± 0.03 b	2.14 ± 0.00 b	2.15 ± 0.00 b	2.13 ± 0.00 b	2.14 ± 0.00 b
C20:2 n-6	0.36 ± 0.02 a	0.27 ± 0.01 b	0.20 ± 0.00 c	0.28 ± 0.00 b	0.21 ± 0.00 c	0.28 ± 0.00 b
C20:3 n-3	0.33 ± 0.02 a	0.22 ± 0.00 d	0.24 ± 0.00 bc	0.25 ± 0.00 b	0.23 ± 0.00 cd	0.25 ± 0.00 b
C23:0	0.40 ± 0.02 c	0.55 ± 0.04 a	0.54 ± 0.00 a	0.53 ± 0.01 ab	0.53 ± 0.00 ab	0.51 ± 0.00 b
Saturated fatty acid (SFA)	27.19 ± 0.11 c	30.22 ± 0.57 a	29.54 ± 0.02 b	30.51 ± 0.00 a	29.76 ± 0.00 b	30.49 ± 0.03 a
Monounsaturated fatty acid (MUFA)	42.73 ± 0.07 a	40.46 ± 0.11 c	40.24 ± 0.01 d	40.88 ± 0.01 b	40.10 ± 0.02 e	40.9 ± 0.02 b
Polyunsaturated fatty acid (PUFA)	29.57 ± 0.09 a	27.52 ± 0.16 c	27.41 ± 0.00 cd	27.79 ± 0.00 b	27.36 ± 0.01 d	27.82 ± 0.01 b
Total *trans* fatty acid (TFA)	0.51 ± 0.04 d	1.79 ± 0.83 b	2.81 ± 0.02 a	0.83 ± 0.00 c	2.78 ± 0.01 a	0.80 ± 0.00 c

ND: not detectable; LLDPE: linear low-density polyethylene film; GF: monolayer gelatin film; E-GF: monolayer gelatin film incorporated with EGCG; GF/EF: bilayer gelatin film; E-GF/EF: bilayer gelatin film incorporated with EGCG.

5.6 Conclusions

The properties of fish gelatin-based films were influenced by the addition of EGCG into film forming solutions and also by the formation of bilayer films. All gelatin films showed very low OP, especially when compared to commercial synthetic films, such as LLDPE. Furthermore, the addition of EGCG reduced the UV transmission of films and increased the tensile strength, thus improving light barrier and mechanical resistance of the resulting films. Oxidative stability of chicken skin oil (CSO) was also influenced by EGCG addition and bilayer formation. CSO packaged in the pouches with EGCG (E-GF and E-GF/EF) had lower PV and TBARS throughout 30 days of storage. Moreover, E-GF/EF pouches could retard the lipid oxidation in CSO and maintain polyunsaturated fatty acids more effectively. Therefore, the pouch based on bilayer gelatin film containing EGCG could be applied for shelf-life extension of non-aqueous food products, especially those prone to lipid oxidation.

5.7 References

AOAC. 2000. Official method of analysis. Association of Official Chemists. Washington.

Barker, D., Lankhaar, J. and Stals, P. 2004. Primary processing of poultry. *In* Poultry meat processing and quality. p. 90-107. Elsevier.

Benbettaïeb, N., Debeaufort, F. and Karbowiak, T. 2018. Bioactive edible films for food applications: mechanisms of antimicrobial and antioxidant activity. Crit. Rev. Food Sci. Nutr. 1-25.

Bertan, L. C., Tanada-Palmu, P. S., Siani, A. C. and Grosso, C. R. F. 2005. Effect of fatty acids and ‘Brazilian elemi’ on composite films based on gelatin. Food Hydrocolloid. 19: 73-82.

Buamard, N. and Benjakul, S. 2017. Ethanolic coconut husk extract: In vitro antioxidative activity and effect on oxidative stability of shrimp oil emulsion. Eur. J. Lipid Sci. Technol. 119: 1700131.

Buege, J. A. and Aust, S. D. 1978. Microsomal lipid peroxidation. *In* Methods in enzymology. Vol. 52. (Flesicher, S. and Packer, L., eds.). p. 302–310. Academic Press. New York.

Chantachum, S., Benjakul, S. and Sriwirat, N. 2000. Separation and quality of fish oil from precooked and non-precooked tuna heads. Food Chem. 69: 289-294.

Cho, S. Y., Lee, S. Y. and Rhee, C. 2010. Edible oxygen barrier bilayer film pouches from corn zein and soy protein isolate for olive oil packaging. LWT-Food Sci. Technol. 43: 1234-1239.

Farmani, J. and Rostammiri, L. 2015. Characterization of chicken waste fat for application in food technology. Journal of Food Measurement and Characterization. 9: 143-150.

Frankel, E. N. 2014. Lipid oxidation. Elsevier. California.

Gennadios, A., Hanna, M. A. and Kurth, L. B. 1997. Application of edible coatings on meats, poultry and seafoods: a review. LWT-Food Sci. Technol. 30: 337-350.

Gennadios, A., McHugh, T. H., Weller, C. L. and Krochta, J. M. 1994. Edible coatings and films based on proteins. *In* Edible coatings and films to improve food quality. (Krochta, J. M. *et al.*, eds.). p. 210–278. Technomic Pub. Co., Inc. Lancaster, NC.

Gennadios, A., Weller, C. L., Hanna, M. A. and Froning, G. W. 1996. Mechanical and barrier properties of egg albumen films. J. Food Sci. 61: 585-589.

Gómez-Estaca, J., Bravo, L., Gómez-Guillén, M. C., Alemán, A. and Montero, P. 2009. Antioxidant properties of tuna-skin and bovine-hide gelatin films induced by the addition of oregano and rosemary extracts. Food Chem. 112: 18-25.

Gómez-Guillén, M. C., Pérez-Mateos, M., Gómez-Estaca, J., López-Caballero, E., Giménez, B. and Montero, P. 2009. Fish gelatin: A renewable material for developing active biodegradable films. Trends Food Sci. Technol. 20: 3-16.

Han, J. H. and Floros, J. D. 1997. Casting antimicrobial packaging films and measuring their physical properties and antimicrobial activity. J. Plast. Film Sheet. 13: 287-298.

Hoque, M. S., Benjakul, S. and Prodpran, T. 2011a. Properties of film from cuttlefish (*Sepia pharaonis*) skin gelatin incorporated with cinnamon, clove and star anise extracts. Food Hydrocolloid. 25: 1085-1097.

Hoque, M. S., Benjakul, S., Prodpran, T. and Songtipya, P. 2011b. Properties of blend film based on cuttlefish (*Sepia pharaonis*) skin gelatin and mungbean protein isolate. Int. J. Biol. Macromol. 49: 663-673.

Hu, M., McClements, D. J. and Decker, E. A. 2003. Lipid oxidation in corn oil-in-water emulsions stabilized by casein, whey protein isolate, and soy protein isolate. J. Agric. Food Chem. 51: 1696-1700.

Iglesias, J. and Medina, I. 2008. Solid-phase microextraction method for the determination of volatile compounds associated to oxidation of fish muscle. J. Chromatogr. A. 1192: 9-16.

Intarasirisawat, R., Benjakul, S., Vissessanguan, W., Maqsood, S. and Osako, K. 2015. Skipjack roe protein hydrolysate combined with tannic acid increases the stability of fish oil upon microencapsulation. Eur. J. Lipid Sci. Technol. 117: 646-656.

Iwata, K. I., Ishizaki, S. H., Handa, A. K. and Tanaka, M. U. 2000. Preparation and characterization of edible films from fish water-soluble proteins. Fish. Sci. 66: 372-378.

Jacobsen, C. 2010. Oxidation of fish oils and foods enriched with omega-3 polyunsaturated fatty acids. *In* Oxidation in Foods and Beverages and Antioxidant Applications. (Decker, E. A. *et al.*, eds.). p. 156-180. Woodhead Publishing. Cambridge.

Jongjareonrak, A., Benjakul, S., Visessanguan, W., Prodpran, T. and Tanaka, M. 2006. Characterization of edible films from skin gelatin of brownstripe red snapper and bigeye snapper. Food Hydrocolloid. 20: 492-501.

Kallio, H., Yli-Jokipii, K., Kurvinen, J.-P., Sjövall, O. and Tahvonen, R. 2001. Regioisomerism of triacylglycerols in lard, tallow, yolk, chicken skin, palm oil, palm olein, palm stearin, and a transesterified blend of palm stearin and coconut oil analyzed by tandem mass spectrometry. J. Agric. Food Chem. 49: 3363-3369.

Kurek, M., Galus, S. and Debeaufort, F. 2014. Surface, mechanical and barrier properties of bio-based composite films based on chitosan and whey protein. Food Pack. Shelf Life. 1: 56-67.

Lee, J. and Min, D. B. 2010. Analysis of volatile compounds from chlorophyll photosensitized linoleic acid by headspace solid-phase microextraction (HS-SPME). Food Science and Biotechnology. 19: 611-616.

Lee, K.-Y. and Song, K. B. 2017. Preparation and characterization of an olive flounder (*Paralichthys olivaceus*) skin gelatin and polylactic acid bilayer film. J. Food Sci. 82: 706-710.

Li, Y., Li, Y. B. and Liu, C. J. 2017. Changes in lipid oxidation and fatty acids in Altay sheep fat during a long time of low temperature storage. Journal of Oleo Science. 66: 321-327.

Limpisophon, K. and Schleining, G. 2017. Use of gallic acid to enhance the antioxidant and mechanical properties of active fish gelatin film. J. Food Sci. 82: 80-89.

Limpisophon, K., Tanaka, M. and Osako, K. 2010. Characterisation of gelatin–fatty acid emulsion films based on blue shark (*Prionace glauca*) skin gelatin. Food Chem. 122: 1095-1101.

Lu, T.-M., Lee, C.-C., Mau, J.-L. and Lin, S.-D. 2010. Quality and antioxidant property of green tea sponge cake. Food Chem. 119: 1090-1095.

Maryam Adilah, Z. A., Jamilah, B. and Nur Hanani, Z. A. 2018. Functional and antioxidant properties of protein-based films incorporated with mango kernel extract for active packaging. Food Hydrocolloid. 74: 207-218.

Nilsuwan, K., Benjakul, S. and Prodpran, T. 2016a. Effects of soy lecithin levels and microfluidization conditions on properties of fish gelatin-based film incorporated with palm oil. Int. J. Food Eng. 12: 647-660.

Nilsuwan, K., Benjakul, S. and Prodpran, T. 2016b. Quality changes of shrimp cracker covered with fish gelatin film without and with palm oil incorporated during storage. Int. Aquat. Res. 8: 227-238.

Nilsuwan, K., Benjakul, S. and Prodpran, T. 2017. Properties, microstructure and heat seal ability of bilayer films based on fish gelatin and emulsified gelatin films. Food Biophys. 12: 234-243.

Nilsuwan, K., Benjakul, S. and Prodpran, T. 2018a. Physical/thermal properties and heat seal ability of bilayer films based on fish gelatin and poly(lactic acid). Food Hydrocolloid. 77: 248-256.

Nilsuwan, K., Benjakul, S. and Prodpran, T. 2018b. Properties and antioxidative activity of fish gelatin-based film incorporated with epigallocatechin gallate. Food Hydrocolloid. 80: 212-221.

Nuthong, P., Benjakul, S. and Prodpran, T. 2009. Effect of phenolic compounds on the properties of porcine plasma protein-based film. Food Hydrocolloid. 23: 736-741.

Rhim, J.-W., Mohanty, K. A., Singh, S. P. and Ng, P. K. W. 2006. Preparation and properties of biodegradable multilayer films based on soy protein isolate and poly (lactide). Industrial and Engineering Chemistry Research. 45: 3059-3066.

Ross, C. F. and Smith, D. M. 2006. Use of volatiles as indicators of lipid oxidation in muscle foods. Compr. Rev. Food Sci. Food Saf. 5: 18-25.

Sae-leaw, T. and Benjakul, S. 2017. Lipids from visceral depot fat of Asian seabass (*Lates calcarifer*): Compositions and storage stability as affected by extraction methods. Eur. J. Lipid Sci. Technol. 119: 1700198.

Shahidi, F. and Zhong, Y. 2010. Lipid oxidation and improving the oxidative stability. Chem. Soc. Rev. 39: 4067-4079.

Shiku, Y., Hamaguchi, P. Y., Benjakul, S., Visessanguan, W. and Tanaka, M. 2004. Effect of surimi quality on properties of edible films based on Alaska pollack. Food Chem. 86: 493-499.

Song, S., Zhang, X., Hayat, K., Liu, P., Jia, C., Xia, S., Xiao, Z., Tian, H. and Niu, Y. 2011. Formation of the beef flavour precursors and their correlation with chemical parameters during the controlled thermal oxidation of tallow. Food Chem. 124: 203-209.

Takeungwongtrakul, S., Benjakul, S. and H-kittikun, A. 2012. Lipids from cephalothorax and hepatopancreas of Pacific white shrimp (*Litopenaeus vannamei*): Compositions and deterioration as affected by iced storage. Food Chem. 134: 2066-2074.

Thiansilakul, Y., Benjakul, S. and Richards, M. P. 2011. Effect of myoglobin from Eastern little tuna muscle on lipid oxidation of washed Asian seabass mince at different pH conditions. J. Food Sci. 76: C242-C249.

Tongnuanchan, P., Benjakul, S. and Prodpran, T. 2014. Comparative studies on properties and antioxidative activity of fish skin gelatin films incorporated with essential oils from various sources. Int. Aquat. Res. 6: 62.

Tongnuanchan, P., Benjakul, S., Prodpran, T. and Nilsuwan, K. 2015. Emulsion film based on fish skin gelatin and palm oil: Physical, structural and thermal properties. Food Hydrocolloid. 48: 248-259.

Tongnuanchan, P., Benjakul, S., Prodpran, T. and Songtipya, P. 2013. Properties and stability of protein-based films from red tilapia (*Oreochromis niloticus*) protein isolate incorporated with antioxidant during storage. Food Bioprocess Tech. 6: 1113-1126.

Vanin, F. M., Sobral, P. J. A., Menegalli, F. C., Carvalho, R. A. and Habitante, A. M. Q. B. 2005. Effects of plasticizers and their concentrations on thermal and functional properties of gelatin-based films. Food Hydrocolloid. 19: 899-907.

Zaveri, N. T. 2006. Green tea and its polyphenolic catechins: Medicinal uses in cancer and noncancer applications. Life Sci. 78: 2073-2080.

CHAPTER 6

PROPERTIES OF FISH GELATIN FILM CONTAINING EPIGALLOCATECHIN GALLATE FABRICATED BY THERMO-COMPRESSION MOLDING

6.1 Abstract

An alternative approach towards more producible active films based on fish gelatin and epigallocatechin gallate (EGCG) fabricated by thermo-compression molding was investigated in this study. This strategy permitted the reduction of production times. Furthermore, EGCG, used as a natural antioxidant, promoted the interaction with gelatin, as shown by Fourier transform infrared spectroscopy, total soluble matter, X-ray diffraction and thermogravimetric analyses. This interaction led to the formation of homogeneous structures, as observed by scanning electron microscopy, indicating a good compatibility among all the components of the mixture. Films with EGCG at 5.71% and 17.14% showed good mechanical properties, both tensile strength and elongation at break. In addition, EGCG provided films with lower gloss and mass loss as well as slow release profile with DPPH radical scavenging activity. Therefore, optimum level of EGCG rendered satisfactory functional properties for thermocompression molded gelatin films, which could be used for food or pharmaceutical applications.

6.2 Introduction

Gelatin is an animal protein derived from the partial hydrolysis of native collagens, which are the most abundant structural proteins found in the skins, bones and connective tissues (Muralidharan *et al.*, 2013). Generally, the skin and bones of pigs and cows are typically sources of gelatin. However, Halal and Kosher food markets and outbreaks of Bovine Spongiform Encephalopathy (BSE) have increased the interest in the production of fish gelatin from fish skins and bones as alternative sources (Arpi *et al.*, 2018; Gómez-Estaca *et al.*, 2009; Karim and Bhat, 2009). Gelatin has received attention for the development of edible films due to its abundance, biodegradability and

excellent film-forming ability (Etxabide *et al.*, 2016). Gelatin films possess outstanding properties such as transparency, biodegradability as well as gas and aroma barrier properties, which are appropriate for applications as biodegradable packaging (Etxabide *et al.*, 2016; Nilsuwan *et al.*, 2016). Recently, phenolic compounds and plant extracts such as epigallocatechin gallate (EGCG) (Nilsuwan *et al.*, 2018), anthocyanins (Uranga *et al.*, 2018) and mango kernel extract (Maryam Adilah *et al.*, 2018) have been incorporated in order to enhance the functional properties of gelatin-based films and, at the same time, to contribute to the reduction in the use of synthetic chemicals in film forming formulations.

Regarding the manufacture processes, there are two main methods used to prepare protein films: wet and dry processes (Guerrero *et al.*, 2010; Prodpran *et al.*, 2017). The wet process is based on the dispersion or solubilization of proteins in a solvent medium, while the dry process includes hot-pressing or compression molding as well as melt and extrusion techniques to prepare films (Ciannamea *et al.*, 2016; Guerrero *et al.*, 2010). Compression and extrusion techniques are faster and more efficient and, thus, more appropriate for industrial scale production, but research on both formulations and processing conditions are still needed to improve the properties of the final products (Chuaynukul *et al.*, 2018; Guerrero *et al.*, 2010). In this regard, compression molding was used in this work with the aim of reducing the production times of gelatin films.

6.3 Objective

To study the physicochemical, optical, morphological, mechanical, barrier and thermal properties of thermo-compression molded fish gelatin film incorporated with different concentrations of EGCG.

6.4 Materials and methods

6.4.1 Materials and chemicals

Fish gelatin produced from tilapia skin (~240 bloom) was procured from Lapi Gelatine S.p.A (Empoli, Italy). (-)-epigallocatechin gallate (EGCG) was obtained

from Chengdu Biopurify Phytochemicals Ltd., (Sichuan, China). The purity of EGCG was greater than 98% as determined by HPLC. 2,4,6-Tri (2-pyridyl)-S-triazine (TPTZ) was procured from Fluka Chemicals (Buchs, Switzerland). 6-Hydroxy-2,5,7,8-tetramethylchroman-2-carboxylic acid (Trolox), 2,2-diphenyl-1-picryhydrazyl (DPPH), ferrous sulfate ($FeSO_4.7H_2O$), ferric chloride ($FeCl_3.6H_2O$), 2,2-azino-bis-(3-ethylbenzothiazoline-6-sulfonic acid) diammonium salt (ABTS), potassium persulfate, hydrogen peroxide (H_2O_2) were purchased from Sigma-Aldrich, Inc. (St. Louis, MO). Glycerol and hydrochloric acid were procured from PanReac AppliChem (Spain). Methanol and ethanol were obtained from Merck (Darmstadt, Germany). All chemicals were of analytical grade.

6.4.2 Preparation of films

Fish gelatin films were prepared according to the method of Uranga *et al.* (2018) with slight modifications. Fish gelatin powder (3.5 g protein content), 0.2, 0.6, and 1.0 g EGCG (5.71, 17.14 and 28.57 wt %, based on protein content), glycerol (30 wt %, based on protein content), and water (45.94 wt %, based on protein content) were manually mixed. Mixtures were thermally compacted using a caver laboratory press (Atlas™, Sanitech Engineers & Consultants Pvt. Ltd., India). Samples were placed between two sheets of silicone papers and covered with aluminium plates, which were pre-heated without pressure at 60 °C for 1 min and then,a pressure of 0.8 MPa was applied for 2 min. Those temperature and pressure conditions were selected since films could not be obtained at lower temperatures and pressures. After that, the plates were allowed to cool at room temperature for 24 h before removing films. All samples were conditioned in an ACS Sunrise 700 V bio-chamber (Alava Ingenieros, Madrid, Spain) at 25 °C and 50% relative humidity for 48 h before testing.

6.4.3 Film thickness

Film thickness was measured to the nearest 0.001 mm with a hand-held QuantuMike digimatic micrometer (Mitutoyo Spain, Elgoibar, Spain). Five positions on film sample were measured to calculate the average thickness.

6.4.4 Physicochemical properties

Films were cut (20 mm × 20 mm), weighed (W_0), and dehydrated in an air-circulating oven at 105 °C for 24 h. The dry samples were reweighed (W_1) and moisture contents (MC) was calculated as follows:

$$MC\ (\%) = \frac{(W_0 - W_1)}{W_0} \times 100$$

Total soluble matter (TSM) was determined according to Etxabide *et al*. (2015). Film samples were immersed in 30 mL distilled water at 25 °C for 24 h in the presence of sodium azide (0.02 g/100 mL). Thereafter, specimens were filtrated and dried in an air-circulating oven at 105 °C for 24 h and weighed (W_2). TSM (% dry basis) was calculated as follows:

$$TSM\ (\%\ dry\ basis) = \frac{(W_1 - W_2)}{W_1} \times 100$$

Fourier transformed infrared (FTIR) spectra of the films were carried out on a Nicolet Nexus FTIR spectrometer using ATR Golden Gate (Specac). A total of 2 scans were performed at 4 cm^{-1} resolution. The measurements were recorded between 4000 and 800 cm^{-1}. FTIR spectra were smoothed out and their baselines were corrected automatically by using Thermo Scientific OMNIC software.

6.4.5 Optical properties

Color was analyzed with a CR-400 Konica Minolta Chroma-Meter. *L**, *a** and *b** parameters were measured by placing the films on the surface of a standard white plate. The CIELAB color scale was used: *L** = 0 (black) to *L** = 100 (white), -*a** (greenness) to +*a** (redness), and -*b** (blueness) to +*b** (yellowness). Color difference (Δ*E**) was calculated based on the control film:

$$\Delta E^* = \sqrt{(\Delta L^*)^2 + (\Delta a^*)^2 + (\Delta b^*)^2}$$

The light barrier properties of films were measured by V-630 UV-vis spectrophotometer (Jasco, Madrid, Spain) at wavelengths from 200 nm to 800 nm.

Film gloss was determined using a Multi Gloss 268 Plus gloss meter. Gloss values were measured at 60° incidence angle, since films exhibit low gloss according to ASTM D523-99 (ASTM, 2008).

6.4.6 Scanning electron microscopy (SEM)

The morphology of the cross-section of the films was visualized using a Hitachi S-4800 scanning electron microscopy (Hitachi, Spain). The cross-section was prepared using mechanical means like conventional cutter. Then, samples were mounted on a metal stub with double-side adhesive tape and coated under vacuum with gold, using a JEOL fine-coat ion sputter JFC-1100 (Izasa, Spain) in an argon atmosphere prior to observation. All samples were examined using an accelerating voltage of 15 kV.

6.4.7 X-ray diffraction (XRD)

XRD of thermo-compression molded films was performed with a diffraction unit (PANalytical Xpert PRO) operating at 40 kV and 40 mA (Guerrero *et al.*, 2012). The radiation was generated from a Cu-Kα (λ = 1.5418 Ǻ) source. The diffraction data were collected from 2θ values from 2.5° to 50°, where θ is the angle of incidence of the X-ray beam on the sample.

6.4.8 Mechanical properties

Tensile strength (TS), elastic modulus (EM) and elongation at break (EB) were measured for each film at least five times on an electromechanical Insight 10 testing system (MTS Systems, Barcelona, Spain) at 25 °C, according to ASTM D1708-93 (ASTM, 1993). Samples were cut into strips of 4.75 mm × 22.25 mm.

6.4.9 Thermal properties

Differential scanning calorimetry (DSC) experiments were performed using a Mettler Toledo DSC 822 as described by Guerrero and de la Caba (2010). Samples (3 mg) were weighed and sealed in aluminium pans. All runs were carried out

from 25 °C up to 250 °C at a heating rate of 10 °C /min. Experiments were carried out under nitrogen atmosphere, and the nitrogen gas flow employed was 10 mL/min.

Thermal stability of films was also analyzed by thermo-gravimetric analysis (TGA). Non-isothermal degradation measurements were performed in a Mettler Toledo TGA SDTA 851. Tests were running from room temperature up to 800 °C at a heating rate of 10 °C/min under nitrogen atmosphere (10 mL/min) to avoid thermo-oxidative reactions (Guerrero and de la Caba, 2010).

6.4.10 Functional properties

The EGCG release was determined as method described by (Etxabide *et al.*, 2018) with slight modification. Firstly, wavelength of maximum absorbance for EGCG in 95% ethanol was measured (λ_{max} = 274 nm). Standard solution of EGCG (0.50 – 20 µg/mL) were then prepared to achieve a calibration curve (y = 0.0387x – 0.0095, R^2=1). Film samples (20 mm × 40 mm) were immersed in 95% ethanol (6 mL) in glass vessels with light protection. The samples were stirred with magnetic stirrer (RT15, IKA®, Staufen, Germany) at 200 rpm under the room temperature (14.0 ± 4.3 °C). At particular interval times during 30 days, the 2.5 mL of simulant were collected from testing vessels and replaced with fresh 95% ethanol. UV-vis spectroscopy (Perkin-Elmer Lambda 18 spectrometer, Perkin-Elmer, Courtaboeuf, France) was used to measure light absorption at 274 nm. The results were expressed as accumulative release with employing the calibration curve. Light absorption of control film was used as a subtracting reference. The experiments of each composition were carried out triplicate. OriginPro 9.1 (OriginLab Corporation, Northampton, MA, USA) was used for plotting the curve and obtained non-linear regression equation.

After film immersion for 30 days, 95% ethanol and films were subjected to analyse the DPPH radical scavenging activity and mass loss, respectively. DPPH radical scavenging activity was measured according to the method of Wu *et al.* (2003) with slight modification. The samples (2 mL) were mixed with DPPH solution (75 µM DPPH in 95% ethanol) (2 mL) and allowed to stand in dark at room temperature for 30 min. The absorbance of the solution was measured at 517 nm using a

spectrophotometer. A standard curve was prepared using EGCG in the range of 0–15 μM. The activity was calculated and expressed as μmol EGCG/mL ethanol. All the test were carried out in triplicate.

Film samples were removed and dried at room temperature for 48 h prior to weighting. Three samples were used for each composition and the mass loss of each film was calculated with the following equation:

$$\text{Mass loss } (\%) = (1 - \frac{W_{30}}{W_0}) \times 100$$

where W_0 is the weight of the films before immersion and W_{30} is the weight of the films after 30 days of immersion.

6.4.11 Statistical analysis

Analysis of variance (ANOVA) was used to determine the significance of differences among the samples. The analysis was performed with a SPSS package (SPSS for windows, SPSS Inc., Chicago, IL, USA) and Duncan's multiple range tests was used for multiple comparisons. Differences were statistically significant at the $P < 0.05$ level.

6.5 Results and discussion

6.5.1 Physicochemical properties

Fish gelatin films incorporated with different concentrations of EGCG (0, 5.71, 17.14 and 28.57 wt %) and prepared by thermo-compression molding were homogenous, transparent and easy to handle. Control film (without EGCG) visually exhibited lightness and transparent, while the films incorporated with EGCG occurred more yellowish and darker particularly when higher concentration was used (Figure 22).

Figure 22. Appearance of fish gelatin films incorporated with different concentrations of EGCG.

Film thickness was in range of 0.145 – 0.172 mm (Table 21). When EGCG higher than 5.71 wt %, a significant increase ($P < 0.05$) of film thickness was observed, probably due to the different microstructure formed as a consequence of EGCG addition. Moisture content (MC) and total soluble matter (TSM) of fish gelatin films incorporated with different concentrations of EGCG are shown in Table 21. The highest ($P < 0.05$) MC value was observed for the control film (without EGCG). A lower ($P < 0.05$) MC was observed when higher concentrations of EGCG were used, related to the interactions between gelatin chains and EGCG, which caused a decrease of available hydrophilic groups to bind with water. Regarding film solubility, the decrement ($P < 0.05$) of TSM value occurred when high concentrations of EGCG was used (17.14 wt % and 28.54 wt %). It is worth noting that lower solubility of gelatin films incorporated with phenolic compounds might result from the formation of a denser structure of the film network due to a higher extent of protein-polyphenol interactions (Bodini *et al.*, 2013; Luchese *et al.*, 2018), in accordance with the MC values measured.

In order to analyze those interactions between gelatin and EGCG, FTIR spectroscopy was carried out and FTIR spectra of the films are shown in Figure 23. A spectra of fish gelatin films generally displayed the major bands at 3290 cm^{-1} (amide A, representative of N–H stretching, coupled with hydrogen bonding), 1631 cm^{-1}

Table 21. Thickness, moisture content (MC), and total soluble matter (TSM) of fish gelatin films incorporated with different concentrations of EGCG.

EGCG (wt %)	Thickness (mm)	MC (%)	TSM (%)
0	0.145 ± 0.011 b	13.08 ± 0.24 a	99.55 ± 0.04 a
5.71	0.155 ± 0.011 b	11.88 ± 0.20 b	95.67 ± 1.80 a
17.14	0.172 ± 0.012 a	10.42 ± 0.08 c	69.11 ± 4.19 b
28.57	0.172 ± 0.005 a	9.40 ± 0.10 d	35.36 ± 2.45 c

Two means followed by the same letter in the same parameter are not significantly ($P > 0.05$) different through the Duncan's Multiple Range Tests. $n = 3$ is the minimum number of replication.

(amide I, representative of C=O stretching/hydrogen bonding coupled with COO^-), 1546 cm^{-1} (amide II, representative of N–H bending coupled with C–N stretching) and 1239 cm^{-1} (amide III, representative of the vibrations in-plane of C–N and N–H groups of bound amide or vibrations of CH_2 groups of glycine) (Muyonga *et al.*, 2004; Nilsuwan *et al.*, 2017; Tongnuanchan *et al.*, 2014). The band at the wavenumber range of 3400-3300 cm^{-1} was also attributed to O–H stretching of alcohols and phenols (Smith, 1998). All film samples exhibited similar spectra. However, the shift to lower wavenumbers of amide A, I and II and III bands was exhibited from 3283, 1629, 1545 and 1239 cm^{-1} in the control film to 3276-3272, 1629-1627, 1544-1534 and 1238-1234 cm^{-1} in the gelatin films containing different levels of EGCG. The shift to lower wavenumbers of those bands is associated with the interaction between gelatin and EGCG. Aewsiri *et al.* (2010) reported that the amide I, II and III bands of gelatin modified with 5% oxidized tannic acid had a lower wavenumber than control gelatin, due to more intermolecular cross-links in the modified gelatin. Moreover, the infrared spectra of the gelatin containing different levels of EGCG revealed the notable changes occurring in the 1500–1000 cm^{-1} region, as compared to the control film. The bands at ~1350, ~1143 and ~1080 cm^{-1} were related to O–H bending, –OH aromatic ring and C–O stretching in phenols and alcohols (Park *et al.*, 2010; Smith, 1998). Additionally, the band situated at the wavenumber of 1036-1037 cm^{-1} was found in all film samples, corresponding to the OH group, associated with glycerol added as a plasticizer and the incorporated EGCG (Bergo and Sobral, 2007; Nilsuwan *et al.*, 2018). A lower

wavenumber along with a higher amplitude of the bands at the wavenumbers range of 1337-1335, 1149-1148 and 1099-1097 cm^{-1} were found for the films containing EGCG, indicative of the interactions between gelatin and EGCG.

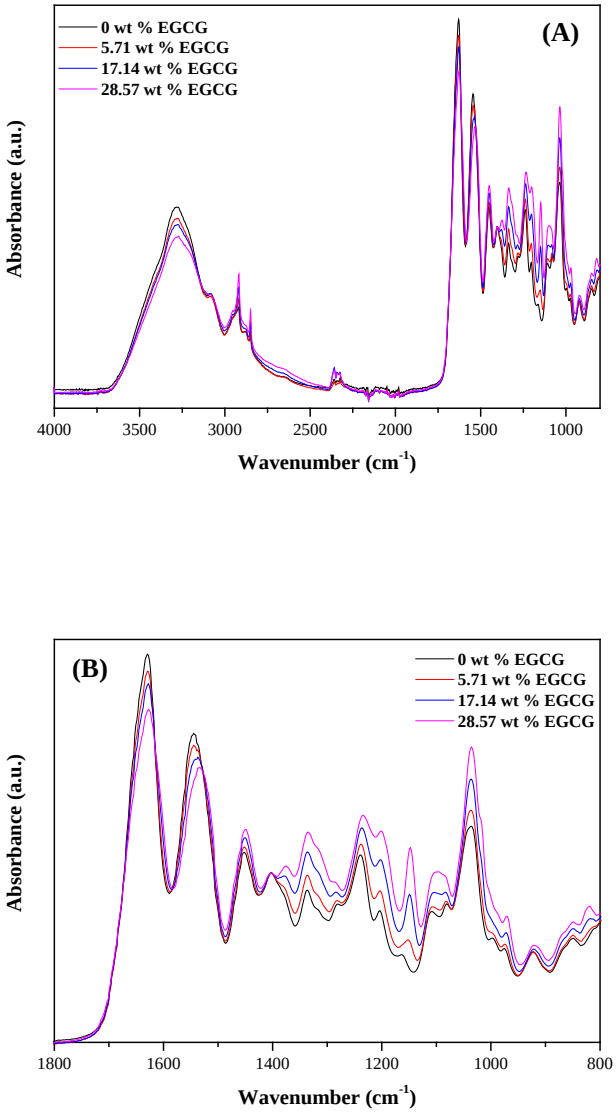

Figure 23. ATR-FTIR spectra of fish gelatin films incorporated with different concentrations of EGCG from 4000 to 800 cm^{-1} (A) and from 1800 to 800 cm^{-1} (B).

6.5.2 Optical properties

Color of thermo-compression molded films incorporated with different concentrations of EGCG is showed in Table 22. Control film (without EGCG) expressed high *L** value (96.07) but low *a** (-0.31) and *b** (4.15) values. As EGCG at different concentrations was incorporated, the decrease in *L** value along with increases in *a** and *b** values were observed. The lowest *L** (93.81) value along with the highest ($P < 0.05$) *b** (7.15) and Δ*E** (3.78) values were found for the film containing 28.57 wt % EGCG. It was noted that the addition of antioxidants affected the *L**, *a** and *b** values of resulting films (Hwang *et al.*, 2012). These could be attributed to the incorporation of EGCG, which influenced on darkness, redness and yellowness of the film, particularly when high concentration of EGCG was applied, due to the fact that EGCG is pale yellow in color (Nilsuwan *et al.*, 2018). Wang *et al.* (2018) also reported a decrease of lightness (*L**) and increases in redness (*a**) and yellowness (*b**) in chitosan films incorporated with increasing concentrations of EGCG (0-30 wt %). Since this is a soft color and films maintained their transparency, this change is not considered as a drawback for the film applications.

Table 22. Color and gloss of fish gelatin films incorporated with different concentrations of EGCG.

EGCG (wt %)	*L**	*a**	*b**	Δ*E**	Gloss (°)
0	96.05 ± 0.05 a	-0.31 ± 0.01 c	4.15 ± 0.01 d	-	16.05 ± 0.3 b
5.71	94.99 ± 0.06 c	-0.37 ± 0.02 d	5.15 ± 0.02 c	1.48 ± 0.03 c	17.38 ± 0.41 a
17.14	95.25 ± 0.08 b	-0.18 ± 0.02 b	5.46 ± 0.02 b	1.54 ± 0.03 b	15.83 ± 0.36 b
28.57	93.81 ± 0.03 d	0.07 ± 0.02 a	7.15 ± 0.01 a	3.78 ± 0.01 a	14.62 ± 0.48 c

Two means followed by the same letter in the same parameter are not significantly ($P > 0.05$) different through the Duncan's Multiple Range Tests. $n = 3$ is the minimum number of replication.

Additionally, absorption spectra of UV and visible light at wavelength range of 200-800 nm of thermo-compression molded films incorporated with different concentrations of EGCG are shown in Figure 24. All gelatin films exhibited a high protection against UV light in the range of 200-250 nm. This is commonly related to

the polypeptide backbone of gelatin (Etxabide *et al.*, 2015; Goldfarb, 1953). The absorption in the range of 250-300 nm is mainly due to the presence of aromatic compounds, such as tyrosine and phenylalanine, in gelatin (Benjakul *et al.*, 2009; Bonilla and Sobral, 2016). Accordingly, a rise of UV absorption was found for gelatin films when EGCG was added, related to the high content of aromatic groups exiting in EGCG. Moreover, the addition of EGCG extended UV-light absorption of films to the wavelength of 300-400 nm, which might be associated with a higher content of chromophores.

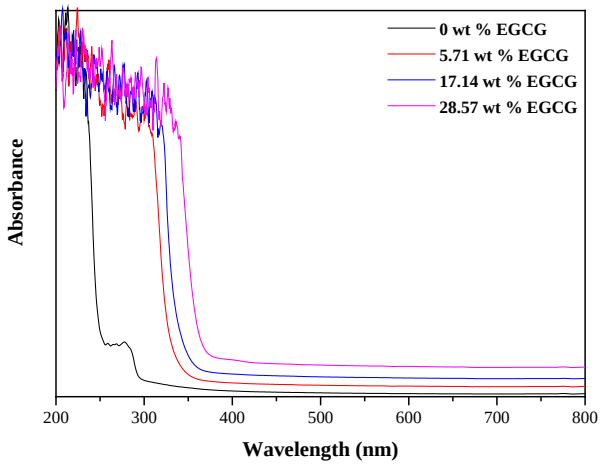

Figure 24. UV-visible light absorption of fish gelatin films incorporated with different concentrations of EGCG.

Gloss is determined in order to evaluate surface attributes. Gloss is directly related to surface smoothness, being higher when surface is smoother (Etxabide *et al.*, 2015; Trezza and Krochta, 2008). Gloss values of all gelatin films were in the range of 13.0-17.4 (Table 22), indicating non-glossy and rough surfaces of resulting films. This might be related to micro voids left over film surface by evaporation of moisture during thermo-compression molding (Park *et al.*, 2008). Moreover, a decrease of gloss values from 16.6 to 13.0 was observed when the concentration of EGCG was increased from 5.71 wt % to 28.57 wt %, which might be related to the morphological changes occurred in the film due to gelatin EGCG interactions.

6.5.3 Morphological and mechanical properties

In order to study the influence of EGCG addition on the film structure, control and EGCG-containing films were analyzed by SEM. As shown in Figure 25, no difference could be appreciated between the cross-sections of control film and film containing 5.71% EGCG. Smoother and more compact cross-sections were observed for the films containing higher concentration of EGCG (≥ 17.14 wt %), indicating that the increased number of non-covalent protein-polyphenol interactions contribute to the formation of a more compact film structure (Hoque *et al.*, 2011). Similar results were found for gelatin film added with different concentrations of EGCG (1-5 wt % w/w) (Wang *et al.*, 2019). It is also worth noting that the microstructure of gelatin films was homogeneous with absence of EGCG particles, regardless of the concentration used, demonstrating that thermo-compression molding was a suitable process for the incorporation of high concentration of EGCG into gelatin films.

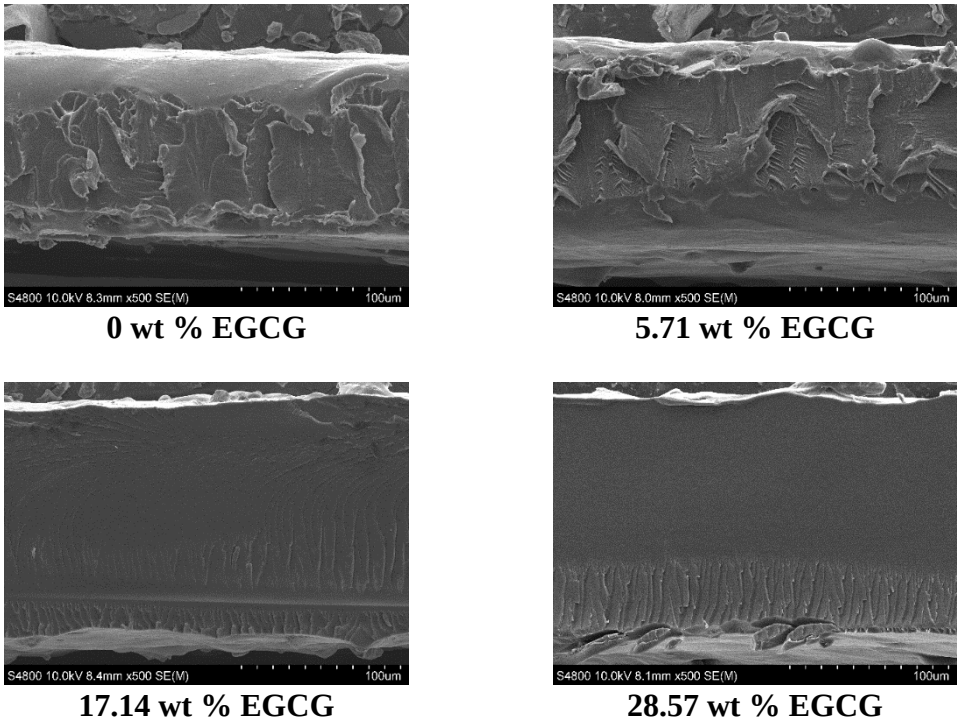

Figure 25. Cross-section SEM micrographs (500×) of fish gelatin films incorporated with different concentrations of EGCG.

Furthermore, this behavior can be related to the amorphous structure of the films incorporated with EGCG, as shown by X-ray diffraction in Figure 26. All samples exhibited a single broad peak at 2θ ≈ 21°, characteristic of an amorphous structure (Pereda *et al.*, 2011), with the absence of collagen-like helix-coil structure. This result indicated that gelatin did not have an ordered structure (Figueroa-Lopez *et al.*, 2018). In addition, a higher peak intensity and a shift towards higher angles were observed for film containing high concentration of EGCG, compared to control film. This result was attributed to a higher number of interactions between gelatin-EGCG via hydrogen bonding.

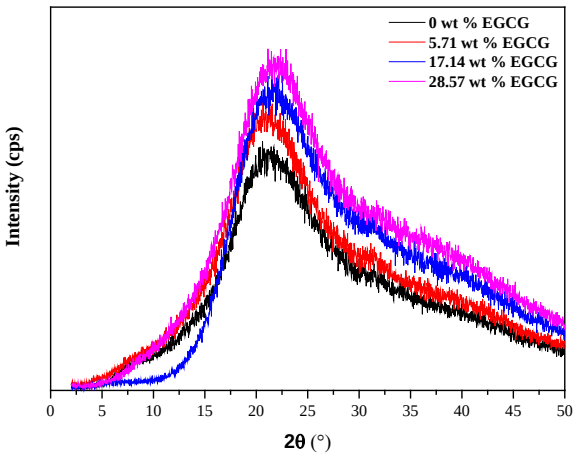

Figure 26. X-ray diffraction pattern of fish gelatin films incorporated with different concentrations of EGCG.

Tensile strength (TS), elongation at break (EAB) and Young's modulus (E) were measured and the values obtained are shown in Table 23. As can be seen, the increase of EGCG content generally increased E and TS values, together with a decrease in EAB values. This behavior might be due to the interactions between gelatin and EGCG, which made film more resistance to fracture, as also shown in previous works (Nilsuwan *et al.*, 2018). Interestingly, 5.71 wt % EGCG concentration promoted the strength together with the maintenance of elasticity in the resulting film. However, the highest level of EGCG (28.57 wt %) seemed to be an excessive content since it

caused a brittle behavior of the film, as indicated by the reduction of TS and EAB values. Therefore, lower levels of EGCG would be more appropriate to reinforce the film by intermolecular hydrogen bonding, leading to resistant films with satisfactory elasticity.

Table 23. Young's modulus (E), tensile strength (TS), and elongation at break (EAB) of fish gelatin films incorporated with different concentrations of EGCG.

EGCG (wt %)	**E (MPa)**	**TS (MPa)**	**EAB (%)**
0	1350.06 ± 114.06 c	31.26 ± 2.18 b	3.26 ± 0.22 a
5.71	1715.31 ± 86.91 b	38.85 ± 2.03 a	3.15 ± 0.35 a
17.14	1872.71 ± 105.18 ab	37.37 ± 3.97 a	2.43 ± 0.21 b
28.57	1993.41 ± 48.02 a	27.33 ± 2.6 b	1.51 ± 0.12 c

Two means followed by the same letter in the same parameter are not significantly ($P > 0.05$) different through the Duncan's Multiple Range Tests. $n = 3$ is the minimum number of replication.

6.5.4 Thermal properties

DSC thermograms showed glass transition (T_g) of gelatin films at around 71-73 °C. The T_g of the films incorporated with EGCG was slightly higher than that of the control film (Figure 27A) due to the interactions of gelatin with EGCG. Peak transition at above 100 °C was attributed to the evaporation of entrapped water. When EGCG was incorporated, a broader peak was observed, suggesting a denser structure, caused by the interactions between gelatin and EGCG, which required more energy for water evaporation.

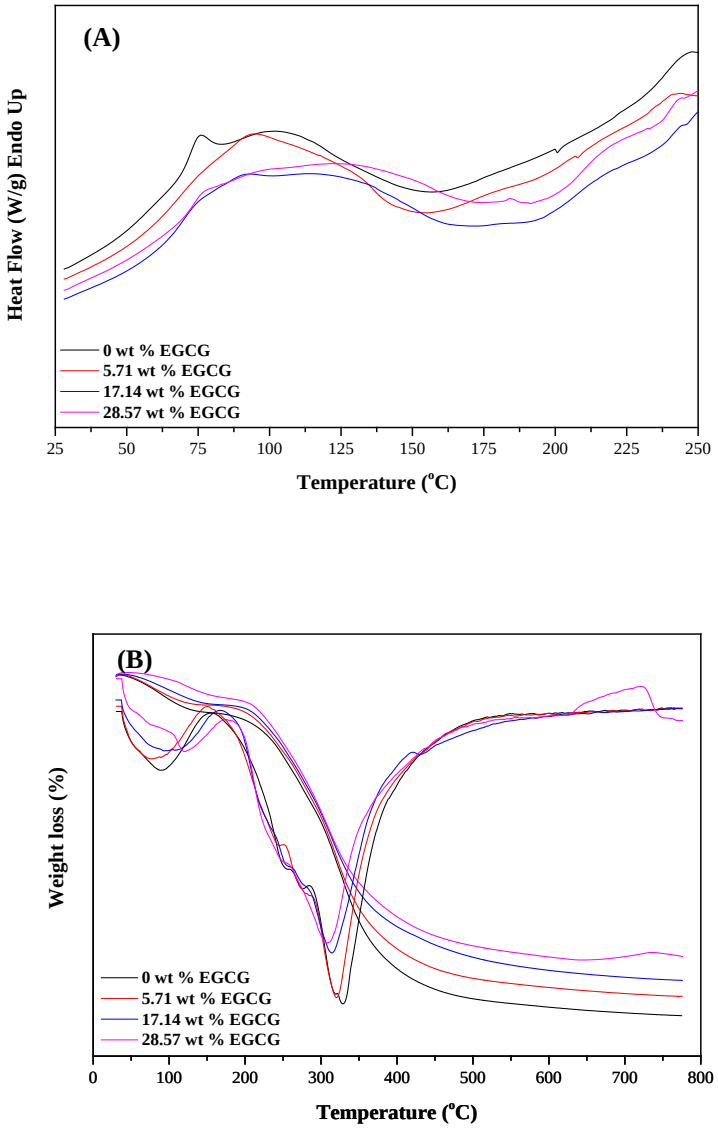

Figure 27. DSC thermograms (A) as well as TGA and DTG curves (B) of fish gelatin films incorporated with different concentrations of EGCG.

In order to analyze the enhancement of thermal stability due to gelatin-EGCG interactions, TGA expressed as weight loss and derivative weight (DTG) are shown in Figure 27B as a function of EGCG concentration in fish gelatin films. All gelatin films presented similar behavior with three weight loss stages. The first stage of weight loss (Δw_1 = 5.95-8.88%) was observed approximately at the temperature range of 88-127 °C, related to the loss of free and absorbed water (Hoque *et al.*, 2011). The second stage of weight loss (Δw_2 = 10.60-12.32%) at temperature about 190-260 °C

was most likely associated with the loss of low molecular weight protein fractions, plasticizer and structurally bounded water (Wetzel *et al.*, 1987). This second stage appeared at temperatures higher than the glycerol boiling point (182 °C), suggesting the existence of interactions, such as hydrogen bonds, between gelatin and glycerol (Guerrero *et al.*, 2011). Furthermore, lower weight loss at about 230 °C was observed when higher concentration of EGCG was used. This result was plausibly related with the interactions of EGCG and glycerol hindering the glycerol degradation. Additionally, the third stage of weight loss (Δw_3 = 50.65-58.13%) was observed at 307-336 °C for all films and was related to the degradation of the larger size or highly associated gelatin fractions. A lower weight loss of this third stage was observed in the films incorporated with EGCG, compared to the control film. This was mostly due to the interactions between the components of the films, suggesting that bonding between EGCG and gelatin molecules yielded a stronger film network, leading to a higher heat resistance of the resulting films, as well as to a higher mechanical resistance as abovementioned (Table 23).

6.5.5 Functional properties

Release profile of EGCG-containing film expressed as accumulative EGCG release is presented in Figure 28. As can be seen in, a continuous increase of accumulative release throughout 30 days of immersion was observed for all films treated. At the same immersion time, film containing 28.57 wt % EGCG generally showed the highest release. This result was noted that increase of incorporation concentration provided more amount of EGCG release. Benbettaieb *et al.* (2018) reported that the increase of released caffeic acid and *p*-courmaric acid in 96% ethanol from chitosan-gelatin film was found when the incorporation concentration was increased from 5 to 10 wt %. Furthermore, the released EGCG from all films after 30 days of immersion was 5.87-8.60% (based on total amount in each film). The interaction between antioxidant and biopolymer plausibly caused to the slow migration of antioxidant from the films (Benbettaieb *et al.*, 2018; Nilsuwan *et al.*, 2018; Soto-Valdez *et al.*, 2011).

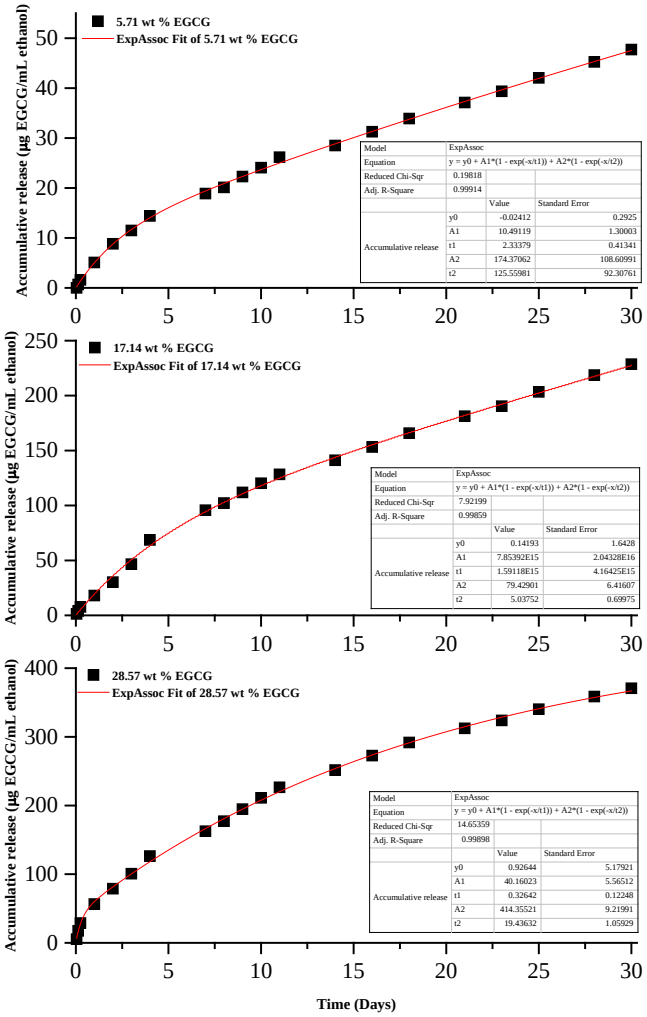

Figure 28. Accumulative of EGCG from fish gelatin films incorporated with different concentrations of EGCG.

DPPH radical scavenging activity was carried out to assess the antioxidant activity of released EGCG in 95% ethanol after 30 days of film immersion. Antioxidant activity was found for 95% ethanol immerged with all films containing EGCG but no activity was observed for film without EGCG (Table 24). This indicated that the EGCG had been released from gelatin film into 95% ethanol. Additionally, higher DPPH radical scavenging activity was observed when the incorporation concentration of EGCG was increased ($P < 0.05$). The highest DPPH radical scavenging activity was obtained for 95% ethanol immerged with gelatin containing 28.57 wt % EGCG ($P < 0.05$). DPPH radical inhibition of food simulant associated with the incorporation

concentration of active compound (Zhu *et al.*, 2018). This was supported by high accumulative of EGCG released from gelatin film containing high incorporation concentration (Figure 28). Regarding the values of mass loss (Table 24), films containing 17.14 and 28.57 wt % EGCG had lower mass loss than film without EGCG ($P < 0.05$). This result probably related with the loss of moisture and glycerol contents during 30 days of immersion. The incorporation of EGCG might be enhanced more interaction of film matrix which lowered the loss of film components. Thus, the developed gelatin film with appropriated EGCG concentration used could provide a satisfactory functional properties which was useful for applying as packaging material to extend shelf-life of fatty food product during storage.

Table 24. DPPH radical scavenging activity of 95% ethanol and mass loss of fish gelatin films incorporated with different concentrations of EGCG after 30 days of film immersion.

EGCG (wt %)	DPPH radical scavenging activity (μmol EGCG/mL ethanol)	Mass loss (%)
0	ND	8.28 ± 0.42 a
5.71	4.90 ± 1.16 c	7.62 ± 0.23 a
17.14	24.72 ± 3.77 b	5.50 ± 0.56 b
28.57	50.33 ± 0.12 a	2.90 ± 0.50 c

Two means followed by the same letter in the same parameter are not significantly ($P > 0.05$) different through the Duncan's Multiple Range Tests. $n = 3$ is the minimum number of replication. ND: Not detected

6.6 Conclusions

Films based on fish gelatin and EGCG fabricated by thermo-compression molding with homogenous and transparent appearance were successfully obtained. The incorporation of EGCG improved the properties of the resulting films depending on the concentration used. Films incorporated with 5.71 wt % and 17.54 wt % EGCG rendered a great integrity after water immersion, compact structure, mechanical resistance, high UV-light barrier and thermal stability as well as satisfactory

release profile and antioxidant activity in controlled way. Therefore, these developed films seemed to be a promising material to prepare films as active food packaging.

6.7 References

Aewsiri, T., Benjakul, S., Visessanguan, W., Wierenga, P. A. and Gruppen, H. 2010. Antioxidative activity and emulsifying properties of cuttlefish skin gelatin–tannic acid complex as influenced by types of interaction. Innov. Food Sci. Emerg. Technol. 11: 712-720.

Arpi, N., Fahrizal and Novita, M. 2018. Isolation of fish skin and bone gelatin from tilapia (*Oreochromis niloticus*): Response surface approach. IOP Conference Series: Materials Science and Engineering. 334: 012061.

ASTM. 1993. Standard test method for tensile properties of plastics by use of microtensile specimens. *In* Annual book of ASTM standards. American Society for Testing and Materials. Philadelphia, PA.

ASTM. 2008. Standard test method for specular gloss, D523-99. *In* Annual book of ASTM standards. American Society for Testing and Materials. Philadelphia, PA.

Benbettaieb, N., Nyagaya, J., Seuvre, A.-M. and Debeaufort, F. 2018. Antioxidant activity and release kinetics of caffeic and *p*-coumaric acids from hydrocolloid-based active films for healthy packaged food. J. Agric. Food Chem. 66: 6906-6916.

Benjakul, S., Oungbho, K., Visessanguan, W., Thiansilakul, Y. and Roytrakul, S. 2009. Characteristics of gelatin from the skins of bigeye snapper, *Priacanthus tayenus* and *Priacanthus macracanthus*. Food Chem. 116: 445-451.

Bergo, P. and Sobral, P. J. A. 2007. Effects of plasticizer on physical properties of pig skin gelatin films. Food Hydrocolloid. 21: 1285-1289.

Bodini, R. B., Sobral, P. J. A., Favaro-Trindade, C. S. and Carvalho, R. A. 2013. Properties of gelatin-based films with added ethanol–propolis extract. LWT-Food Sci. Technol. 51: 104-110.

Bonilla, J. and Sobral, P. J. A. 2016. Investigation of the physicochemical, antimicrobial and antioxidant properties of gelatin-chitosan edible film mixed with plant ethanolic extracts. Food Bioscience. 16: 17-25.

Chuaynukul, K., Nagarajan, M., Prodpran, T., Benjakul, S., Songtipya, P. and Songtipya, L. 2018. Comparative characterization of bovine and fish gelatin films fabricated by compression molding and solution casting methods. J. Polym. Mater. 26: 1239-1252.

Ciannamea, E. M., Stefani, P. M. and Ruseckaite, R. A. 2016. Properties and antioxidant activity of soy protein concentrate films incorporated with red grape extract processed by casting and compression molding. LWT-Food Sci. Technol. 74: 353-362.

Etxabide, A., Leceta, I., Cabezudo, S., Guerrero, P. and de la Caba, K. 2016. Sustainable fish gelatin films: from food processing waste to compost. ACS Sustainable Chemistry & Engineering. 4: 4626-4634.

Etxabide, A., Ribeiro, R. D. C., Guerrero, P., Ferreira, A. M., Stafford, G. P., Dalgarno, K., de la Caba, K. and Gentile, P. 2018. Lactose-crosslinked fish gelatin-based porous scaffolds embedded with tetrahydrocurcumin for cartilage regeneration. Int. J. Biol. Macromol. 117: 199-208.

Etxabide, A., Uranga, J., Guerrero, P. and de la Caba, K. 2015. Improvement of barrier properties of fish gelatin films promoted by gelatin glycation with lactose at high temperatures. LWT-Food Sci. Technol. 63: 315-321.

Figueroa-Lopez, J. K., Andrade-Mahecha, M. M. and Torres-Vargas, L. O. 2018. Development of antimicrobial biocomposite films to preserve the quality of bread. Molecules. 23:

Goldfarb, A. R. 1953. Absorption spectrum of the peptide bond: ii. Influence of chain length. Journal of Biological Chemistry. 201: 317-320.

Gómez-Estaca, J., Montero, P., Fernández-Martín, F. and Gómez-Guillén, M. C. 2009. Physico-chemical and film-forming properties of bovine-hide and tuna-skin gelatin: A comparative study. J. Food Eng. 90: 480-486.

Guerrero, P., Beatty, E., Kerry, J. P. and de la Caba, K. 2012. Extrusion of soy protein with gelatin and sugars at low moisture content. J. Food Eng. 110: 53-59.

Guerrero, P. and de la Caba, K. 2010. Thermal and mechanical properties of soy protein films processed at different pH by compression. J. Food Eng. 100: 261-269.

Guerrero, P., Nur Hanani, Z. A., Kerry, J. P. and de la Caba, K. 2011. Characterization of soy protein-based films prepared with acids and oils by compression. J. Food Eng. 107: 41-49.

Guerrero, P., Retegi, A., Gabilondo, N. and de la Caba, K. 2010. Mechanical and thermal properties of soy protein films processed by casting and compression. J. Food Eng. 100: 145-151.

Hoque, M. S., Benjakul, S. and Prodpran, T. 2011. Properties of film from cuttlefish (*Sepia pharaonis*) skin gelatin incorporated with cinnamon, clove and star anise extracts. Food Hydrocolloid. 25: 1085-1097.

Hwang, S. W., Shim, J. K., Selke, S. E. M., Soto-Valdez, H., Matuana, L., Rubino, M. and Auras, R. 2012. Poly(L-lactic acid) with added α-tocopherol and resveratrol: optical, physical, thermal and mechanical properties. Polymer International. 61: 418-425.

Karim, A. A. and Bhat, R. 2009. Fish gelatin: properties, challenges, and prospects as an alternative to mammalian gelatins. Food Hydrocolloid. 23: 563-576.

Luchese, C. L., Uranga, J., Spada, J. C., Tessaro, I. C. and de la Caba, K. 2018. Valorisation of blueberry waste and use of compression to manufacture sustainable starch films with enhanced properties. Int. J. Biol. Macromol. 115: 955-960.

Maryam Adilah, Z. A., Jamilah, B. and Nur Hanani, Z. A. 2018. Functional and antioxidant properties of protein-based films incorporated with mango kernel extract for active packaging. Food Hydrocolloid. 74: 207-218.

Muralidharan, N., Jeya Shakila, R., Sukumar, D. and Jeyasekaran, G. 2013. Skin, bone and muscle collagen extraction from the trash fish, leather jacket (*Odonus niger*) and their characterization. J. Food Sci. Technol. 50: 1106-1113.

Muyonga, J. H., Cole, C. G. B. and Duodu, K. G. 2004. Characterisation of acid soluble collagen from skins of young and adult Nile perch (*Lates niloticus*). Food Chem. 85: 81-89.

Nilsuwan, K., Benjakul, S. and Prodpran, T. 2016. Quality changes of shrimp cracker covered with fish gelatin film without and with palm oil incorporated during storage. Int. Aquat. Res. 8: 227-238.

Nilsuwan, K., Benjakul, S. and Prodpran, T. 2017. Properties, microstructure and heat seal ability of bilayer films based on fish gelatin and emulsified gelatin films. Food Biophys. 12: 234-243.

Nilsuwan, K., Benjakul, S. and Prodpran, T. 2018. Properties and antioxidative activity of fish gelatin-based film incorporated with epigallocatechin gallate. Food Hydrocolloid. 80: 212-221.

Park, J. W., Scott Whiteside, W. and Cho, S. Y. 2008. Mechanical and water vapor barrier properties of extruded and heat-pressed gelatin films. LWT-Food Sci. Technol. 41: 692-700.

Park, Y.-S., Lee, M.-K., Heo, B.-G., Ham, K.-S., Kang, S.-G., Cho, J.-Y. and Gorinstein, S. 2010. Comparison of the Nutrient and Chemical Contents of Traditional Korean Chungtaejeon and Green Teas. Plant Foods for Human Nutrition. 65: 186-191.

Pereda, M., Ponce, A. G., Marcovich, N. E., Ruseckaite, R. A. and Martucci, J. F. 2011. Chitosan-gelatin composites and bi-layer films with potential antimicrobial activity. Food Hydrocolloid. 25: 1372-1381.

Prodpran, T., Chuaynukul, K., Nagarajan, M., Benjakul, S. and Prasarpran, S. 2017. Impacts of plasticizer and pre-heating conditions on properties of bovine and fish gelatin films fabricated by thermo-compression molding technique. Italian Journal of Food Science. 29: 487-504.

Smith, B. C. 1998. Infrared spectral interpretation: a systematic approach. CRC press.

Soto-Valdez, H., Auras, R. and Peralta, E. 2011. Fabrication of poly(lactic acid) films with resveratrol and the diffusion of resveratrol into ethanol. J. Appl. Polym. Sci. 121: 970-978.

Tongnuanchan, P., Benjakul, S. and Prodpran, T. 2014. Structural, morphological and thermal behaviour characterisations of fish gelatin film incorporated with basil and citronella essential oils as affected by surfactants. Food Hydrocolloid. 41: 33-43.

Trezza, T. A. and Krochta, J. M. 2008. The gloss of edible coatings as affected by surfactants, lipids, relative humidity, and time. J. Food Sci. 65: 658-662.

Uranga, J., Etxabide, A., Guerrero, P. and de la Caba, K. 2018. Development of active fish gelatin films with anthocyanins by compression molding. Food Hydrocolloid. 84: 313-320.

Wang, Q., Cao, J., Yu, H., Zhang, J., Yuan, Y., Shen, X. and Li, C. 2019. The effects of EGCG on the mechanical, bioactivities, cross-linking and release properties of gelatin film. Food Chem. 271: 204-210.

Wang, X., Xie, Y., Ge, H., Chen, L., Wang, J., Zhang, S., Guo, Y., Li, Z. and Feng, X. 2018. Physical properties and antioxidant capacity of chitosan/epigallocatechin-3-gallate films reinforced with nano-bacterial cellulose. Carbohydr Polym. 179: 207-220.

Wetzel, R., Buder, E., Hermel, H. and Hüttner, A. 1987. Conformations of different gelatins in solutions and in films an analysis of circular dichroism (CD) measurements. Colloid and Polymer Science. 265: 1036-1045.

Wu, H.-C., Chen, H.-M. and Shiau, C.-Y. 2003. Free amino acids and peptides as related to antioxidant properties in protein hydrolysates of mackerel (*Scomber austriasicus*). Food Res. Int. 36: 949-957.

Zhu, J.-Y., Tang, C.-H., Yin, S.-W. and Yang, X.-Q. 2018. Development and characterization of novel antimicrobial bilayer films based on Polylactic acid (PLA)/Pickering emulsions. Carbohydr Polym. 181: 727-735.

CHAPTER 7

PROPERTIES AND APPLICATION OF BILAYER FILMS BASED ON POLY (LACTIC ACID) AND FISH GELATIN CONTAINING EPIGALLOCATECHIN GALLATE FABRICATED BY THERMO-COMPRESSION MOLDING

7.1 Abstract

An alternative approach towards production of active bilayer films based on poly (lactic acid) (PLA) and fish gelatin incorporated with epigallocatechin gallate (EGCG) fabricated by thermo-compression molding was investigated. This strategy permitted the reduction of production times and avoided the uses of inorganic solvents. Thermo-compression molded bilayer films showed good handling, transparency and low water vapor permeability. The incorporation of EGCG promoted interactions with gelatin, as shown by Fourier transform infrared spectroscopy. These interactions contributed to homogeneous structures, as observed by scanning electron microscopy. Bilayer films with 12 wt % EGCG showed good mechanical properties, high water and UV-visible light barrier properties as well as a high DPPH radical scavenging activity. These bilayer films were used to produce bags, in which striped catfish slices (SCS) were packaged. After 7 days of storage at 4 °C, SCS packaged in bags prepared with12 wt % EGCG had lower psychrophilic bacteria count, weight loss, peroxide value, and thiobarbituric acid reactive substances (TBARS) value along with higher docosahexaenoic acid (C22:6 *n*-3) content than those packaged in bags prepared without EGCG or in LLDPE bags. No difference in overall likeness score was found among all the samples packaged in different bags after 7 days of storage. Therefore, PLA/gelatin bilayer films containing 12 wt % EGCG possessed satisfactory film properties with augmented antioxidant activity, and thus they could be used as active food packaging, especially for fish slices with high lipid content.

7.2 Introduction

Polymeric materials for packaging applications have been considered carefully, due to the constraints and regulations related to primary and postconsumer plastic waste management. In order to reduce the use of synthetic polymers, biopolymers such as carbohydrates, lipids, and proteins have been utilized; among them, gelatin has been widely used as a starting material for film formation since it has a good film forming ability and excellent oxygen barrier properties (Lee and Song, 2017; Nilsuwan *et al.*, 2016). However, gelatin-based films have poor water vapor barrier properties, due to the hydrophilic nature of gelatin (Hoque *et al.*, 2011). Several strategies have been proposed to improve the moisture resistance of gelatin–based films, such as chemical and enzymatic crosslinking (Bigi *et al.*, 2001; de Carvalho and Grosso, 2004). Lamination is a means to improve the performance of polymeric films by combining the properties of different films into one sheet (Rakotonirainy and Padua, 2001). In general, the outer layers impart moisture resistance and mechanical stability, while the inner one acts as a gas barrier (Fang *et al.*, 2005). Poly (lactic acid) (PLA), classified as GRAS (Generally Recognized As Safe, GRAS) (Martino *et al.*, 2009), has gained increasing attention as renewable and readily biodegradable material (Cabedo *et al.*, 2006). Consequently, laminated films with improved properties can be produced for food packaging applications (Rhim *et al.*, 2007). Regarding the lamination processes, two main methods are used to prepare bilayer films: wet and dry processes. The wet process or solution casting is based on the dispersion or solubilization of materials in a solvent medium, while the dry process includes hot-pressing or compression molding to prepare films (Martucci and Ruseckaite, 2010; Nagarajan *et al.*, 2017; Nilsuwan *et al.*, 2018a). Compression is faster and more efficient and, thus, more appropriate for industrial scale production (Chuaynukul *et al.*, 2018; Guerrero *et al.*, 2010). In this regard, compression molding was used in this work with the aim of avoiding the use of inorganic solvents and the subsequent drying process, thus, reducing the production time.

Due to the increasing concern of food quality and safety, the interest in the development of active packaging has risen in order to extend food shelf-life; in particular, antioxidant packaging to inhibit lipid oxidation (Zhu *et al.*, 2018). In this

regard, active compounds, such as phenolic compounds from plant extracts, have been incorporated into packaging materials to provide antioxidant activity (Kaewprachu *et al.*, 2015; Maryam Adilah *et al.*, 2018; Nuthong *et al.*, 2009). Among all natural antioxidants, epigallocatechin gallate (EGCG), the major phenolic compound in tea, has gained increasing interest (Zaveri, 2006). EGCG has been reported to exhibit antioxidant activity, dependent on the amount of extract used (Lu *et al.*, 2010).

7.3 Objective

To investigate the properties of bilayer films based on PLA and fish gelatin incorporated with EGCG at different concentrations and its effect on striped catfish slice (SCS) packaged in the bags developed with the bilayers films.

7.4 Materials and methods

7.4.1 Materials

Fish gelatin produced from tilapia skin (~240 bloom) was procured from Lapi Gelatine S.p.A (Empoli, Italy). (-)-epigallocatechin gallate (EGCG) was obtained from Chengdu Biopurify Phytochemicals Ltd., (Sichuan, China). The purity of EGCG was greater than 98% as determined by HPLC. Poly (lactic acid) pellets (4032D, extrusion grade, Mn = 88,500 g/mol and Mw/Mn = 1.8) were obtained from Nature Work Co. Ltd. (Blair, NE, USA). 2,2-diphenyl-1-picryhydrazyl (DPPH), cumene hydroperoxide and 1,1,3,3-tetramethoxypropane (MDA) were purchased from Sigma-Aldrich, Inc. (St. Louis, MO). Glycerol and hydrochloric acid were procured from Panreac AppliChem (Spain). Ethanol and sodium chloride were obtained from Merck (Darmstadt, Germany). All chemicals were of analytical grade.

7.4.2 Preparation of bilayer films

PLA (5 g) was processed by compression molding at 190 °C in a hot press. The material was pre-heated between the platens at atmospheric pressure for 30 s and then pressed at 0.1 MPa for 15 s before cooling and removing the film.

Gelatin films incorporated with EGCG were prepared as described by Nilsuwan *et al.* (2018b) with slight modifications. Film forming solution was prepared by mixing fish gelatin powder (3.5%, w/v), 30 wt % glycerol and EGCG at concentration of 0, 3, 6, 9 and 12 wt % in distilled water. The mixtures were heated at 70 °C for 30 min. The mixture (26 mL) was cast onto petri dish plates (diameter = 150 mm) and dried at room temperature for 48 h. Films were manually peeled off and conditioned in an ACS Sunrise 700 V bio-chamber (Alava Ingenieros, Madrid, Spain) at 25 °C and 50% relative humidity for 24 h before compression.

The bilayer films were prepared by stacking PLA film and gelatin film before pre-heating at 60 °C for 1 min. Thereafter, a pressure of 0.1 MPa was applied for 1 min. All samples were cooled at room temperature and conditioned at 25 °C and 50% relative humidity for 48 h before film characterization.

7.4.3 Film thickness

Film thickness was measured to the nearest 0.001 mm with a hand-held QuantuMike digimatic micrometer (Mitutoyo Spain, Elgoibar, Spain). Five positions on film sample were measured to calculate the average thickness.

7.4.4 Physicochemical properties

Films were cut (20 mm × 20 mm), weighed (W_0), and dehydrated in an air-circulating oven at 105 °C for 24 h. The dry samples were reweighed (W_1) and moisture content (MC) was calculated as follows:

$$\text{MC (\%)} = \frac{(W_0 - W_1)}{W_0} \times 100$$

In order to determine total soluble matter (TSM), film samples were immersed into 30 mL distilled water at 25 °C for 24 h in the presence of sodium azide (0.02 g/100 mL). Thereafter, specimens were filtrated and dried in an air-circulating oven at 105 °C for 24 h and weighed (W_2). TSM (%) was calculated as follows:

$$\text{TSM (\%)} = \frac{(W_1\text{-}W_2)}{W_1} \times 100$$

In order to determine water vapor absorption, films were cut (20 mm × 10 mm), dehydrated as abovementioned and weighed (W_1). The dry samples were stored in a desiccator containing water at 25 °C. Film samples were weighed at different times during 0.5 – 168 h (W_t). Water vapor absorption was calculated as follows:

$$\text{Water vapor absorption (\%)} = \frac{(W_t\text{-}W_1)}{W_1} \times 100$$

Fourier transformed infrared (FTIR) spectra of the films were determined on a Nicolet Nexus FTIR spectrometer using ATR Golden Gate (Specac). A total of 32 scans were performed at 4 cm^{-1} resolution. The measurements were recorded between 4000 and 800 cm^{-1}.

7.4.5 Optical and morphological properties

Color was analyzed with a CR-400 (Konica Minolta Chroma-Meter, Valencia, Spain). The color was expressed as *L**-value (lightness), *a**-value (redness/greenness) and *b**-value (yellowness/blueness). *L**, *a** and *b** parameters were measured by placing the films on the surface of a standard white plate. Color difference (ΔE^*) was calculated based on the control film (without EGCG):

$$\Delta E^* = \sqrt{(\Delta L^*)^2 + (\Delta a^*)^2 + (\Delta b^*)^2}$$

Film gloss was determined according to ASTM D523-99 (ASTM, 2008), using a Multi Gloss 268 Plus gloss meter. Gloss values were measured at 60° incidence angle.

The morphology of the cross-section of the films was visualized using a Hitachi S-4800 scanning electron microscopy (Hitachi, Spain). The cross-section was prepared using mechanical means by a conventional cutter. Then, samples were mounted on a metal stub with double-side adhesive tape and coated under vacuum with

gold, using a JEOL fine-coat ion sputter JFC-1100 (Izasa, Spain) in an argon atmosphere prior to observation. All samples were examined using an accelerating voltage of 15 kV.

7.4.6 Mechanical and barrier properties

Tensile strength (TS), Young's modulus (E) and elongation at break (EAB) were measured at least five times for each film, using an electromechanical Insight 10 testing system (MTS Systems, Barcelona, Spain) at 25 °C, according to ASTM D1708-93 (ASTM, 1993). Samples were cut into dog bone shaped specimens of 4.75 mm × 22.25 mm.

Water vapor permeability (WVP) measurements were carried out in a controlled humidity environment chamber PERME™ W3/0120 (Labthink Instruments Co. Ltd., Shandong, China). Bilayer films were cut in samples of 7.4 cm diameter and a test area of 33 cm^2. Films were maintained at a temperature of 38 °C and a relative humidity of 90%, according to ASTM E96-00 (ASTM, 2000) and WVP was determined gravimetrically until constant weight. Firstly, water vapor transmission rate (WVTR) was determined and then, water vapor permeability (WVP):

$$\mathrm{WVP}\left(\frac{\mathrm{g}}{\mathrm{m\ s\ Pa}}\right) = \frac{\mathrm{WVTR} \times \mathrm{L}}{\Delta P}$$

where L is the thickness of the samples and ΔP is the partial pressure difference of water vapor across the film.

The light barrier properties of films were measured by using a V-630 UV-vis spectrophotometer (Jasco, Madrid, Spain) at wavelengths from 200 nm to 800 nm.

7.4.7 Antioxidant activity

The EGCG release was determined using UV-vis spectroscopy (Perkin-Elmer Lambda 18 spectrometer, Perkin-Elmer, Courtaboeuf, France). Firstly, the wavelength of the maximum absorbance for EGCG in 95% ethanol was measured (λ_{max}

= 274 nm). Standard solutions of EGCG (0.50 – 20 µg/mL) were then prepared to achieve a calibration curve. Film samples (2 cm × 4 cm) were immersed into 95% ethanol (6 mL) in glass vessels with light protection. The samples were stirred with magnetic stirrer (RT15, IKA®, Staufen, Germany) at 200 rpm at room temperature (14.0 ± 4.3 °C). After 7 days, 2.5 mL of simulant were collected from testing vessels and light absorption was measured at 274 nm using UV-vis spectroscopy. The release was obtained by employing the calibration curve. Light absorption of control film was used as the subtracting reference. The experiments of each composition were carried out in triplicate.

Additionally, film samples removed after 7 days of immersion were dried at room temperature for 48 h and weighed (W_7). Three samples were used for each composition and the mass loss of each film was calculated with the following equation:

$$\text{Mass loss (\%)} = (1-\frac{W_7}{W_0}) \times 100$$

In order to measure DPPH radical scavenging activity, samples (2 mL) were mixed with DPPH solution (75 µM DPPH in 95% ethanol) (2 mL) and allowed to stand in dark at room temperature for 30 min. The absorbance of the solution was measured at 517 nm using a spectrophotometer. A standard curve was prepared using EGCG in the range of 0–15 µM. The activity was calculated and expressed as µmol EGCG/mL ethanol. All the tests were carried out in triplicate.

7.4.8 Quality changes of striped catfish slices packaged in bags

7.4.8.1 Preparation of bags

The prepared bilayer films (BL) without and with 12 wt % EGCG or linear low-density polyethylene (LLDPE) were used for preparation of bags using an impulse sealer with a magnet model ME-300HIM (S.N.MARK Ltd., Park, Nonthaburi, Thailand) and the bags obtained were named as ‘BL’, ‘BL-12EGCG’ and ‘LLDPE’ bags, respectively. Films (60 mm × 60 mm) were sealed at 150 ± 0.5 °C for 1.25 s, followed by cooling for 1.50 s. The width of seal area was 2 mm.

7.4.8.2 Packaging of striped catfish slices in bags

Fresh striped catfish was purchased from a market located at Hat Yai, Songkhla, Thailand. Fish was packaged in an insulated box containing ice with an ice/fish ratio of 3:1 (w/w) and transported to the laboratory. Striped catfish slices (SCS) (45 mm × 45 mm) with a thickness of 8 – 10 mm and weight of 10 – 12 g were prepared and inserted manually into the bags before heat-sealing. SCS packaged in LLDPE bag was used as the control. All samples were stored in a refrigerator (4 ± 1 °C). The samples were randomly taken for analysis at 0, 3, 5 and 7 days of storage.

7.4.8.3 Determinations of fish slice quality

7.4.8.3.1 Physical changes

Color was analyzed with a CIE colorimeter (Hunter associates laboratory, Inc., Reston, VA, USA). L^*, a^* and b^* parameters were measured by placing the flesh on a measure cell with a 30 mm opening. Total color difference (ΔE^*) was calculated relative to fresh SCS (Day 0).

The texture of SCS was determined as described by Kaewprachu *et al.* (2017a) using a texture analyzer (Stable Micro Systems, Guildford, UK) equipped with a cylindrical plunger (20 mm in diameter) at a constant speed of 0.5 mm/s and at a penetration of 2.5 mm into the flesh. Hardness was defined as the maximum force (N).

7.4.8.3.2 Microbiological changes

Spread plate method as described by Sallam (2007) was adopted. Total viable count (TVC) and psychrophilic bacteria count (PBC) of SCS were enumerated on standard plate count agar incubated at 37 °C for 3 days and at 4 °C for 7 days, respectively. Samples were collected aseptically and used as the composite sample. The sample (2.5 g) was placed in a Stomacher bag containing 22.5 ml of 0.85% (w/v) NaCl solution and mixed for 1 min at 230 rpm in a Stomacher blender (Stomacher M400, Seward Ltd., Worthington, England). Subsequently, serial dilutions were made from

the homogenate using 0.85% NaCl solution as the diluent. Appropriate dilutions were used for analysis.

7.4.8.3.3 Chemical changes

The weight loss was determined by comparison between the weights of the initial sample and those of samples after storage at the designated time. Peroxide value (PV) was measured according to the method of Richards and Hultin (2002) and expressed as mg cumene hydroperoxide/kg sample. The thiobarbituric acid reactive substances (TBARS) value was examined as tailored by Buege and Aust (1978). TBARS values were calculated and expressed as mg malonaldehyde/kg sample.

For fatty acid composition, extraction of total lipids and preparation of fatty acid methyl esters (FAMEs) using alkali catalyzed transmethylation were carried out as described by Muhammed *et al.* (2015). The resulting FAMEs (1 µL) were subjected to gas chromatography system 7890B series (Agilent Technologies, Santa Clara, CA, USA) equipped with flame ionization detector (FID) and CP-Sil 88 capillary column (J & W Scientific Column from Agilent Technologies) length of 100 m with 0.25 mm (ID) and 0.20 mm (film thickness). The GC inlet temperature and FID detector temperature were maintained at 240 °C, and the initial column temperature was set at 140 °C. The column temperature was increased at a rate of 4 °C/min up to 240 °C. Helium was used as the mobile phase at 1 mL/min. Peak identification was done based on the retention time of external standard from Supelco (37 Component FAME Mix). The identified peaks were integrated and calibrated against the standards curve using the software Open LAB CDS (Chem Station edition, Agilent Technologies, Santa Clara, CA, USA).

7.4.8.3.4 Sensory evaluation

Sensory evaluation in terms of appearance, color, rancidity, fishy odor and overall likeness of SCS stored in different bags was performed with fifty untrained panelists as described by Meilgaard *et al.* (1999). Nine-point hedonic scale was used, in which score ‘1’ represents ‘unaccepted and dislike extremely’ and nine denoted

'accepted and like extremely'. The average score of 5 was used as the limit of overall acceptability (Olatunde *et al.*, 2019).

7.4.9 Statistical analysis

Analysis of variance (ANOVA) was done and the differences among the samples were determined using Duncan's multiple range test. Differences were statistically significant at the $P < 0.05$ level. The analysis was performed with a SPSS package (SPSS for windows, SPSS Inc., Chicago, IL, USA).

7.5 Results and discussion

7.5.1 Physicochemical properties

The appearance of bilayer films incorporated with EGCG at different concentrations is shown in Figure 29. All bilayer films showed good handling and transparency. High lightness was occurred for control film (without EGCG), while a slight yellowish was observed for the films containing EGCG.

Figure 29. Appearance of PLA-gelatin bilayer films incorporated with different concentrations of EGCG.

Film thickness of bilayer films was in the range of 0.179 – 0.195 mm (Table 25). No significant ($P > 0.05$) difference was observed for the thickness of all film samples. Regarding moisture content, low MC values (4.3-5.4%) were obtained for all films, which could be associated to the moisture content of the gelatin layer. Moreover, bilayer films containing EGCG showed slightly lower ($P < 0.05$) MC values than the

control film (without EGCG). This could be associated to the interactions between gelatin and EGCG, which decreased the hydrophilic groups available to interact with water. As considering film solubility, all films exhibited a similar ($P > 0.05$) TSM in the range of 38.0 – 39.1%, indicating that the incorporation of EGCG did not affect the solubility of the resulting films.

Table 25. Thickness, moisture content (MC), and total soluble matter (TSM) of PLA-gelatin bilayer films incorporated with different concentrations of EGCG.

EGCG (wt %)	Thickness (mm)	MC (%)	TSM (%)
0	0.179 ±0.009 a	5.4 ± 0.4 a	38.0 ± 1.7 a
3	0.185 ±0.006 a	5.2 ± 0.4 ab	39.0 ± 0.9 a
6	0.181 ±0.012 a	4.4 ± 0.2 bc	39.1 ± 2.6 a
9	0.195 ±0.005 a	4.3 ± 0.5 c	37.9 ± 3.7 a
12	0.186 ±0.008 a	4.5 ± 0.5 bc	38.2 ± 2.4 a

Two means followed by the same letter in the same parameter are not significantly ($P > 0.05$) different through the Duncan's Multiple Range Test. $n = 3$ is the minimum number of replication.

Additionally, water vapor absorption of bilayer films incorporated with EGCG at different concentrations is shown in Figure 30. Continuous increase of water absorption was observed for all films for 168 h of storage. This could be mainly related to the gelatin layer, which is hydrophilic in nature, while PLA, had relatively low moisture sorption capacity (Auras *et al.*, 2004). Control film (without EGCG) generally exhibited high water vapor absorption. The lowest ($P < 0.05$) water vapor absorption was obtained for the film containing 9 wt % EGCG. This result was probably due to the high extend of gelatin and EGCG interactions, which lowered the amount of hydrophilic groups available to bind with water, in accordance with the lower MC value shown in Table 25. However, when the highest concentration (12 wt % EGCG) was used, higher values were found probably due to an excessive EGCG amount.

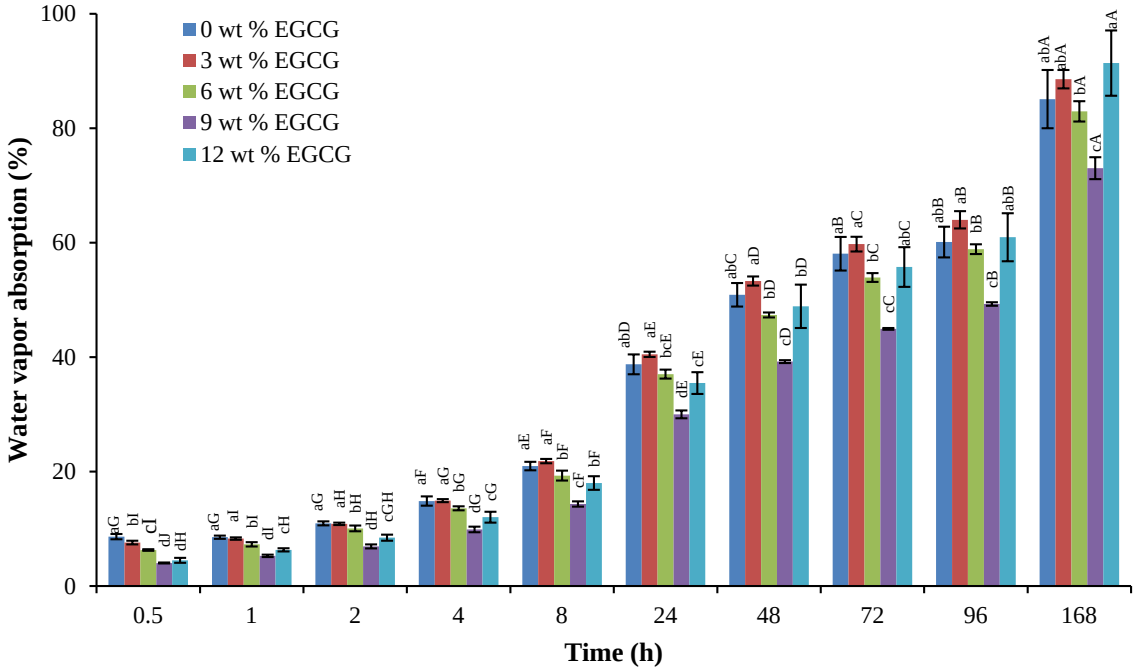

Figure 30. Water vapor absorption of PLA-gelatin bilayer films incorporated with different concentrations of EGCG. Two means followed by the same letter in the same parameter are not significantly (P > 0.05) different through the Duncan's Multiple Range Test. *n* = 3 is the minimum number of replication. Bar represents standard deviation values.

In order to study the interactions between gelatin and EGCG, FTIR spectroscopy was carried out with the gelatin layer incorporated with different concentrations of EGCG and spectra are shown in Figure 31. The characteristic bands of gelatin appeared at 3290 cm^{-1} (amide A, representative of N–H stretching, coupled with hydrogen bonding), 1631 cm^{-1} (amide I, representative of C=O stretching/hydrogen bonding coupled with COO^-), 1546 cm^{-1} (amide II, representative of N–H bending coupled with C–N stretching) and 1239 cm^{-1} (amide III, representative of the vibrations in-plane of C–N and N–H groups of bound amide or vibrations of CH_2 groups of glycine) (Muyonga *et al.*, 2004; Nilsuwan *et al.*, 2017; Tongnuanchan *et al.*, 2014). The band at the wavenumber range of 3400-3300 cm^{-1} was attributed to O–H stretching of alcohols and phenols and the bands at ~1350, ~1143 and ~1080 cm^{-1} were related to O–H bending, –OH aromatic ring and C–O stretching in phenols and

alcohols (Park *et al.*, 2010; Smith, 1998). The band situated at 1036 cm^{-1} corresponded to hydroxyl groups associated with the glycerol added as plasticizer (Bergo & Sobral, 2007) and the incorporated EGCG (Bergo and Sobral, 2007; Nilsuwan *et al.*, 2018b). It is worth noting that amide-A and amide-II bands shifted from 3291 to 3285 and from 1543 to 1537 cm^{-1}, respectively, suggesting the interaction between gelatin and EGCG molecules. Additionally, the changes exhibited in the 1500–1000 cm^{-1} region denoted the interactions with EGCG.

7.5.2 Optical and morphological properties

Color parameters of bilayer films are shown in Table 26. As can be seen, no significant difference ($P > 0.05$) of L^* values was found, but an increase of a^*, b^* and ΔE^* values was observed when the EGCG concentration was increased. The effect of the addition of antioxidants on L^*, a^* and b^* values of the resulting films has also been found by other authors (Hwang *et al.*, 2012).

Moreover, gloss was determined on the gelatin layer in order to assess the surface attributes. All films showed high gloss values (> 70 GU), indicating the smooth and glossy surface (Trezza and Krochta, 2008). Fish gelatin films generally have high gloss values (119.75 – 142.50 GU) (Etxabide *et al.*, 2015). As EGCG was incorporated at different concentrations, lower gloss values occurred, in comparison to control film (without EGCG). This change can be explained by the interactions among the components of the film forming solution.

In order to investigate the microstructure of bilayer films, SEM was carried out and the cross-section of films is presented in Figure 32. The cross-section of all films showed the good adhesion between the two layers of the film: PLA (upper layer) and gelatin (lower layer). Smoother and more compact cross-section was found for the gelatin layer, while a rougher cross-section was observed for the PLA layer. When EGCG content was increased, the adhesion between layers seemed to be enhanced and gelatin layer (lower layer) became rougher.

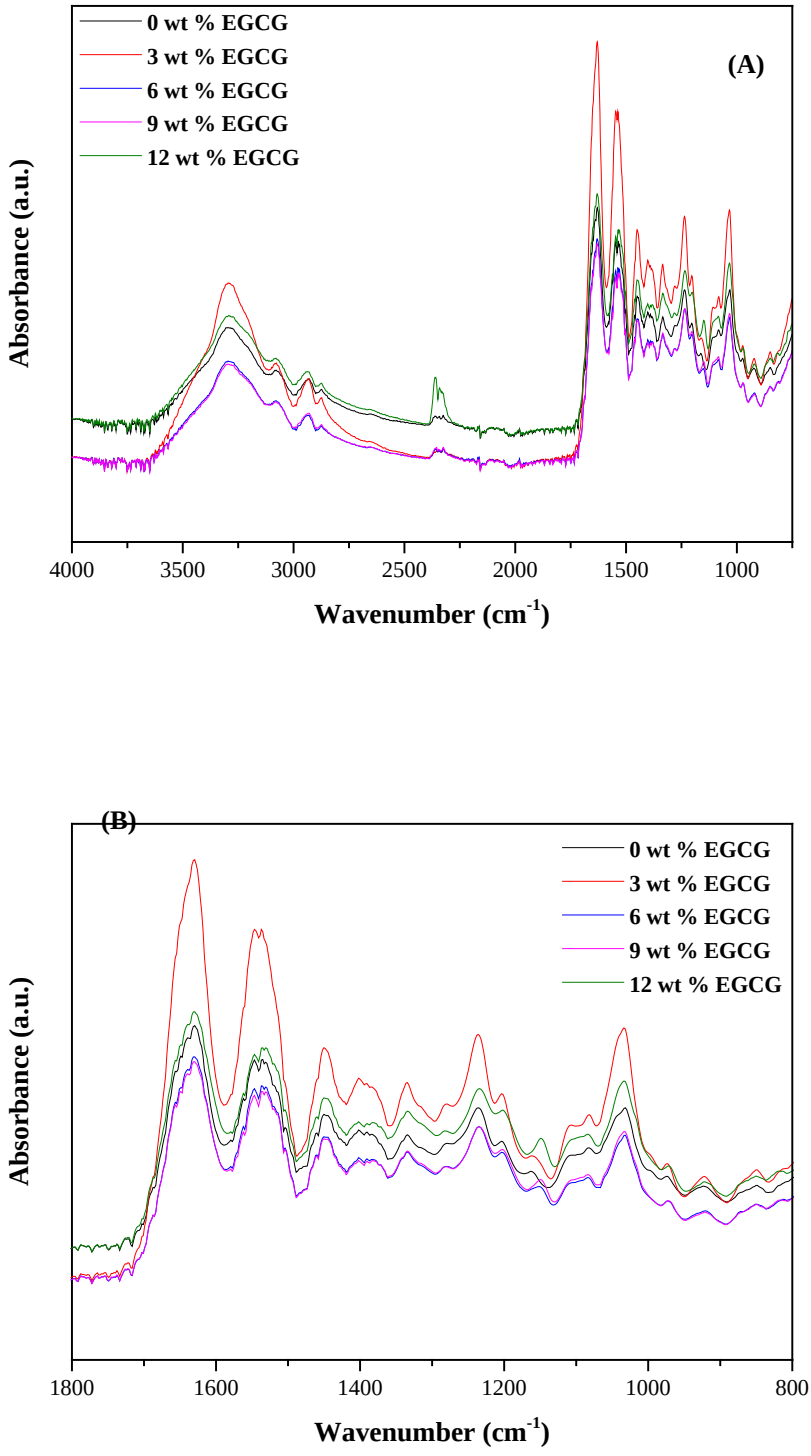

Figure 31. ATR-FTIR spectra of gelatin layer incorporated with different concentrations of EGCG: (A) from 4000 to 800 cm^{-1} and (B) from 1800 to 800 cm^{-1}.

Table 26. Color and gloss of PLA-gelatin bilayer films incorporated with different concentrations of EGCG.

EGCG (wt %)	*L**	*a**	*b**	Δ*E**	Gloss$_{60}$ (GU)
0	95.33 ± 0.21 a	-0.36 ± 0.02 c	3.30 ± 0.05 c	-	152 ± 3 a
3	95.33 ± 0.23 a	-0.25 ± 0.03 b	3.59 ± 0.08 b	0.36 ± 0.12 b	108 ± 4 b
6	95.20 ± 0.05 a	-0.24 ± 0.01 b	3.97 ± 0.03 a	0.69 ± 0.04 a	79 ± 4 c
9	95.16 ± 0.16 a	-0.17 ± 0.01 a	3.93 ± 0.03 a	0.69 ± 0.06 a	77 ± 3 c
12	95.20 ± 0.05 a	-0.15 ± 0.02 a	4.05 ± 0.18 a	0.79 ± 0.18 a	78 ± 3 c

Two means followed by the same letter in the same parameter are not significantly (P > 0.05) different through the Duncan's Multiple Range Test. n = 3 is the minimum number of replication.

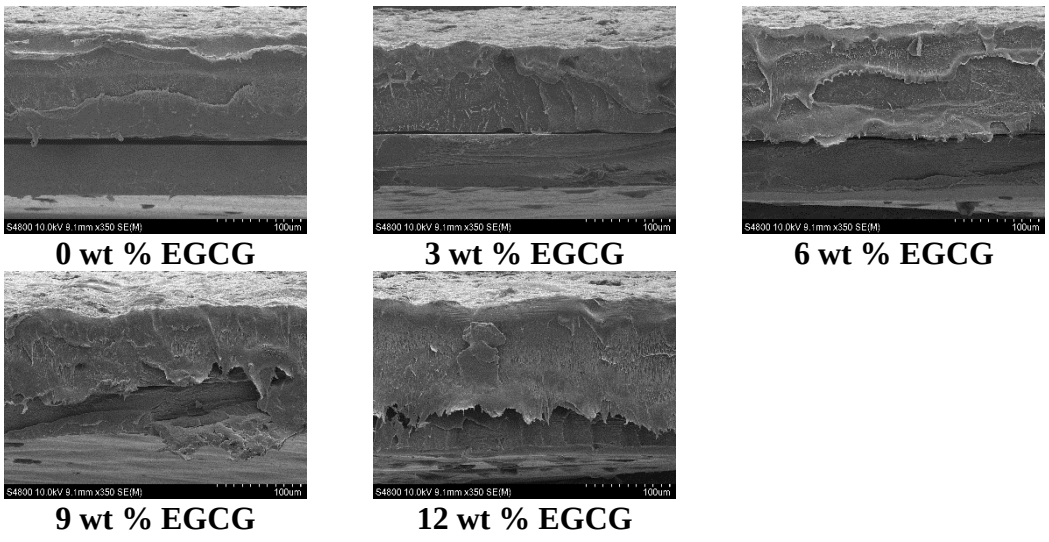

Figure 32. SEM micrographs (350×) of the cross-sections of bilayer films with different concentrations of EGCG.

7.5.3 Mechanical and barrier properties

Tensile strength (TS), elongation at break (EAB) and Young's modulus (E) were measured and the values are shown in Table 27. As can be seen, similar values were found for all films, regardless of EGCG content. In general, resistant films were obtained with TS values higher than 20 MPa. This behavior might be associated to the

high resistance of the PLA layer, which plays a major role in the mechanical properties of the bilayer films. Martucci and Ruseckaite (2010) have also reported that PLA films show high E and TS values.

WVP was determined in order to evaluate the water vapor barrier of the resulting films. No significant ($P < 0.05$) difference of WVP values was observed for all bilayer films (Table 27), regardless of the EGCG concentration used. Bilayer films showed low WVP values associated with the low WVP of PLA films (Nilsuwan *et al.*, 2018a; Zhu *et al.*, 2017).

Table 27. Young's modulus (E), tensile strength (TS), elongation at break (EAB), and water vapor permeability (WVP) of PLA-gelatin bilayer films incorporated with different concentrations of EGCG.

EGCG (wt %)	E (MPa)	TS (MPa)	EAB (%)	WVP ($\times 10^{-13}$ g/m s Pa)
0	1777 ± 213 a	26 ± 4 a	1.5 ± 0.1 a	2.01 ± 0.01 a
3	1596 ± 156 a	20 ± 4 a	1.3 ± 0.2 ab	2.06 ± 0.03 a
6	1770 ± 200 a	24 ± 5 a	1.3 ± 0.1 ab	2.01 ± 0.02 a
9	1752 ± 150 a	24 ± 3 a	1.4 ± 0.2 ab	2.02 ± 0.02 a
12	1737 ± 94 a	20 ± 4 a	1.2 ± 0.2 b	2.15 ± 0.01 a

Two means followed by the same letter in the same parameter are not significantly ($P > 0.05$) different through the Duncan's Multiple Range Test. $n = 3$ is the minimum number of replication.

Furthermore, UV and visible light absorption spectra at the wavelength range of 200-800 nm for bilayer films incorporated with different concentrations of EGCG are shown in Figure 33. High UV light protection in the range of 200 – 250 nm was exhibited for all bilayer films. This is commonly related to the absorption of the polypeptide backbone of gelatin (Etxabide *et al.*, 2015; Goldfarb, 1953). The absorption in the range of 250 - 300 nm is mainly due to the presence of aromatic compounds, such as tyrosine and phenylalanine, in gelatin (Benjakul *et al.*, 2009; Bonilla and Sobral, 2016). Accordingly, a rise of UV absorption was found for gelatin films when EGCG was added due to the high content of aromatic groups existing in EGCG. In addition,

films containing EGCG showed higher visible light absorption in the range of 400 - 800 nm, which might be associated with higher content of chromophores.

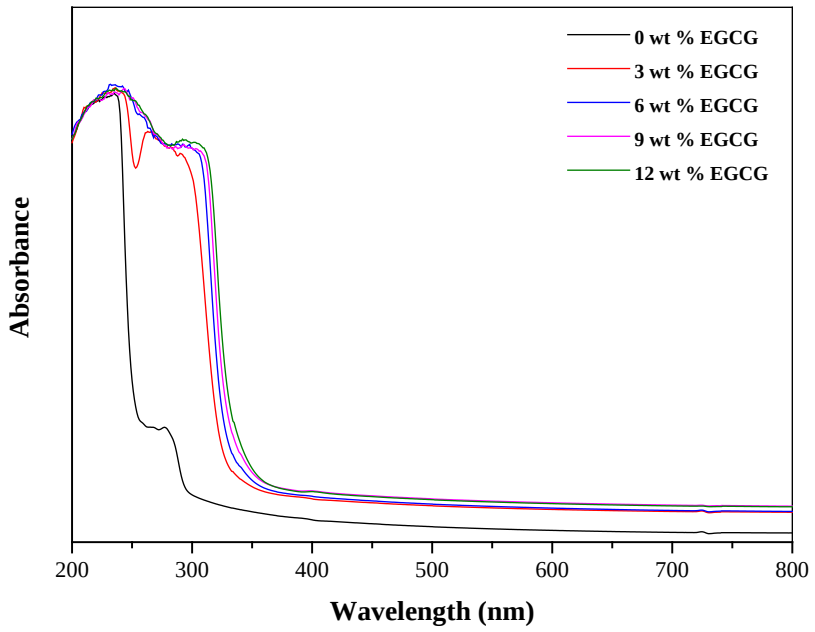

Figure 33. UV-visible light absorption of PLA-gelatin bilayer films incorporated with different concentrations of EGCG.

7.5.4 Antioxidant activity

The release of EGCG from bilayer films into 95% ethanol after 7 days of immersion is shown in Table 28. The EGCG released from all bilayer films was in the range of 0.82 - 1.69 µg EGCG/mL ethanol. Higher ($P < 0.05$) release of EGCG was observed when the concentration of EGCG increased. The highest ($P < 0.05$) release of EGCG was observed for bilayer films containing 12 wt % EGCG, suggesting that the release of active compounds is associated with the concentration used (Benbettaieb *et al.*, 2018). Additionally, in order to evaluate antioxidant activity, DPPH radical scavenging activity was measured in 95% ethanol after 7 days of film immersion. As can be seen in Table 28, an increase of DPPH radical scavenging activity was found when higher concentrations of EGCG were used. Bilayer films containing 12 wt %

EGCG showed the highest ($P < 0.05$) DPPH radical scavenging activity. This was supported by the highest release of EGCG (1.69 µg EGCG/mL ethanol). Finally, regarding mass loss, this can be related to the loss of moisture and glycerol during film immersion. The highest ($P < 0.05$) mass loss was found for the control film (without EGCG); however, no mass loss could be appreciated for bilayer films incorporated with 9 and 12 wt % EGCG. This might be related to the interactions between EGCG and gelatin, thus decreasing mass loss. Therefore, the appropriate EGCG concentrations could provide the developed PLA-gelatin bilayer film with satisfactory functional properties, which play a crucial role for packaging materials used to extend shelf-life of fatty food products during storage.

Table 28. Release and DPPH radical scavenging activity of PLA-gelatin bilayer films incorporated with different concentrations of EGCG after 7 days of immersion in 95% ethanol.

EGCG (wt %)	Release (µg EGCG/mL ethanol)	DPPH radical scavenging activity (µmol EGCG/mL ethanol)	Mass loss (%)
0	ND	ND	1.65 ± 0.27 a
3	0.82 ± 0.17 c	2.36 ± 0.52 c	0.72 ± 0.09 b
6	0.95 ± 0.17 bc	2.97 ± 0.38 bc	0.39 ± 0.09 b
9	1.14 ± 0.08 b	3.77 ± 0.70 b	ND
12	1.69 ± 0.04 a	6.69 ± 0.33 a	ND

Two means followed by the same letter in the same parameter are not significantly ($P > 0.05$) different through the Duncan's Multiple Range Test. $n = 3$ is the minimum number of replication. ND: Not detected.

7.5.5 Quality changes of striped catfish slice packaged in bags during refrigerated storage

7.5.5.1 Physical changes and weight loss

Color changes of striped catfish slices (SCS) packaged in different bags during 7 days of storage are depicted in Figure 34. Overall, fresh SCS had high L^* (61.2) and b^* (26.6) values with low a^* value (5.2), indicating the bright orangish color. When storage time increased, the decrease in L^* value was observed for all the samples. No changes ($P > 0.05$) in a^* and b* values were obtained throughout the storage. This result

suggested that SCS became slightly darker, which might be related to the loss of some moisture during storage (Bjørlykke *et al.*, 2011). Nevertheless, the Δ*E** value of SCS packaged in LLDPE bag was lower after 7 days of storage, indicating the BL bags could retard discoloration of SCS to some extent. Additionally, EGCG with antioxidant activity could retard lipid oxidation or prevent the oxidation of pigments, myoglobin or haemoglobin, in SCS. This led to the lowered change in color of SCS packaged in BL-12EGCG bag.

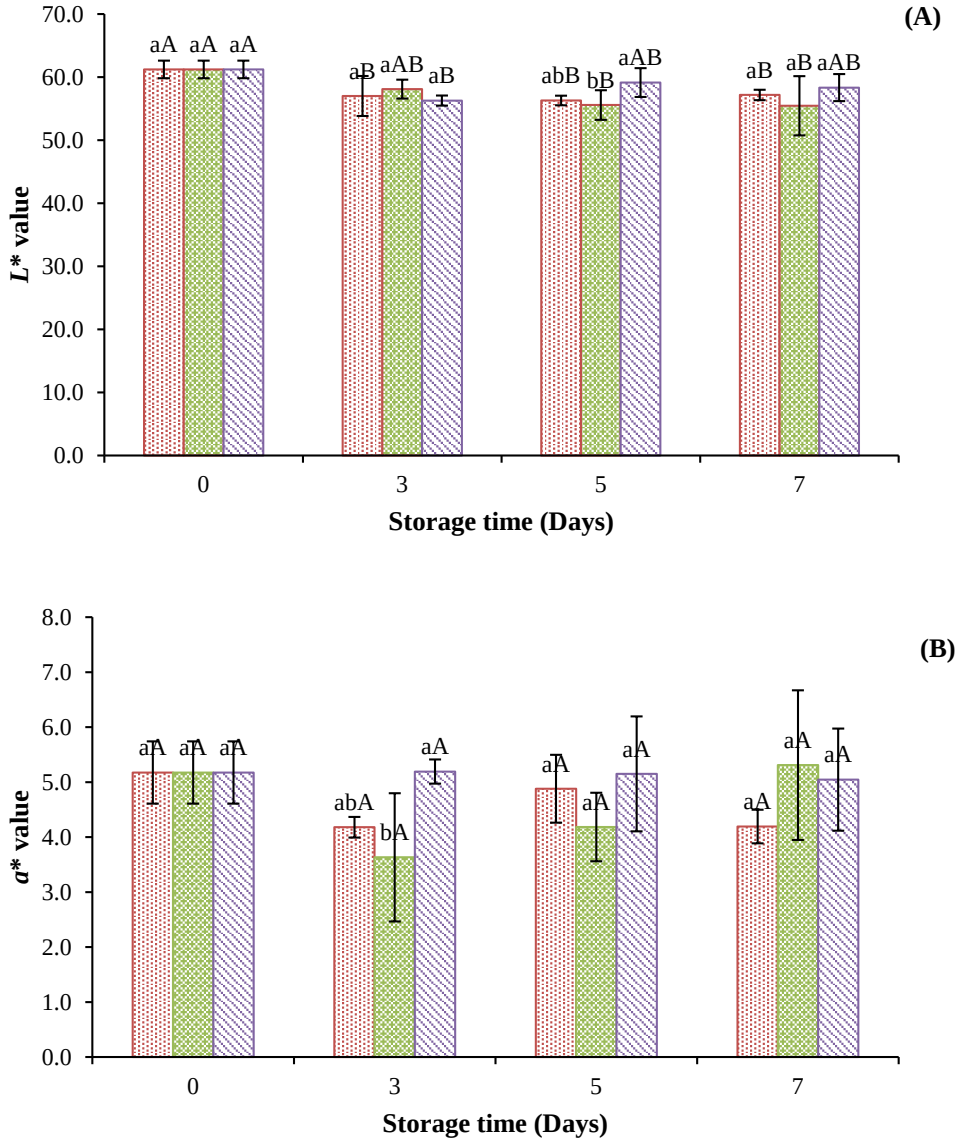

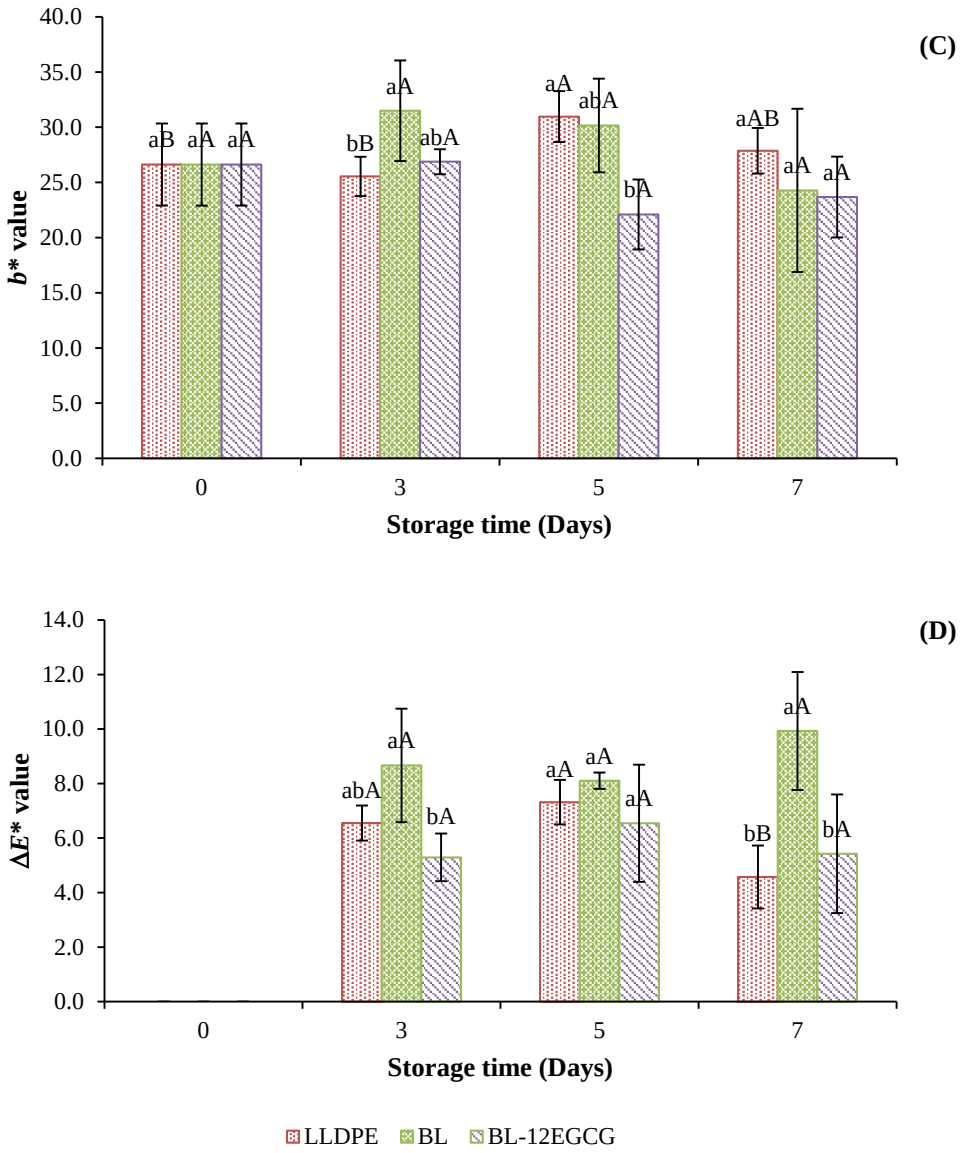

Figure 34. Changes in color of striped catfish slices stored in different bags during storage of 7 days at 4 °C. Two means followed by the same uppercase letter in the same bag and two means followed by the same lowercase letter in the same storage time are not significantly ($P > 0.05$) different through the Duncan's Multiple Range Test. $n = 3$ is the minimum number of replication. Bar represents standard deviation values.

Texture is a quality parameter associated with consumer acceptance. The change in hardness values of SCS packaged in different bags during 7 days of refrigerated storage is shown in Figure 35A. Hardness value of fresh SCS was 5.1 N. During 7 days of storage, changes ($P < 0.05$) in hardness value were observed for all

samples. This plausibly caused by the augmented oxidation of lipids and/or proteins as well as dehydration of flesh during the extended storage (Estévez *et al.*, 2006). For the sample packaged in LLDPE bag, the increase ($P < 0.05$) in hardness was observed at day 7. On the other hand, sample packaged in BL bag had the increase after 3 days but no difference ($P < 0.05$) was found during 3 – 7 days. No difference ($P > 0.05$) in hardness was observed for samples packaged in BL-12EGCG bag during 5 – 7 days of storage. In particular, at the same storage time, a higher hardness value was generally obtained for SCS packaged in BL bag during 3 – 7 days of storage. It might be related to higher weight loss occurring in SCS packaged in BL bag, as indicated in Figure 35B. Nevertheless, the increase in hardness value of SCS packaged in BL-12EGCG bag might also be associated with the interaction of proteins in striped catfish muscle and EGCG released from BL-12EGCG bag.

For weight loss, the lowest weight loss ($P < 0.05$) was found in SCS packaged in LLDPE bag at all storage times. This was related to a lower water vapor permeability (WVP) of LLDPE film. On the other hand, the highest weight loss was attained in SCS packaged in BL bag, but lower ($P < 0.05$) weight loss was found in those packaged in BL-12EGCG bags during the storage of 7 days. The high weight loss could be caused by the water absorption of packaging evidenced by high water absorption of gelatin film, as presented in Figure 30. The incorporation of EGCG could consequently reduce the water absorption of gelatin films by the enhancement of interactions between EGCG and gelatin. Kaewprachu *et al.* (2017b) reported that the incorporation of catechin-Kradon extract in fish myofibrillar protein film could decrease the diffusion rate of the water molecules due to crosslinking of fish myofibrillar protein with catechin-Kradon extract by intermolecular bonding (e.g. hydrogen bonding). EGCG might induce the cross-linking of protein and, thus, a denser network was developed, leading to a higher barrier for water migration.

7.5.5.2 Microbiological changes

At day 0, total viable count (TVC) and psychrophilic bacteria count (PBC) of fresh SCS was 2.89 and 1.95 log CFU/g sample, respectively (Figure 36). TVC and PBC of all packaged SCS were continuously increased up to7 days of storage. Lower

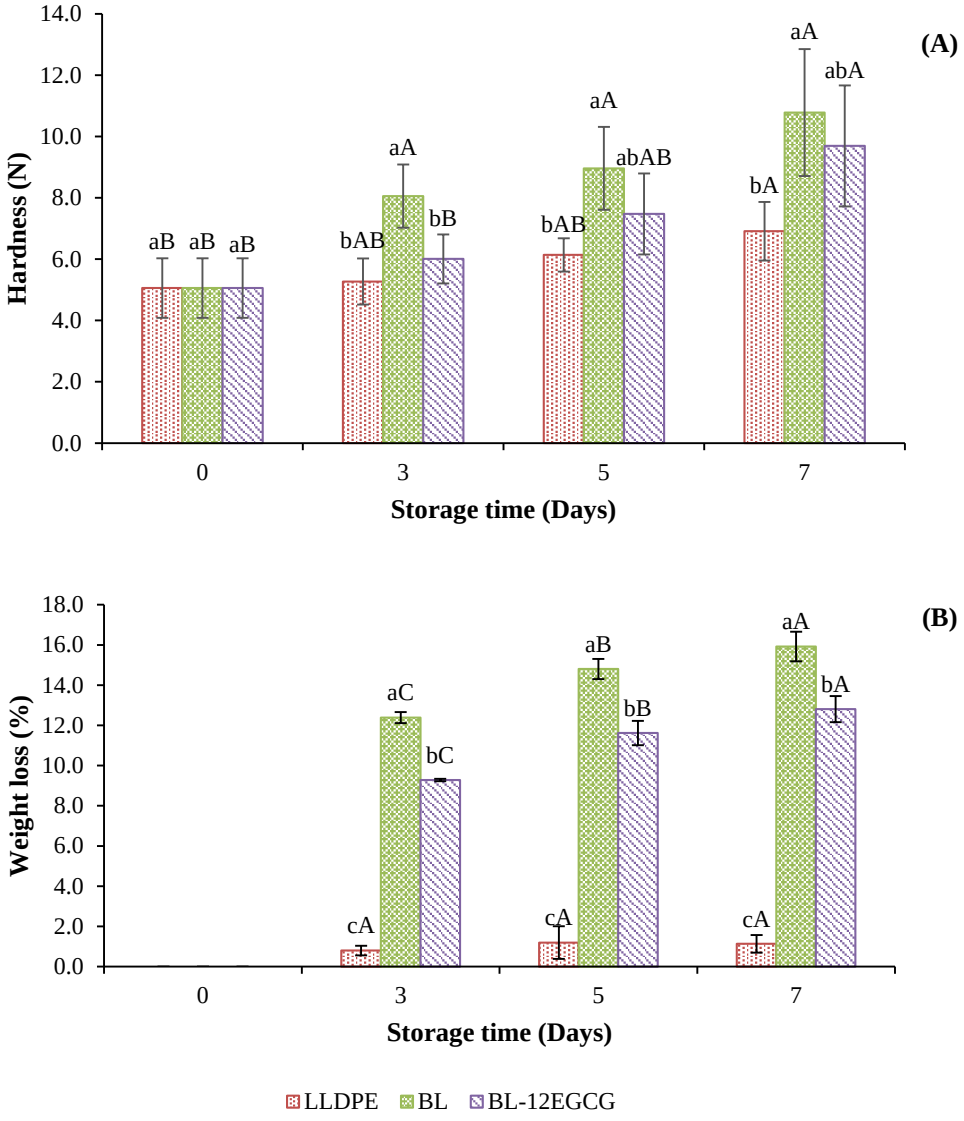

Figure 35. Changes in hardness (A) and weight loss (B) of striped catfish slices stored in different bags during storage of 7 days at 4 °C. Two means followed by the same uppercase letter in the same bag and two means followed by the same lowercase letter in the same storage time are not significantly ($P > 0.05$) different through the Duncan's Multiple Range Test. $n = 3$ is the minimum number of replication. Bar represents standard deviation values.

($P < 0.05$) PBC was observed for SCS packaged in BL-12EGCG bag throughout 7 days of storage. It is worth noting that the incorporated EGCG could be released into the flesh and acted as antimicrobial agent for inhibition of microbial growth during

extended storage. There was no difference ($P > 0.05$) in TVC between sample packaged in BL bag and LLDPE bag throughout the storage. The highest ($P < 0.05$) PBC was found for SCS packaged in LLDPE bag. As the storage time increased, psychrophilic bacteria grew and became predominant, which played a role in spoilage of slices during extended storage (Mol *et al.*, 2007). After 7 days of storage, the PBC of SCS packaged in LLDPE bag exceeded the limit (6 log CFU/g sample) recommended for fish and fish products (Mol *et al.*, 2007). Conversely, SCS samples packaged in BL and BL-12EGCG bags had PBC in the range of 5.57 – 5.85 log CFU/g sample, indicating their acceptable quality. The developed bilayer films, particularly those incorporated with 12% EGCG, could extend the shelf-life of SCS stored at refrigerated temperature by retarding the growth of microorganisms. EGCG has been known to have antimicrobial activity, mainly via injury or rupture of bacterial cell wall (Reygaert, 2018).

7.5.5.3 Chemical changes

7.5.5.3.1 Peroxide value (PV)

In general, the highly unsaturated lipids of fish become oxidized easily, resulting in alterations in smell, taste, texture, color and nutritional value (Olafsdóttir *et al.*, 1997). PV is typically used for the measurement of the concentration of hydroperoxides formed at the initial stage of lipid oxidation (Shahidi and Zhong, 2010). PV of fresh SCS (day 0) was 15.48 mg cumene hydroperoxide/kg sample (Figure 37A), suggesting the lipid oxidation took place in fish after capture or during dressing. After 3 days of refrigerated storage, the rapid increase in PV was observed for SCS packaged in BL bag, while a decrease in PV was found for SCS packaged in LLDPE bag. No change ($P > 0.05$) of PV was obtained for sample packaged in BL-12EGCG bag up to 3 days, suggesting the addition of EGCG could enhance antioxidant activity of packaging. At day 5 of storage, PV of all SCS samples were risen up to high level, regardless of the bag type used, and similar PV values ($P > 0.05$) were obtained. This result might be related to the propagation stage of lipid oxidation. After 7 days of storage, the decrease in PV was found for SCS packaged in all bags, indicating the decomposition of hydroperoxides to secondary products (Shahidi and Zhong, 2010). Among all the samples, that packaged in BL-12EGCG bag had the lowest ($P < 0.05$) PV.

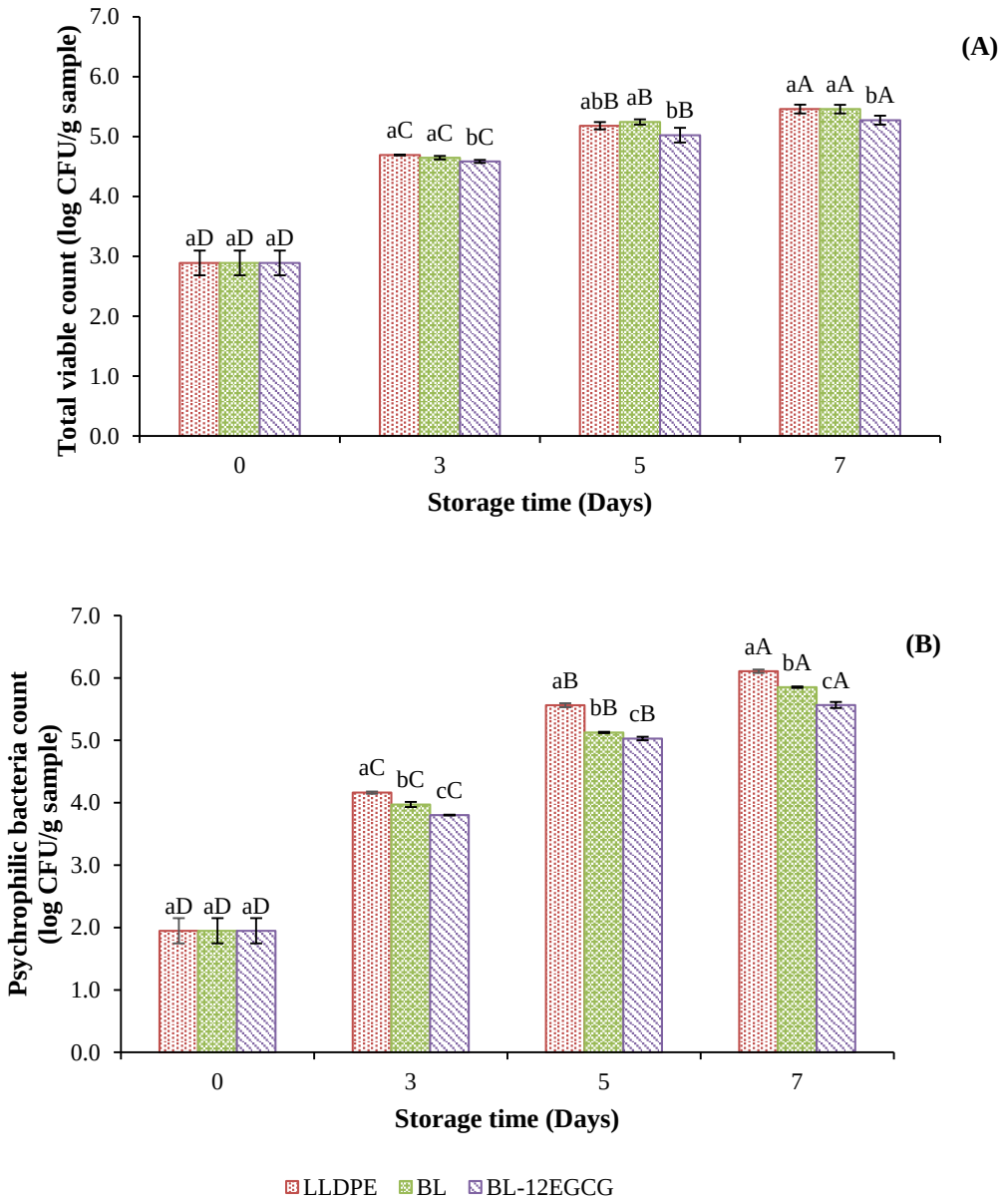

Figure 36. Changes in total viable count (A) and psychrophilic bacteria count (B) of striped catfish slices stored in different bags during storage of 7 days at 4 °C. Two means followed by the same uppercase letter in the same bag and two means followed by the same lowercase letter in the same storage time are not significantly ($P > 0.05$) different through the Duncan's Multiple Range Test. $n = 3$ is the minimum number of replication. Bar represents standard deviation values.

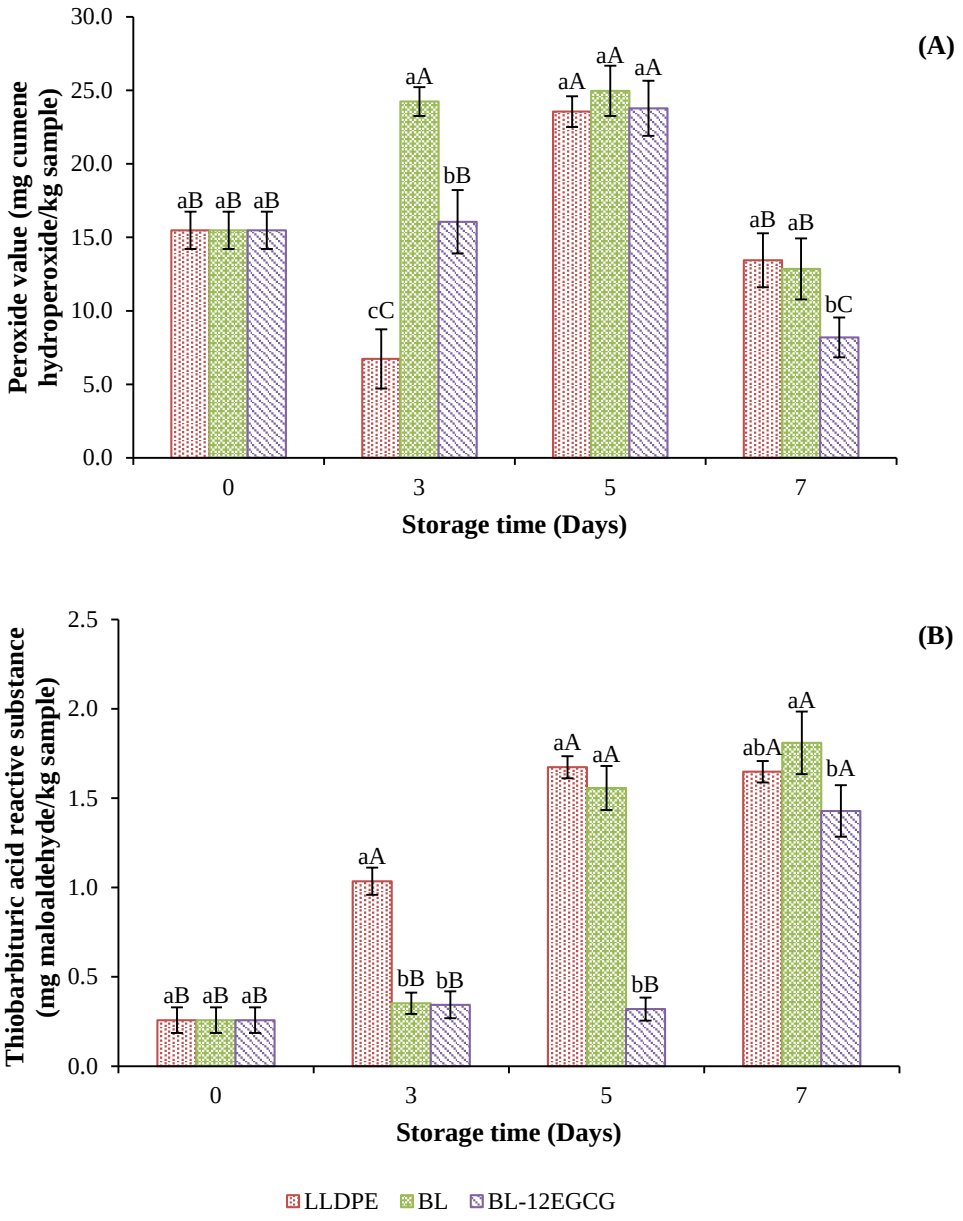

Figure 37. Changes in peroxide value (A) and thiobarbituric acid reactive substances (B) of striped catfish slices stored in different bags during storage of 7 days at 4 °C. Two means followed by the same uppercase letter in the same bag and two means followed by the same lowercase letter in the same storage time are not significantly ($P > 0.05$) different through the Duncan's Multiple Range Test. $n = 3$ is the minimum number of replication. Bar represents standard deviation values.

7.5.5.3.2 Thiobarbituric acid reactive substances (TBARS)

TBARS value was determined in order to assess the secondary oxidation products, mainly generated from decomposition of peroxides to aldehydes and ketones (Maqsood and Benjakul, 2010). TBARS value of fresh SCS was 0.23 mg malonaldehyde/kg sample (Figure 37B). Generally, the increase of TBARS values was observed for all SCS samples throughout 7 days of storage. In particular, a rapid increase ($P < 0.05$) of TBARS values was obtained for SCS packaged in LLDPE bag after 3 days of storage. This result might be related to lower oxygen barrier properties of LLDPE (Nilsuwan *et al.*, 2019). A lower ($P < 0.05$) TBARS value was observed for SCS packaged in BL-12EGCG bag during 3-5 days of storage. It is worth noting that the incorporated EGCG, which possessed an antioxidant activity, could be released into fish slice during storage, thus lowering the oxidation of lipids in slices. However, the increase ($P < 0.05$) in TBARS values was also observed at day 7 for SCS packaged in BL-12EGCG bag.

7.5.5.3.3 Fatty acid profile

Fatty acid compositions of SCS at day 0 and those after 7 days of storage are shown in Table 29. Fresh SCS had 53.60% saturated fatty acid (SFA), 31.38% monounsaturated fatty acid (MUFA) and 15.02% polyunsaturated fatty acid (PUFA). Among the fatty acids, palmitic acid (C16:0) (29.11%) and oleic acid (C18:1 *n*-9) (28.30%) were the most abundant fatty acids found in SCS. The result was in accordance with Domiszewski *et al.* (2011), who reported that the palmitic and oleic acids were the predominant fatty acids in lipids from striped catfish. The SCS also contained polyunsaturated fatty acids such as docosahexaenoic acid (DHA) (C22:6 *n*-3) and linoleic acid (C18:2 *n*-6) at high content. After 7 days of refrigerated storage, the decreases of PUFA, including linoleic, dihomolinoleic, cis-8,11,14-eicosatrienoic, cis-13,16-docosadienoic and cis-5,8,11,14,17-eicosapentaenoic (EPA) acids, along with the coincidental increases in SFA and MUFA, including lauric, cis-10-heptadecanoic, elaidic and arachidic acids, were observed for all the SCS samples. This result suggested that the PUFA were more susceptible to oxidation, thereby increasing the proportion of both SFA and MUFA, which were more stable toward oxidation

(Olatunde *et al.*, 2019). Nevertheless, SCS packaged in BL-12EGCG bag had higher ($P < 0.05$) PUFA content (14.37) than those of SCS packaged in other bags. The highest ($P < 0.05$) DHA content was found in SCS packaged in BL-12EGCG bag at day 7 of storage. It is worth noting that the incorporated EGCG could prevent lipid oxidation in SCS during storage. This result was in line with the lower TBARS values, as presented in Figure 37B.

Table 29. Fatty acid compositions of fresh striped catfish slice and those stored in different bags after 7 days of storage at 4 °C.

Formula	Fatty acids	Day 0	Day 7		
		Fresh	LLDPE	BL	BL-12EGCG
C10:0	Capric acid	ND	ND	0.79 ± 0.09 a	0.76 ± 0.08 a
C12:0	Lauric acid	ND	0.41 ± 0.06 c	1.07 ± 0.07 a	0.86 ± 0.08 b
C14:0	Myristic acid	4.54 ± 0.04 a	4.12 ± 0.05 b	3.86 ± 0.10 c	3.79 ± 0.04 c
C15:0	Pentadecanoic acid	1.18 ± 0.04 a	0.84 ± 0.12 b	0.77 ± 0.08 b	0.73 ± 0.01 b
C16:0	Palmitic acid	29.11 ± 0.15 a	30.01 ± 0.54 a	29.59 ± 0.49 a	29.45 ± 0.55 a
C16:1	Palmitoleic acid	1.39 ± 0.03 a	1.28 ± 0.11 ab	1.14 ± 0.05 b	1.22 ± 0.11 b
C17:0	Heptadecanoic acid	1.51 ± 0.03 a	1.13 ± 0.11 b	1.12 ± 0.07 b	1.04 ± 0.02 b
C17:1	Cis-10-heptadecanoic acid	ND	ND	0.63 ± 0.10 a	0.63 ± 0.07 a
C18:0	Stearic acid	10.16 ± 0.02 a	10.00 ± 0.03 b	9.86 ± 0.06 b	9.89 ± 0.12 bc
C18:1 *trans*-9	Elaidic acid	ND	0.78 ± 0.12 a	0.69 ± 0.09 a	0.70 ± 0.10 a
C18:1 *n*-9	Oleic acid	28.30 ± 0.18 a	29.17 ± 0.61 a	29.06 ± 0.56 a	28.46 ± 0.37 a
C18:2 *n*-6	Linoleic acid	4.42 ± 0.02 a	4.31 ± 0.00 b	4.25 ± 0.02 b	4.29 ± 0.07 b
C20:0	Arachidic acid	ND	1.36 ± 0.11 a	1.09 ± 0.1 b	1.03 ± 0.05 b
C20:1 *n*-9	Gondoic acid	1.69 ± 0.02 a	1.42 ± 0.04 b	1.04 ± 0.13 c	1.39 ± 0.07 b
C21:0	Heneicosanoic acid	1.53 ± 0.05 a	1.18 ± 0.10 b	1.13 ± 0.07 b	1.18 ± 0.10 b
C20:2 *n*-6	Dihomolinoleic acid	1.31 ± 0.03 a	0.96 ± 0.07 b	0.93 ± 0.07 b	1.00 ± 0.08 b
C22:0	Behenic acid	2.02 ± 0.06 a	1.09 ± 0.09 b	1.04 ± 0.11 b	1.05 ± 0.08 b
C20:3 *n*-6	Cis-8,11,14-eicosatrienoic acid	1.56 ± 0.03 a	1.29 ± 0.01 b	1.17 ± 0.01 c	1.28 ± 0.05 b
C20:4 *n*-3	Cis-5,8,11,14-eicosatetrienoic acid	ND	0.70 ± 0.12 a	0.63 ± 0.08 a	0.63 ± 0.07 a
C23:0	Tricosanoic acid	3.54 ± 0.01 a	3.27 ± 0.03 c	3.30 ± 0.01 c	3.42 ± 0.04 b
C22:2 *n*-6	Cis-13,16-docosadienoic acid	1.12 ± 0.04 a	0.75 ± 0.07 b	0.74 ± 0.07 b	0.77 ± 0.08 b
C20:5 *n*-3	Cis-5,8,11,14,17-eicosapentaenoic acid (EPA)	1.62 ± 0.02 a	1.24 ± 0.07 b	1.23 ± 0.02 b	1.30 ± 0.08 b
C22:6 *n*-3	Cis-4,7,10,13,16,19-docosahexaenoic acid (DHA)	4.99 ± 0.02 ab	4.67 ± 0.03 c	4.88 ± 0.04 b	5.10 ± 0.18 a
Saturated fatty acids (SFA)		53.60 ± 0.03 a	53.42 ± 0.10 a	53.62 ± 0.14 a	53.23 ± 0.17 a
Monounsaturated fatty acids (MUFA)		31.38 ± 0.13 a	31.88 ± 0.47 a	31.88 ± 0.41 a	31.70 ± 0.14 a
Polyunsaturated fatty acids (PUFA)		15.02 ± 0.10 a	13.92 ± 0.28 c	13.82 ± 0.18 c	14.37 ± 0.21 b
Trans fatty acids		ND	0.78 ± 0.12 a	0.69 ± 0.09 a	0.70 ± 0.10 a

Two means followed by the same letter in the same row are not significantly ($P > 0.05$) different through the Duncan's Multiple Range Test. Values are expressed as mean ± SD. $n = 3$ is the minimum number of replication. ND: Not detected.

7.5.5.4 Sensory evaluation

Fresh SCS showed high likeness score (> 7) (Figure 38) for all attributes tested, suggesting the high quality fish used for making slices. When SCS were kept for 7 days, appearance, color and overall likeness scores were decreased to 6.1 – 6.6, 5.9 – 6.5 and 6.0 – 6.4, respectively, indicating the quality loss of SCS occurred during storage. The rancidity and fishy odor likeness scores of SCS stored in LLDPE or BL was decreased to 5.8 – 6.1 and 6.1 – 6.4, respectively. Higher ($P < 0.05$) likeness score for rancidity and fishy odor were observed for SCS packaged in BL-12EGCG bag. A lower likeness score for rancidity and fishy odor was related with the increased rancidity occurred in the sample. Lipid oxidation was the major cause for the formation of fishy odor (Sae-leaw and Benjakul, 2014). This result indicated that the incorporated EGCG could be released into fish slice during storage to some extent and retarded the oxidation of lipids in slices. Additionally, all SCS samples exhibited high overall likeness scores, which was higher than the acceptable limit for human consumption (> 5.0 likeness score) (Olatunde *et al.*, 2019). However, SCS stored in BL-12EGCG showed higher ($P < 0.05$) overall likeness score than others after 7 days. It is worth noting that the bags from bilayer films, particularly those containing EGCG at 12% could maintain the sensory quality of fish slice during refrigerated storage.

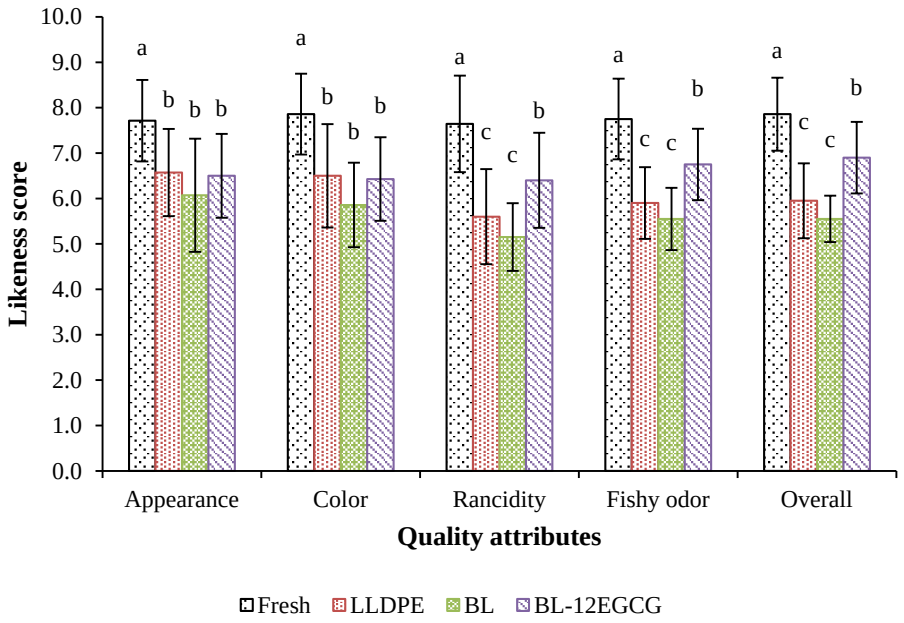

Figure 38. Changes in likeness scores of striped catfish slices stored in different bags during storage of 7 days at 4 °C. Two means followed by the same lowercase letters in the same quality attributes are not significantly ($P > 0.05$) different through the Duncan's Multiple Range Test.

7.6 Conclusions

Easy-to-handle and transparent bilayer films based on poly (lactic acid) and fish gelatin incorporated with EGCG were fabricated by thermo-compression molding. Lamination with PLA enhanced water barrier property of the resulting films. Furthermore, the incorporation of EGCG improved the properties of the bilayer films, depending on the concentration used. Bilayer films incorporated with 12 wt % EGCG rendered high water and UV-visible light barrier as well as a controlled bioactive release and antioxidant activity. The quality of striped catfish slice (SCS) packaged in bags was influenced by the EGCG incorporation into bags. The SCS packaged in BL-12EGCG bag had good quality during 7 days of storage, as indicated by low physical, microbiological, and chemical changes along with high likeness scores. Therefore, the bags based on the bilayer films containing EGCG could be applied as active packaging for shelf-life extension of high lipid-containing fish or fish products.

7.7 References

ASTM. 1993. Standard test method for tensile properties of plastics by use of microtensile specimens. *In* Annual book of ASTM standards. American Society for Testing and Materials. Philadelphia, PA.

ASTM. 2000. Standard test methods for water vapor transmission of materials, E96-00. *In* Annual book of ASTM standards. American Society for Testing and Materials. Philadelphia, PA.

ASTM. 2008. Standard test method for specular gloss, D523-99. *In* Annual book of ASTM standards. American Society for Testing and Materials. Philadelphia, PA.

Auras, R., Harte, B. and Selke, S. 2004. An overview of polylactides as packaging materials. Macromolecular Bioscience. 4: 835-864.

Benbettaieb, N., Nyagaya, J., Seuvre, A.-M. and Debeaufort, F. 2018. Antioxidant activity and release kinetics of caffeic and *p*-coumaric acids from hydrocolloid-based active films for healthy packaged food. J. Agric. Food Chem. 66: 6906-6916.

Benjakul, S., Oungbho, K., Visessanguan, W., Thiansilakul, Y. and Roytrakul, S. 2009. Characteristics of gelatin from the skins of bigeye snapper, *Priacanthus tayenus* and *Priacanthus macracanthus*. Food Chem. 116: 445-451.

Bergo, P. and Sobral, P. J. A. 2007. Effects of plasticizer on physical properties of pig skin gelatin films. Food Hydrocolloid. 21: 1285-1289.

Bigi, A., Cojazzi, G., Panzavolta, S., Rubini, K. and Roveri, N. 2001. Mechanical and thermal properties of gelatin films at different degrees of glutaraldehyde cross-linking. Biomaterials. 22: 763-768.

Bjørlykke, G. A., Roth, B., Sørheim, O., Kvamme, B. O. and Slinde, E. 2011. The effects of carbon monoxide on Atlantic salmon (*Salmo salar* L.). Food Chem. 127: 1706-1711.

Bonilla, J. and Sobral, P. J. A. 2016. Investigation of the physicochemical, antimicrobial and antioxidant properties of gelatin-chitosan edible film mixed with plant ethanolic extracts. Food Bioscience. 16: 17-25.

Buege, J. A. and Aust, S. D. 1978. Microsomal lipid peroxidation. *In* Methods in enzymology. Vol. 52. (Flesicher, S. and Packer, L., eds.). p. 302–310. Academic Press. New York.

Cabedo, L., Luis Feijoo, J., Pilar Villanueva, M., Lagarón, J. M. and Giménez, E. 2006. Optimization of biodegradable nanocomposites based on a PLA/PCL blends for food packaging applications. Macromol. Symp. 233: 191-197.

Chuaynukul, K., Nagarajan, M., Prodpran, T., Benjakul, S., Songtipya, P. and Songtipya, L. 2018. Comparative characterization of bovine and fish gelatin films fabricated by compression molding and solution casting methods. J. Polym. Mater. 26: 1239-1252.

de Carvalho, R. A. and Grosso, C. R. F. 2004. Characterization of gelatin based films modified with transglutaminase, glyoxal and formaldehyde. Food Hydrocolloid. 18: 717-726.

Domiszewski, Z., Bienkiewicz, G. and Plust, D. 2011. Effects of different heat treatments on lipid quality of striped catfish (*Pangasius hypophthalmus*). Acta Sci. Pol. Technol. Aliment. 10: 359-373.

Estévez, M., Ventanas, S. and Cava, R. 2006. Effect of natural and synthetic antioxidants on protein oxidation and colour and texture changes in refrigerated stored porcine liver pâté. Meat Sci. 74: 396-403.

Etxabide, A., Uranga, J., Guerrero, P. and de la Caba, K. 2015. Improvement of barrier properties of fish gelatin films promoted by gelatin glycation with lactose at high temperatures. LWT-Food Sci. Technol. 63: 315-321.

Fang, J. M., Fowler, P. A., Escrig, C., Gonzalez, R., Costa, J. A. and Chamudis, L. 2005. Development of biodegradable laminate films derived from naturally occurring carbohydrate polymers. Carbohydr Polym. 60: 39-42.

Goldfarb, A. R. 1953. Absorption spectrum of the peptide bond: ii. Influence of chain length. Journal of Biological Chemistry. 201: 317-320.

Guerrero, P., Retegi, A., Gabilondo, N. and de la Caba, K. 2010. Mechanical and thermal properties of soy protein films processed by casting and compression. J. Food Eng. 100: 145-151.

Hoque, M. S., Benjakul, S. and Prodpran, T. 2011. Effects of partial hydrolysis and plasticizer content on the properties of film from cuttlefish (*Sepia pharaonis*) skin gelatin. Food Hydrocolloid. 25: 82-90.

Hwang, S. W., Shim, J. K., Selke, S. E. M., Soto-Valdez, H., Matuana, L., Rubino, M. and Auras, R. 2012. Poly(L-lactic acid) with added α-tocopherol and resveratrol: optical, physical, thermal and mechanical properties. Polymer International. 61: 418-425.

Kaewprachu, P., Osako, K., Benjakul, S. and Rawdkuen, S. 2015. Quality attributes of minced pork wrapped with catechin–lysozyme incorporated gelatin film. Food Pack. Shelf Life. 3: 88-96.

Kaewprachu, P., Osako, K., Benjakul, S., Suthiluk, P. and Rawdkuen, S. 2017a. Shelf life extension for Bluefin tuna slices (*Thunnus thynnus*) wrapped with myofibrillar protein film incorporated with catechin-Kradon extract. Food Control. 79: 333-343.

Kaewprachu, P., Rungraeng, N., Osako, K. and Rawdkuen, S. 2017b. Properties of fish myofibrillar protein film incorporated with catechin-Kradon extract. Food Pack. Shelf Life. 13: 56-65.

Lee, K.-Y. and Song, K. B. 2017. Preparation and characterization of an olive flounder (*Paralichthys olivaceus*) skin gelatin and polylactic acid bilayer film. J. Food Sci. 82: 706-710.

Lu, T.-M., Lee, C.-C., Mau, J.-L. and Lin, S.-D. 2010. Quality and antioxidant property of green tea sponge cake. Food Chem. 119: 1090-1095.

Maqsood, S. and Benjakul, S. 2010. Comparative studies of four different phenolic compounds on in vitro antioxidative activity and the preventive effect on lipid oxidation of fish oil emulsion and fish mince. Food Chem. 119: 123-132.

Martino, V. P., Jiménez, A. and Ruseckaite, R. A. 2009. Processing and characterization of poly(lactic acid) films plasticized with commercial adipates. J. Appl. Polym. Sci. 112: 2010-2018.

Martucci, J. F. and Ruseckaite, R. A. 2010. Three-layer sheets based on gelatin and poly(lactic acid), part 1: Preparation and properties. J. Appl. Polym. Sci. 118: 3102-3110.

Maryam Adilah, Z. A., Jamilah, B. and Nur Hanani, Z. A. 2018. Functional and antioxidant properties of protein-based films incorporated with mango kernel extract for active packaging. Food Hydrocolloid. 74: 207-218.

Meilgaard, M. C., Carr, B. T. and Civille, G. V. 1999. Sensory evaluation techniques. CRC press.

Mol, S., Erkan, N., ÜÇOk, D. and Tosun, Ş. Y. 2007. Effect of psychrophilic bacteria to estimate fish quality. Journal of Muscle Foods. 18: 120-128.

Muhammed, M. A., Domendra, D., Muthukumar, S. P., Sakhare, P. Z. and Bhaskar, N. 2015. Effects of fermentatively recovered fish waste lipids on the growth and composition of broiler meat. British poultry science. 56: 79-87.

Muyonga, J. H., Cole, C. G. B. and Duodu, K. G. 2004. Characterisation of acid soluble collagen from skins of young and adult Nile perch (*Lates niloticus*). Food Chem. 85: 81-89.

Nagarajan, M., Prodpran, T., Benjakul, S. and Songtipya, P. 2017. Properties and characteristics of multi-layered films from tilapia skin gelatin and poly(lactic acid). Food Biophys. 1-12.

Nilsuwan, K., Benjakul, S. and Prodpran, T. 2016. Influence of palm oil and glycerol on properties of fish skin gelatin-based films. J. Food Sci. Technol. 53: 2715-2724.

Nilsuwan, K., Benjakul, S. and Prodpran, T. 2017. Properties, microstructure and heat seal ability of bilayer films based on fish gelatin and emulsified gelatin films. Food Biophys. 12: 234-243.

Nilsuwan, K., Benjakul, S. and Prodpran, T. 2018a. Physical/thermal properties and heat seal ability of bilayer films based on fish gelatin and poly(lactic acid). Food Hydrocolloid. 77: 248-256.

Nilsuwan, K., Benjakul, S. and Prodpran, T. 2018b. Properties and antioxidative activity of fish gelatin-based film incorporated with epigallocatechin gallate. Food Hydrocolloid. 80: 212-221.

Nilsuwan, K., Benjakul, S., Prodpran, T. and de la Caba, K. 2019. Fish gelatin monolayer and bilayer films incorporated with epigallocatechin gallate: Properties and their use as pouches for storage of chicken skin oil. Food Hydrocolloid. 89: 783-791.

Nuthong, P., Benjakul, S. and Prodpran, T. 2009. Effect of phenolic compounds on the properties of porcine plasma protein-based film. Food Hydrocolloid. 23: 736-741.

Olafsdóttir, G., Martinsdóttir, E., Oehlenschläger, J., Dalgaard, P., Jensen, B., Undeland, I., Mackie, I. M., Henehan, G., Nielsen, J. and Nilsen, H. 1997. Methods to evaluate fish freshness in research and industry. Trends Food Sci. Technol. 8: 258-265.

Olatunde, O. O., Benjakul, S. and Vongkamjan, K. 2019. Combined effects of high voltage cold atmospheric plasma and antioxidants on the qualities and shelf-life of Asian sea bass slices. Innov. Food Sci. Emerg. Technol. 54: 113-122.

Park, Y.-S., Lee, M.-K., Heo, B.-G., Ham, K.-S., Kang, S.-G., Cho, J.-Y. and Gorinstein, S. 2010. Comparison of the Nutrient and Chemical Contents of Traditional Korean Chungtaejeon and Green Teas. Plant Foods for Human Nutrition. 65: 186-191.

Rakotonirainy, A. M. and Padua, G. W. 2001. Effects of lamination and coating with drying oils on tensile and barrier properties of zein films. J. Agric. Food Chem. 49: 2860-2863.

Reygaert, W. C. 2018. Green tea catechins: Their use in treating and preventing infectious diseases. BioMed research international. 2018:

Rhim, J.-W., Lee, J. H. and Ng, P. K. W. 2007. Mechanical and barrier properties of biodegradable soy protein isolate-based films coated with polylactic acid. LWT-Food Sci. Technol. 40: 232-238.

Richards, M. P. and Hultin, H. O. 2002. Contributions of blood and blood components to lipid oxidation in fish muscle. J. Agric. Food Chem. 50: 555-564.

Sae-leaw, T. and Benjakul, S. 2014. Fatty acid composition, lipid oxidation, and fishy odour development in seabass (*Lates calcarifer*) skin during iced storage. Eur. J. Lipid Sci. Technol. 116: 885-894.

Sallam, K. I. 2007. Antimicrobial and antioxidant effects of sodium acetate, sodium lactate, and sodium citrate in refrigerated sliced salmon. Food Control. 18: 566-575.

Shahidi, F. and Zhong, Y. 2010. Lipid oxidation and improving the oxidative stability. Chem. Soc. Rev. 39: 4067-4079.

Smith, B. C. 1998. Infrared spectral interpretation: a systematic approach. CRC press.

Tongnuanchan, P., Benjakul, S. and Prodpran, T. 2014. Structural, morphological and thermal behaviour characterisations of fish gelatin film incorporated with basil and citronella essential oils as affected by surfactants. Food Hydrocolloid. 41: 33-43.

Trezza, T. A. and Krochta, J. M. 2008. The gloss of edible coatings as affected by surfactants, lipids, relative humidity, and time. J. Food Sci. 65: 658-662.

Zaveri, N. T. 2006. Green tea and its polyphenolic catechins: Medicinal uses in cancer and noncancer applications. Life Sci. 78: 2073-2080.

Zhu, J.-Y., Tang, C.-H., Yin, S.-W. and Yang, X.-Q. 2018. Development and characterization of novel antimicrobial bilayer films based on Polylactic acid (PLA)/Pickering emulsions. Carbohydr Polym. 181: 727-735.

Zhu, J. Y., Tang, C. H., Yin, S. W. and Yang, X. Q. 2017. Development and characterisation of polylactic acid–gliadin bilayer/trilayer films as carriers of thymol. International Journal of Food Science and Technology. 53: 608-618.

CHAPTER 8

CONCLUSION AND SUGGESTION

8.1 Conclusions

1. Properties of bilayer film prepared from GF and EF were influenced by the GF/EF thickness ratio. Increasing thickness ratio of GF increased the oxygen barrier property, while increasing ratio of EF decreased water permeability of bilayer film. Thermal stability of GF was increased when laminated with EF and it was governed by GF/EF thickness ratio. All bilayer films were heat sealable. The seal strength and seal efficiency of bilayer films proportionally increased as the thickness of GF layer increased.

2. Properties of bilayer film prepared from GF and PLA were also influenced by the GF/PLA layer thickness ratio. The increasing thickness ratio of PLA layer increased the water vapor barrier property, while increasing ratio of GF layer increased UV-light barrier properties of bilayer film.

3. EGCG possessed antioxidant activities with varying modes of actions.

4. The properties of fish gelatin-based film was affected by the concentrations of EGCG added. EGCG enhanced the mechanical and UV-light barrier properties of the film. EGCG at 5.71 wt % provided smooth surface and compact cross-section as well as high seal strength and seal efficiency of films. The highest migration of EGCG from film was also obtained in film containing 5.71 wt % EGCG. Incorporation of 5.71 wt % EGCG increased glass transition temperature of gelatin film. FTIR analysis revealed that the OH group in film matrix was increased and interaction via H-bond.

4. Oxidative stability of chicken skin oil (CSO) was also influenced by EGCG addition and bilayer formation. CSO packaged in the pouches with EGCG (E-GF and E-GF/EF) had lower PV and TBARS throughout 30 days of storage. Moreover,

E-GF/EF pouches could retard the lipid oxidation in CSO and maintain polyunsaturated fatty acids more effectively.

5. Films based on fish gelatin and EGCG fabricated by thermo-compression molding with homogenous and transparent appearance were successfully obtained. The incorporation of EGCG improved the properties of the resulting films depending on the concentration used. Films incorporated with 5.71 wt % and 17.54 wt % EGCG rendered a great integrity after water immersion, compact structure, mechanical resistance, high UV-light barrier and thermal stability as well as satisfactory release profile and antioxidant activity in controlled way.

6. Easy-to-handle and transparent bilayer films based on poly (lactic acid) and fish gelatin incorporated with EGCG were fabricated by thermo-compression molding. Lamination with PLA enhanced water barrier property of the resulting films. Furthermore, the incorporation of EGCG improved the properties of the bilayer films, depending on the concentration used. Bilayer films incorporated with 12 wt % EGCG rendered high water and UV-visible light barrier as well as a controlled bioactive release and antioxidant activity.

7. The quality of striped catfish slice (SCS) packaged in bags was also influenced by the EGCG incorporation into bags. The SCS packaged in BL-12EGCG bag had good quality during 7 days of storage, as indicated by low physical, microbiological, and chemical changes along with high likeness scores.

8.2 Suggestions

1. Interaction between both layers of bilayer film should be evaluated.

2. Lamination between gelatin and other protein should be investigated.